



UNIVERSIDADE ESTADUAL DE
CAMPINAS
FACULDADE DE ENGENHARIA MECÂNICA

LUCAS NEVES EGÍDIO

Contributions to Switched Affine Systems Control Theory with Applications in Power Electronics

Contribuições à Teoria de Controle de Sistemas
Afins com Comutação com Aplicações em
Eletrônica de Potência

CAMPINAS
2020

LUCAS NEVES EGÍDIO

**Contributions to Switched Affine Systems Control Theory with
Applications in Power Electronics**

**Contribuições à Teoria de Controle de Sistemas Afins com
Comutação com Aplicações em Eletrônica de Potência**

Thesis presented to the School of Mechanical Engineering of the University of Campinas in partial fulfillment of the requirements for the degree of Doctor in Mechanical Engineering, in the area of Mechatronics.

Tese apresentada à Faculdade de Engenharia Mecânica da Universidade Estadual de Campinas como parte dos requisitos exigidos para a obtenção do título de Doutor em Engenharia Mecânica, na área de Mecatrônica.

Orientadora: Profa. Dra. Grace Silva Deaecto

ESTE TRABALHO CORRESPONDE À VERSÃO FINAL DA TESE
DEFENDIDA PELO ALUNO LUCAS NEVES EGÍDIO, E ORIEN-
TADA PELA PROFA. DRA. GRACE SILVA DEAECTO

CAMPINAS
2020

Ficha catalográfica
Universidade Estadual de Campinas
Biblioteca da Área de Engenharia e Arquitetura
Luciana Pietrosanto Milla - CRB 8/8129

Egídio, Lucas Neves, 1992-
Eg41c Contributions to switched affine systems control theory with applications in power electronics / Lucas Neves Egídio. – Campinas, SP : [s.n.], 2020.

Orientador: Grace Silva Deaecto.
Tese (doutorado) – Universidade Estadual de Campinas, Faculdade de Engenharia Mecânica.

1. Sistemas com comutação. 2. Sistemas de controle por realimentação. 3. Desigualdades matriciais lineares. 4. Teoria do controle. 5. Eletrônica de potência. I. Deaecto, Grace Silva, 1983-. II. Universidade Estadual de Campinas. Faculdade de Engenharia Mecânica. III. Título.

Informações para Biblioteca Digital

Título em outro idioma: Contribuições à teoria de controle de sistemas afins com comutação com aplicações em eletrônica de potência

Palavras-chave em inglês:

Switched systems
Feedback control systems
Linear matrix inequalities
Control theory
Power electronics

Área de concentração: Mecatrônica

Titulação: Doutor em Engenharia Mecânica

Banca examinadora:

Grace Silva Deaecto [Orientador]
João Pedro Hespanha
Marcelo Dutra Fragoso
Ricardo Coração de Leão Fontoura de Oliveira
Eric Fujiwara

Data de defesa: 10-01-2020

Programa de Pós-Graduação: Engenharia Mecânica

Identificação e informações acadêmicas do(a) aluno(a)

- ORCID do autor: <https://orcid.org/0000-0003-4096-5969>
- Currículo Lattes do autor: <http://lattes.cnpq.br/6360282705868142>

UNIVERSIDADE ESTADUAL DE CAMPINAS
FACULDADE DE ENGENHARIA MECÂNICA

COMISSÃO DE PÓS GRADUAÇÃO EM ENGENHARIA MECÂNICA

DEPARTAMENTO DE MECÂNICA COMPUTACIONAL

TESE DE DOUTORADO ACADÊMICO

**Contributions to Switched Affine Systems Control Theory with
Applications in Power Electronics**

**Contribuições à Teoria de Controle de Sistemas Afins com
Comutação com Aplicações em Eletrônica de Potência**

Autor: Lucas Neves Egídio

Orientadora: Profa. Dra. Grace Silva Deaecto

A Banca Examinadora composta pelos membros abaixo aprovou esta Tese:

Profa. Dra. Grace Silva Deaecto (Presidente)

Departamento de Mecânica Computacional, Faculdade de Engenharia Mecânica, UNICAMP

Prof. Dr. Eric Fujiwara

Departamento de Sistemas Integrados, Faculdade de Engenharia Mecânica, UNICAMP

Prof. Dr. Ricardo Coração de Leão Fontoura de Oliveira

Departamento de Sistemas e Energia, Faculdade de Engenharia Elétrica e de Computação, UNICAMP

Prof. Dr. Marcelo Dutra Fragoso

Coordenação de Sistemas e Controle, Laboratório Nacional de Computação Científica (LNCC)

Prof. Dr. João Pedro Hespanha

Electrical and Computer Engineering Department, University of California, Santa Barbara

A Ata de Defesa com as respectivas assinaturas dos membros encontra-se no SIGA/Sistema de Fluxo de Dissertação/Tese e na Secretaria do Programa da Unidade.

Campinas, 10 de Janeiro de 2020.

ACKNOWLEDGEMENTS (Agradecimentos)

Primeiramente, gostaria de agradecer aos meus pais, Ângela e Maurício pelo apoio incondicional ao longo de minha vida e trajetória acadêmica, nunca medindo esforços para que eu pudesse alcançar este objetivo e por sempre me mostrarem que a educação forma a essência do ser humano e a chave para libertar-se e crescer. Sou também grato a todas as pessoas da minha família, em especial meus irmãos Arthur e Alice, que sempre estiveram ao meu lado nos momentos das mais diversas naturezas.

Manifesto também minha gratidão à Profa. Grace S. Deaecto que, desde 2014, vem me orientando tanto academicamente como pessoalmente. Muitos foram os seus conselhos, dicas e ensinamentos diluídos em reuniões, ora bem descontraídas, ora mais sérias, mas que sempre contaram com o rigor exigido pela ciência, o comprometimento com a realização de um trabalho sério e a certeza de que sempre devemos dar o melhor de nós.

Não posso deixar também de agradecer ao Prof. José C. Geromel que com muito conhecimento e sabedoria realçados com seu bom humor pôde contribuir ativamente com a realização das pesquisas contidas nesta tese e com a minha formação.

Por me mostrar sempre que há muito mais ao nosso redor no que pensar além de equações diferenciais e problemas de otimização, sou grato à Fernanda pelo companheirismo e carinho que me acompanharam integralmente desde os tempos de graduação.

Agradeço também aos meus colegas de laboratório Helder Daiha, Guilherme Kolotelo, José Lima Luz e Arturo Flores. Estes me proporcionaram discussões construtivas, momentos de descontração e camaradagem além de se mostrarem ótimos parceiros de trabalho.

Reconheço também o apoio de toda a comunidade da Unicamp, a começar pelos meus colegas de graduação da ECA010 e demais cursos, os amigos da pós-graduação do DMC e demais departamentos, os professores e funcionários de todas as unidades, dos restaurantes e da área da saúde. De fato, agradeço a cada pessoa com quem tive contato ao longo dos meus 10 anos de vínculo com esta universidade que tem sua excelência mantida inquestionável graças ao esforço contínuo e coletivo de sua comunidade. Em especial, por todo apoio técnico na realização dos experimentos desta tese, sou grato ao Marcílio Messias, ao Fernando Ortolano, ao Murilo Nicolau e ao José Luís.

I'm also thankful to the whole community of the University of California, Santa Barbara and, specially, to professor João P. Hespanha for receiving me as a visiting scholar, putting me in contact with many new horizons and research perspectives, and also for his helpful comments on this work. I would like to thank also all the friends I've met in Santa Barbara, in special, Henrique Ferraz and Raphael Chinchilla for making me feel like at home.

Pelos comentários pertinentes e reflexões interessantes a respeito deste trabalho, agradeço à banca avaliadora que me permitiu lançar um segundo olhar mais crítico sobre os resultados e discussões aqui apresentados. Também agradeço à Flávia Carneiro pelo *proofreading* e ao Craig Massey pela ajuda com a apresentação.

Finalmente, deixo meu sincero reconhecimento ao povo brasileiro que, por meio de tributos recolhidos das mais diversas formas, financiou meus estudos desde o ensino médio no CAP-COLUNI/UFV até o doutorado. Recebendo bolsas da Coordenação de Aperfeiçoamento de Pessoal de Nível Superior (CAPES) e outros recursos do Conselho Nacional de Desenvolvimento Científico e Tecnológico (CNPq), da Fundação de Amparo à Pesquisa do Estado de São Paulo (FAPESP) e da própria Unicamp, fui capaz de realizar os trabalhos descritos nesta tese. Logo, desejo profundamente que estes resultados e os conhecimentos gerados possam contribuir de alguma forma com o desenvolvimento tecnológico e científico do nosso país, retribuindo o investimento realizado em mim.

Muito obrigado!

* O presente trabalho foi realizado com apoio da Coordenação de Aperfeiçoamento de Pessoal de Nível Superior - Brasil (CAPES) - Código de Financiamento 001.

RESUMO

Esta tese é dedicada ao estudo da teoria de controle de sistemas afins com comutação e algumas de suas aplicações no contexto de eletrônica de potência. Após discussões preliminares, as contribuições principais são apresentadas. O objetivo comum ao longo deste trabalho é desenvolver, sob a perspectiva de otimização convexa, estratégias capazes de governar eventos de chaveamento em sistemas dinâmicos afins de maneira a levar a trajetória do estado a um ponto de referência desejado ou a rastrear uma trajetória variante no tempo. Metodologias de projeto, baseadas em uma função de Lyapunov quadrática generalizada, para função de comutação dependente do estado ou da saída são fornecidas para sistemas afins com comutação a tempo discreto para os quais apenas estabilidade prática é possível de ser assegurada. Subsequentemente, novas condições para estabilidade prática são introduzidas baseadas em desigualdades de Lyapunov-Metzler e levando em conta uma função de Lyapunov do tipo mínimo, que permite reduzir o conservadorismo referente à garantia de estabilidade. Uma metodologia para projetar ciclos limites e assegurar a estabilidade assintótica global foi também apresentada, que leva em conta uma função de Lyapunov variante no tempo e permite tratar otimização de desempenho \mathcal{H}_2 e \mathcal{H}_∞ . Ademais, novas discussões sobre a estabilidade de uma classe de sistemas não-lineares com comutação a tempo contínuo são introduzidas, nas quais o problema de rastreamento de trajetória é tratado. O estudo desta classe é de interesse visto que ela modela o comportamento dinâmico de conversores de potência CA-CC e de máquinas síncronas de ímã permanente alimentadas por inversores de tensão. Esta nova abordagem permite o controle de forma mais simples quando comparada a estratégias clássicas de controle vetorial. Finalmente, alguns resultados experimentais são apresentados, validando as estratégias de controle desenvolvidas. As condições de estabilidade e projeto são majoritariamente escritas em termos de desigualdades matriciais lineares e, logo, podem ser resolvidas de forma eficiente por resolvedores de programação semi-definida prontamente disponíveis.

Palavras-chave: Sistemas com comutação, Sistemas de controle por realimentação, Desigualdades matriciais lineares, Teoria do controle, Eletrônica de potência

ABSTRACT

This dissertation is devoted to the study of switched affine systems control theory and some of its applications in power electronics context. After some preliminary discussions, the main contributions are presented. The common goal throughout this work is to develop, from a convex optimization viewpoint, strategies capable of governing switching events in dynamical affine systems in order to bring the state variable to a desired reference value or to track a time-varying trajectory profile. Design methodologies for state or output dependent switching function based on a generalized Lyapunov function are provided for discrete-time switched affine systems, where only practical stability is possible to be assured. Subsequently, novel practical stability conditions are proposed, based on Lyapunov-Metzler inequalities and taking into account a min-type Lyapunov function, which allows us to reduce conservativeness regarding stability guarantee. A methodology for designing limit cycles and assuring their global asymptotic stability is also presented, which takes into account a time-varying Lyapunov function and permits to cope with \mathcal{H}_2 and \mathcal{H}_∞ performance optimization. Afterward, novel discussions on the stability of a continuous-time switched nonlinear systems class are introduced, where the trajectory-tracking problem is addressed. The study about this class is of interest as it models the dynamic behavior of AC-DC power converters and permanent magnet synchronous machines fed by voltage source inverters. This new approach allows their control in a simpler manner when compared to classical field-oriented control strategies. Finally, some experimental results are presented, validating the developed control strategies. Stability and design conditions are mostly written as linear matrix inequalities and, thus, can be efficiently solved by readily available semi-definite programming solvers.

Keywords: Switched systems, Feedback control systems, Linear matrix inequalities, Control theory, Power electronics

LIST OF FIGURES

1.1 Power versus switching frequency for various power electronic devices, as in Chow and Guo (2019)	18
2.1 Phase portrait for the Hare-Lynx problem.	25
2.2 System trajectories evolving from x_0 when x_e is a stable (1), asymptotically stable (2) and unstable (3) equilibrium point.	26
2.3 Temperature trajectories under switching function $u_h(\theta(t))$ (left) and $u_a(t)$ (right).	42
2.4 State trajectory “sliding” on the switching surface \mathcal{C} .	43
2.5 State trajectories for system \mathcal{G}_s (left) and \mathcal{G}_u (right).	45
2.6 Set X_e^c with equilibrium points x_e (black circle), x_{e1} (red triangle) and x_{e2} (red circle).	54
2.7 Phase portrait of the switched affine system.	55
2.8 Time evolution for a system trajectory along with corresponding switching signal.	55
2.9 Time evolution of the Lyapunov function $v(\xi)$ for different T .	56
3.1 Phase portrait of state trajectory evolving from $x_0 = [0 \ 5]'$, being attracted to \mathcal{X} .	66
3.2 Time evolution of state trajectory from $x_0 = [0 \ 5]'$, and resulting switching sequence.	67
3.3 Block diagram showing the proposed output-dependent switching strategy.	70
3.4 System and filter state over time under the output-dependent switching rule.	78
3.5 Switching signal generated by the output-dependent switching rule.	78
3.6 Differential-drive robot.	79
3.7 System and filter state over time.	81
3.8 Phase portraits for both system and filter.	81
3.9 Obtained switching signal.	81
3.10 Graphical representation of a nonconvex set of attraction provided by Theorem 3.6.	85
3.11 State trajectory ξ and sets of attraction assured from Corollary 3.3.	89
3.12 Time evolution of trajectories $\xi[n]$ and switching sequence $\sigma[n]$, obtained from Corollary 3.3.	90
3.13 Lyapunov function trajectory and the upper bound r_* for the invariant set together with the switching function (3.102).	91
3.14 Phase portrait of a state trajectory converging to the invariant set of attraction \mathcal{V} , in red.	92
3.15 Area of the set of attraction \mathcal{X} calculated from Theorem 3.1 (solid black) and Corollary 3.3 (dashed red) for various sampling periods T .	94
3.16 State trajectory $x[n]$ and limit cycle \mathcal{X}_e^*	101
3.17 Time evolution of the auxiliary state $\xi[n]$.	101
3.18 Obtained switching signal $\sigma[n]$.	101
3.19 Schematic of a three-cell converter.	105
3.20 State trajectories for \mathcal{H}_2 control design.	107

3.21	Obtained switching signal for \mathcal{H}_2 control design.	108
3.22	State trajectories converging to the limit cycle \mathcal{X}_e^* .	108
3.23	Zoom showing the limit cycle \mathcal{X}_e^* in steady-state.	108
3.24	Discrete-time state $\xi[n]$ for \mathcal{H}_∞ control design.	109
3.25	State trajectories for \mathcal{H}_∞ control design.	109
4.1	Phase portrait of a trajectory $x(t)$ along with some level sets \mathcal{V}_t .	113
4.2	Level sets of the Lyapunov function evaluated along the trajectory $x(t)$ (in blue).	113
4.3	PMSM and inverter schematic.	115
4.4	Graphical representation of polytope \mathbb{P} and inscribed circumference.	120
4.5	Phase currents of a PMSM controled by switching rule (4.36).	126
4.6	Rotational velocity of a PMSM controled by switching rule (4.36) and desired reference ω^* (dashed line).	126
4.7	Corresponding switching signal associated to the switching rule (4.36).	127
4.8	Three-phase AC-DC power converter.	129
4.9	Representation of X^* (in red) as $\mathcal{E} \cap \mathcal{H}$.	131
4.10	Graphical representation of polytope \mathbb{P} and inscribed circumference.	135
4.11	Phase currents $i_a(t)$ (blue) and $i_b(t)$ (red) and steady-state references (dashed lines).	138
4.12	Output voltage $v_o(t)$ and correspondent steady-state reference (dashed line).	138
4.13	Switching signal $\sigma(t)$ generated by the proposed switching function.	138
4.14	Steady-state response of current $i_a(t)$ (above) and voltage $v_o(t)$ (below) for several values of T .	139
5.1	Buck-boost circuit schematic.	141
5.2	Photo of the developed buck-boost converter.	142
5.3	Experimental response of a buck-boost converter controled by the switching function (3.10).	144
5.4	Buck-boost and DC-motor circuit schematic.	144
5.5	Friction torque in function of the rotational velocity.	145
5.6	Photo of the considered DC motor.	146
5.7	Attainable rotational velocities for continuous and discrete-time switched control techniques.	147
5.8	Experimental response of a DC motor fed by buck-boost converter under several switching functions.	148
5.9	State trajectory ξ under u_V , obtained experimentally, and sets \mathcal{V} and \mathcal{X} .	148
5.10	Photo of the experimental setup for controlling the PMSM.	150
5.11	Experimental and simulated rotational velocities for $\omega^* = 100$ rad/s.	151
5.12	Experimental and simulated phase current $i_a(t)$ correspondent to $\omega^* = 100$ rad/s.	151
5.13	Switching signal for a constant $\omega^* = 100$ rad/s.	151
5.14	Experimental rotational velocity $\omega(t)$ and correspoding reference $\omega^*(t)$.	152
5.15	Experimental phase currents $i_a(t)$ obtained considering the reference $\omega^*(t)$.	152

LIST OF TABLES

3.1	Switching states and corresponding applied voltages for the differential-drive robot.	80
3.2	System parameters adopted for the differential-drive robot.	80
3.3	Volume comparison for several switching functions and system data.	90
3.4	Number of candidate limit cycles, upper bound $\bar{\mathcal{J}}_2$ and actual cost \mathcal{J}_2 for several κ .	103
3.5	Values u_1 , u_2 , and u_3 for each operation mode i	106
4.1	Modes σ , switches state and phase voltages.	116
4.2	System data employed	125
4.3	Absolute current peak and settling time for $\omega(t)$ obtained for several values of d .	128
4.4	Modes σ , switch states and vector S_i	130
4.5	System parameters adopted in simulations.	137
5.1	Identified parameters for the built buck-boost converter.	142
5.2	Identified parameters for the DC motor.	146
5.3	Quantitative comparison of switching functions.	149
5.4	Identified system parameters.	150

NOMENCLATURE

Abbreviations

AC	Alternating Current
ADC	Analog-to-Digital Converter
BMI	Bilinear Matrix Inequality
DAC	Digital-to-Analog Converter
DC	Direct Current
DTC	Direct-Torque Control
FOC	Field-Oriented Control
IC	Integrated Circuit
IGBT	Insulated Gate Bipolar Transistors
LMI	Linear Matrix Inequality
LTI	Linear Time-Invariant
PID	Proportional-Integral-Derivative
PMSM	Permanent Magnet Synchronous Machine
PWM	Pulse-Width Modulation
RMS	Root Mean Square
s.t.	subject to
VSI	Voltage Source Inveter

Latin Letters

\mathcal{C}	Switching surface
\mathcal{G}	Dynamical system
\mathcal{H}_2	The \mathcal{H}_2 -norm
\mathcal{H}_∞	The \mathcal{H}_∞ -norm

j	Imaginary unit
\mathcal{J}	Quadratic performance cost
\mathcal{J}_2	\mathcal{H}_2 performance index
\mathcal{J}_∞	\mathcal{H}_∞ performance index
\mathcal{L}	Laplace transform
\mathcal{L}_2^c	Set of signals such that the \mathcal{L}_2^c -norm exists
\mathcal{L}_2^d	Set of sequences such that the \mathcal{L}_2^d -norm exists
\mathcal{M}_c	Subset of Metzler matrices for continuous-time
\mathcal{M}_d	Subset of Metzler matrices for discrete-time
\mathbb{K}	Set of N first positive natural numbers $\{1, \dots, N\}$
\mathbb{N}	Set of natural numbers
\mathbb{N}_+	Set of positive natural numbers
\mathbb{N}_-	Set of natural numbers and -1 (i.e. $\mathbb{N}_- = \mathbb{N} \cup \{-1\}$)
\mathbb{R}	Set of real numbers
$\mathbb{R}^{n \times m}$	Set of real matrices of dimension $n \times m$.
\mathbb{R}^n	Set of real vectors of dimension n .
\mathbb{R}_+	Set of real positive numbers
\mathbb{R}_{0+}	Set of real nonnegative numbers
\mathbb{S}	Set of switching signals
\mathbb{Z}	Set of integers
\mathcal{Z}	Z transform
\mathcal{O}_i	i -th operating region
s	Laplace domain variable
z	Z domain variable
e	A vector $e = [1, \dots, 1]'$ of appropriate dimensions
$k(n)$	$n \bmod \kappa$ for some $\kappa \in \mathbb{N}_+$

N	Number of available subsystems or operation modes
n	Discrete-time instant
t	Continuous-time instant
t_n	n -th sampling or switching instant
u	Switching function
v	Lyapunov function
w	Exogenous input
x	State variable
x^*	Reference value
x_e	Equilibrium point
y	Measured output
z	Controlled output

Greek Letters

δ	Unit impulse signal
$\Gamma(X)$	Gamma function
$\gamma_i(X)$	i -th eigenvalue of matrix X
Λ	Unit simplex, i.e. $\Lambda = \left\{ \lambda \in \mathbb{R}^N : \lambda_i \geq 0, \sum_{i \in \mathbb{K}} \lambda_i = 1 \right\}$
λ	Convex combination vector in Λ
ω	Angular frequency or velocity
Π	A Metzler matrix in \mathcal{M}_c or \mathcal{M}_d
π_{ki}	Element (k, i) of a Metzler matrix Π
σ	Switching signal or sequence
$\sigma_m(X)$	Maximum singular value of matrix X
θ	Angular position or electrical angle
ξ	Auxiliary state variable

Superscripts

X'	Transpose of matrix X .
X^\sim	Conjugate transpose of matrix X .

Subscripts

λ_i	i -th element of vector λ
\mathcal{X}_*	Optimal or chosen \mathcal{X}
$T_{wz}(\cdot)$	Transfer matrix from input w to output z

Symbols

•	Symmetric matrix block
$\Delta x[n]$	Difference operator, i.e., $\Delta x[n] = x[n+1] - x[n]$
$\ \cdot\ $	Euclidean norm
$ \cdot $	Absolute value of a scalar or cardinality of a set
$\ \cdot\ _2$	\mathcal{H}_2 -norm for systems, \mathcal{L}_2^c -norm for signals or \mathcal{L}_2^d -norm for sequences
$\ \cdot\ _\infty$	\mathcal{H}_∞ -norm for systems or $\max_{i \in \{1, \dots, n\}} x_i $ for a vector $x \in \mathbb{R}^n$
\otimes	Kronecker product between matrices
$\text{diag}(X, Y)$	Block diagonal matrix, whose elements are X and Y
$\text{tr}(X)$	Trace of matrix X

Notations

$\prod_{k=n_0}^n X_k$	Product over a set, i.e., $\prod_{k=n_0}^n X_k = X_{n_0} X_{n_0+1} \cdots X_n$
$\text{He}(X)$	Hermitian operator of a real matrix X , i.e., $\text{He}(X) = X + X'$
$x(t)$	Continuous-time signal
$x[n]$	Discrete-time sequence

TABLE OF CONTENTS

1	Introduction and Motivation	17
1.1	Organization	20
2	Preliminaries	23
2.1	Nonlinear Systems	23
2.1.1	Lyapunov Stability	26
2.2	Linear Time-Invariant Systems	28
2.2.1	Stability	29
2.2.2	\mathcal{H}_2 and \mathcal{H}_∞ Performance	33
2.2.3	Sampled-Data LTI Systems	39
2.3	Switched Systems	40
2.3.1	Stability under Arbitrary Switching	45
2.4	Switched Linear Systems	46
2.4.1	Stability and Performance - Continuous-Time Domain	46
2.4.2	Stability and Performance - Discrete-Time Domain	49
2.5	Switched Affine Systems	51
2.5.1	Sampled-Data Switched Affine Systems	57
2.6	Concluding Remarks	58
3	Discrete-Time Switched Affine Systems	59
3.1	Problem Formulation	59
3.2	Practical Stability	60
3.2.1	State-dependent Switching	62
3.2.2	Output-dependent Switching	69
3.2.3	Min-type Lyapunov Functions	82
3.2.4	Sampled-data Application	92
3.3	Limit Cycle Stability	94
3.3.1	Problem Statement	95
3.3.2	Limit Cycle Generation	97
3.3.3	State and Time-dependent Switching	98
3.3.4	\mathcal{H}_2 Performance	102
3.3.5	\mathcal{H}_∞ Performance	103
3.3.6	Application for DC-DC Conversion	105
3.4	Concluding Remarks	110

4 Switched Nonlinear Systems	111
4.1 Parameter-dependent Lyapunov Function	112
4.2 Permanent Magnet Synchronous Machines	114
4.2.1 Mathematical Properties of Function $f(\theta)$	117
4.2.2 Switching Function Design	117
4.2.3 Computational Analysis	124
4.2.4 Simulation Results	125
4.3 AC-DC Converter	128
4.3.1 Trigonometric Properties	131
4.3.2 Switching Function Design	132
4.3.3 Averaged Model Comparison	136
4.3.4 Computational Analysis	136
4.3.5 Simulation Results	137
4.4 Concluding Remarks	139
5 Experimental Results	141
5.1 Buck-boost DC-DC Converter	141
5.2 DC-DC Converter Feeding DC Motor	144
5.3 PMSM and Voltage Source Inverter	149
5.4 Concluding Remarks	153
6 Conclusions and Future Works	155
6.1 Conclusions	155
6.2 Future Works	156
References	157
A Important Lemmas	169
A.1 Rayleigh quotient	169
A.2 Matrix Inversion Lemma	169
A.3 Schur Complement Lemma	169
A.4 S-procedure	170
A.5 Convex maximization	171
B Linear Matrix Inequalities	173
B.1 BMIs	174
C Ellipsoids	175
C.1 Volume	175
C.2 Projection	176

INTRODUCTION AND MOTIVATION

“Eu ando bem normal como se deve andar / Pois eu tenho que ir adiante.”

— LUIZ CARLOS SÁ, GUARABYRA & ZÉ RODRÍX, ADIANTE (1973)

History of electrical switching devices starts alongside the invention of relays and vacuum tubes between the 19th and 20th centuries. A more mature state was attained with the large-scale industrial production of semiconductor devices, which provided scope for the development of many nowadays ubiquitous technologies. Fields such as telecommunications, power generation and distribution, electrical machines and computing, widely benefited from the ability of electrically controlling current through circuits. Nevertheless, switching phenomena are not exclusive of electrical engineering creations. Valves, for instance, were employed since the late 17th century as safety devices by the French physicist Denis Papin and for controlling steam flow in the Thomas Savery's early steam pump, see [Farey \(1827\)](#). Later and until now, these mechanic devices were used in all sorts of combustion engines, hydraulic and pneumatic systems, fostering transportation, manufacturing and many other industries.

The main motivation for the theoretical control studies carried out during this Ph.D. resides, however, in the power electronics domain. Quoting [Mohan et al. \(2003\)](#), “the task of power electronics is to process and control the flow of electric energy by supplying voltages and currents in a form that is optimally suited for user loads”. To efficiently perform this task, it is crucial that devices called power converters employ semiconductor elements such as bipolar junction transistors (BJTs), metal-oxide-semiconductor field effect transistors (MOSFETs), gate turn-off thyristors (GTOs) and insulated gate bipolar transistors (IGBTs), among others. These elements work as switches, whose state can be assigned as opened or closed by some logic controller. Recent advancements in replacing silicon semiconductors by gallium nitride (GaN) or silicon carbide (SiC) ones have enhanced the switching frequency and power ranges on which power converters can operate, as shown in Figure 1.1, presented in [Chow and Guo \(2019\)](#). Despite this increase in the switching rate upper bound, reducing the overall number of switching cycles is highly desirable in many applications, since power losses in semiconductors grow linearly with the switching frequency. Regarding the control of these devices, the majority of the available techniques relies upon the premise that the switching events happen arbitrarily fast, which might not be the case in many high power applications, for instance high-voltage direct current (HVDC) systems, see [Qin and Saeedifard \(2013\)](#).

The mathematical modeling of switched power converters can be generally given in terms of switched dynamical systems – a particular case of hybrid systems, wherein the system dynamics interact with discrete events. Switched systems consist of a set of subsystems and a switching signal responsible for selecting one of them to govern the system behavior at each instant of time. Some classical references on this topic are the books [Liberzon \(2003\)](#); [Sun and Ge \(2011\)](#) and the surveys [DeCarlo et al. \(2000\)](#); [Shorten et al. \(2007\)](#); [Lin and Antsaklis \(2009\)](#). Far beyond the power electronics domain, the interest in studying switched systems grew in the past decades as they have shown to be relevant in contexts such as supervisory control [Hespanha et al. \(2003\)](#), control of time-varying polytopic systems [Deaecto et al. \(2011b\)](#), fault-tolerant control [Seron et al. \(2008\)](#), multi-agent systems [Xiao and Wang \(2008\)](#), and networked control systems [Hespanha et al. \(2007\)](#). As it will be

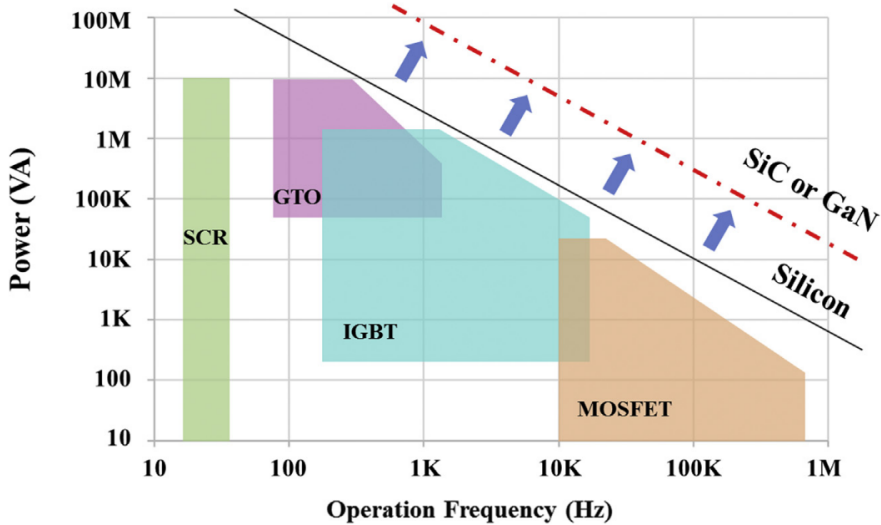


Figure 1.1: Power versus switching frequency for various power electronic devices, as in [Chow and Guo \(2019\)](#)

discussed later in this dissertation, the switching signal can act as a disturbance or a control variable. In this work, the control case is particularly discussed and the switching function design is the goal in every presented problem.

Control and stability for the subclass of switched linear systems have been extensively studied in the literature in both time domains, see for instance [Hespanha \(2004\)](#); [Geromel and Colaneri \(2006a,b\)](#); [Deaecto et al. \(2011a\)](#); [Lin and Antsaklis \(2009\)](#); [Sun and Ge \(2011\)](#); [Fiacchini and Jungers \(2014\)](#); [Deaecto and Geromel \(2018\)](#). The general problem, in this case, is to assess stability of the origin, which is a common equilibrium point among all subsystems. A more general subclass is that of switched affine systems, which are the principal topic of interest in this dissertation, being capable of modeling, among other devices, several DC-DC power converters, see [Deaecto et al. \(2010\)](#). These systems intrigue researchers due to the presence of affine terms in their dynamic equation, responsible for the existence of a set of equilibrium points in the state-space that are attainable by a suitable switching policy. This control problem is more involving since the main interest is generally to stabilize the system towards an equilibrium point that is not common to any subsystem. For this reason, as will be discussed, asymptotic stability is only possible in the continuous-time domain, and some results are available in the literature for this case, see [Bolzern and Spinelli \(2004\)](#); [Corona et al. \(2007\)](#); [Patino et al. \(2009\)](#); [Trofino et al. \(2009\)](#); [Deaecto et al. \(2010\)](#); [Trofino et al. \(2012\)](#); [Scharlau et al. \(2014\)](#); [Deaecto and Santos \(2015\)](#); [Albea et al. \(2015\)](#); [Deaecto \(2016\)](#), among others. In these cases there is a costly price to be paid: to assure asymptotic stability of a desired equilibrium point is the same as requiring that the system trajectories remain fixed at this point; consequently, an arbitrarily high switching frequency is mandatory and the so-called Fillipov solutions arise. It is not hard to imagine that several existing switches cannot operate in this scenario, preventing these theoretical results to be implementable such as they are. Moreover, high switching frequencies are not desirable since, as already mentioned, they lead to power losses. Efforts from the scientific community to bound this frequency are various, see for instance [Hetel and Fridman \(2013\)](#), [Deaecto et al. \(2014\)](#) and [Sanchez et al. \(2019a\)](#). In the general context of switched affine systems under limited switching frequency, asymptotic

stability of an equilibrium point of interest is impossible to be obtained and practical stability is often addressed.

Part of the contributions in this dissertation relies on tackling this problem in the discrete-time domain, where the switching rate is naturally limited. Besides intrinsic discrete-time systems, all continuous-time switched affine models can be represented exactly as discrete-time ones by imposing, for example, a constant period of time during which the switching signal is held constant. In this case, the responses of both systems, continuous and discrete, are identical at the switching instants. See the references [Deaecto et al. \(2014\)](#); [Souza et al. \(2014\)](#); [Chen and Francis \(2012\)](#) for more details about exact discretization. Unfortunately, for the class of discrete-time switched affine systems, the control design is a problem to which the literature has not dedicated many efforts up to now. In this sense, two approaches are developed in this dissertation. The first one deals with the design of a state-dependent switching function to assure practical stability and minimize a set of attraction to where the state trajectories are attracted. Subsequently, these results are generalized to cope with output feedback control, see [Egidio and Deaecto \(nd\)](#). In both cases, the design conditions are based on a general quadratic Lyapunov function and described in terms of linear matrix inequalities (LMIs). For the state-feedback case, alternative conditions are also proposed based on Lyapunov-Metzler inequalities that are less conservative in terms of conditions for the existence of a set of attraction, but not comparable to the previous ones with respect to optimality, see [Egidio and Deaecto \(2019\)](#). It is important to remark that in practical stability studies, the behavior of the trajectories inside the set of attraction cannot be assessed *a priori* and, therefore, nothing can be concluded about performance in the steady state. To overcome this issue, a second approach is provided, which consists in designing limit cycles and assuring their global asymptotic stability. Through this methodology, the limit cycle is determined according to aspect of interest defined by the designer, for instance, the fundamental frequency, amplitude and mean value of the trajectories in steady state. Moreover, due to the asymptotic stability, classical performance indexes such as \mathcal{H}_2 and \mathcal{H}_∞ can be adopted and the transient response of the system is taken into account in the switching function design, see [Egidio et al. \(2020\)](#). For this case, the proposed design conditions are based on a time-varying periodic Lyapunov function and can be described in terms LMIs, being simple to solve using classical optimization tools, see [Boyd et al. \(1994\)](#) for important aspects related to LMIs.

Other contributions within this work concern switched nonlinear systems, whose dynamic equations depend harmonically on a time-varying parameter. Precisely, the nonlinearities are in the form of trigonometric functions that crucially impact the system behavior and naturally entails the study of trajectory tracking problems. For an efficient switching function design, we propose more elaborate non-quadratic Lyapunov functions that are able to capture the harmonic dependency of these systems to provide design conditions also given in terms of LMIs. The goal is to suitably design the switching rule to asymptotically stabilize the system toward an equilibrium trajectory that keeps part of the state at a constant reference while the remaining system variables evolve periodically. The capability of these systems to model AC devices is the main motivation for these studies. Indeed, a regular switched affine system can be used for AC power systems under constant AC frequency, employing exosystems or auxiliary reference frames see, [Sanchez et al. \(2019b\)](#); [Hadjeras et al. \(2019\)](#). However, these models might not be enough to capture AC power systems whose frequency varies, for example, when

feeding or being fed by AC machines. Moreover, classical controllers for these systems are based on cascade control loops, reference frame transformations and take into account modulation strategies. The proposed switched approach controls the system variables in a single control loop and requires low computational effort. Two applications in the power electronics domain are presented, namely, an AC-DC controlled rectifier, see [Egidio et al. \(nd\)](#), and a permanent magnet synchronous machine fed by a voltage source inverter, see [Egidio et al. \(2019\)](#). Regarding the latter, experimental validation is performed, highlighting the efficiency and applicability of these results.

Finally, studying new control strategies for these classes of systems is highly relevant in the current moment as society is moving towards the employment of sustainable and renewable energy sources, such as photovoltaic, wind and other innovative sources, which depend drastically on efficient power conversion, see [Bose \(2010\)](#). Moreover, energy storage and its wise utilization are critical for electrical and hybrid terrestrial or aerial vehicles, which also heavily rely upon effective control of power converters, see [Chan \(2007\)](#); [Shakhatreh et al. \(2019\)](#).

1.1 Organization

The organization of this dissertation obeys the following structure.

- [Chapter 1](#): An introduction with practical and theoretical motivations and general information about this work are presented.
- [Chapter 2](#): Some classical contents are provided along the sections, regarding dynamical systems theory and Lyapunov stability for the reader who is not familiarized with these contents. Additionally, well-known results regarding switched systems that are relevant for the following chapters are discussed.
- [Chapter 3](#): Novel results concerning global stability of discrete-time switched affine systems are presented. Conditions for state or output-dependent switching function design are proposed to assure the existence of a set of attraction, to where system trajectories are globally attracted. Afterward, methodologies for controlling the steady-state behavior through the suitable design of a globally asymptotically stable limit cycle are presented. In this context, the optimization of \mathcal{H}_2 and \mathcal{H}_∞ performance indexes is taken into account in order to assure a suitable transient response.
- [Chapter 4](#): New approaches to model and control particular classes of switched systems, capable of modeling AC systems are discussed here. More specifically, two cases are studied regarding DC-AC and AC-DC conversion. The first one regards the control of the switches in a voltage source inverter feeding a permanent magnet synchronous machine, while the latter regards the rectification of a three-phase voltage source. Trajectory tracking problems naturally arise as sinusoidal currents must be tracked.
- [Chapter 5](#): Experimental results regarding the last two chapters are presented. More specifically, a buck-boost DC-DC converter is used to control the rotational velocity of a DC motor and a voltage

source inverter is employed to control a permanent magnet synchronous machine. The adopted switched control strategy permits the control of these assemblies in a single control loop, contrasting with classical methodologies where cascade controllers are required.

- [Chapter 6](#): Discussions and perspectives regarding future works that should arise from this dissertation are provided.
- [Appendix A](#): Some mathematical tools, as lemmas and theorems, that are employed in our main results are gathered in this appendix.
- [Appendix B](#): A brief discussion about linear matrix inequalities and how some optimization problems in this thesis were solved.
- [Appendix C](#): Discussions about ellipsoids, their volumes and projections.

Figures, tables, examples and mathematical structures, such as equations, definitions, theorems, etc., are numbered as they appear, per chapter. Hyperlinks are denoted by red text. To ease the navigation, each reference is followed by a list of the pages in which they are cited. All simulations presented in examples were performed by using MATLAB and the optimization problems were solved using functions available in the **Robust Control Toolbox**.

Derived Publications

The scientific articles originated throughout this Ph.D. are listed below, categorized by the form of publication.

Journal papers

1. Egidio, L. N. and Deaecto, G. S. (2019). Novel practical stability conditions for discrete-time switched affine systems. *IEEE Transactions on Automatic Control*, 64(11):4705–4710.
2. Egidio, L. N., Daiha, H. R., and Deaecto, G. S. (2020). Limit cycle global asymptotic stability and $\mathcal{H}_2/\mathcal{H}_\infty$ performance of discrete-time switched affine systems. *Automatica*, Accepted.
3. Egidio, L. N. and Deaecto, G. S. (n.d.). Dynamic output feedback control of discrete-time switched affine systems. Submitted.

International conference papers

1. Egidio, L. N., Deaecto, G. S., Hespanha, J. P., and Geromel, J. C. (2019). A nonlinear switched control strategy for permanent magnet synchronous machines. In *IEEE Conference on Decision and Control (CDC)*, pages 3411–3416.
2. Kolotelo, G. K., Egidio, L. N., and Deaecto, G. S. (2018). \mathcal{H}_2 and \mathcal{H}_∞ filtering for continuous-time switched affine systems. In *IFAC Symposium on Robust Control Design (ROCOND)*, volume 51, pages 184–189.

3. Egidio, L. N., Daiha, H. R., Deaecto, G. S., and Geromel, J. C. (2017). DC motor speed control via buck-boost converter through a state dependent limited frequency switching rule. In *IEEE Conference on Decision and Control (CDC)*, pages 2072–2077.
4. Daiha, H. R., Egidio, L. N., Deaecto, G. S., and Geromel, J. C. (2017). \mathcal{H}_∞ state feedback control design of discrete-time switched linear systems. In *IEEE Conference on Decision and Control (CDC)*, pages 5882–5887.
5. Deaecto, G. S. and Egidio, L. N. (2016). Practical stability of discrete-time switched affine systems. In *European Control Conference (ECC)*, pages 2048–2053.
6. Egidio, L. N., Deaecto, G. S., and Barros, T. A. S. (n.d.). Switched control of three-phase ac-dc power converter. Submitted.
7. Egidio, L. N., Deaecto, G. S., and Geromel, J. C. (n.d.). Limit cycle global asymptotic stability of continuous-time switched affine systems. Submitted.

National conference papers

1. Egidio, L. N., Deaecto, G. S. (2019). Estabilidade prática de sistemas afins com comutação a tempo discreto e ponto de equilíbrio parcialmente conhecido. In *Anais do Simpósio Brasileiro de Automação Inteligente (SBAI)*, pp. 804–809.
2. Kolotelo, G. K., Egidio, L. N., Deaecto, G. S. (2018), Projeto de filtros com comutação \mathcal{H}_2 e \mathcal{H}_∞ para sistemas afins a tempo contínuo. In *Anais do Congresso Brasileiro de Automática (CBA)*.
3. Egidio, L. N., Luz Netto, J. L., Deaecto, G. S. (2018). Controle cooperativo \mathcal{H}_∞ via rede de comunicação. In *Anais do Congresso Brasileiro de Automática (CBA)*.
4. Luz Netto, J. L., Egidio, L. N., Ferreira, J. V., Deaecto, G. S. (2017). Controle cooperativo com comutação \mathcal{H}_2 : Implementação em pêndulos invertidos via rede de comunicação. In *Anais do Simpósio Brasileiro de Automação Inteligente (SBAI)*, pp. 171–176.
5. Egidio, L. N., Daiha, H. R., Deaecto, G. S. (2017). Projeto e implementação prática de uma regra de comutação para o controle de velocidade de um motor CC via conversor Buck-Boost. In *Anais do Simpósio Brasileiro de Automação Inteligente (SBAI)*, pp. 295–300.
6. Daiha, H. R., Egidio, L. N., Deaecto, G. S. (2017). Síntese de controle \mathcal{H}_∞ via realimentação de estado para sistemas lineares com comutação a tempo discreto. In *Anais do Simpósio Brasileiro de Automação Inteligente (SBAI)*, pp. 301–306.

“Se oriente, rapaz / Pela constelação do Cruzeiro do Sul.”

— GILBERTO GIL, ORIENTE (1972)

THIS chapter is thoroughly dedicated to present important concepts upon which the main results of this dissertation rely. Its contents are gathered from papers and books that have been previously published and forms a brief review of dynamical systems analysis and performance in both, continuous and discrete-time domains. The main purpose of this presentation is to enlighten colleagues who are being introduced to the switched systems framework as well as help those who are already familiar with these ideas to recapitulate main formalisms.

Firstly, classic stability conditions for general nonlinear autonomous systems are presented, introducing the concept of Lyapunov stability, which is the main foundation of all results to be presented. After that, a summary of linear systems stability and performance is presented. This is done under the convex optimization point of view, that is, writing conditions as constraints expressed in terms of a **linear matrix inequality (LMI)** or more, see [Boyd et al. \(1994\)](#) for further details. The reader may refer to Appendix B for an overview of the main tools required for the full comprehension of this approach. Finally, results on switched systems are gathered from the literature to date and presented as a motivational basis for the developments to come in Chapters 3 and 4.

2.1 Nonlinear Systems

A general n_x -th order **nonlinear system** in the continuous-time domain is defined by the vector differential equation

$$\dot{x}(t) = g(x(t), t), \quad x(0) = x_0 \quad (2.1)$$

where $x : \mathbb{R}_{0+} \rightarrow \mathbb{R}^{n_x}$ is the continuous-time **state vector**, responsible to capture the entire system configuration by putting together all the system variables, and $g : \mathbb{R}^{n_x} \times \mathbb{R}_{0+} \rightarrow \mathbb{R}^{n_x}$ is a locally Lipschitz function in x (see [Khalil \(2002\)](#)) and measurable on t defining, at each instant of time $t \in \mathbb{R}_{0+}$, the evolution of the state $x(t)$ starting from an initial condition $x_0 \in \mathbb{R}^{n_x}$. For the discrete-time domain this system is given as

$$x[n+1] = g(x[n], n), \quad x[0] = x_0 \quad (2.2)$$

being $x : \mathbb{N} \rightarrow \mathbb{R}^{n_x}$ the discrete-time state vector and $g : \mathbb{R}^{n_x} \times \mathbb{N} \rightarrow \mathbb{R}^{n_x}$, the vector field defining its evolution at every instant of time $n \in \mathbb{N}$. For both time domains, the behavior of these systems is fully represented by the dynamic equations (2.1) and (2.2).

The Euclidean space \mathbb{R}^{n_x} of order $n_x \in \mathbb{N}_+$ whence the state vector takes values is called the **state-space** and an arbitrary vector $x \in \mathbb{R}^{n_x}$ is also referred to as a point. Naturally, the length of $x \in \mathbb{R}^{n_x}$ is given by the **Euclidean norm** $\|x\| = \sqrt{(x'x)}$ and a distance between points $x_1, x_2 \in \mathbb{R}^{n_x}$ is defined as $\|x_1 - x_2\|$. A function

$x(t)$ is called a **system trajectory** for the system (2.1) whenever $x(t)$ is a solution of its dynamic equation for some $x_0 \in \mathbb{R}^{n_x}$. The same can be stated about a sequence $x[n]$ regarding the discrete-time system (2.2). The Lipschitz and measurable conditions over the vector fields for the continuous-time case assure the uniqueness of these trajectories for each $x_0 \in \mathbb{R}^{n_x}$ (see Hale (1969); Khalil (2002)) while, for the discrete-time case, the uniqueness is trivial.

Determining the behavior of a system trajectory is essential for a control theory study. Indeed, performance and stability guarantees are the main metrics for evaluating a control system and, even though closed-form solutions might not be available in most cases, being able to characterize growth rates, limit behaviors and other aspects is usually enough within our context, see Luenberger (1979) for some discussions. To this end, let us first define what an equilibrium point is and how can it be categorized, following definitions provided in Luenberger (1979), Slotine et al. (1991) and Khalil (2002).

Definition 2.1 (Equilibrium point). *A vector $x_e \in \mathbb{R}^{n_x}$ is an **equilibrium point** for a continuous-time dynamical system (2.1) if, for all $t \in \mathbb{R}_{0+}$, it satisfies*

$$g(x_e, t) = 0 \quad (2.3)$$

or for a discrete-time dynamical system (2.1) if, for all $n \in \mathbb{N}$, it satisfies

$$g(x_e, n) = x_e \quad (2.4)$$

Notice that, given this definition, we can conclude that whenever the system trajectory attains an equilibrium point, it never leaves it in subsequent time instants unless a non-modeled dynamic or disturbance take action. Formally, we have that if $x(t_0) = x_e$ for some $t_0 \in \mathbb{R}_{0+}$ then $x(t) = x_e, \forall t \geq t_0$ in the continuous-time domain, and that if $x[n_0] = x_e$ for some $n_0 \in \mathbb{N}_+$ then $x[n] = x_e, \forall n \geq n_0$ in the discrete-time counterpart. A nonlinear system can possess either none, one or several equilibrium points scattered or clustered over the state-space. Each one of these points can be classified as stable or unstable depending on how the system trajectories starting in its close neighborhood behave.

Definition 2.2 (Stable and unstable equilibrium points). *An equilibrium point x_e of a continuous-time system is said to be a **stable equilibrium point** if and only if the following holds: for all $R \in \mathbb{R}_+$, there exists another $r \in \mathbb{R}_+$ such that $\|x(t_0) - x_e\| < r$, $t_0 \in \mathbb{R}_{0+}$ implies in $\|x(t) - x_e\| < R$, $\forall t \geq t_0$. Otherwise, x_e is an **unstable equilibrium point**. This definition is analogous for discrete-time systems.*

To illustrate these definitions, the following example recalls a classical (and somewhat controversial, see Gilpin (1973)) ecological system.

Example 2.1 (*The Hare-Lynx System*). Consider the Lotka-Volterra model for prey-predator systems

$$\dot{h}(t) = h(t)(r_h + c_{hl}l(t)), \quad h(0) = h_0 \quad (2.5)$$

$$\dot{l}(t) = l(t)(r_l + c_{lh}h(t)), \quad l(0) = l_0 \quad (2.6)$$

where the nonnegative variables $h(t)$ and $l(t)$ represent, respectively, the hare and lynx populations sharing

a habitat, $r_h > 0$, $r_l < 0$ are growth rates and $c_{hl} < 0$, $c_{lh} > 0$ are coupling constants. Considering a state vector $x(t) = [h(t) \ l(t)]'$, this system has two equilibrium points $x_{e1} = [0 \ 0]'$ and $x_{e2} = [h_e \ l_e]'$, with $h_e = -\frac{r_l}{c_{lh}}$, $l_e = -\frac{r_h}{c_{lh}}$. It is not hard to verify from Definition 2.2 that x_{e1} is unstable since for $x(0) = [r \ 0]'$, $r \in \mathbb{R}_+$ there exists no R such that $\|x(t) - x_{e1}\| < R$, $\forall t > 0$. That is, in the absence of predators (lynxes), the prey population grows indefinitely according to this model. However, x_{e2} is known to be a stable equilibrium point and both prey and predator populations tend to orbit it, forming bounded system trajectories. A phase portrait for $r_h = 0.7$, $r_l = -0.2$, $c_{hl} = -0.03$ and $c_{lh} = 0.05$ is presented in Figure 2.1.

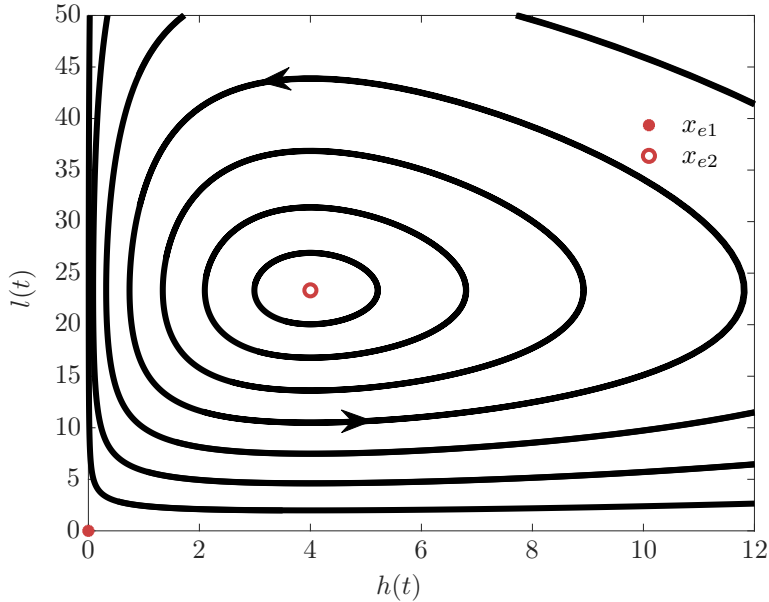


Figure 2.1: Phase portrait for the Hare-Lynx problem.

The general definition of stability for equilibrium points allows us to identify particular cases of interest. In fact, a stable equilibrium point is not required to attract every trajectory of the system regardless its initial condition. Generally, one should only infer from stability that every system trajectory starting sufficiently close to x_e will have the distance $\|x(t) - x_e\|$ bounded by some scalar R . No further knowledge can be derived about its steady-state behavior or how far away from x_e can one choose the starting point x_0 . For that reason, let us define specific types of stable equilibrium points.

Definition 2.3 ((Globally) asymptotically stable equilibrium point). *An equilibrium point x_e is said to be an **asymptotically stable equilibrium point** of a dynamical system (2.1) if and only if there exists an $r \in \mathbb{R}_+$ for which every trajectory $x(t)$ such that $\|x(t_0) - x_e\| < r$, $t_0 \in \mathbb{R}_{0+}$ satisfies $\lim_{t \rightarrow \infty} x(t) = x_e$. Moreover, x_e is said to be a **globally asymptotically stable equilibrium point** if that holds for every $r \in \mathbb{R}_+$. For a discrete-time dynamical system (2.2) this definition is analogous.*

Asymptotic stability of an equilibrium point is a stronger characteristic, imposing that nearby trajectories will not only remain within a bounded distance to x_e but will progressively approach it as time evolves. Additionally, it is readily demonstrated by contradiction that the existence of a globally asymptotically stable equilibrium point imposes that no other equilibrium point exists. Figure 2.2 illustrates possible system trajectories

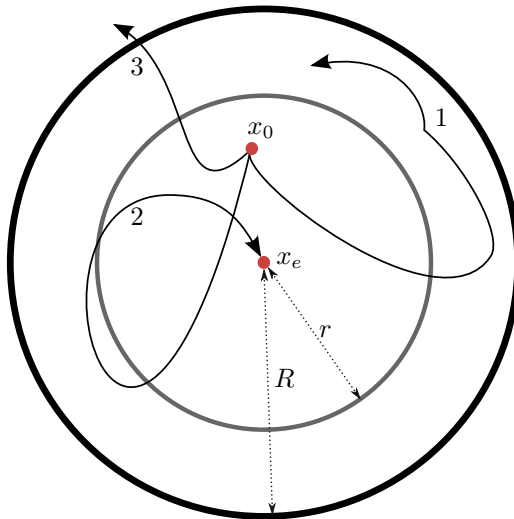


Figure 2.2: System trajectories evolving from x_0 when x_e is a stable (1), asymptotically stable (2) and unstable (3) equilibrium point.

starting at some x_0 near an equilibrium point x_e of different natures.

Controllers capable of assuring asymptotic stability of some desired point x_e are generally of great interest under a control theory perspective, as this means that every system trajectory that gets close enough to x_e will converge to it. However, it is not always possible to design this kind of controllers, especially in the discrete-time domain, as it will be clear in the next sections. Based on discussions in Vangipuram et al. (1990), a weaker type of stability is defined in the sequel for a point that will be sometimes referred to as an equilibrium point, although, rigorously, it does not satisfy Definition 2.1.

Definition 2.4 ((Globally) practically stable equilibrium point). *A point x_e is said to be a **practically stable equilibrium point** of a dynamical system (2.1) if and only if there exists a pair $r, R \in \mathbb{R}_+$ for which every trajectory $x(t)$ satisfying $\|x(t_0) - x_e\| < r$, $t_0 \in \mathbb{R}_{0+}$ fulfills $\|x(t) - x_e\| < R$, $\forall t > t_n$ for some $t_n > t_0$. Moreover, x_e is said to be a **globally practically stable equilibrium point** if that holds for every $r \in \mathbb{R}_+$. For a discrete-time dynamical system (2.2) this definition is analogous.*

Certainly, practical stability may not be the most desirable situation but it is, in many cases, sufficiently satisfactory. This is a context-sensitive matter but, the quality of a practically stabilizing controller should be generally evaluated according to the size and shape of the region to where the system trajectories are attracted in steady state. Notice that the existence of a practically stable equilibrium point is linked to the existence of a region in the state-space to where system trajectories are attracted and, once inside, they never leave it. This region will be formally defined at an adequate moment.

2.1.1 Lyapunov Stability

Within this subsection, we discuss a powerful tool to study the stability of equilibrium points: the **Lyapunov Stability Theorem**. The framework provided by this theorem, developed by the Russian mathematician Aleksandr M. Lyapunov, is the basis upon which much of modern control theory holds for both time domains. The key point of Lyapunov stability is that it allows for a function capable of roughly condensing information

about a system behavior, without giving full account of details. In this sense, we use these functions to simplify the search for a stability certificate. Nevertheless, a formal definition must precede the theorem statement.

Definition 2.5 (Lyapunov function). *Considering an equilibrium point $x_e \in D$, a function $v : D \subseteq \mathbb{R}^{n_x} \rightarrow \mathbb{R}_{0+}$ is called a **Lyapunov function** for a continuous-time (or discrete-time) dynamical system (2.1) (or (2.2)) if the following conditions hold simultaneously:*

1. *v is continuous over D .*
2. *$v(x) = 0$ if $x = x_e$ and $v(x) > 0$ otherwise.*
3. *$\dot{v}(x(t)) \leq 0$ (or $\Delta v(x[n]) \leq 0$), which means that it is non-increasing with time if $x(t)$ (or $x[n]$) is a system trajectory.*

Moreover, if D is unbounded, $v(x)$ must be radially unbounded¹.

Lyapunov functions can be regarded as distance or energy functions that do not increase over time (or when we allow them to do so, they must admit a non-increasing upper bound), guiding the system state towards some sort of minimum value. Certainly, the existence of such function allows us to conclude that a system trajectory starting in D will remain in D and when D is the whole state-space, the trajectory is not getting arbitrarily far away from x_e . The Lyapunov Stability Theorems for both time domains are presented below and proofs are available in Luenberger (1979) and Khalil (2002).

Theorem 2.1 (Lyapunov Stability Theorem – Continuous-Time). *Let $x_e \in D$ be an equilibrium point for the continuous-time dynamical system (2.1). If there exists a Lyapunov Function $v(x)$ as given in Definition 2.5 then x_e is stable. Moreover, if $\dot{v}(x(t)) < 0, \forall x \in D \setminus \{x_e\}$, then x_e is asymptotically stable. If $D = \mathbb{R}^{n_x}$, then the stability is global.*

Theorem 2.2 (Lyapunov Stability Theorem – Discrete-Time). *Let $x_e \in D$ be an equilibrium point for the discrete-time dynamical system (2.2). If there exists a Lyapunov Function $v(x)$ as given in Definition 2.5 then x_e is stable. Moreover, if $\Delta v(x[n]) < 0, \forall x \in D \setminus \{x_e\}$, then x_e is asymptotically stable. If $D = \mathbb{R}^{n_x}$, then the stability is global.*

The following example, based on discussions in Luenberger (1979), presents a Lyapunov function.

Example 2.2 (A Lyapunov function). Consider again the Hare-Lynx system presented in Example 2.1. The nonnegative function

$$v(h, l) = p_h \left(h - h_e - h_e \ln \left(\frac{h}{h_e} \right) \right) + p_l \left(l - l_e - l_e \ln \left(\frac{l}{l_e} \right) \right) \quad (2.7)$$

defined in the domain $D = \mathbb{R}_+^2$ is a Lyapunov Function for system (2.5)-(2.6) with respect to $x_{e2} = [h_e \ l_e]'$ with $p_h = -(c_{lh}/c_{hl})p_l$ and $p_l > 0$. Indeed, $v(h, l)$ is continuous, nonnegative and $v(h, l) = 0$ uniquely for

¹A radially unbounded function is a function such that $\|x\| \rightarrow \infty \implies f(x) \rightarrow \infty$.

$h = h_e$ and $l = l_e$. The demonstration that $\dot{v}(h, l) \leq 0$ for all $x = [h \ l]' \in D$ is done by evaluating

$$\dot{v}(h, l) = p_h \left(1 - \frac{h_e}{h} \right) \dot{h} + p_l \left(1 - \frac{l_e}{l} \right) \dot{l} = 0 \quad (2.8)$$

showing that all conditions in Definition 2.5 hold and thus x_{e2} is stable according to Theorem 2.1.

For this last example, we can say that the Lyapunov function (2.7) is a stability certificate for the point x_{e2} and system (2.5)-(2.6). However, for a general nonlinear system, finding a Lyapunov function for a stable equilibrium point is not a trivial task. Fortunately, there are specific forms of Lyapunov function candidates that might speed this search up for some classes of dynamical systems, sometimes providing a sufficiently limited search domain. This means that, for given system classes, the problem of determining whether an equilibrium point x_e is stable or not is a decidable problem. In other words, there exists an algorithmic procedure capable of finding a Lyapunov function, whenever there exists one, and determining the stability or instability of x_e within a finite amount of time. Some of these are presented in the following sections of this chapter.

2.2 Linear Time-Invariant Systems

The state-space representation of a **Linear Time-Invariant System (LTI)** of order $n_x \in \mathbb{N}_+$ is given in the continuous-time domain by the set of linear differential equations

$$\begin{cases} \dot{x}(t) &= Ax(t) + Hw(t), \quad x(0) = x_0 \\ z(t) &= Ex(t) + Gw(t) \end{cases} \quad (2.9)$$

for which, $x : \mathbb{R}_{0+} \rightarrow \mathbb{R}^{n_x}$ denotes the state vector, $w : \mathbb{R}_{0+} \rightarrow \mathbb{R}^{n_w}$ represents an external input signal and $z : \mathbb{R}_{0+} \rightarrow \mathbb{R}^{n_z}$ is a controlled (or performance) output. The first equation defines, as (2.1), the behavior of system trajectories and is called the dynamic equation. The second one, referred to as the output equation, is used to determine the output of the system. An LTI system is fully described by the 4-tuple of matrices $\mathcal{G}_c = (A, H, E, G)$, of suitable dimensions. This system presents a closed-form solution for any given initial condition x_0 , see Chen (1995), defined by

$$x(t) = e^{At}x(0) + \int_0^t e^{A(t-\tau)}Hw(\tau)d\tau \quad (2.10)$$

Similarly, an LTI system in the discrete-time domain is given by the state-space representation

$$\begin{cases} x[n+1] &= Ax[n] + Hw[n], \quad x[0] = x_0 \\ z[n] &= Ex[n] + Gw[n] \end{cases} \quad (2.11)$$

for which $x : \mathbb{N} \rightarrow \mathbb{R}^{n_x}$ is the state vector, $w : \mathbb{N} \rightarrow \mathbb{R}^{n_w}$ is the external input and $z : \mathbb{N} \rightarrow \mathbb{R}^{n_z}$ is the controlled output. The closed-form solution for this system is given by

$$x[n] = A^n x_0 + \sum_{k=0}^{n-1} A^{n-1-k} H w[k] \quad (2.12)$$

A classical alternative representation for an LTI system can be done in the frequency domain by means of

its **transfer function**. Assuming null initial conditions and applying the Laplace Transform operator to (2.9) and Z Transform operator to (2.11) yields, respectively, the continuous-time and discrete-time transfer functions

$$T_{wz}(\mathbf{s}) = E(\mathbf{s}I - A)^{-1}H + G \quad (2.13)$$

$$T_{wz}(\mathbf{z}) = E(\mathbf{z}I - A)^{-1}H + G \quad (2.14)$$

Both transfer functions are proper (or strictly proper) rational polynomial functions, that is, the ratio between two polynomials such that the degree of the numerator is less than or equal to (strictly less than) the degree of the denominator. The roots of the numerator and denominator are the **zeros** and the **poles** of the transfer function, respectively. These functions are responsible to map the inputs onto the outputs in the frequency domain. That is, consider for the continuous-time the Laplace Transforms $\mathcal{L}(w(t)) = \hat{w}(\mathbf{s})$ and $\mathcal{L}(z(t)) = \hat{z}(\mathbf{s})$ while for the discrete-time, the Z Transforms $\mathcal{Z}(w[n]) = \hat{w}(\mathbf{z})$ and $\mathcal{Z}(z[n]) = \hat{z}(\mathbf{z})$. Then, the following equalities are verified

$$T_{wz}(\mathbf{s}) = \frac{\hat{z}(\mathbf{s})}{\hat{w}(\mathbf{s})} \quad (2.15)$$

$$T_{wz}(\mathbf{z}) = \frac{\hat{z}(\mathbf{z})}{\hat{w}(\mathbf{z})} \quad (2.16)$$

It is important to remark that, although an LTI system is not often encountered in real-world, its model is a fair approximation of a general nonlinear system around its equilibrium point. For deeper discussions on linearization, see Slotine et al. (1991); Khalil (2002); Hespanha (2018) or, for Lusophones, Geromel and Korogui (2011).

2.2.1 Stability

In this subsection, let us assume $w = 0$. Notice that, in this case, the origin is an equilibrium point of any LTI system. Additionally, whenever A is regular for the continuous-time system or $A - I$ is regular for the discrete-time one, $x_e = 0$ is the only equilibrium point in the state-space. As a consequence, an LTI system is said to be a **stable LTI system** if its origin is stable.

There is no difficulty in assessing the stability of an LTI system by analyzing the eigenvalues of the matrix A or the poles of its transfer function, which match each other when the minimal realization is considered. Indeed, asymptotic stability is assured if and only if, for the continuous-time domain, $\text{Re}(\gamma_i(A)) < 0$, $\forall i \in \{1, \dots, n_x\}$ or, for the discrete-time domain, $|\gamma_i(A)| < 1$, $\forall i \in \{1, \dots, n_x\}$. However, the Lyapunov theory may also be used to decide whether the origin of a linear system is a stable equilibrium. The following theorem presents some necessary and sufficient conditions for global asymptotic stability in continuous-time.

Theorem 2.3 (LTI system stability – Continuous-time). *Consider a continuous-time LTI system $\mathcal{G}_c = (A, H, E, G)$ as given in (2.9) along with $w(t) = 0$ for all $t \in \mathbb{R}_{0+}$. These statements are equivalent:*

1. *The system \mathcal{G}_c is globally asymptotically stable, that is, $x_e = 0$ is a globally asymptotically stable equilibrium point.*
2. *A is a **Hurwitz stable matrix**, that is, the eigenvalues of A satisfy $\text{Re}(\gamma_i(A)) < 0$, $\forall i \in \{1, \dots, n_x\}$.*
3. *Every pole p of the system transfer function (2.13) satisfies $\text{Re}(p) < 0$.*

4. There exists one symmetric positive definite matrix $P \in \mathbb{R}^{n_x \times n_x}$ solution of the **continuous-time Lyapunov equation**

$$A'P + PA + Q = 0 \quad (2.17)$$

for an arbitrary positive definite matrix $Q \in \mathbb{R}^{n_x \times n_x}$.

Proof: This proof will be split in 4 demonstrations of necessity, sufficiency or equivalence between the statements. More specifically, let us show that $1 \equiv 2$, $2 \equiv 3$, $4 \Rightarrow 1$ and $4 \Leftarrow 1$.

$1 \equiv 2$ Notice that the solution (2.10) can be rewritten as

$$x(t) = V^{-1}e^{Dt}Vx(0) = V^{-1}e^{\text{Re}(D)t}e^{\text{Im}(D)\text{j}t}Vx(0) \quad (2.18)$$

where V and $D = \text{diag}(\gamma_1(A), \dots, \gamma_{n_x}(A))$ form the eigendecomposition of $A = V^{-1}DV$. From this equation, we can conclude that $\lim_{t \rightarrow \infty} x(t) = 0$ for any $x_0 \in \mathbb{R}^{n_x}$ if and only if $\text{Re}(\gamma_i(A)) < 0$ for all $i \in \{1, \dots, n_x\}$.

$2 \equiv 3$ To demonstrate this, let us show that the poles of the transfer function $T_{wz}(\mathbf{s})$ and the eigenvalues of A coincide. Take the definition given in (2.13) and rewrite it as

$$T_{wz}(\mathbf{s}) = \frac{1}{\det(\mathbf{s}I - A)}(E\text{adj}(\mathbf{s}I - A)H + G\det(\mathbf{s}I - A)) \quad (2.19)$$

This shows that every pole p of $T_{wz}(\mathbf{s})$ is also a root of $\det(\mathbf{s}I - A) = 0$, which is an eigenvalue of A . The converse holds if \mathcal{G}_c is in minimal realization.

$4 \Rightarrow 1$ Let us assume that the continuous-time Lyapunov equation is satisfied by $P > 0$ for an arbitrary $Q > 0$. Hence, a Lyapunov function for the LTI system \mathcal{G}_c is the **quadratic Lyapunov function**

$$v(x(t)) = x(t)'Px(t) \quad (2.20)$$

with time derivative given by

$$\begin{aligned} \dot{v}(x(t)) &= x(t)'(A'P + PA)x(t) \\ &= -x(t)'Qx(t) < 0 \end{aligned}$$

for all $x(t) \neq 0$. Then, from Theorem 2.1 the equilibrium point $x_e = 0$ is globally asymptotically stable.

$4 \Leftarrow 1$ Assume that the origin is a globally asymptotically stable equilibrium point. Let us show that for an arbitrary $Q > 0$ there exists $P > 0$ solution of (2.17) and it is given by

$$P = \int_0^\infty e^{A't}Qe^{At}dt \quad (2.21)$$

This improper integral exists since, by assumption, condition 2 assures $\text{Re}\{\gamma_i(A)\} < 0$, $\forall i \in \{1, \dots, n_x\}$. Multiplying (2.21) to the right by a non-null vector $x_0 \in \mathbb{R}^{n_x}$ and to the left by its transpose yields

$$x_0'Px_0 = \int_0^\infty x(t)'Qx(t)dt > 0 \quad (2.22)$$

where $x(t) = e^{At}x_0$ is the solution starting from $x(0) = x_0$, which shows that P is positive definite. Now, replacing the given P in the Lyapunov equation (2.17), we obtain

$$\begin{aligned} A'P + PA &= A' \left(\int_0^\infty e^{A't} Q e^{At} dt \right) + \left(\int_0^\infty e^{A't} Q e^{At} dt \right) A \\ &= \int_0^\infty \frac{d}{dt} e^{A't} Q e^{At} dt = e^{A't} Q e^{At} \Big|_0^\infty \\ &= \lim_{t \rightarrow \infty} e^{A't} Q e^{At} - Q \\ &= -Q \end{aligned} \tag{2.23}$$

where the last equality, arising from the fact that A is Hurwitz stable, reveals that P is a solution for the Lyapunov equation.

Finally, the uniqueness of this solution is verified by contradiction, assuming another \tilde{P} to solve $A'\tilde{P} + \tilde{P}A = -Q$. Subtracting this equality from (2.17), we have

$$A'(P - \tilde{P}) + (P - \tilde{P})A = 0 \tag{2.24}$$

which, multiplied to the left by $e^{A't}$ and to the right by its transpose, results in

$$e^{A't} \left(A'(P - \tilde{P}) + (P - \tilde{P})A \right) e^{At} = \frac{d}{dt} \left(e^{A't}(P - \tilde{P})e^{At} \right) = 0 \tag{2.25}$$

This last equality shows that the matrix $e^{A't}(P - \tilde{P})e^{At}$ is time-independent. Evaluating it for $t = 0$ and $t \rightarrow \infty$ and equating both expressions provides

$$P - \tilde{P} = \lim_{t \rightarrow \infty} e^{A't}(P - \tilde{P})e^{At} = 0 \tag{2.26}$$

demonstrating that $P = \tilde{P}$. □

This theorem deals with global asymptotic stability of LTI continuous-time systems and shows that the only form of Lyapunov function to be investigated when trying to verify the asymptotic stability of these systems is the quadratic one, given in (2.20). It surely alleviates the task of searching for a stability certificate as the set of positive definite matrices P is a convex cone and the convex optimization framework can be readily employed. Similar conclusions can be presented for discrete-time LTI systems, as the following theorem presents.

Theorem 2.4 (LTI system stability – Discrete-time). *Consider a discrete-time LTI system $\mathcal{G}_d = (A, H, E, G)$ as given in (2.11) along with $w[n] = 0$ for all $n \in \mathbb{N}$. These statements are equivalent:*

1. *The system \mathcal{G}_d is globally asymptotically stable, that is, $x_e = 0$ is a globally asymptotically stable equilibrium point.*
2. *A is a **Schur stable matrix**, that is, the eigenvalues of A satisfy $|\gamma_i(A)| < 1$, $\forall i \in \{1, \dots, n_x\}$.*
3. *Every pole p of the system transfer function (2.14) satisfies $|p| < 1$.*
4. *There exists one symmetric positive definite matrix $P \in \mathbb{R}^{n_x \times n_x}$ solution of the **discrete-time Lyapunov equation***

$$A'PA - P + Q = 0 \quad (2.27)$$

for an arbitrary positive definite matrix $Q \in \mathbb{R}^{n_x \times n_x}$.

Proof: This proof is again split in 4 demonstrations of $1 \equiv 2$, $2 \equiv 3$, $4 \Rightarrow 1$ and $4 \Leftarrow 1$.

$1 \equiv 2$ Notice that the solution (2.12) can be rewritten as

$$x[n] = V^{-1}D^nVx[0] \quad (2.28)$$

where V and $D = \text{diag}(\gamma_1(A), \dots, \gamma_{n_x}(A))$ form the eigendecomposition of $A = V^{-1}DV$. From this equation we can conclude that $\lim_{n \rightarrow \infty} x[n] = 0$ for any $x_0 \in \mathbb{R}^{n_x}$ if and only if $|\gamma_i(A)| < 1$ for all $i \in \{1, \dots, n_x\}$.

$2 \equiv 3$ This is analogous to the demonstration presented in Theorem 2.3 and, therefore, omitted.

$4 \Rightarrow 1$ Let us assume that the discrete-time Lyapunov equation is satisfied by $P > 0$ for an arbitrary $Q > 0$. Hence, a Lyapunov function for the LTI system \mathcal{G}_d is also the **quadratic Lyapunov function**

$$v(x[n]) = x[n]'Px[n] \quad (2.29)$$

with the difference operator given by

$$\begin{aligned} \Delta v(x[n]) &= x[n]'(A'PA - P)x[n] \\ &= -x[n]'Qx[n] < 0 \end{aligned}$$

for all $x[n] \neq 0$. Then, from Theorem 2.2 the equilibrium point $x_e = 0$ is globally asymptotically stable.

$4 \Leftarrow 1$ Assume that the origin is a global asymptotically stable equilibrium point. Let us show that an arbitrary $Q > 0$ there exists $P > 0$ solution of (2.27) and it is given by

$$P = \sum_{n=0}^{\infty} (A')^n Q (A)^n \quad (2.30)$$

Observe that this series converges since, by assumption, condition 2 assures $|\gamma_i(A)| < 1$, $\forall i \in \{1, \dots, n_x\}$.

Multiplying (2.30) to the right by a non-null vector $x_0 \in \mathbb{R}^{n_x}$ and to the left by its transpose yields

$$x_0'Px_0 = \sum_{n=0}^{\infty} x[n]'Qx[n] > 0 \quad (2.31)$$

where $x[n] = A^n x_0$ is the solution starting from $x[0] = x_0$, which shows that P is positive definite. Now, replacing the given P in the Lyapunov equation (2.27), we obtain

$$\begin{aligned} A'PA - P &= A' \left(\sum_{n=0}^{\infty} (A')^n Q (A)^n \right) A - \sum_{n=0}^{\infty} (A')^n Q (A)^n \\ &= -(A')^0 Q (A)^0 \\ &= -Q, \end{aligned}$$

showing that P is a solution for the Lyapunov equation. The uniqueness of this solution is once more verified by contradiction, assuming another \tilde{P} to solve $A'\tilde{P}A - \tilde{P} = -Q$. Subtracting this equality from (2.27), we have

$$A'(P - \tilde{P})A - (P - \tilde{P}) = 0 \quad (2.32)$$

which, multiplied to the left by $(A')^n$, to the right by $(A)^n$ and summed from $n = 0$ up to infinity, provides

$$\sum_{n=0}^{\infty} (A')^{n+1}(P - \tilde{P})(A)^{n+1} - \sum_{n=0}^{\infty} (A')^n(P - \tilde{P})(A)^n = -(A')^0(P - \tilde{P})(A)^0 = 0 \quad (2.33)$$

demonstrating that $P = \tilde{P}$. \square

2.2.2 \mathcal{H}_2 and \mathcal{H}_{∞} Performance

Now that stability conditions have been presented for LTI systems, we can formulate performance metrics that will serve as a basis for more general indices to be later defined. To this end, it is important to define measures for trajectories in both time domains as follows.

Definition 2.6 (\mathcal{L}_2^c -norm). *The \mathcal{L}_2^c -norm of a continuous vector function $f : \mathbb{R}_{0+} \rightarrow \mathbb{R}^m$ is defined as*

$$\|f\|_2 = \left(\int_0^{\infty} f(\tau)' f(\tau) d\tau \right)^{1/2} \quad (2.34)$$

and the set of functions f such that this integral exists is called \mathcal{L}_2^c space.

Definition 2.7 (\mathcal{L}_2^d -norm). *The \mathcal{L}_2^d -norm of a discrete vector function $f : \mathbb{N} \rightarrow \mathbb{R}^m$ is defined as*

$$\|f\|_2 = \left(\sum_{n=0}^{\infty} f[n]' f[n] \right)^{1/2} \quad (2.35)$$

and the set of functions f such that this series converges is called \mathcal{L}_2^d space.

From this point, continuous and discrete-time domains will be treated separately to avoid troublesome notations.

Two classic measures for performance of an LTI system in optimal control theory are the \mathcal{H}_2 and \mathcal{H}_{∞} norms. These indexes are defined in the frequency domain for a globally asymptotically stable continuous-time linear system \mathcal{G}_c and can be equivalently rewritten in the time domain after some algebraic manipulations. Considering $G = 0$ and $x(0) = 0$, the system \mathcal{G}_c presents a strictly proper transfer function $T_{wz}(\mathbf{s})$ and its \mathcal{H}_2 norm is defined as an integral over the imaginary axis given by

$$\|\mathcal{G}_c\|_2 = \left(\frac{1}{2\pi} \int_{-\infty}^{\infty} \text{tr}(T_{wz}(j\omega) \sim T_{wz}(j\omega)) d\omega \right)^{1/2} \quad (2.36)$$

From the Parseval's theorem (see Oppenheim et al. (1997)), equality (2.36) squared provides

$$\|\mathcal{G}_c\|_2^2 = \int_0^{\infty} \text{tr}(h(t)h(t)') dt \quad (2.37)$$

with $h(t)$ defining the **impulse response** of \mathcal{G}_c as the inverse Laplace transform $h(t) = \mathcal{L}^{-1}(T_{wz}(\mathbf{s}))$. Notice that the linear nature of the system allows to rewrite this expression by considering inputs $w(t) = e_k \delta(t)$, $k \in$

$\{1, \dots, n_w\}$ where $\delta(t)$ is the unitary impulse and e_k is the k -th vector of the standard basis of \mathbb{R}^{n_w} . As done in Doyle et al. (1989), for each of these impulsive inputs, $z_k(t) = Ee^{At}He_k$ denotes the associated outputs satisfying

$$\begin{aligned}\|\mathcal{G}_c\|_2^2 &= \sum_{k=0}^{n_w} \int_0^\infty z_k(t)' z_k(t) dt \\ &= \sum_{k=0}^{n_w} e_k' H' \left(\int_0^\infty e^{A't} E' E e^{At} dt \right) H e_k \\ &= \text{tr}(H' P_o H)\end{aligned}\tag{2.38}$$

where the matrix $P_o = \int_0^\infty e^{A't} E' E e^{At} dt$ is the **observability gramian**, the solution of the continuous-time Lyapunov equation (2.17) for $Q = E'E$. Due to the **circularity of the trace operator**², it is possible to formulate a dual procedure to evaluate $\|\mathcal{G}_c\|_2$ as

$$\begin{aligned}\|\mathcal{G}_c\|_2^2 &= \text{tr} \left(H' \int_0^\infty e^{A't} E' E e^{At} dt H \right) \\ &= \text{tr} \left(E \int_0^\infty e^{At} H H' e^{A't} dt E' \right) \\ &= \text{tr}(EP_cE')\end{aligned}\tag{2.39}$$

where the matrix $P_c = \int_0^\infty e^{At} H H' e^{A't} dt$ is the **controllability gramian**, satisfying the continuous-time Lyapunov equation $AP_c + P_c A' + HH' = 0$. At this point, we are able to state the first performance-related theorem of this dissertation.

Theorem 2.5 (LTI \mathcal{H}_2 performance – continuous-time). *Consider a continuous-time LTI system \mathcal{G}_c given by (2.9). The \mathcal{H}_2 norm of the system can be exactly computed by the following procedures.*

1. From the observability or controllability gramians, P_o or P_c , we have

$$\|\mathcal{G}_c\|_2 = \sqrt{\text{tr}(H' P_o H)} = \sqrt{\text{tr}(EP_cE')}\tag{2.40}$$

2. From the integration, we have

$$\|\mathcal{G}_c\|_2 = \int_0^\infty \text{tr}(h(t)h(t)') dt\tag{2.41}$$

3. From the limit solution of the primal convex optimization problem

$$\|\mathcal{G}_c\|_2^2 = \inf_{P>0} \text{tr}(H' PH) \quad \text{s.t.}\tag{2.42}$$

$$A'P + PA + E'E < 0\tag{2.43}$$

4. From the limit solution of the dual convex optimization problem

$$\|\mathcal{G}_c\|_2^2 = \inf_{S>0} \text{tr}(ESE') \quad \text{s.t.}\tag{2.44}$$

$$AS + SA' + HH' < 0\tag{2.45}$$

²The circularity property of $\text{tr}(\cdot)$ assures that for any matrices A, B of adequate dimensions $\text{tr}(AB) = \text{tr}(BA)$.

Proof: The first procedure is verified from equations (2.38) and (2.39), the second one comes from the time-domain definition (2.37) and both, third and fourth, from the fact that the optimal solutions to the indicated optimization problems satisfy the Lyapunov equations $A'P + PA + E'E = -\epsilon I$ and $AS + SA' + HH' = -\epsilon I$, respectively, for a precision $\epsilon > 0$. \square

Control theory advancements in the last decades have been largely explored formulations that are similar to those given in the optimization problems (2.42) and (2.44). One of the key observations that allowed these advancements is the fact that a constraint like (2.43) or (2.45), called a **linear matrix inequality** or an **LMI**, defines a convex solution set and, thus, casts an optimization problem which is efficiently³ decidable. According to Boyd et al. (1994), developments of interior-point algorithms in the late 1980's and early 1990's, for example in Nesterov and Nemirovskii (1994), allowed the existence nowadays of some off-the-shelf toolboxes for numerically solving an extensive amount of control problems. Again, the reader is invited to visit Appendix B for further details about this topic.

Let us now take the same LTI system \mathcal{G}_c , considering the proper or strictly proper transfer function $T_{wz}(\mathbf{s})$ and a generic non-null input $w(t) \in \mathcal{L}_2^c$. The \mathcal{H}_∞ **norm** of this system is defined as

$$\|\mathcal{G}_c\|_\infty = \sup_{\omega \in \mathbb{R}} \sigma_m(T_{wz}(j\omega)) \quad (2.46)$$

where $\sigma_m(\cdot)$ returns the maximum singular value of a matrix. Notice that, evaluating $\|z\|_2^2$ for a generic input $w(t) \neq 0$ with Laplace transform given by $\mathcal{L}(w(t)) = \hat{w}(s)$, we have

$$\begin{aligned} \|z\|_2^2 &= \int_0^\infty z(t)' z(t) dt \\ &= \frac{1}{2\pi} \int_{-\infty}^\infty \hat{w}(j\omega)' T_{wz}(j\omega) T_{wz}(j\omega) \hat{w}(j\omega) d\omega \\ &\leq \sup_{\omega_s \in \mathbb{R}} \frac{1}{2\pi} \int_{-\infty}^\infty \hat{w}(j\omega)' T_{wz}(j\omega_s)' T_{wz}(j\omega_s) \hat{w}(j\omega) d\omega \\ &\leq \frac{\|\mathcal{G}_c\|_\infty^2}{2\pi} \int_{-\infty}^\infty \hat{w}(j\omega)' \hat{w}(j\omega) d\omega \\ &= \|\mathcal{G}_c\|_\infty^2 \|w\|_2^2 \end{aligned} \quad (2.47)$$

where the second equality holds from Parseval's Theorem (see Oppenheim et al. (1997)) and from (2.15), the first inequality is a consequence of the sup operator, the next one holds from the upper-bound provided in Lemma A.1 together with (2.46) and, finally, the last equality is again a consequence of Parseval's Theorem. This last derivation allows us to conclude that for all $w(t) \in \mathcal{L}_2^c$

$$\|z\|_2^2 \leq \rho \|w\|_2^2 \iff \|\mathcal{G}_c\|_\infty^2 \leq \rho \quad (2.48)$$

for some $\rho \in \mathbb{R}_+$. For this reason, the \mathcal{H}_∞ norm can also be calculated as

$$\|\mathcal{G}_c\|_\infty = \max_{w \in \mathcal{L}_2^c \setminus \{0\}} \frac{\|z\|_2}{\|w\|_2} \quad (2.49)$$

The next theorem can now be expounded.

³By efficiently, it is meant “with polynomial time complexity”.

Theorem 2.6 (LTI \mathcal{H}_∞ performance – continuous-time). Consider a continuous-time LTI system \mathcal{G}_c given by (2.9). The \mathcal{H}_∞ norm of the system can be computed by the following procedures.

1. From the numerical evaluation of its definition (2.46)
2. From $\|\mathcal{G}_c\|_\infty^2 = \rho_*$ where ρ_* is the limit solution of the primal convex optimization problem

$$\rho_* = \inf_{P > 0, \rho > 0} \rho \quad \text{s.t.} \quad (2.50)$$

$$\begin{bmatrix} A'P + PA & \bullet & \bullet \\ H'P & -\rho I & \bullet \\ E & G & -I \end{bmatrix} < 0 \quad (2.51)$$

3. From $\|\mathcal{G}_c\|_\infty^2 = \rho_*$ where ρ_* is the limit solution of the dual convex optimization problem

$$\rho_* = \inf_{S > 0, \rho > 0} \rho \quad \text{s.t.} \quad (2.52)$$

$$\begin{bmatrix} AS + SA' & \bullet & \bullet \\ H' & -I & \bullet \\ ES & G & -\rho I \end{bmatrix} < 0 \quad (2.53)$$

Proof: The first procedure is the very own definition of the \mathcal{H}_∞ norm. Now take into account a quadratic Lyapunov function $v(x(t)) = x(t)'Px(t)$. Evaluating its time derivative, one can write the equation

$$\dot{v}(x(t)) = \begin{bmatrix} x(t) \\ w(t) \end{bmatrix}' \begin{bmatrix} A'P + PA + E'E & \bullet \\ H'P + G'E & G'G - \rho I \end{bmatrix} \begin{bmatrix} x(t) \\ w(t) \end{bmatrix} - z(t)'z(t) + \rho w(t)'w(t) \quad (2.54)$$

which was obtained by summing and subtracting $z(t)'z(t) - \rho w(t)'w(t)$ for some $\rho \in \mathbb{R}_+$. Notice that applying the Schur Complement Lemma (see Appendix A.3) with respect to the last diagonal block of (2.51) shows that this constraint is equivalent to

$$\begin{bmatrix} A'P + PA + E'E & \bullet \\ H'P + G'E & G'G - \rho I \end{bmatrix} < 0 \quad (2.55)$$

which, multiplying by $[x(t)' \ w(t)']$ to the left and by its transpose to the right, provides

$$\dot{v}(x(t)) < -z(t)'z(t) + \rho w(t)'w(t) \quad (2.56)$$

Integrating this last equation from $t = 0$ up to $t \rightarrow \infty$, yields

$$\begin{aligned} \int_0^\infty \dot{v}(x(t)) dt &< - \int_0^\infty z(t)'z(t) dt + \int_0^\infty \rho w(t)'w(t) dt \\ v(x(t)) \Big|_0^\infty &< -\|z\|_2^2 + \rho \|w\|_2^2 \\ 0 &< -\|z\|_2^2 + \rho \|w\|_2^2 \end{aligned} \quad (2.57)$$

since $v(x(0)) = 0$ (from $x(0) = 0$) and $\lim_{t \rightarrow \infty} v(x(t)) = 0$, because \mathcal{G}_c is asymptotically stable and $\|w\|_2$ exists. From the equivalent statements in (2.48), this shows that the infimum with respect to ρ shall coincide with the square \mathcal{H}_∞ norm $\|\mathcal{G}_c\|_\infty^2$. Finally, the primal and dual problems are equivalent taking $S = \rho P^{-1}$ what can be

verified by multiplying (2.51) to both sides by $\text{diag}(S, I, \rho I)$. \square

The above theorem concludes the study on \mathcal{H}_2 and \mathcal{H}_∞ norms for continuous-time LTI systems. Similarly, we start the discussion about the norms for discrete-time LTI systems, given by the state-space realization (2.11) evolving from a null initial condition, i.e. $x[0] = 0$. Consider a discrete-time LTI system \mathcal{G}_d with transfer function $T_{wz}(\mathbf{z})$. The \mathcal{H}_2 norm of \mathcal{G}_d is defined in the frequency domain as the integral over the unit circle of the complex plane given by

$$\|\mathcal{G}_d\|_2 = \left(\frac{1}{2\pi} \int_{-\pi}^{\pi} \text{tr}(T_{wz}(e^{j\omega})^\sim T_{wz}(e^{j\omega})) d\omega \right)^{1/2} \quad (2.58)$$

From the Parseval theorem (see Oppenheim and Schafer (2014)), equality (2.58) squared provides

$$\|\mathcal{G}_d\|_2^2 = \sum_{n=0}^{\infty} \text{tr}(h[n]h[n]') \quad (2.59)$$

with $h[n]$ defining the **impulse response** of \mathcal{G}_d as the inverse Z transform $h[n] = \mathcal{Z}^{-1}(T_{wz}(\mathbf{z}))$. Notice again that the linear nature of the system allows rewriting this expression by considering inputs $w[n] = e_k \delta[n]$, $k \in \{1, \dots, n_w\}$ where $\delta[n]$ is the unitary discrete-time impulse and e_k is the k -th vector of the standard basis of \mathbb{R}^{n_w} . In a similar fashion to the continuous-time case, for each of these impulsive inputs, denote $z_k[n]$ the associated output satisfying

$$\|\mathcal{G}_d\|_2^2 = \sum_{k=0}^{n_w} \sum_{n=0}^{\infty} z_k[n]' z_k[n] \quad (2.60)$$

Analogous developments to (2.38) using $z_k[n] = EA^{n-1}He_k$, $n \geq 1$ and $z_k[n] = Ge_k$, $n = 0$, lead to an alternative manner to evaluate this norm through gramians. Indeed, one has

$$\|\mathcal{G}_d\|_2^2 = \text{tr}(H'P_oH + G'G) = \text{tr}(EP_cE' + GG') \quad (2.61)$$

where P_o and P_c are, respectively the **observability gramian** and the **controllability gramian**, satisfying the Lyapunov equations $A'P_oA - P_o + E'E = 0$ and $AP_cA' - P_c + HH' = 0$. Hence, we can state the next theorem.

Theorem 2.7 (LTI \mathcal{H}_2 performance – discrete-time). *Consider a discrete-time LTI system \mathcal{G}_d given by (2.11). The \mathcal{H}_2 norm of the system can be exactly computed by the following procedures.*

1. *From the observability or controllability gramians, P_o or P_c , we have*

$$\|\mathcal{G}_d\|_2 = \sqrt{\text{tr}(H'P_oH + G'G)} = \sqrt{\text{tr}(EP_cE' + GG')} \quad (2.62)$$

2. *From the summation, we have*

$$\|\mathcal{G}_d\|_2 = \sum_{n=0}^{\infty} \text{tr}(h[n]h[n]') \quad (2.63)$$

3. *From the limit solution of the primal convex optimization problem*

$$\|\mathcal{G}_d\|_2^2 = \inf_{P>0} \text{tr}(H'PH + G'G) \quad \text{s.t.} \quad (2.64)$$

$$A'PA - P + E'E < 0 \quad (2.65)$$

4. From the limit solution of the dual convex optimization problem

$$\|\mathcal{G}_d\|_2^2 = \inf_{S>0} \text{tr}(ESE' + GG') \quad \text{s.t.} \quad (2.66)$$

$$ASA' - S + HH' < 0 \quad (2.67)$$

Proof: This proof is analogous to the one of Theorem 2.5 and is, thus, omitted. \square

Regarding the \mathcal{H}_∞ performance, the \mathcal{H}_∞ **norm** norm is defined for the same system \mathcal{G}_d , evolving from null initial conditions, by the maximum

$$\|\mathcal{G}_d\|_\infty = \max_{\theta \in [-\pi, \pi]} \sigma_m(T_{wz}(e^{j\theta})) \quad (2.68)$$

Through equivalent reasoning to the one presented in the continuous-time case, this norm can be shown to satisfy

$$\|z\|_2^2 \leq \rho \|w\|_2^2 \iff \|\mathcal{G}_d\|_\infty^2 \leq \rho \quad (2.69)$$

for all pair of trajectories $z[n]$ and $w[n] \in \mathcal{L}_2^d \setminus \{0\}$ and some $\rho \in \mathbb{R}_+$. Hence, the \mathcal{H}_∞ may also be given as

$$\|\mathcal{G}_d\|_\infty = \max_{w \in \mathcal{L}_2^d \setminus \{0\}} \frac{\|z\|_2}{\|w\|_2} \quad (2.70)$$

The following theorem presents equivalent manners to evaluate this norm.

Theorem 2.8 (LTI \mathcal{H}_∞ performance – discrete-time). Consider a discrete-time LTI system \mathcal{G}_d given by (2.11). The \mathcal{H}_∞ norm of the system can be computed by the following procedures.

1. From the numerical evaluation of its definition (2.68)

2. From $\|\mathcal{G}_d\|_\infty^2 = \rho_*$ where ρ_* is the limit solution of the primal convex optimization problem

$$\rho_* = \inf_{P>0, \rho>0} \rho \quad \text{s.t.} \quad (2.71)$$

$$\begin{bmatrix} P & \bullet & \bullet & \bullet \\ 0 & \rho I & \bullet & \bullet \\ PA & PH & P & \bullet \\ E & G & 0 & I \end{bmatrix} > 0 \quad (2.72)$$

3. From $\|\mathcal{G}_d\|_\infty^2 = \rho_*$ where ρ_* is the limit solution of the dual convex optimization problem

$$\rho_* = \inf_{S>0, \rho>0} \rho \quad \text{s.t.} \quad (2.73)$$

$$\begin{bmatrix} S & \bullet & \bullet & \bullet \\ 0 & \rho I & \bullet & \bullet \\ SA' & SE' & S & \bullet \\ H' & G' & 0 & I \end{bmatrix} > 0 \quad (2.74)$$

Proof: The proof follows similar steps as in Theorem 2.6 and is, therefore, omitted. \square

2.2.3 Sampled-Data LTI Systems

At this moment, let us point out some facts about **sampled-data LTI systems**. These systems, denoted by \mathcal{G}_{sd} , consist of a continuous-time LTI system and a set of sampling instants $\{t_0, t_1, \dots\}$ satisfying $t_0 = 0$ and $t_{n+1} > t_n$, for all $n \in \mathbb{N}$. The main difference between these systems and generic continuous-time systems is that some of its signals satisfy

$$s(t) = s(t_n), \quad \forall t \in [t_n, t_{n+1}) \quad (2.75)$$

that is, signals whose values are held constant between successive sampling instants. These signals can be inputs, outputs or both of them and are generally related to the fact that their values are being sampled by an analog-to-digital converter (ADC) or held constant by an digital-to-analog converter (DAC). Scenarios of this type arise typically in contexts as networked control systems (see [Hespanha et al. \(2007\)](#)) where analog signals must be sampled to be sent over through a digital network, and general digital control systems, where a microprocessor samples continuous-time signals to compute outputs that are kept constant until an updated sample is available. A particular case of interest considers uniformly distributed sampling instants, which take into account a constant sampling period $T = t_{n+1} - t_n$ for all $n \in \mathbb{N}$. For these cases, considering the input $w(t)$ of the form (2.75), one may define an equivalent discrete-time system \mathcal{G}_d which models exactly the dynamics of the sampled-data system \mathcal{G}_{sd} at $\{t_0, t_1, \dots\}$. Such a procedure is derived by taking the solution (2.10) evaluated between sampling instants. That is,

$$\begin{aligned} x(t_{n+1}) &= e^{A(t_{n+1}-t_n)}x(t_n) + \left(\int_{t_n}^{t_{n+1}} e^{A(t_{n+1}-\psi)} d\psi \right) Hw(t_n) \\ &= e^{AT}x(t_n) + \left(\int_0^T e^{A\tau} d\tau \right) Hw(t_n) \end{aligned} \quad (2.76)$$

where, in the second term of the sum, we have made the change of variables $\tau = t_{n+1} - \psi$. Choosing the discrete-time state $x[n] = x(t_n)$, $w[n] = w(t_n)$ and $z[n] = z(t_n)$, we can describe a discrete-time linear system in the form (2.11), whose response is exactly equal to \mathcal{G}_{sd} at sampling instants. Therefore, the discrete-time system is given by $\mathcal{G}_d = \{A_d, H_d, E, G\}$ with

$$A_d = e^{AT}, \quad H_d = \left(\int_0^T e^{A\tau} d\tau \right) H \quad (2.77)$$

which can be calculated for a nonsingular A as $H_d = A^{-1}(e^{AT} - I)H$. A discrete-time system obtained by such manner is called a **discretized system** and this specific procedure is defined as a **step-invariant discretization** since it preserves exactly the value of the step response (and, therefore, every other system response for piecewise constant inputs as (2.75)) at sampling instants.

Even though this discretization procedure assures that $z[n] = z(t_n)$, it does not assure the equivalence between the \mathcal{L}_2^d and \mathcal{L}_2^c norms of the discrete and continuous-time outputs. Consequently, a discrete-time control project that makes conclusions about the \mathcal{L}_2^d norm of $z[n]$ may not lead to the same results regarding the continuous-time \mathcal{L}_2^c norm. To overcome this issue, reference [Chen and Francis \(2012\)](#) presented a discrete-time

output vector $z_d[n]$ such that $\|z_d\|_2 = \|z\|_2$. This output is defined as

$$z_d[n] = E_d x[n] + G_d w[n] \quad (2.78)$$

such that $[E_d \ G_d]$ is the Cholesky decomposition of the integral

$$\int_0^T e^{\mathcal{A}'\tau} \mathcal{E}' \mathcal{E} e^{\mathcal{A}\tau} d\tau = \begin{bmatrix} E'_d \\ G'_d \end{bmatrix} \begin{bmatrix} E'_d \\ G'_d \end{bmatrix}' \quad (2.79)$$

with

$$\mathcal{A} = \begin{bmatrix} A & H \\ 0 & 0 \end{bmatrix}, \quad \mathcal{E} = \begin{bmatrix} E & G \end{bmatrix} \quad (2.80)$$

delivering the discretized system $\mathcal{G}_d = \{A_d, H_d, E_d, G_d\}$. For the sake of efficiency, matrices A_d and H_d can be also calculated as

$$\begin{bmatrix} A_d & H_d \\ 0 & I \end{bmatrix} = e^{\mathcal{A}T} \quad (2.81)$$

The procedure to obtain this system is called a **norm-equivalent discretization** as it guarantees the equivalence

$$\|z_d\|_2 = \|z\|_2 \quad (2.82)$$

The demonstration of this equivalence can be done by the definition of the \mathcal{L}_2^c -norm of the continuous-time signal $\|z(t)\|_2$ and the reader can refer to [Chen and Francis \(2012\)](#) for further details.

2.3 Switched Systems

Let us now briefly discuss some definitions and characteristics regarding switched systems, the main purpose of this thesis. Roughly, these systems are composed of a finite set of dynamic equations and some logic that chooses one of them to define the time evolution of the system state. A general **switched system** is given for both time domains by the state-space representations

$$\dot{x}(t) = g_{\sigma(t)}(x(t), t), \quad x(0) = x_0, \quad (2.83)$$

$$x[n+1] = g_{\sigma[n]}(x[n], n), \quad x[0] = x_0, \quad (2.84)$$

where, $\sigma : \mathbb{R}_{0+} \rightarrow \mathbb{K} = \{1, \dots, N\}$ is for the continuous-time domain a **switching signal** and $\sigma : \mathbb{N} \rightarrow \mathbb{K}$, for the discrete-time, is a **switching sequence**, indistinctly referred to as switching laws. In both time domains, σ is responsible for choosing one out of N vector fields, composing the finite set $\{g_1, \dots, g_N\}$, at each instant of time, to define the right-hand side of the dynamical equation. Notice that, for the continuous-time case, $g_i, i \in \mathbb{K}$ must be locally Lipschitz function in x and measurable in t , so the system admits a unique solution, see [Liberzon \(2003\)](#). These vector fields define the **subsystems** $\{\mathcal{G}_{s1}, \dots, \mathcal{G}_{sN}\}$ available to be activated by the switching law. As discussed in [Hespanha \(2004\)](#), the main distinction between these formulations and the generic nonlinear systems given in (2.1) and (2.2) is the existence of the switching law σ along with the admissible switching set

\mathbb{S} which, for the continuous-time, defines all possible switching signals $\sigma(t) \in \mathbb{S}$ and, for the discrete-time, all possible switching sequences $\sigma[n] \in \mathbb{S}$. Therefore, while the study of (2.1) and (2.2) is oriented towards the solution evolving from a given initial condition, the switched systems framework considers the set of possible solutions as σ ranges over \mathbb{S} or some proper subset, which can create unexpected nonlinear behaviors. Indeed, (2.83) and (2.84) become (2.1) and (2.2) if \mathbb{S} is restricted to a singleton set⁴.

It is not hard to notice that switched systems form a special class of hybrid systems, where continuous-time or discrete-time dynamics interact with discrete events, in our case, the switching. Naturally, some researchers studying switched systems might decide to employ hybrid system formulations, see Branicky (1998) for some discussion or Sanchez et al. (2019a) as an example.

Often, a switched control system problem emerges when the switching law is constrained to belong to some set $\mathbb{S}_s \subset \mathbb{S}$. This is generally the case when considering **dwell-time** or some other structures for a switching signal. This topic will be recalled at an opportune moment.

According to Liberzon (2003), a classical book about switched systems, the nature of the switching law can be classified as one of the following:

- *state-dependent* versus *time-dependent*
- *autonomous* versus *controlled*

A **state-dependent switching law** is the one whose switching events occur as a function of the state while a **time-dependent switching law** is governed by the time. Notice that every state-dependent switching law can be rewritten as a time-dependent one by suitably evaluating *a priori* (numerically, for example) the corresponding system trajectory. However, the converse does not hold. A state-dependent switching function is linked to the existence of **switching surfaces** \mathcal{C} . These surfaces partition the state-space in several subsets called **operating regions**, each of which has an associated subsystem $i \in \mathbb{K}$. The i -th operating region is defined as $\mathcal{O}_i = \{x \in \mathbb{R}^{n_x} : \sigma(x) = i, i \in \mathbb{K}\}$. Therefore, when the state trajectory hits a switching surface its dynamic behavior is expected to change. It is important to remark that the formulation presented in Liberzon (2003) allows for a structure called the **reset map**, which is not considered in our context.

Moreover, an **autonomous switching law** allows no way to design the mechanism that will orchestrate the switching events. This is analogous to the notion of autonomous systems that admit no input. On the other hand, a **controlled switching law** can be defined by a designer, which is generally done to assure stability or performance. Notice that both cases can be state or time-dependent. For instance, an autonomous switching law can be either predetermined by a state and/or time-dependent switching logic. In the same way, a designer can always assign a state and/or time-dependent switching function to govern σ . The next illustrative example explores the fact that multiple switching laws can coexist in the same system and how this phenomenon is frequently found in our everyday life.

⁴A **singleton set** is a set with cardinality 1, i.e., containing a single element.

Example 2.3 (The Refrigerator). Consider a refrigerator model, adapted from [Angeli and Kountouriotis \(2011\)](#), described as a continuous-time switched system given by

$$\dot{\theta}(t) = -a_{\sigma_1(t)}(\theta(t) - \hat{\theta}_{\sigma_1(t)\sigma_2(t)}), \quad \theta(0) = \theta_0 \quad (2.85)$$

where $\theta(t)$ is the current temperature at a point inside the refrigerator. The value $\hat{\theta}_{11}$ is the equilibrium temperature of this point when the cooling device is kept functioning with the door closed, $\hat{\theta}_{21}$ is the equilibrium temperature for the door open and the cooling functioning and, finally, $\hat{\theta}_{12}$ and $\hat{\theta}_{22}$ are the equilibrium temperatures with the cooling turned off when the door is closed or open, respectively. The value a_{σ_1} is a system parameter based on thermal insulation and thermal mass. Notice the presence of two switching signals $\sigma_1(t) \in \mathbb{K}_1 = \{1, 2\}$ and $\sigma_2(t) \in \mathbb{K}_2 = \{1, 2\}$. The first one corresponds to whether the refrigerator door is closed ($\sigma_1(t) = 1$) or open ($\sigma_1(t) = 2$), which defines two parameters a_1 and a_2 , respectively. The second switching signal determines when the cooling device must be turned on ($\sigma_2(t) = 1$) or off ($\sigma_2(t) = 2$) and is regarded as a control variable.

Notice that $\sigma_1(t)$ is an autonomous switching signal that is time-dependent as it changes exclusively at the instants for which the door is open or closed. However, $\sigma_2(t)$ is a control input that can be suitably orchestrated to stabilize the system temperature around a desired reference θ_e . Consider that the temperature is measured in degrees Celsius [$^{\circ}\text{C}$] and the time, in minutes [min]. Let us suppose $\hat{\theta}_{11} = -40$, $\hat{\theta}_{21} = 8$, $\hat{\theta}_{12} = \hat{\theta}_{22} = 20$, $a_1 = 2.5 \times 10^{-4}$ and $a_2 = 10^{-2}$. Starting from $\theta_0 = 4$, two methodologies of control were chosen to regulate $\theta(t)$ around $\theta_e = 5$. The first one is a hysteresis based switching function

$$\sigma_2(t) = u_h(\theta(t)) = \begin{cases} 1, & \text{if } \theta > 6 \\ 2, & \text{if } \theta < 4 \\ \sigma_2(t_-), & \text{otherwise} \end{cases} \quad (2.86)$$

while the second one is a switching function based on the average system, given as

$$\sigma_2(t) = u_a(t) = \begin{cases} 1, & \text{if } (t \bmod 4) < 1 \\ 2, & \text{otherwise} \end{cases} \quad (2.87)$$

which turns on the cooling for 25% of time.

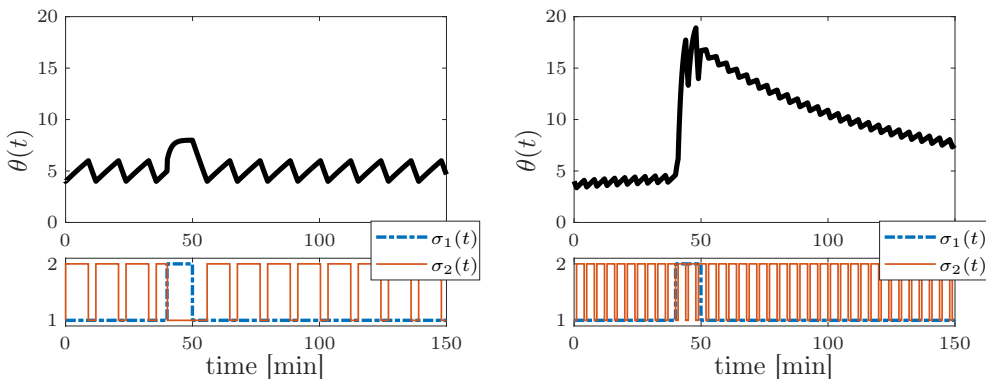


Figure 2.3: Temperature trajectories under switching function $u_h(\theta(t))$ (left) and $u_a(t)$ (right).

System trajectories under both control functions and the corresponding switching signals were

obtained via numerical simulations and are provided in Figure 2.3, assuming that the door was open for 10 minutes after 40 minutes from the initial instant $t = 0$ and remained closed for all the subsequent instants. Intuitively, the state-dependent switching function $u_h(\theta(t))$ may overcome the time-dependent one since $u_h(\theta(t))$ can benefit from important information about the system state to which $u_a(t)$ has no access. Finally, notice that $u_h(\theta(t))$ is rigorously defined as both state and time-dependent since the hysteresis requires knowledge about the system state in previous instants of time.

This example presented a system with two switching signals σ_1 and σ_2 performing different roles. Indeed, one of them is designed to control a system variable, while the other acts as a disturbance, impairing the proper operation of the device. Moreover, notice that different choices for the **switching function** $u(\cdot)$ to govern the switching signal yielded notably distinct behavior. All switched control problems presented in the next chapters share in common the search for an optimal or sub-optimal switching control $u(\cdot)$ to govern σ .

A possible question that may arise at the beginning of Example 2.3 is whether a system with multiple switching laws $\{\sigma_1, \dots, \sigma_M\}$ can be written in the general form (2.83) or (2.84). In fact, this can always be done by defining a new augmented switching law $\tilde{\sigma} = (\sigma_1, \dots, \sigma_M)$ and defining the vector fields $g_{i_1 \dots i_M}$ for every combination of subsystems $(i_1, \dots, i_M) \in \mathbb{K}_1 \times \dots \times \mathbb{K}_M$.

An important theoretical aspect of continuous-time switched systems as (2.83) is the fact that the number of switching events might be infinite within a finite amount of time. The so-called **Zeno Behavior** (see Liberzon (2003); Goebel and Sanfelice (2012)), is an example of this phenomenon, possibly leading to some unexpected system behaviors. Indeed, arbitrarily fast switching among subsystems can force the system trajectory to evolve according to an extra dynamics, different from those of the isolated subsystems. For state-dependent switching this might occur when the switching trajectory $x(t)$, evolving from $x(0)$ reaches the switching surface \mathcal{C} separating two operating regions, for instance, \mathcal{O}_1 and \mathcal{O}_2 . If \mathcal{C} is attained at a point $x(t_h)$ for some $t_h \geq 0$ such that the vector fields $g_1(x(t_h), t_h)$ and $g_2(x(t_h), t_h)$ are oriented towards the operating regions \mathcal{O}_2 and \mathcal{O}_1 , respectively, then the trajectory “slides” on \mathcal{C} . This behavior is illustrated in Figure 2.4 and the segment of the switching surface \mathcal{C} which produces this “sliding” evolution is called a **sliding mode** or a **sliding surface**.

Regarding time-dependent switching laws, sliding modes also occur in a limit case. Consider the periodic switching function

$$\sigma(t) = u_a(t) = \begin{cases} 1, & \text{if } (t \bmod T_a) < \alpha T_a \\ 2, & \text{otherwise} \end{cases} \quad (2.88)$$

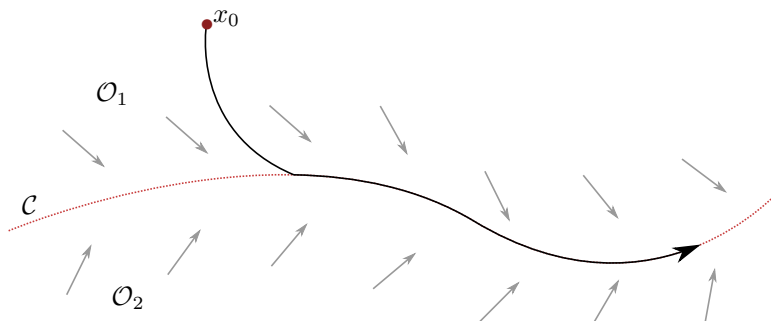


Figure 2.4: State trajectory “sliding” on the switching surface \mathcal{C} .

where the period $T_a \in \mathbb{R}_+$ and the scalar $\alpha \in [0, 1]$ are given. Taking into account that the function $g_{\sigma(t)}(x(t), t)$ is piecewise continuous with respect to t , a solution to the differential equation (2.83) in the sense of Carathéodory, according to Liberzon (2003) for all $t \in \mathbb{R}_{0+}$ is

$$x(t) = x(t - T_a) + \int_{t-T_a}^t g_{\sigma(\tau)}(x(\tau), \tau) d\tau \quad (2.89)$$

Evaluating this equation for arbitrary instants $t \in \{T_a, 2T_a, \dots\}$, yields

$$x(t) = x(t - T_a) + \int_{t-T_a}^{t-(1-\alpha)T_a} g_1(x(\tau), \tau) d\tau + \int_{t-(1-\alpha)T_a}^t g_2(x(\tau), \tau) d\tau \quad (2.90)$$

Dividing both sides by T_a , we can rewrite the first integral

$$\frac{1}{T_a} \int_{t-T_a}^{t-(1-\alpha)T_a} g_1(x(\tau), \tau) d\tau = \frac{\alpha}{\alpha T_a} \int_0^{\alpha T_a} g_1(x(\psi + t - T_a), \psi + t - T_a) d\psi \quad (2.91)$$

where the change of variables $\psi = \tau - t + T_a$ was considered. An analogous procedure can be made for the second integral. Then, at the limit situation where $T_a \rightarrow 0$, we have

$$\lim_{T_a \rightarrow 0} \frac{x(t) - x(t - T_a)}{T_a} = \alpha g_1(x(t), t) + (1 - \alpha) g_2(x(t), t) \quad (2.92)$$

which allows us to conclude that the time evolution of the trajectory is given by a time-average of the dynamics g_1 and g_2 . The system given by this weighted average is called the **averaged system**, where α is the instantaneous weight. This approach is a common approximation in power electronics analysis for systems commanded by **pulse-width modulated (PWM)** signals of the form (2.88), see Cuk and Middlebrook (1977) for instance. In that context, α might also be referred to as a **duty cycle**.

Along a sliding mode, the system trajectory is not a solution for the dynamic equation in the sense of Carathéodory anymore since it no longer verifies (2.83). For this reason, one must seek solutions in the sense of Filippov (see Filippov (1967); Liberzon (2003)) that shall satisfy the **differential inclusion**

$$\dot{x} \in \{g_\lambda(x, t) : \lambda \in \Lambda\} \quad (2.93)$$

where Λ is the unit simplex given by

$$\Lambda = \left\{ \lambda \in \mathbb{R}^N : \lambda_i \geq 0, \sum_{i \in \mathbb{K}} \lambda_i = 1 \right\} \quad (2.94)$$

and $g_\lambda(x, t) = \sum_{i \in \mathbb{K}} \lambda_i g_i(x, t)$. In other words, the set of possible dynamics that a continuous-time switched system can assume does not only contain the subsystem dynamics but also includes all of their possible convex combinations.

So far, we discussed how important is the switching law for defining the system behavior. Certainly, many interesting situations may occur depending on the switching pattern, as it is illustrated in the following example.

Example 2.4 (Two switched systems). Consider two discrete-time switched systems $(\mathcal{G}_s, \mathcal{G}_u)$ given by the

state-space representation

$$x[n+1] = A_{\sigma[n]}x[n], \quad x[0] = x_0 \quad (2.95)$$

where the switching signal is time-dependent and governed by the sequence $\sigma = (1, 2, 1, 2, \dots)$. The first system \mathcal{G}_s is defined by two stable subsystems

$$A_1 = \begin{bmatrix} 0.9 & 0 \\ 0.9 & 0.9 \end{bmatrix}, \quad A_2 = \begin{bmatrix} 0.7 & 0.8 \\ 0.1 & 0.1 \end{bmatrix} \quad (2.96)$$

while the second system \mathcal{G}_u is given by the unstable subsystems

$$A_1 = \begin{bmatrix} 0 & 0.6 \\ 0.2 & 0.9 \end{bmatrix}, \quad A_2 = \begin{bmatrix} 0.8 & 0.3 \\ 0.8 & 0.2 \end{bmatrix} \quad (2.97)$$

Interestingly, for the first system \mathcal{G}_s we have that $x[n] \rightarrow \infty$ as $n \rightarrow \infty$ for all $x_0 \neq 0$ and for the second system \mathcal{G}_u we have that $x[n] \rightarrow 0$ as $n \rightarrow \infty$ for any x_0 . This can be verified by evaluating $\max_{i \in \{1,2\}} |\gamma_i(A_2 A_1)|$ for both cases and observing that the system solution is given by $x[n] = \prod_{k=1}^n A_{\sigma[n-k]} x_0$ for every $x_0 \in \mathbb{R}^{n_x}$, where $\prod_{k=1}^n A_{\sigma[n-k]}$ is known as monodromy matrix [Bittanti and Colaneri \(2009\)](#). Time trajectories evolving from $x_0 = [1 \ -1]'$ are presented for both cases in Figure 2.5.

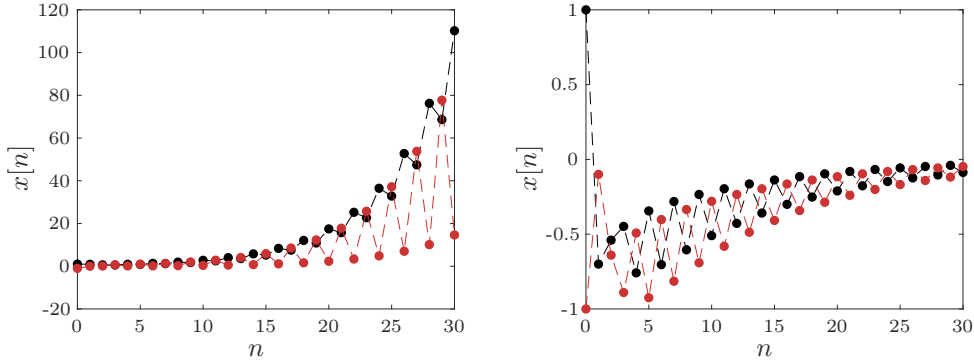


Figure 2.5: State trajectories for system \mathcal{G}_s (left) and \mathcal{G}_u (right).

We just presented how particular switching laws can stabilize trajectories governed by unstable subsystems or destabilize trajectories derived from stable subsystems. This allows us to provide the following definition

Definition 2.8 (Stabilizability of switched systems). *A switched system is said to be **stabilizable** with respect to an equilibrium point $x_e \in \mathbb{R}^{n_x}$ if there exists at least one switching law $\sigma \in \mathbb{S}$ such that x_e is a stable equilibrium point.*

Indeed, all the discussed topics in this section corroborate the fact that the stability study of switched systems is an intricate problem. A brief discussion on stability under arbitrary switching signals is presented in the sequel.

2.3.1 Stability under Arbitrary Switching

It is a well-known fact about switched systems (see [Dayawansa and Martin \(1999\)](#); [Lin and Antsaklis \(2009\)](#)) that a necessary and sufficient condition for global asymptotic stability of an equilibrium point under an arbitrary

switching law is the existence of a **common Lyapunov function** for all subsystems $i \in \mathbb{K}$. That is, there exists a radially unbounded Lyapunov function $v(x)$ that decreases along every trajectory of each subsystem $\{\mathcal{G}_{s1}, \dots, \mathcal{G}_{sN}\}$. Many efforts emerge from researchers to treat this problem in both time domains where several classes of switching laws and various Lyapunov function structures are considered, see Branicky (1998); Geromel and Colaneri (2006a,b); Shorten et al. (2007); Zhao et al. (2016); Philippe et al. (2018) as some instances. Nevertheless, further discussions on this topic are beyond the scope of this thesis, where the design of state and output-dependent switching functions is the main goal. The last two sections of this chapter summarize stability and performance conditions for two subclasses of switched systems.

2.4 Switched Linear Systems

Conditions for designing a state-dependent switching function for switched linear systems are presented in this section. Firstly, results for the continuous-time domain will be presented and then some discrete-time results will follow. Both rely upon stability conditions based on Lyapunov-Metzler inequalities, which will be generalized in Chapter 3 to cope with practical stability of switched affine systems. Important aspects of these inequalities will be highlighted.

2.4.1 Stability and Performance - Continuous-Time Domain

A **continuous-time switched linear system** is defined by the state-space representation

$$\begin{cases} \dot{x}(t) = A_{\sigma(t)}x(t) + H_{\sigma(t)}w(t), & x(0) = 0 \\ z(t) = E_{\sigma(t)}x(t) + G_{\sigma(t)}w(t) \end{cases} \quad (2.98)$$

for which $x : \mathbb{R}_{0+} \rightarrow \mathbb{R}^{n_x}$ denotes the state vector, $w : \mathbb{R}_{0+} \rightarrow \mathbb{R}^{n_w}$ represents an external input signal and $z : \mathbb{R}_{0+} \rightarrow \mathbb{R}^{n_z}$ is a controlled (or performance) output. The switching signal $\sigma : \mathbb{R}_{0+} \rightarrow \mathbb{K}$ is again responsible for choosing, at each instant of time, one subsystem $\mathcal{G}_{si} = (A_i, H_i, E_i, G_i)$, $i \in \mathbb{K}$, out of N available ones to be activated. As for LTI systems, the origin is generally the only equilibrium point common to all subsystems. Assuming $w(t) = 0$, the stability problem consists of determining a switching function

$$\sigma(t) = u(x(t)) \quad (2.99)$$

to orchestrate the switching and, along with a Lyapunov function $v(x)$, assure the global asymptotic stability of the origin. A basic approach to this problem assumes a simple quadratic Lyapunov function of the form (2.20) and the switching function

$$u(x(t)) = \arg \min_{i \in \mathbb{K}} x(t)' A_i P x(t) \quad (2.100)$$

where P is the solution of the Lyapunov inequality $A_\lambda' P + P A_\lambda < 0$ for some $\lambda \in \Lambda$, which shows that the existence of a $\lambda \in \Lambda$ such that A_λ is Hurwitz stable is a sufficient condition for stabilizability of the system. Hence, global asymptotic stability can be obtained even when all subsystems are unstable. Nonetheless, finding $\lambda \in \Lambda$ such that A_λ is Hurwitz is known to be an NP-hard problem, see Blondel and Tsitsiklis (1997). More

sophisticate Lyapunov functions can be adopted to provide less conservative stability conditions. One of them was proposed by Geromel and Colaneri (2006a) which takes into account the **min-type Lyapunov function**

$$v(x(t)) = \min_{i \in \mathbb{K}} x(t)' P_i x(t) \quad (2.101)$$

along with the existence of a matrix $\Pi \in \mathcal{M}_c$, where the set \mathcal{M}_c is a subset of the Metzler matrix set, defined by

$$\mathcal{M}_c = \left\{ \Pi = \{\pi_{ki}\} \in \mathbb{R}^{N \times N} : \sum_{k=1}^N \pi_{ki} = 0, \pi_{ki} \geq 0 \forall k \neq i \right\} \quad (2.102)$$

Before presenting the corresponding theorem, let us define the matrix $P_{\pi i} = \sum_{k \in \mathbb{K}} \pi_{ki} P_k$.

Theorem 2.9. Consider system (2.98) with $w(t) = 0$, $\forall t \geq 0$ and $x(0) = x_0$. Let $Q_i \geq 0$ be given for all $i \in \mathbb{K}$. Assume that there exist a set of positive definite matrices $\{P_1, \dots, P_N\}$ and $\Pi \in \mathcal{M}_c$ satisfying the **Lyapunov-Metzler inequalities**

$$A_i' P_i + P_i A_i + P_{\pi i} + Q_i < 0, \quad \forall i \in \mathbb{K} \quad (2.103)$$

The state-dependent switching control (2.99) with

$$u(x(t)) = \arg \min_{i \in \mathbb{K}} x(t)' P_i x(t) \quad (2.104)$$

makes the equilibrium point $x = 0$ of (2.98) globally asymptotically stable and

$$\int_0^\infty x(t)' Q_{\sigma(t)} x(t) dt < \min_{i \in \mathbb{K}} x_0' P_i x_0 \quad (2.105)$$

Proof: See Geromel and Colaneri (2006a). □

The design conditions just presented contains those based on the quadratic Lyapunov function (2.20), see Geromel and Colaneri (2006a). Moreover, notice that a necessary condition for the feasibility of (2.103) is that the inequalities

$$\left(A_i + \frac{\pi_{ii}}{2} I \right)' P_i + P_i \left(A_i + \frac{\pi_{ii}}{2} I \right) < 0, \quad i \in \mathbb{K} \quad (2.106)$$

be verified, which has been obtained by making $P_{\pi i} = \sum_{k \neq i=1}^N \pi_{ki} P_k + \pi_{ii} P_i$ in (2.103). Since $\pi_{ii} = -\sum_{k \neq i \in \mathbb{K}} \pi_{ki} < 0$, it is not required any property of the matrices A_i , $i \in \mathbb{K}$ isolatedly considered. Then, as before, the switching function is able to assure global asymptotic stability even if all subsystems \mathcal{G}_{si} , $i \in \mathbb{K}$ are unstable. However, notice that the products between matrices P_i and the Metzler matrix Π make (2.103) a set of nonconvex constraints. Fortunately, for a given matrix $\Pi \in \mathcal{M}_c$ these conditions become LMIs, opening doors for strategies to determine a solution $\{\Pi, P_1, \dots, P_N\}$ based on a set of convex optimization problems. More comments about this can be found in Geromel and Colaneri (2006a) but will also be addressed in the next chapter.

Regarding performance indices, notice that \mathcal{H}_2 and \mathcal{H}_∞ norms are only defined for LTI systems. Nevertheless, the literature presents generalizations of these indices regarding the presence of switching in the system dynamic. For the continuous-time domain, let us adopt indices as defined in Deaecto et al. (2012), which are:

- **\mathcal{H}_2 performance index:** Similarly to the time domain definition (2.37) for LTI systems, this index is

defined for an asymptotically stable continuous-time switched system (2.98) with $G_i = 0, \forall i \in \mathbb{K}$ as

$$\mathcal{J}_2 = \sum_{k=1}^{n_w} \|z_k\|_2^2 \quad (2.107)$$

where $z_k(t)$ represents the output when the system is disturbed by an impulsive response $w(t) = e_k \delta(t)$ with $k \in \{1, \dots, n_w\}$, where the set $\{e_1, \dots, e_{n_w}\}$ forms the standard basis of \mathbb{R}^{n_w} .

- **\mathcal{H}_∞ performance index:** Considering a generic input $w(t) \in \mathcal{L}_2^c \setminus \{0\}$, this index is defined for an asymptotically stable continuous-time switched system (2.98) by the equation

$$\mathcal{J}_\infty = \max_{w \in \mathcal{L}_2^c \setminus \{0\}} \frac{\|z\|_2^2}{\|w\|_2^2} \quad (2.108)$$

Notice that these indices equal the \mathcal{H}_2 and \mathcal{H}_∞ squared norm of the i -th subsystem whenever the switching signal is chosen $\sigma(t) = i$ for all $t \in \mathbb{R}_{0+}$. However, as discussed in Geromel et al. (2013), whenever a switching function $u(x(t))$ is consistently designed, these indices are less than or equal to the least squared norm of the isolated subsystems.

It is a particularly difficult problem to design $u(x(t))$ such that the optimality of these indices is assured. For this reason, available design conditions usually tackle the minimization of some upper bound for \mathcal{J}_2 or \mathcal{J}_∞ , which is called a **guaranteed cost**. The next theorems provide results in this fashion.

Theorem 2.10. *For the system (2.98) with $G_i = 0$, for all $i \in \mathbb{K}$, the switching function (2.104) is globally asymptotically stabilizing and assures the guaranteed cost*

$$\mathcal{J}_2 < \min_{i \in \mathbb{K}} \text{tr}(H'_{\sigma(0)} P_i H_{\sigma(0)}) \quad (2.109)$$

whenever $P_i, \forall i \in \mathbb{K}$ satisfy the Lyapunov-Metzler inequalities (2.103) replacing $E'_i E_i \rightarrow Q_i$.

Proof: It is presented in Geromel et al. (2008) and, thus, omitted. \square

Theorem 2.11. *For the system (2.98), the switching function (2.104) is globally asymptotically stabilizing and assures the guaranteed cost*

$$\mathcal{J}_\infty < \rho \quad (2.110)$$

whenever $P_i, \forall i \in \mathbb{K}$ and $\rho \in \mathbb{R}_+$ satisfy the Riccati-Metzler inequalities

$$\begin{bmatrix} A'_i P_i + P_i A_i + P_{\pi i} & \bullet & \bullet \\ H'_i P_i & -\rho I & \bullet \\ E_i & G_i & -I \end{bmatrix} < 0, \quad \forall i \in \mathbb{K} \quad (2.111)$$

Proof: It is presented in Deaecto and Geromel (2010) and, thus, omitted. \square

In the next subsection, similar results will be obtained for discrete-time systems.

2.4.2 Stability and Performance - Discrete-Time Domain

Let us now consider a **discrete-time switched linear system**, given by the state-space representation

$$\begin{cases} x[n+1] = A_{\sigma[n]}x[n] + H_{\sigma[n]}w[n], & x[0] = 0 \\ z[n] = E_{\sigma[n]}x[n] + G_{\sigma[n]}w[n] \end{cases} \quad (2.112)$$

Design conditions for a switching function are available in the literature considering several types of Lyapunov functions, ranging from a simple quadratic to a time-varying one. The one presented by Geromel and Colaneri (2006b) is again based on a min-type Lyapunov function

$$v(x[n]) = \min_{i \in \mathbb{K}} x[n]' P_i x[n] \quad (2.113)$$

However, the class of Metzler matrices considered in this case is different, being defined as

$$\mathcal{M}_d = \left\{ \Pi = \{\pi_{ki}\} \in \mathbb{R}^{N \times N} : \sum_{k=1}^N \pi_{ki} = 1, \pi_{ki} \geq 0 \right\} \quad (2.114)$$

The following theorem presents design conditions for a global asymptotic stabilizing switching function.

Theorem 2.12. Consider system (2.112) with $w[n] = 0, \forall n \in \mathbb{N}$ and $x[0] = x_0$. Let $Q_i \geq 0$ be given. Assume that there exist a set of positive definite matrices $\{P_1, \dots, P_N\}$ and $\Pi \in \mathcal{M}_d$ satisfying the **Lyapunov-Metzler inequalities**

$$A_i' P_{\pi i} A_i - P_i + Q_i < 0, \quad \forall i \in \mathbb{K} \quad (2.115)$$

The state-dependent switching control (2.99) with

$$u(x[n]) = \arg \min_{i \in \mathbb{K}} x[n]' P_i x[n] \quad (2.116)$$

makes the equilibrium point $x = 0$ of (2.112) globally asymptotically stable and assures

$$\sum_{n=0}^{\infty} x[n]' Q_{\sigma[n]} x[n] < \min_{i \in \mathbb{K}} x_0' P_i x_0 \quad (2.117)$$

Proof: See Geromel and Colaneri (2006b). \square

As in the continuous-time case, the switching function is able to assure global asymptotic stability even if all subsystems $\mathcal{G}_{si}, i \in \mathbb{K}$ are unstable. In fact, a necessary condition for the feasibility of (2.115) is that the inequalities

$$(\sqrt{\pi_{ii}} A_i)' P_i (\sqrt{\pi_{ii}} A_i) - P_i < 0, \quad i \in \mathbb{K} \quad (2.118)$$

are verified, which has been obtained by making $P_{\pi i} = \sum_{k \neq i=1}^N \pi_{ki} P_k + \pi_{ii} P_i$ in (2.115). Since the inequalities $0 \leq \sqrt{\pi_{ii}} \leq 1$ hold, then it is not required any stability property of matrices $A_i, \forall i \in \mathbb{K}$ considered separately. As in the continuous-time case, the conditions (2.115) are nonconvex and difficult to solve. However, whenever matrix $\Pi \in \mathcal{M}_d$ is known, the conditions are expressed in terms of LMIs. See Geromel and Colaneri (2006b) for a discussion about alternative conditions that are easier to solve. Now, let us define the analogous performance indices for a discrete-time switched system as follows:

- **\mathcal{H}_2 performance index:** Consider system (2.112), but evolving from $x[-1] = 0$. Similarly to definition (2.59), this index is defined for an asymptotically stable discrete-time switched system (2.112) as

$$\mathcal{J}_2 = \sum_{k=1}^{n_w} \|z_k\|_2^2 + e'_k G'_{\sigma[-1]} G_{\sigma[-1]} e_k \quad (2.119)$$

where $z_k[n]$ represents the output when the system is disturbed by an impulsive response $w[n] = e_k \delta[n+1]$ with $k \in \{1, \dots, n_w\}$, where the set $\{e_1, \dots, e_{n_w}\}$ forms the standard basis.

- **\mathcal{H}_∞ performance index:** Considering a generic non-null input $w[n] \in \mathcal{L}_2^d$, this index is defined for an asymptotically stable discrete-time switched system (2.112) with $x[0] = 0$ by the equation

$$\mathcal{J}_\infty = \max_{w \in \mathcal{L}_2^d \setminus \{0\}} \frac{\|z\|_2^2}{\|w\|_2^2} \quad (2.120)$$

Notice that, differently from the \mathcal{H}_2 norm for LTI systems, the \mathcal{J}_2 performance index for discrete-time switched systems is calculated from the instant $n = -1$. This time shift does not change the fact that the index \mathcal{J}_2 equals the squared \mathcal{H}_2 norm of the i -th subsystem when $\sigma(t) = i$, $\forall t \in \mathbb{R}_{0+}$ and eases the forthcoming developments. See reference Geromel et al. (2008) for more details about this point. The next theorems present design conditions for a globally stabilizing switching function assuring guaranteed costs for both \mathcal{J}_2 and \mathcal{J}_∞ .

Theorem 2.13. *For the system (2.112) with $x[-1] = 0$, the switching function (2.116) is globally asymptotically stabilizing and assures the guaranteed cost*

$$\mathcal{J}_2 < \min_{i \in \mathbb{K}} \text{tr}(H'_{\sigma[-1]} P_i H_{\sigma[-1]} + G'_{\sigma[-1]} G_{\sigma[-1]}) \quad (2.121)$$

whenever P_i , $i \in \mathbb{K}$ satisfy the Lyapunov-Metzler inequalities (2.115) replacing $E'_i E_i \rightarrow Q_i$.

Proof: It is presented in Geromel et al. (2008) and, thus, omitted. \square

Theorem 2.14. *For the system (2.112) with $x[0] = 0$, the switching function (2.116) is globally asymptotically stabilizing and assures the guaranteed cost*

$$\mathcal{J}_\infty < \rho \quad (2.122)$$

whenever P_i , $i \in \mathbb{K}$ and ρ satisfy the Riccati-Metzler inequalities

$$\begin{bmatrix} P_i & \bullet & \bullet & \bullet \\ 0 & \rho I & \bullet & \bullet \\ P_{\pi i} A_i & P_{\pi i} H_i & P_{\pi i} & \bullet \\ E_i & G_i & 0 & I \end{bmatrix} > 0, \quad \forall i \in \mathbb{K} \quad (2.123)$$

Proof: It is presented in Deaecto et al. (2011a) and, thus, omitted. \square

Necessary and sufficient conditions for stabilizability of this class of systems are presented in Fiacchini and Jungers (2014) under a set-theory approach. Nevertheless, they are often computationally unaffordable, as they require to check whether some particular set is contained in the union of others and are very difficult to generalize to cope with problems of great interest in control theory, for example, state and output feedback control design. Alternatively, sufficient design conditions based on time-varying Lyapunov functions are available

in Deaecto and Geromel (2018) and Daiha et al. (2017), which are more adapted to generalizations. These conditions are described in terms of LMIs and, in some cases, overcome those based on Lyapunov-Metzler inequalities in terms of conservativeness. In fact, these LMIs are a special case of time-varying Lyapunov-Metzler inequalities, available in Daiha et al. (2017), with Metzler matrices given by $\Pi[n] = [\lambda[n] \cdots \lambda[n]] \in \mathcal{M}_d$, $\lambda \in \Lambda$, and can benefit of their time-varying nature to enhance performance when compared to previously presented Lyapunov-Metzler inequalities. See reference Daiha et al. (2017) for a more detailed discussion about this topic. Chapter 3 presents a generalization of these LMI conditions to cope with limit cycle control design in switched affine systems. The next section presents some results already available in the literature related to switched affine systems, since they are our main concern in this work.

2.5 Switched Affine Systems

This section is devoted to discussing results available in Bolzern and Spinelli (2004) and Deaecto et al. (2010) about the global asymptotic stability of continuous-time switched systems whose models are affine switched functions on the state vector. More specifically, these references present design conditions for a state-dependent switching function capable of assuring global asymptotic stability of an equilibrium point chosen by the designer, inside a set of attainable ones. As it will be clear afterward, these guarantees come with the existence of sliding modes, requiring an arbitrarily high switching frequency. This is not the most desirable scenario in engineering contexts since power loss equations are often increasing functions of the switching frequency, see Mohan et al. (2003); Rashid (2014). That being so, our goal in this section is to emphasize the principal aspects of this class of systems and investigate the effects of imposing bounds to the switching frequency, especially in the sampled-data context. The next two chapters of this thesis will deeply rely upon the results to be presented in the sequence.

Consider a continuous-time **switched affine system** given by the state-space representation

$$\begin{cases} \dot{x}(t) &= A_{\sigma(t)}x(t) + b_{\sigma(t)}, \quad x(0) = x_0 \\ z(t) &= E_{\sigma(t)}x(t) \end{cases} \quad (2.124)$$

where $x : \mathbb{R}_{0+} \rightarrow \mathbb{R}^{n_x}$ is the state, $z : \mathbb{R}_{0+} \rightarrow \mathbb{R}^{n_z}$ is the output and $\sigma : \mathbb{R}_{0+} \rightarrow \mathbb{K}$ is the switching signal, selecting one of the subsystems $\mathcal{G}_{si} = (A_i, b_i, E_i)$, $i \in \mathbb{K}$ at each instant of time. This dynamic model is more comprehensive than the one of switched linear systems, given in (2.98), considering $w(t) = 0$, $\forall t \in \mathbb{R}_{0+}$. The affine vector field allows us to model several switching power converters for DC-DC conversion, such as buck, boost, buck-boost (see Deaecto et al. (2010)), Ćuk (see Goudarzian and Khosravi (2019)), flyback (see Kolotelo et al. (2018); Beneux et al. (2019)) and multilevel (see Patino et al. (2009)), among others. Recently, some works also paid attention to DC-AC conversion, modeling one-phase (see Sanchez et al. (2019b)) and three-phase (see Egidio et al. (2019)) voltage source inverters as well as AC-DC conversion (see Hadjeras et al. (2019); Egidio et al. (nd)). For this reason, the study on switched affine systems is particularly interesting inside the power electronics domain.

In contrast to a switched linear system, the introduction of affine terms b_i , $i \in \mathbb{K}$ implies in the existence

of a region of attainable equilibrium points, composing the subset of the state-space

$$X_e^c = \{x_e \in \mathbb{R}^{n_x} : x_e = -A_\lambda^{-1}b_\lambda, \lambda \in \Lambda\} \quad (2.125)$$

Indeed, as discussed in [Albea et al. \(2015\)](#), notice that if we expect to obtain Filippov solutions satisfying the differential inclusion (2.93), then an equilibrium point x_e must possess an associated $\lambda \in \Lambda$ such that $\dot{x}(t) = 0$ satisfies this differential inclusion for all $t \in \mathbb{R}_{0+}$. Summarizing, we can state that

$$x_e \in X_e^c \iff \exists \lambda \in \Lambda : \dot{x} = A_\lambda x_e + b_\lambda = 0 \quad (2.126)$$

Hence, this is a necessary and sufficient condition to characterize an equilibrium point for this class of systems, regardless its stability.

The first problem to be investigated in this section is whether or not there exists a state-dependent switching function for which a given $x_e \in X_e^c$ is globally asymptotically stable. Notice that this is a more challenging problem when compared with continuous-time switched linear system because, even if all subsystems \mathcal{G}_{si} , $i \in \mathbb{K}$ are stable, the desired equilibrium point $x_e \in X_e^c$ might not be an equilibrium for any \mathcal{G}_{si} , $i \in \mathbb{K}$ or there might not be a switching function that makes it asymptotically stable.

Results regarding stability analysis for these systems from a switched system point of view are available in [Bolzern and Spinelli \(2004\)](#); [Buisson et al. \(2005\)](#); [Corona et al. \(2007\)](#); [Deaecto et al. \(2010\)](#); [Hetel and Bernuau \(2014\)](#); [Scharlau et al. \(2014\)](#); [Deaecto and Santos \(2015\)](#); [Sanchez et al. \(2019a\)](#); [Beneux et al. \(2019\)](#) where the adoption of quadratic Lyapunov functions is done in most of them. The exceptions are [Scharlau et al. \(2014\)](#), which considers max-type Lyapunov functions, [Corona et al. \(2007\)](#), which tackles the problem from a dynamic programming perspective and [Patino et al. \(2009\)](#) which adopts a neural network to control the system reproducing optimal trajectories. Approaches considering a max-type Lyapunov function lead to non-convex design conditions and, for the particular cases where constraints are introduced to obtain LMI-based conditions (as done in [Trofino et al. \(2012\)](#)), more conservative results may be found. The dynamic programming method benefits from dealing straightly with optimality but it might suffer from the curse of dimensionality as the system order and the number of subsystems increases (see [Bellman \(1961\)](#)).

For a desired equilibrium point $x_e \in X_e^c$, by declaring the auxiliary state variable $\xi(t) = x(t) - x_e$ we can redefine system (2.124) as

$$\begin{cases} \dot{\xi}(t) &= A_{\sigma(t)}\xi(t) + \ell_{\sigma(t)}, \quad \xi(0) = \xi_0 = x_0 - x_e \\ z_e(t) &= E_{\sigma(t)}\xi(t) \end{cases} \quad (2.127)$$

with $\ell_i = A_i x_e + b_i$ and $z_e = z - C_\sigma x_e$. The study of the origin $\xi(t) = 0$ for this alternative system is hereby equivalent to the one of x_e for the original system (2.124). Therefore, we seek a control law $u(\xi(t))$ such that the switching function $\sigma(t) = u(\xi(t))$ assures the global asymptotic stability of the origin $\xi = 0$. The next theorem, from [Deaecto et al. \(2010\)](#), presents such design method by adopting a quadratic Lyapunov function

$$v(\xi(t)) = \xi(t)'P\xi(t) \quad (2.128)$$

with a symmetric positive definite $P \in \mathbb{R}^{n_x \times n_x}$ and defining a guaranteed cost for the \mathcal{L}_2^c -norm of $z_e(t)$

Theorem 2.15. Consider the continuous-time switched affine system (2.127), and let $x_e \in X_e^c$ with its associated $\lambda \in \Lambda$ be given. If there exists a symmetric positive definite matrix P satisfying the LMI

$$A_\lambda' P + P A_\lambda + \sum_{i \in \mathbb{K}} \lambda_i E_i' E_i < 0 \quad (2.129)$$

then the min-type switching function

$$\sigma(t) = u(\xi(t)) = \arg \min_{i \in \mathbb{N}_N} \xi(t)'(Q_i \xi(t) + 2P\ell_i) \quad (2.130)$$

where $Q_i = A_i' P + P A_i + R_i$, assures global asymptotic stability of the equilibrium point $x_e \in X_e^c$ along with the guaranteed cost

$$\|z_e\|_2^2 \leq \xi_0' P \xi_0. \quad (2.131)$$

Proof: The proof is given in [Deaecto et al. \(2010\)](#). \square

At this point, few remarks are in order. Notice that an equivalent condition to (2.129) is that A_λ be a Hurwitz stable matrix. Nothing is imposed directly on matrices A_i , $i \in \mathbb{K}$ so this theorem takes into account the fact that unstable subsystems may generate stable system trajectories. Another concern is the choice of $\lambda \in \Lambda$. From the previous discussions, it follows that a $\lambda \in \Lambda$ is related to a unique $x_e \in X_e^c$ but the converse does not hold. Deciding if a desired $x_e \in \mathbb{R}^{n_x}$ belongs to X_e^c or not can be efficiently done by solving the convex optimization problem

$$(\lambda_*, \mu_*) = \arg \min_{\lambda \in \Lambda, \mu \in \mathbb{R}_+} \mu \quad \text{s.t.} \quad (2.132)$$

$$\begin{bmatrix} \mu & \bullet \\ A_\lambda x_e + b_\lambda & I \end{bmatrix} > 0 \quad (2.133)$$

and verifying if $\mu_* \rightarrow 0$. If so, via Schur Complement Lemma, the LMI (2.133) assures that $\|A_{\lambda_*} x_e + b_{\lambda_*}\|^2 < \mu \approx 0$, showing that $x_e \in X_e^c$. In spite of that, for a given switched affine system, the problem of deciding whether there exists any globally asymptotically stabilizable $x_e \in X_e^c$ is NP-Hard. This is a consequence of the fact that the mentioned problem is equivalent to verify if there exists a $\lambda \in \Lambda$ such that A_λ is Hurwitz stable. For more information about the NP-hardness of these problems, see [Nemirovskii \(1993\)](#); [Blondel and Tsitsiklis \(1997\)](#); [Henrion et al. \(2001\)](#).

The following example, adapted from [Egidio \(2016\)](#), puts in evidence the control problem for this class of systems.

Example 2.5. Consider a system (2.124) defined by matrices

$$A_1 = \begin{bmatrix} 0 & 1 \\ -5 & 1 \end{bmatrix}, \quad A_2 = \begin{bmatrix} 0 & 1 \\ 2 & -5 \end{bmatrix}, \quad b_1 = \begin{bmatrix} 1 \\ 0 \end{bmatrix}, \quad b_2 = \begin{bmatrix} 0 \\ 1 \end{bmatrix}, \quad (2.134)$$

and $E_1 = E_2 = I$. Note that $\max_{i \in \{1,2\}} \operatorname{Re} \gamma_i(A_1) = 0.5 > 0$ and $\max_{i \in \{1,2\}} \operatorname{Re} \gamma_i(A_2) = 0.3723 > 0$, characterizing the instability of both subsystems. Our goal is to find a state-dependent switching function

$\sigma(t) = u(x(t))$ assuring the global asymptotic stability of a chosen equilibrium point $x_e = [1.2051 \ -0.4700]'$. This point belongs to the set X_e^c , which can be verified from the solution of the optimization problem (2.132)-(2.133). The corresponding convex combination is given by $\lambda = [0.47 \ 0.53] \in \Lambda$. Indeed, the locus of $x_e \in X_e$ is represented as a curve in Figure 2.6 along with the desired x_e (black circle), x_{e1} (red triangle) and x_{e2} (red circle) where x_{e1} and x_{e2} are, respectively, the equilibrium points of subsystems 1 and 2. In blue, a segment of this curve is highlighted and represents the $x_e \in X_e^c$ such that the corresponding $\lambda \in \Lambda$ makes A_λ Hurwitz stable and thus, are stable equilibrium points.

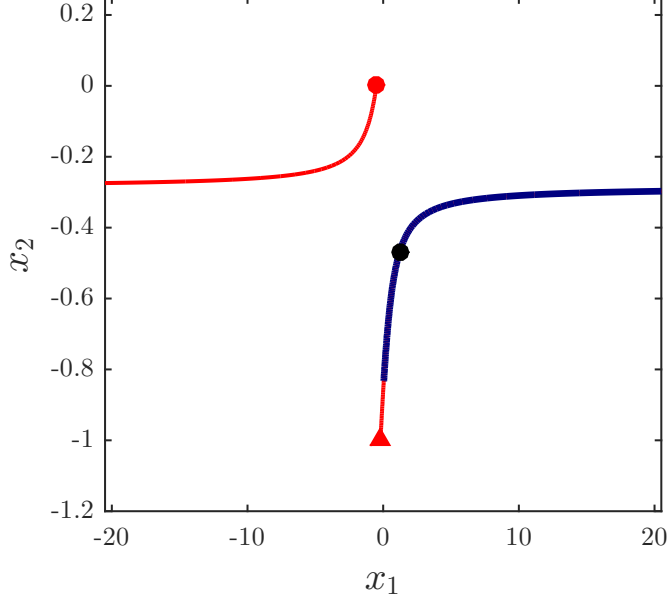


Figure 2.6: Set X_e^c with equilibrium points x_e (black circle), x_{e1} (red triangle) and x_{e2} (red circle).

Taking into account the λ associated with the chosen x_e and solving the optimization problem

$$\min_{P > 0, \mu > 0} \mu \quad \text{s.t.} \quad P < \mu I, \quad (2.129)$$

we can find a matrix

$$P = \begin{bmatrix} 1.3702 & 0.3876 \\ 0.3876 & 0.4072 \end{bmatrix} \quad (2.136)$$

satisfying the conditions of Theorem 2.15. This objective function was chosen to obtain P without taking into account any specific initial condition. Notice that eigenvalues of P are bounded above by μ , which provides the robust upper-bound for the guaranteed cost

$$\|z_e\|_2^2 < \xi_0' P \xi_0 < \mu \|\xi_0\|^2 \quad (2.137)$$

With the obtained P , we can design the state-dependent switching function (2.130). The resulting switching surface \mathcal{C} can be defined as

$$\mathcal{C} = \{\xi \in \mathbb{R}^{n_x} : (\xi - \xi_c)' \Delta Q (\xi - \xi_c) = r\} \quad (2.138)$$

with, $\Delta Q = Q_1 - Q_2$, $r = \Delta \ell' P (\Delta Q)^{-1} P \Delta \ell$, $\Delta \ell = \ell_1 - \ell_2$ and $\xi_c = -(\Delta Q)^{-1} P \Delta \ell$. This expression comes from the equality $\xi' (Q_1 \xi + 2P\ell_1) = \xi' (Q_2 \xi + 2P\ell_2)$, which defines the set of $x \in \mathbb{R}^{n_x}$ such that

the min operator in (2.130) accepts two arguments. The eigenvalues of ΔQ are $\gamma_1(\Delta Q) = -5.4530$ and $\gamma_2(\Delta Q) = 4.9125$, implying that \mathcal{C} is a hyperbole. The phase portrait of this system is represented in Figure 2.7. The gray dashed line represents the switching surface \mathcal{C} and the blue, green and black curves describe system trajectories evolving with respect to subsystem 1, subsystem 2 and sliding modes, respectively.

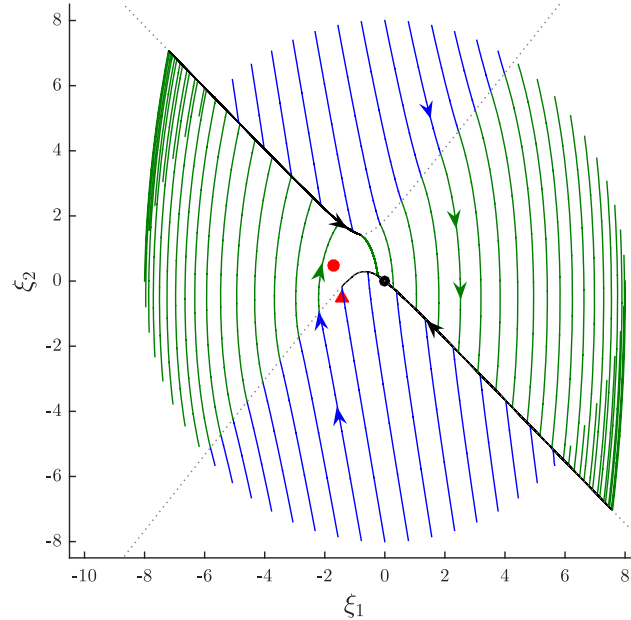


Figure 2.7: Phase portrait of the switched affine system.

Finally, we present in Figure 2.8 the time evolution of a particular system trajectory evolving from $\xi_0 = [-2.3223 \ -7.6555]'$ along with the correspondent switching signal. The zoomed plot highlights the high switching frequency required in order to maintain the simulated system trajectory at the desired equilibrium point. Additionally, the \mathcal{L}_2^c -norm of $\zeta(t)$ was calculated, providing $\|z_e\|_2^2 = 24.4743 < \xi_0' P \xi_0 = 45.0331$, as expected.

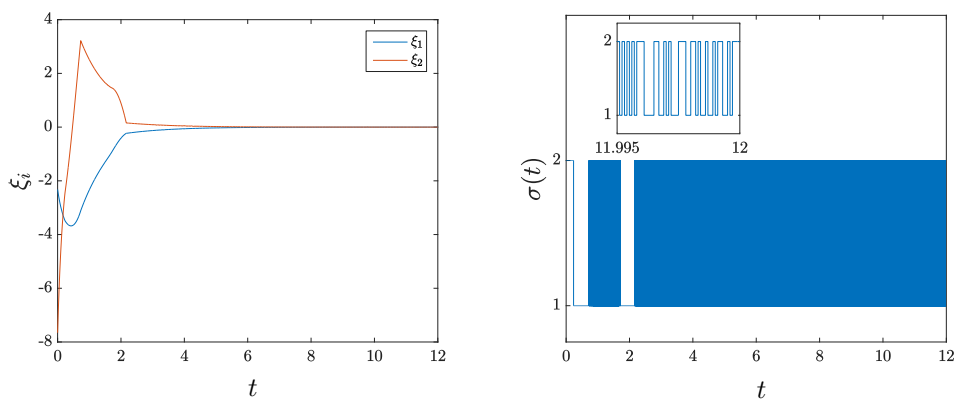


Figure 2.8: Time evolution for a system trajectory along with corresponding switching signal.

As previously discussed, in the switched affine systems context, the price to pay for asymptotic stability of a point, which is not an equilibrium for any subsystem is the arbitrarily high switching frequency characterizing sliding modes, as it was made clear in the previous example. Anyhow, in practical applications the switching frequency must be limited by some intrinsic system property such as sampling periods, response times, slew rates or other issues that prevent sliding surfaces to occur as the theory predicts. The result is a finite frequency oscillation around the theoretical system trajectory jeopardizing the control design, causing component wear or even damages. This unforeseen high frequency oscillation is known as the **chattering phenomenon**, see Khalil (2002); Utkin and Lee (2006) and many are the efforts emerging from the scientific community to suppress it.

To tackle the chattering avoidance problem one must bound the switching frequency by some suitable finite value, which might be done by employing dwell-time (see Deaecto et al. (2014)), hysteresis (see Hespanha et al. (2003)), among others (see Lee and Utkin (2007)). Another feasible approach is to employ a piecewise constant switching function, describing the switching signal as

$$\sigma(t) = u(x(t_n)), \quad \forall t \in [t_n, t_{n+1}) \quad (2.139)$$

where $t_0 = 0$ and $t_{n+1} > t_n$ for all $n \in \mathbb{N}$. This naturally arises when the sampled-data control framework is taken into account in the sense that the state variable is only available to be measured at specific sampling instants. Empirically, the effects produced by such restriction are investigated in the next example.

Example 2.6. Consider the switched affine system defined in Example 2.5 and that the switching function is now replaced by (2.139) with $u(x(t))$ defined in (2.130) with matrix P determined in the previous example and considering a constant length for the piecewise constant intervals, i.e. $T = t_{n+1} - t_n$ for all $n \in \mathbb{N}$.

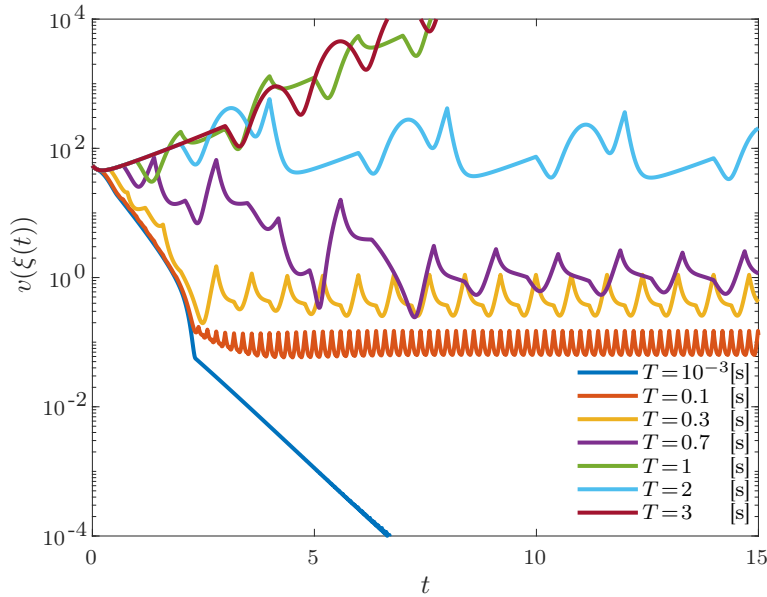


Figure 2.9: Time evolution of the Lyapunov function $v(\xi)$ for different T .

Adopting various values of $T \in \{10^{-3}, 0.1, 0.3, 0.7, 1, 2, 3\}[\text{s}]$ allowed us to analyze different

behaviors for the system trajectory $\xi(t)$ evolving from $\xi_0 = [-4 \ -6]'$. Figure 2.9 presents the time evolution of the Lyapunov function $v(\xi)$ for several values of T . Notice that for $T = 1$ [s] and $T = 3$ [s] the Lyapunov function grows indefinitely, characterizing instability. However, for the remaining values of T , $v(\xi)$ is bounded in steady state, characterizing the practical stability of x_e given in Definition 2.4. Certainly, the system trajectories were attracted to some region in the state-space containing x_e and, once inside, they never left it. It is important to remark that for $T = 2$ [s] the Lyapunov function remains bounded even though for $T = 1$ [s] the correspondent response was unstable, which is a seemingly counterintuitive consequence as all switching signals produced for $T = 2$ [s] could be generated when $T = 1$ [s]. This occurs because the existence of a dwell-time has not been taken into account in the control design of the state-dependent switching function.

Indeed, the investigation provided by this last example is the main motivation for the study of discrete-time switched affine systems, as the discrete-time dynamics naturally bounds the switching frequency and only practical stability can be achieved. Moreover, notice that for switching signals of the form (2.139), the continuous-time system can be described at the sampling instants by a discrete-time switched affine system employing the norm-equivalent discretization procedure introduced in Subsection 2.2.3, discretizing each of the subsystems separately.

2.5.1 Sampled-Data Switched Affine Systems

To conclude this chapter, the present subsection discusses some results available in the literature dealing or adapted to deal with sampled-data control of switched affine systems. These control systems, as previously discussed, will combine the continuous-time dynamics with discrete sampling events, which will produce piecewise constant switching signals, bounding the switching frequency.

In the context of hybrid systems, the reference Rubensson and Lennartson (2000) presented an analysis to assess stability of limit cycles for a given discrete-time switched affine systems. In this case, the switching surfaces are assumed to be given and no control problem arises.

The first reference dealing with the control design, to the best of my knowledge, is Lee and Kouvaritakis (2009), which employs receding horizon control to keep the system trajectories inside an invariant set, close to a reference value. This requires the off-line solution of 2^h semidefinite programming problems where h is the defined discrete-time horizon length.

In Xu et al. (2010), some results about practical stability of discrete-time switched affine systems are presented, which cope with sampled-data systems under constant sampling period. This approach analyzes the quadratic forms generated by the difference operator of a quadratic Lyapunov function, providing the attraction set constructively. However, a procedure to define the Lyapunov matrix P is not provided and the authors suggest employing a common quadratic Lyapunov function, which requires the stability of all subsystems.

Hauroigne et al. (2011) presents three strategies to stabilize the system, being the first one time-dependent (based on PWM signals), the second one selects the subsystem providing the steepest descent for a quadratic Lyapunov function, and the third one minimizes this Lyapunov function over some receding horizon. The global stability guarantee comes from the solution of an optimization problem selecting the worst level set attained after some finite number of switching events N . The complexity of this problem grows exponentially with the number

of subsystems and the number of switching events N considered in the analysis. Additionally, the authors in Hetel and Fridman (2013) have proposed a switching function taking into account an uncertain sampling period and also uncertainties in the model along with design conditions written as LMIs. This result establishes a trade-off between the size of the set to where the system trajectories are attracted and the decay rate of this attraction.

A strategy for bounding the switching frequency was proposed in Bolzern and Spinelli (2004) but it should not be regarded from the sampled-data viewpoint as this upper-bound is not user-defined nor fixed. The same can be concluded about the practical stabilization discussions presented in Xu et al. (2008), Sanchez et al. (2019b) and many others based on hysteresis or non-constant dwell-times. In fact, for digital implementation, non-constant switching frequencies demand a high sampling frequency to detect the exact (or almost exact) instant when a switching event must occur.

For this reason, the next chapter is entirely dedicated to investigating discrete-time switched affine systems governed by both state and output-dependent switching functions. The discrete-time domain approach naturally synchronizes the switching and sampling events and microprocessors can handle the control strategy with no difficulty. Moreover, novel stability conditions are presented, less conservative than preexisting ones in many aspects.

2.6 Concluding Remarks

In this chapter, basic concepts regarding dynamic systems (and particularly switched systems) were presented, allowing the reader to better understand the main results obtained through my Ph.D. studies, presented in the sequel. The key concept illustrated in the last section is to regard the switching signal as the only control variable in the system, which will be extensively explored in Chapters 3 and 4.

For further readings on systems and signals theory, refer to Luenberger (1979); Slotine et al. (1991); Oppenheim et al. (1997); Khalil (2002); Oppenheim and Schafer (2014). Books containing classical results on switched systems are Liberzon (2003); Sun and Ge (2011). More discussions on sampled-data control can be found in Chen and Francis (2012).

DISCRETE-TIME SWITCHED AFFINE SYSTEMS

“Eu já estou com o pé nessa estrada / Qualquer dia a gente se vê / Sei que nada será como antes, amanhã”

— MILTON NASCIMENTO & RONALDO BASTOS, NADA SERÁ COMO ANTES (1970)

PART of the main results obtained throughout these doctoral studies is presented in this chapter. As it was made clear in Section 2.6, not many works concerning stabilizability of discrete-time switched affine systems are available in the literature. With this in mind, conditions for guaranteeing global stability of specific points in the state-space will be developed from a Lyapunov stability perspective. This is a subject of great interest as it might shed light upon the dynamic behavior of this class of systems in a more comprehensive fashion, allowing generalizations from the literature to be incorporated. Moreover, these concepts can be straightforwardly applied in the control of DC-DC converters, allowing to limit the switching frequency by a desired sampling rate, as already discussed in the last chapter.

Firstly, some practical stability results will be presented, where the goal is to determine a set to where the state trajectories are globally attracted. This set, containing the desired equilibrium point, is calculated along with the switching function design, allowing the optimization of some of its metrics. State and output-dependent switching functions will be developed at this part and novel design conditions, based on Lyapunov-Metzler inequalities, are discussed.

Later, a time-varying Lyapunov function approach is considered, addressing global asymptotic stability of limit cycles rather than general practical stability of a specific point. Under this perspective, \mathcal{H}_2 and \mathcal{H}_∞ performances can be taken into account, in contrast with the first methodology.

3.1 Problem Formulation

Consider a **switched affine system** in the discrete-time domain whose model is given by the state-space representation

$$\begin{cases} x[n+1] = A_{\sigma[n]}x[n] + b_{\sigma[n]} + H_{\sigma[n]}w[n], & x[0] = x_0 \\ y[n] = C_{\sigma[n]}(x[n] - x_e) \\ z[n] = E_{\sigma[n]}(x[n] - x_e) + G_{\sigma[n]}w[n] \end{cases} \quad (3.1)$$

where $x : \mathbb{N} \rightarrow \mathbb{R}^{n_x}$ denotes the state vector, $w : \mathbb{N} \rightarrow \mathbb{R}^{n_w}$ represents an exogenous input sequence and $y : \mathbb{N} \rightarrow \mathbb{R}^{n_y}$ and $z : \mathbb{N} \rightarrow \mathbb{R}^{n_z}$ are, respectively, the measured and the controlled outputs. The switching sequence $\sigma : \mathbb{N} \rightarrow \mathbb{K}$ is responsible for choosing, at each instant of time, one subsystem $\mathcal{G}_{si} = (A_i, b_i, H_i, C_i, E_i, G_i)$, $i \in \mathbb{K}$, out of N available ones to be activated.

A goal point $x_e \in \mathbb{R}^{n_x}$ is also considered and, as previously discussed in Chapter 2, it will be called an equilibrium point even though it is not a solution to the dynamic equation. Indeed, the only actual equilibrium points for this system are those of the isolated subsystems and asymptotic stability towards any other point is impossible to be guaranteed. For this reason, this control problem consists of designing a switching function that,

by commanding the switching sequence $\sigma[n]$, can guide the state trajectories starting from any initial condition to as close as possible to x_e . Although the vague concept of “as close as possible” might be subjective, we will analyze different performance metrics throughout this chapter.

Compared to what was discussed in Section 2.5 and references therein, this switched control problem in discrete-time domain is more intricate than in continuous-time, requiring not only the stability certificate but also an evaluation for the steady-state behavior of the state trajectories. The following questions arise: Is it possible to stabilize $x[n]$ to a limit cycle, an invariant set or other structure around x_e ? How to derive an upper bound for $\|x[n] - x_e\|$, $n \geq n_0$ for some $n_0 \in \mathbb{N}$? And what happens to the control problem if x_e is partially known or $x[n]$ is partially available to be measured? These concerns will be addressed in the following sections.

3.2 Practical Stability

In this section, conditions for designing state and output-dependent switching functions to assure practical stability of the desired x_e are presented. The generic concept of global practical stability of equilibrium points, given in Definition 2.4, is recalled at this moment. To assure this feature for a given system (3.1), let us first define the auxiliary state variable $\xi[n] = x[n] - x_e$ and rewrite the state-space representation of (3.1) as

$$\begin{cases} \xi[n+1] = A_{\sigma[n]}\xi[n] + \ell_{\sigma[n]} + H_{\sigma[n]}w[n], & \xi[0] = \xi_0 \\ y[n] = C_{\sigma[n]}\xi[n] \\ z[n] = E_{\sigma[n]}\xi[n] + G_{\sigma[n]}w[n] \end{cases} \quad (3.2)$$

where $\ell_i = (A_i - I)x_e + b_i$ is the new associated affine vector and $\xi_0 = x_0 - x_e$. For this system, the origin $\xi = 0$ is equivalent to $x = x_e$ for the original system (3.1). This alternative system considerably eases the forthcoming developments.

Consider now the existence of a Lyapunov function $v(\xi)$ and a switching function $\sigma[n] = u(\cdot)$ which assure that the time-difference operator of $v(\xi)$ is negative for points ξ far enough from $\xi = 0$, but this statement fails inside some bounded set containing $\xi = 0$. It is not hard to imagine that this scenario is sufficient to assure that system trajectories will be attracted toward the origin but may never attain it. This idea is formalized using the following definitions, presented in Deaecto and Geromel (2017); Egidio et al. (2017).

Definition 3.1 (Set of attraction). *A bounded set $\mathcal{X} \subset \mathbb{R}^n$ is a **set of attraction** of system (3.2) guided by a switching function $\sigma[n] = u(\cdot)$ if there exists a Lyapunov function $v(\xi)$ such that the following conditions are simultaneously satisfied:*

1. $0 \in \mathcal{X}$
2. If $\xi[n] \notin \mathcal{X}$ then $\Delta v(\xi[n]) < 0$

Definition 3.2 (Invariant set of attraction). *A bounded set $\mathcal{V} \subset \mathbb{R}^n$ is an **invariant set of attraction** of system (3.2) guided by a switching function $\sigma[n] = u(\cdot)$ if it is a set of attraction and fulfills the invariance property, i.e., $\xi[n] \in \mathcal{V} \implies \xi[n+1] \in \mathcal{V}$.*

These sets are of main importance for the results presented within this section. It is important to remark that the idea of set of attraction is close to the concept of attractor (see Milnor (1985)). However, the sets of

attraction presented in Definitions 3.1 and 3.2 are not themselves attractors. This can be concluded observing that the definition of attractor provided by Milnor (1985) requires that it cannot present another attractor inside of it. The sets of attraction fail in fulfilling this requirement as they might contain one or more attractors in their interiors.

The switching functions we will design in this section present an associated set of attraction which, together with its Lyapunov function, is the practical stability certificate for the switched affine system. To relate the existence of a set of attraction to the generic Definition 2.4, some discussions are in order. Before going any further, let us present the following lemma.

Lemma 3.1. *If there exists an invariant set of attraction \mathcal{V} for a switched affine system (3.2) under a switching function $\sigma[n] = u(\cdot)$, then its origin $\xi = 0$ is a globally practically stable equilibrium point.*

Proof: Given the fact that $0 \in \mathcal{V}$, we can conclude that any system trajectory starting outside of \mathcal{V} is globally attracted to it (because of condition 2 in Definition 3.1). Then, let us define $n_0 \in \mathbb{N}$ as the first time instant $n = n_0$ such that $\xi[n] \in \mathcal{V}$. Given that \mathcal{V} is bounded and has the invariance property, we can define $R = \sup_{\xi \in \mathcal{V}} \|\xi\|$, which satisfies Definition 2.4 as an upper bound for $\|x[n] - x_e\| < R$ for $n > n_0$. \square

The next lemma, inspired by discussions in Deaecto and Geromel (2017), points out that the existence of a set of attraction is actually sufficient for practical stability, regardless of its invariance property. Before introducing its statement, considering boundedness of \mathcal{X} and continuity of $v(\xi)$, let us define $V_M, V_\Delta \in \mathbb{R}_+$ such that $V_M = \max_{\xi[n] \in \mathcal{X}} v(\xi[n])$ and $V_\Delta = \max_{\xi[n] \in \mathcal{X}} \Delta v(\xi[n])$.

Lemma 3.2. *If there exists a set of attraction \mathcal{X} for a switched affine system (3.2) under a switching function $\sigma[n] = u(\cdot)$, then its origin $\xi = 0$ is a globally practically stable equilibrium point.*

Proof: Let us demonstrate that whenever \mathcal{X} exists, there is a corresponding invariant set of attraction \mathcal{V} , which assures global practical stability through Lemma 3.1. This invariant set is constructed as a sublevel set $\mathcal{V} = \{\xi \in \mathbb{R}^{n_x} : v(\xi) \leq V_M + V_\Delta\}$. Firstly, note that \mathcal{X} is a subset of \mathcal{V} since $\mathcal{X} \subseteq \{\xi \in \mathbb{R}^{n_x} : v(\xi) \leq V_M\} \subseteq \mathcal{V}$. The verification that any \mathcal{V} is also a set of attraction is straightforward from the fact that $\mathcal{X} \subseteq \mathcal{V}$. To demonstrate the invariance property, two cases must be analyzed for $\xi[n] \in \mathcal{V}$:

1. $\xi[n] \notin \mathcal{X}$: For this case, we have $\Delta v(\xi[n]) < 0$ and so $\xi[n+1]$ remains in \mathcal{V} .
2. $\xi[n] \in \mathcal{X}$: Now, the fact that $\Delta v(\xi[n]) \leq V_\Delta$ for $\xi[n] \in \mathcal{X}$ yields

$$v(\xi[n+1]) \leq v(\xi[n]) + V_\Delta \quad (3.3)$$

$$\leq V_M + V_\Delta \quad (3.4)$$

concluding that $\xi[n+1]$ also remains in \mathcal{V} .

This proves the invariance of \mathcal{V} , concluding this demonstration. \square

This result will not be directly employed to evaluate invariant sets because, in our particular studies, we will take advantage from the fact that these sets are constructed through ellipsoids. At this moment, the reader

is invited to Appendix C for a brief review on ellipsoids. Nevertheless, the importance of the previous lemma resides in showing that presenting a generic set of attraction \mathcal{X} is sufficient to assess the global practical stability of the desired equilibrium point x_e . With this in mind, let us now turn our attention to the design of globally practically stabilizing state-dependent switching functions.

3.2.1 State-dependent Switching

The following developments assume that the desired equilibrium point x_e is taken within a set of attainable ones in the state-space. As will be clear later, this constraint allows us to draw key conclusions about sampled-data switched affine systems. The considered set of equilibrium points for this class of systems is defined

$$X_e = \{x_e \in \mathbb{R}^{n_x} : x_e = (I - A_\lambda)^{-1}b_\lambda, \lambda \in \Lambda\} \quad (3.5)$$

Analogously to its continuous-time counterpart, each $x_e \in X_e$ has at least one associated vector $\lambda \in \Lambda$ such that $\ell_\lambda = 0$. Additionally, verifying whether a given x_e belongs to X_e can be done in a similar way to (2.132)-(2.133). However, an easier manner to proceed is to find the set X_e by varying $\lambda \in \Lambda$ and choose a point of interest inside it. This procedure is commonly adopted in literature (see Deaecto et al. (2010), Sanchez et al. (2019a), Hetel and Fridman (2013)).

As done in Deaecto and Geromel (2017); Egidio and Deaecto (nd), the Lyapunov function to be considered is a general quadratic one

$$v(\xi) = \begin{bmatrix} \xi \\ 1 \end{bmatrix}' \begin{bmatrix} P & h \\ h' & h'P^{-1}h \end{bmatrix} \begin{bmatrix} \xi \\ 1 \end{bmatrix} \quad (3.6)$$

with $h \in \mathbb{R}^{n_x}$ and $0 < P \in \mathbb{R}^{n_x \times n_x}$, written alternatively as $v(\xi) = (\xi - \xi_c)'P(\xi - \xi_c)$ with center $\xi_c = -P^{-1}h$. Clearly, this is a convex function such that $v(\xi) > 0$ for all $\xi \neq \xi_c$ and $v(\xi_c) = 0$. In Egidio (2016); Deaecto and Egidio (2016) the Lyapunov function was considered centered at the origin, that is, $\xi_c = 0$, while in Deaecto and Geromel (2017) the center ξ_c is determined from the equilibrium solution to a minimax problem. The next theorem, from Egidio and Deaecto (nd), presents the conditions for the state feedback case encompassing results from both references.

Theorem 3.1. Consider system (3.1) with $x[n]$ available for feedback, $w[n] = 0, \forall n \in \mathbb{N}$ and let the equilibrium point $x_e \in X_e$ be given with its associated vector $\lambda \in \Lambda$. If there exist symmetric matrices W, P, Q_i , vectors $h, g, c_i \in \mathbb{R}^{n_x}$ and scalars ρ_i solution to the convex optimization problem

$$\inf_{W, P, Q_i, h, g, c_i, \rho_i} -\ln(\det(W)) \quad \text{s.t.} \quad (3.7)$$

$$\begin{bmatrix} P - Q_i & \bullet & \bullet \\ c'_i + h'(I - A_i) & \rho_i - \ell'_i h - h'\ell_i & \bullet \\ PA_i & P\ell_i & P \end{bmatrix} > 0, \quad i \in \mathbb{K} \quad (3.8)$$

$$\begin{bmatrix} Q_\lambda & \bullet & \bullet \\ -c'_\lambda & 1 - \rho_\lambda & \bullet \\ W & g & W \end{bmatrix} > 0 \quad (3.9)$$

then the state-dependent switching function $\sigma[n] = u(\xi[n])$ with

$$u(\xi[n]) = \arg \min_{i \in \mathbb{K}} -\xi[n]' Q_i \xi[n] + 2c'_i \xi[n] + \rho_i \quad (3.10)$$

assures that the equilibrium point $\xi = 0$ is globally practically stable and that

$$\mathcal{X}_* = \{\xi \in \mathbb{R}^{n_x} : (\xi - \mu)' W (\xi - \mu) \leq 1\} \quad (3.11)$$

with $\mu = -W^{-1}g$, is an ellipsoidal set of attraction of minimum volume.

Proof: Assume that inequalities (3.8)-(3.9) are verified. Time dependency is dropped from this point onward. Evaluating the time-difference operator of the Lyapunov function for an arbitrary trajectory of (3.2), we have

$$\begin{aligned} \Delta v(\xi) &= v(A_\sigma \xi + \ell_\sigma) - v(\xi) \\ &= \begin{bmatrix} \xi \\ 1 \end{bmatrix}' \begin{bmatrix} A'_\sigma P A_\sigma - P & \bullet \\ \ell'_\sigma P A_\sigma + h'(A_\sigma - I) & \ell'_\sigma P \ell_\sigma + 2\ell'_\sigma h \end{bmatrix} \begin{bmatrix} \xi \\ 1 \end{bmatrix} \end{aligned} \quad (3.12)$$

$$\leq \begin{bmatrix} \xi \\ 1 \end{bmatrix}' \begin{bmatrix} -Q_\sigma & \bullet \\ c'_\sigma & \rho_\sigma \end{bmatrix} \begin{bmatrix} \xi \\ 1 \end{bmatrix} \quad (3.13)$$

where this inequality is verified from (3.8) after applying the Schur Complement Lemma with respect to the matrix block (3.3). Now, taking into account the switching function (3.10), we obtain

$$\begin{aligned} \Delta v(\xi) &\leq \min_{i \in \mathbb{K}} \begin{bmatrix} \xi \\ 1 \end{bmatrix}' \begin{bmatrix} -Q_i & \bullet \\ c'_i & \rho_i \end{bmatrix} \begin{bmatrix} \xi \\ 1 \end{bmatrix} \\ &= \min_{\lambda^* \in \Lambda} \begin{bmatrix} \xi \\ 1 \end{bmatrix}' \begin{bmatrix} -Q_{\lambda^*} & \bullet \\ c'_{\lambda^*} & \rho_{\lambda^*} \end{bmatrix} \begin{bmatrix} \xi \\ 1 \end{bmatrix} \\ &\leq \begin{bmatrix} \xi \\ 1 \end{bmatrix}' \begin{bmatrix} -Q_\lambda & \bullet \\ c'_\lambda & \rho_\lambda \end{bmatrix} \begin{bmatrix} \xi \\ 1 \end{bmatrix} \end{aligned} \quad (3.14)$$

which holds for all $\xi \in \mathbb{R}^{n_x}$. Defining the set \mathcal{X}_s as being

$$\mathcal{X}_s = \{\xi \in \mathbb{R}^{n_x} : (\xi - \mu_s)' Q_\lambda (\xi - \mu_s) < c'_\lambda Q_\lambda^{-1} c_\lambda + \rho_\lambda\} \quad (3.15)$$

with $\mu_s = Q_\lambda^{-1} c_\lambda$, and considering the validity of (3.14), two properties hold. The first one is $\xi = 0 \in \mathcal{X}_s$ because, from (3.8), we have that $\rho_i > 2\ell'_i h$, which implies that $\rho_\lambda > 0$ since $\ell_\lambda = 0$. The second one is that $\Delta v(\xi) < 0$, $\forall \xi \notin \mathcal{X}_s$, indicating that \mathcal{X}_s is a set of attraction for the system according to Definition 3.1. Moreover, notice that, by S-procedure (see Appendix Subsection A.4), the set \mathcal{X} , defined in (3.11), contains the ellipsoid \mathcal{X}_s whenever the inequality

$$\begin{bmatrix} W & \bullet \\ -\mu' W & \mu' W \mu - 1 \end{bmatrix} < \beta \begin{bmatrix} Q_\lambda & \bullet \\ -c'_\lambda & -\rho_\lambda \end{bmatrix} \quad (3.16)$$

is satisfied for $\beta > 0$, see Boyd et al. (1994) for details. Actually, both sides of (3.16) can be arbitrarily close and the sign in (3.16) could be replaced by \leq . However, we will maintain it strict, without loss of generality, in order

to describe the problem in terms of strict LMIs. In other words, multiplying both sides of (3.16) to the left by $[\xi' \ 1]$ and to the right by its transpose, the resulting inequality assures that $(\xi - \mu)'W(\xi - \mu) < 1$ whenever $\xi \in \mathcal{X}_s$ and, as a consequence, \mathcal{X} is a set of attraction, since $\mathcal{X} \supseteq \mathcal{X}_s$. Writing (3.16) as

$$\begin{bmatrix} \beta Q_\lambda & \bullet \\ -\beta c'_\lambda & 1 - \beta \rho_\lambda \end{bmatrix} > \begin{bmatrix} W \\ -\mu'W \end{bmatrix} W^{-1} \begin{bmatrix} W \\ -\mu'W \end{bmatrix}' \quad (3.17)$$

By applying the Schur Complement Lemma with respect to W in (3.17) we obtain

$$\begin{bmatrix} \beta Q_\lambda & \bullet & \bullet \\ -\beta c'_\lambda & 1 - \beta \rho_\lambda & \bullet \\ W & g & W \end{bmatrix} > 0 \quad (3.18)$$

Now, notice that (3.8) can be multiplied by the scalar β , without loss of generality. The resultant inequality and (3.18) after redefining, with some abuse of notation, $(Q_i, c_i, \rho_i, P, h) \leftarrow (\beta Q_i, \beta c_i, \beta \rho_i, \beta P, \beta h)$, are exactly the inequalities (3.8)-(3.9), assuring that \mathcal{X} is an ellipsoidal set of attraction. The objective function (3.7) is responsible for minimizing the volume of (3.11) (see Appendix Subsection C.1 for more information about ellipsoids and volume minimization). The proof is concluded. \square

This is the first stability theorem for discrete-time affine switched systems discussed in this dissertation, assuring the existence of an ellipsoidal set of attraction \mathcal{X} . Let us draw a comparison between this result and the one presented in [Deaecto and Geromel \(2017\)](#). This reference provides a design procedure based on the solution to the convex optimization problem

$$\inf_{P>0, W>0} -\ln(\det(W)) \quad \text{s.t.} \quad (3.19)$$

$$\sum_{i \in \mathbb{K}} \lambda_i A'_i P A_i - P < -W, \quad \sum_{i \in \mathbb{K}} \ell'_i P \ell_i < 1 \quad (3.20)$$

which minimizes the volume of $\mathcal{X} = \{\xi \in \mathbb{R}^{n_x} : \xi' W \xi \leq 1\}$. These conditions were obtained departing from an upper bound for the difference operator of the Lyapunov function that is derived adopting the switching function $\sigma[n] = u(\xi[n])$ with $u(\xi) = \arg \min_{i \in \mathbb{K}} v(A_i \xi + \ell_i)$. This upper bound function is given by

$$\Delta v(\xi) < f_u(\xi, h) = \sum_{i \in \mathbb{K}} \lambda_i \begin{bmatrix} \xi \\ h \\ 1 \end{bmatrix}' \begin{bmatrix} A'_i P A_i - P & \bullet & \bullet \\ A_i - I & 0 & \bullet \\ \ell'_i P A_i & \ell'_i & \ell'_i P \ell_i \end{bmatrix} \begin{bmatrix} \xi \\ h \\ 1 \end{bmatrix} \quad (3.21)$$

Assuming that the design conditions are fulfilled, the function $f_u(\xi, h)$ is concave with respect to ξ and linear (or concave-convex) with respect to h . Thus, there exists a saddle point that is the solution to the minimax problem

$$\min_{h \in \mathbb{R}^{n_x}} \max_{\xi \in \mathbb{R}^{n_x}} f_u(\xi, h) \quad (3.22)$$

To define the center of $v(\xi)$ that minimizes the worst-case upper bound for $\Delta v(\xi)$, the vector h is chosen from the equilibrium solution to (3.22) given as $(h_*, \xi_*) = ((I - A'_\lambda)^{-1}(\sum_{i \in \mathbb{K}} \lambda_i A'_i P \ell_i), 0)$, which can be obtained as demonstrated in [Deaecto and Geromel \(2017\)](#). For a broader study about saddle points in convex optimization, see [Rockafellar \(1970\)](#). Back to our context, notice that (3.8), after having applied the Schur Complement

Lemma with respect to the last diagonal block, can be rewritten as

$$\begin{bmatrix} A'_i P A_i - P & \bullet \\ \ell'_i P A_i - h'(I - A_i) & \ell'_i P \ell_i + 2\ell'_i h \end{bmatrix} < \begin{bmatrix} -Q_i & \bullet \\ c'_i & \rho_i \end{bmatrix} \quad (3.23)$$

We can observe that, without loss of generality, the right-hand side of this inequality can take values arbitrarily close to the left-hand side and, therefore, (3.10) becomes the switching function of [Deaecto and Geromel \(2017\)](#). Moreover, inequality (3.23) together with (3.9), after performing the Schur Complement with respect to the last row and column, provide

$$\begin{bmatrix} \sum_{i \in \mathbb{K}} \lambda_i A'_i P A_i - P & \bullet \\ \sum_{i \in \mathbb{K}} \lambda_i \ell'_i P A_i - h'(I - A_\lambda) & \sum_{i \in \mathbb{K}} \lambda_i \ell'_i P \ell_i \end{bmatrix} < \begin{bmatrix} -W & \bullet \\ \mu' W & 1 - \mu' W \mu \end{bmatrix} \quad (3.24)$$

where it has been used the fact that $\ell_\lambda = 0$ since $x_e \in X_e$. Notice that $h = (I - A'_\lambda)^{-1}(\sum_{i \in \mathbb{K}} \lambda_i A'_i P \ell_i - W \mu)$ is the best choice, since this vector makes null the off-diagonal block element, implying that (3.24) is equivalent to $\sum_{i \in \mathbb{K}} \lambda_i A'_i P A_i - P < -W$ and $\sum_{i \in \mathbb{K}} \lambda_i \ell'_i P \ell_i < 1 - \mu' W \mu$. This last inequality allows us to conclude that $\mu = 0$ is the less restrictive choice and, therefore, vector h becomes the optimal solution to the minimax problem (3.22). Moreover, the resultant inequalities become exactly (3.20), putting in evidence that Theorem 3.1 is equivalent to Theorem 1 of [Deaecto and Geromel \(2017\)](#). Although they are equivalent, the great advantage of adopting Theorem 3.1 is that it is more amenable for output feedback generalizations, since it allows us to impose structures on the matrices that define the switching function, making it independent of the state vector. This point will be clear afterward.

Another property of Theorem 3.1 is worthwhile to mention. Notice that the necessary and sufficient condition for the feasibility of this theorem is $\sum_{i \in \mathbb{K}} \lambda_i A'_i P A_i - P < 0$ and, therefore, nothing is required from matrices A_i , $\forall i \in \mathbb{K}$, considered separately. This can be concluded from the discussions in the previous paragraph. Hence, even in cases where all subsystems are unstable, it is possible to obtain practical stability through a suitable action of the switching function (3.10), as discussed in Chapter 2. However, in contrast with the continuous-time case, the Schur stability of A_λ is necessary but not sufficient for feasibility. Indeed, as proved in [Deaecto et al. \(2014\)](#), $\sum_{i \in \mathbb{K}} \lambda_i A'_i P A_i - P < 0$ is satisfied for some $P > 0$ whenever \mathcal{A}_λ is Schur stable, with $\mathcal{A}_i = A'_i \otimes A_i$, where \otimes stands for the Kronecker product.

Finally, it is important to verify whether the center of the Lyapunov function $\xi_c = -P^{-1}h$ and the equilibrium point $\xi = 0$ belong to the set of attraction \mathcal{X} . To demonstrate that $\xi_c \in \mathcal{X}$, notice that (3.14) evaluated for ξ_c provides

$$\begin{bmatrix} \xi_c \\ 1 \end{bmatrix}' \begin{bmatrix} -Q_\lambda & \bullet \\ c'_\lambda & \rho_\lambda \end{bmatrix} \begin{bmatrix} \xi_c \\ 1 \end{bmatrix} > v(A_\sigma \xi_c + \ell_\sigma) \geq 0 \quad (3.25)$$

because $v(\xi_c) = 0$. This inequality, together with (3.9), after applying the Schur Complement with respect to

the last row and column, produces

$$\begin{bmatrix} \xi_c \\ 1 \end{bmatrix}' \begin{bmatrix} W & \bullet \\ -\mu'W & \mu'W\mu - 1 \end{bmatrix} \begin{bmatrix} \xi_c \\ 1 \end{bmatrix} < \begin{bmatrix} \xi_c \\ 1 \end{bmatrix}' \begin{bmatrix} Q_\lambda & \bullet \\ -c'_\lambda & -\rho_\lambda \end{bmatrix} \begin{bmatrix} \xi_c \\ 1 \end{bmatrix} < 0 \quad (3.26)$$

which guarantees that $\xi_c \in \mathcal{X}$. Now, we have that $0 \in \mathcal{X}$ from the simple fact that $0 \in \mathcal{X}_s$ as proved in Theorem 3.1 and $\mathcal{X}_s \subseteq \mathcal{X}$. Concluding these remarks, let us illustrate the effectiveness of these practical stability conditions by means of an academical example.

Example 3.1. Consider a discrete-time switched affine system (3.1) given by matrices

$$A_1 = \begin{bmatrix} -0.1 & 0.8 \\ 0.4 & -0.8 \end{bmatrix}, \quad A_2 = \begin{bmatrix} -0.9 & 0.8 \\ 0.6 & 0.5 \end{bmatrix}, \quad A_3 = \begin{bmatrix} 0.3 & 0.5 \\ 1.0 & 0.7 \end{bmatrix}, \quad A_4 = \begin{bmatrix} -0.5 & 1.0 \\ 0.8 & 0.3 \end{bmatrix} \quad (3.27)$$

$$b_1 = \begin{bmatrix} -0.1 \\ 0 \end{bmatrix}, \quad b_2 = \begin{bmatrix} 0.2 \\ 0.1 \end{bmatrix}, \quad b_3 = \begin{bmatrix} 0 \\ -0.1 \end{bmatrix}, \quad b_4 = \begin{bmatrix} -0.1 \\ 0 \end{bmatrix} \quad (3.28)$$

defining $N = 4$ unstable subsystems. Our goal is to bring the state trajectories, starting from arbitrary initial conditions $x_0 \in \mathbb{R}^2$, to as close as possible to zero. As the desired equilibrium point is already the origin, no auxiliary state variable ξ is needed in this case.

There is no difficulty in verifying that $0 \in X_e$ associated with the convex combination vector $\lambda = [0.05 \ 0.25 \ 0.25 \ 0.45] \in \Lambda$. Solving the convex optimization problem proposed in Theorem 3.1, we have obtained matrices

$$P = \begin{bmatrix} 56.1502 & -8.7082 \\ -8.7082 & 48.9259 \end{bmatrix}, \quad h = \begin{bmatrix} -7.9537 \\ -12.2851 \end{bmatrix}, \quad W = \begin{bmatrix} 1.8397 & -0.2487 \\ -0.2487 & 1.8291 \end{bmatrix}, \quad g = 0 \quad (3.29)$$

and Q_i , c_i , ρ_i , $i \in \mathbb{K}$, which assure the existence of an elliptical set of attraction \mathcal{X} centered at the origin and with a minimum area equals to 1.7286, as given in (3.11). This allowed us to implement the state-dependent switching function (3.10), which can orchestrate the switching to assure global practical stability of $x = 0$.

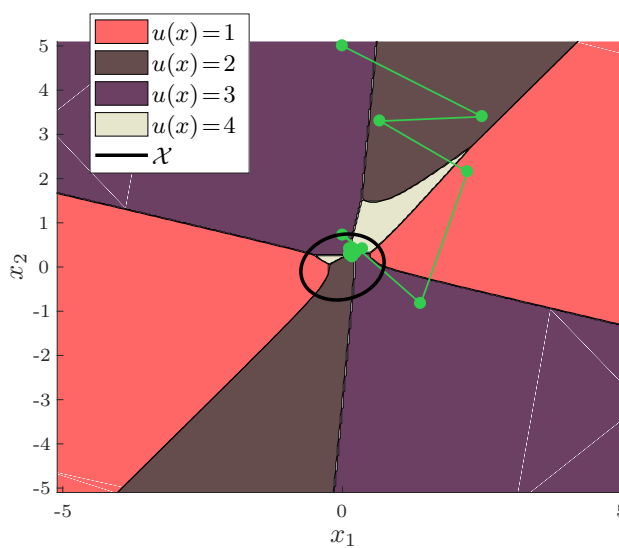


Figure 3.1: Phase portrait of state trajectory evolving from $x_0 = [0 \ 5]'$, being attracted to \mathcal{X} .

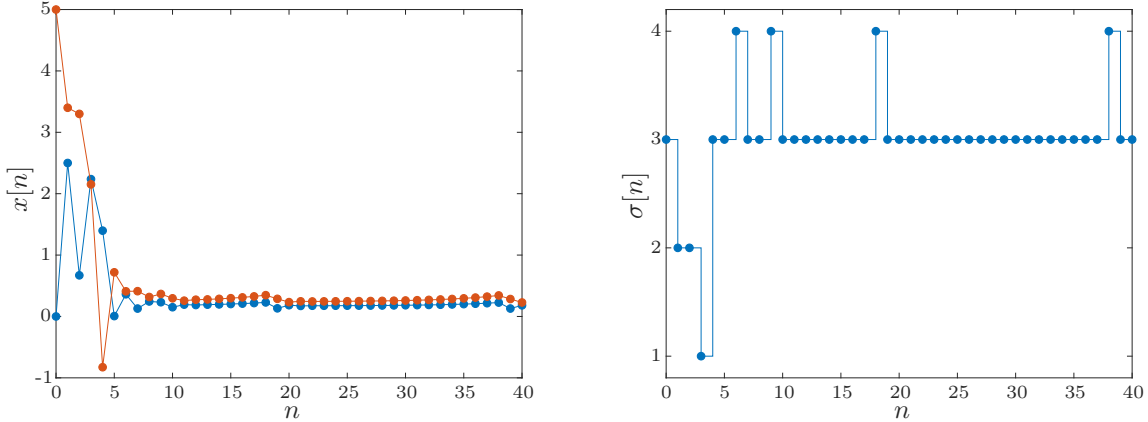


Figure 3.2: Time evolution of state trajectory from $x_0 = [0 \ 5]'$, and resulting switching sequence.

For an initial condition $x_0 = [0 \ 5]'$, we could obtain the simulated system response, displayed in the phase portrait in Figure 3.1 and as a function of time in Figure 3.2 along with the resultant switching sequence. Notice in Figure 3.1, the operating regions of each switching function $\sigma[n] = u(\xi[n]) \in \{1 \dots, 4\}$ as well as the set of attraction \mathcal{X} .

This last example highlights the state-dependent switching function design for a switched affine system. Despite the fact that this system comprises only unstable dynamics, the proposed methodology was successful in assessing global practical stability. The next example provides a comparison between Theorem 3.1 and the results presented in Xu et al. (2010).

Example 3.2. Consider the discrete-time switched affine system (3.1) defined by matrices

$$A_i = e^{A_{ci}T}, \quad b_i = \int_0^T e^{A_{ci}\tau} d\tau \ b_{ci} \quad (3.30)$$

discretized by the step invariant discretization (2.77) with

$$A_{c1} = \begin{bmatrix} 1 & 10 \\ -100 & 1 \end{bmatrix}, \quad A_{c2} = \begin{bmatrix} -1 & 1 \\ -1 & -1 \end{bmatrix}, \quad A_{c3} = \begin{bmatrix} -0.1 & 2 \\ -2 & -0.2 \end{bmatrix} \quad (3.31)$$

$$b_{c1} = \begin{bmatrix} -0.7 \\ -0.7 \end{bmatrix}, \quad b_{c2} = \begin{bmatrix} 0.8 \\ -0.5 \end{bmatrix}, \quad b_{c3} = \begin{bmatrix} -0.5 \\ 0.8 \end{bmatrix} \quad (3.32)$$

provided in Example 1 of Xu et al. (2010). Authors in Xu et al. (2010) proposed a strategy to assess practical stability of the origin for a discrete-time switched affine system. When this strategy is applied to this discretized system, the maximal value of T for which Xu et al. (2010) can assure stability is $T = 0.01239$ s. However, Theorem 3.1 can guarantee practical stability of this same point for sampling periods up to $T = 0.0227$ s, which is 83% greater than Xu et al. (2010). For this value, the associated $\lambda \in \Lambda$, assuring $0 \in X_e$ is $\lambda = [0.3306 \ 0.4437 \ 0.2256]$. The solution matrices defining the ellipsoid \mathcal{X} , the corresponding

Lyapunov function and the switching function (3.10) are

$$W = \begin{bmatrix} 0.0597 & -0.0012 \\ -0.0012 & 0.0072 \end{bmatrix}, \quad P = \begin{bmatrix} 3.7437 \times 10^3 & 80.0148 \\ 80.0148 & 449.4066 \end{bmatrix}, \quad h = \begin{bmatrix} 44.8749 \\ 0.1895 \end{bmatrix} \quad (3.33)$$

$$Q_1 = \begin{bmatrix} -250.5197 & 191.6029 \\ 191.6029 & -13.1692 \end{bmatrix}, \quad Q_2 = \begin{bmatrix} 171.0821 & -67.7403 \\ -67.7403 & 14.8413 \end{bmatrix}, \quad Q_3 = \begin{bmatrix} 30.8845 & -147.5359 \\ -147.5359 & -9.8596 \end{bmatrix} \quad (3.34)$$

$$c_1 = \begin{bmatrix} -57.8769 \\ -3.6003 \end{bmatrix}, \quad c_2 = \begin{bmatrix} 63.3281 \\ -1.1718 \end{bmatrix}, \quad c_3 = \begin{bmatrix} -39.7399 \\ 7.5801 \end{bmatrix}, \quad \rho_1 = -0.4658, \quad \rho_2 = 2.8075, \quad \rho_3 = -0.4071 \quad (3.35)$$

Let us now turn our attention to the invariance property of the set of attraction. Although the existence of a simple set of attraction \mathcal{X} is sufficient to assess practical stability, as discussed in Lemma 3.1, a different methodology based on a convex optimization problem to obtain an invariant set of attraction is presented in the next theorem, borrowed from [Deaecto and Geromel \(2017\)](#).

Theorem 3.2. *Consider system (3.1) with $x[n]$ available for feedback, $w[n] = 0, \forall n \in \mathbb{N}$ and let the set of attraction \mathcal{X} , obtained from Theorem 3.1 be given, along with solution matrices P , W and h . If there exist scalars $r, \beta > 0$, solution to the convex optimization problem*

$$\inf_{r, \beta > 0} r \quad \text{s.t.} \quad (3.36)$$

$$\begin{bmatrix} r - \beta & \bullet & \bullet \\ h & P & \bullet \\ 0 & P & \beta W \end{bmatrix} > 0 \quad (3.37)$$

then the ellipsoidal set

$$\mathcal{V} = \{\xi \in \mathbb{R}^{n_x} : v(\xi) < r\} \quad (3.38)$$

is an invariant set of attraction with $\mathcal{X} \subset \mathcal{V}$.

Proof: Available in [Deaecto and Geromel \(2017\)](#). □

This last theorem provides a convex optimization problem whose solution defines an invariant sublevel set for the Lyapunov function. Notice this is done for the specific case where $g = 0$, i.e., \mathcal{X} is centralized at the equilibrium point. However, Theorem 3.2 may be employed in the general case after defining another translated state variable $\xi_T = \xi - \mu$ which makes $h \leftarrow h - P\mu$ in (3.37). A possibly smaller sublevel set could be obtained if, instead of minimizing the volume of \mathcal{X} and then calculating \mathcal{V} , the designer adopted the following theorem which deals directly with the invariant set minimization.

Theorem 3.3. *Consider system (3.1) with $x[n]$ available for feedback, $w[n] = 0, \forall n \in \mathbb{N}$ and let the equilibrium point $x_e \in X_e$ be given with its associated vector $\lambda \in \Lambda$. If there exist symmetric matrices P , Q_i , vectors $h, c_i \in \mathbb{R}^{n_x}$ and scalars ρ_i, β solution to the optimization problem*

$$\inf_{P, Q_i, h, c_i, \rho_i, \beta} -\ln(\det(P)) \quad \text{s.t.} \quad (3.39)$$

$$\begin{bmatrix} P - Q_i & \bullet & \bullet \\ c'_i + h'(I - A_i) & \rho_i - \ell'_i h - h' \ell_i & \bullet \\ PA_i & P\ell_i & P \end{bmatrix} > 0, \quad i \in \mathbb{K} \quad (3.40)$$

$$\begin{bmatrix} \beta Q_\lambda & \bullet & \bullet \\ -\beta c'_\lambda & 1 - \beta \rho_\lambda & \bullet \\ P & h & P \end{bmatrix} > 0, \quad \beta > 0 \quad (3.41)$$

then the state-dependent switching function (3.10) assures that $\xi = 0$ is a globally practically stable equilibrium point and that

$$\mathcal{V} = \{\xi \in \mathbb{R}^{n_x} : v(\xi) \leq 1\} \quad (3.42)$$

is an ellipsoidal invariant set of attraction of minimum volume.

Proof: The proof that \mathcal{V} is a set of attraction of minimum volume is straightforward from Theorem 1, observing that $\mathcal{X} = \mathcal{V} \supseteq \mathcal{X}_s$ is assured as (3.9) is equivalent to (3.41) with $W = P$ and $g = h$. Notice that the S-procedure multiplier β could not be incorporated into the problem variables in this case. The invariance property is verified by analyzing the following cases when $\xi[n] \in \mathcal{V}$:

1. $\xi[n] \notin \mathcal{X}_s$: For this case, we have $\Delta v(\xi[n]) < 0$ and so $\xi[n+1]$ remains in \mathcal{V} .

2. $\xi[n] \in \mathcal{X}_s$: Now, from (3.14), we have

$$v(\xi[n+1]) < \begin{bmatrix} \xi \\ 1 \end{bmatrix}' \begin{bmatrix} P - Q_\lambda & \bullet \\ h' + c'_\lambda & h' P^{-1} h + \rho_\lambda \end{bmatrix} \begin{bmatrix} \xi \\ 1 \end{bmatrix} \quad (3.43)$$

$$\leq \max_{\xi \in \mathcal{X}_s} \begin{bmatrix} \xi \\ 1 \end{bmatrix}' \begin{bmatrix} P - Q_\lambda & \bullet \\ h' + c'_\lambda & h' P^{-1} h + \rho_\lambda \end{bmatrix} \begin{bmatrix} \xi \\ 1 \end{bmatrix} \quad (3.44)$$

$$= \max_{\xi \in \mathcal{X}_s} \begin{bmatrix} \xi \\ 1 \end{bmatrix}' \begin{bmatrix} P & \bullet \\ h' & h' P^{-1} h \end{bmatrix} \begin{bmatrix} \xi \\ 1 \end{bmatrix} \quad (3.45)$$

$$= 1 \quad (3.46)$$

where the first equality comes from Lemma A.5 along with the fact that $P - Q_i > 0$ for all $i \in \mathbb{K}$ from (3.40) and the last equality is a consequence of $\mathcal{V} \supseteq \mathcal{X}_s$. Hence, $\xi[n+1] \in \mathcal{V}$.

This proves the invariance of \mathcal{V} concluding this demonstration. \square

Notice that this invariance proof is less restrictive than the one provided by Lemma 3.1 since it takes the maximum of the entire upper bound of $v(\xi[n+1])$ while in the previous lemma the maximum is taken individually from each term bounding $v(\xi[n+1])$. More discussions about invariant sets are provided at the end of the next subsection where the output-dependent switching case will be studied.

3.2.2 Output-dependent Switching

To the best of my knowledge, all of the references to date studying switching function design for discrete-time switched affine systems deal exclusively with state and/or time-dependent switching. Considering that in

practical applications the state is seldom fully available, coping with this more realistic situation is an important project feature. In this case, the switching strategy must take into account only a measured output to determine which subsystem must be activated at each instant, assuring system global stability. Some methodologies in other contexts can serve as inspiration, for instance Deaecto et al. (2011a); Pinto and Trofino (2014); Deaecto (2016); Kolotelo et al. (2018).

Departing from Theorem 3.1, we will now address dynamic output feedback control design of switched affine systems in the discrete-time domain. The design conditions to be presented were submitted for publication in Egidio and Deaecto (nd) and assure global practical stability of a desired equilibrium point. When compared to the results in Deaecto and Geromel (2017), the generalization of Theorem 3.1 to cope with the output feedback control design requires less imposed structures on matrix variables to make the switching rule independent of the system state, even though both methodologies are theoretically equivalent.

The proposed switching function takes into account a **full-order switched affine filter** given by the state-space realization

$$\hat{\xi}[n+1] = \hat{A}_{\sigma[n]} \hat{\xi}[n] + \hat{B}_{\sigma[n]} y[n] + \hat{\ell}_{\sigma[n]}, \quad \hat{\xi}[0] = \hat{\xi}_0 \quad (3.47)$$

with $\hat{\xi} : \mathbb{N} \rightarrow \mathbb{R}^{n_x}$ being the filter state variable and the matrices $(\hat{A}_i, \hat{B}_i, \hat{\ell}_i)$, $i \in \mathbb{K}$ to be suitably designed. Notice that the filter (3.47) is not an observer but a generic dynamic system. Actually, $\hat{\xi}$ does not necessarily converge to the system state ξ . Its objective is to provide essential information for the switching function $\sigma[n] = u(\hat{\xi}[n])$, making the switching strategy dependent only on the measured output $y \in \mathbb{R}^{n_y}$ through $\hat{\xi} \in \mathbb{R}^{n_x}$. Figure 3.3 illustrates the proposed approach.

Defining the augmented state variable $\tilde{\xi} = [\xi' \ \hat{\xi}']'$ and connecting the filter (3.47) to the system (3.2) with $w[n] = 0$, $\forall i \in \mathbb{K}$ and $E_i = E$, $\forall i \in \mathbb{K}$, we obtain

$$\begin{cases} \tilde{\xi}[n+1] = \tilde{A}_{\sigma[n]} \tilde{\xi}[n] + \tilde{\ell}_{\sigma[n]}, \quad \tilde{\xi}[0] = \tilde{\xi}_0 \\ z[n] = \tilde{E} \tilde{\xi}[n] \end{cases} \quad (3.48)$$

with matrices

$$\tilde{A}_i = \begin{bmatrix} A_i & 0 \\ \hat{B}_i C_i & \hat{A}_i \end{bmatrix}, \quad \tilde{\ell}_i = \begin{bmatrix} \ell_i \\ \hat{\ell}_i \end{bmatrix}, \quad \tilde{E}' = \begin{bmatrix} E' \\ 0 \end{bmatrix}, \quad i \in \mathbb{K} \quad (3.49)$$

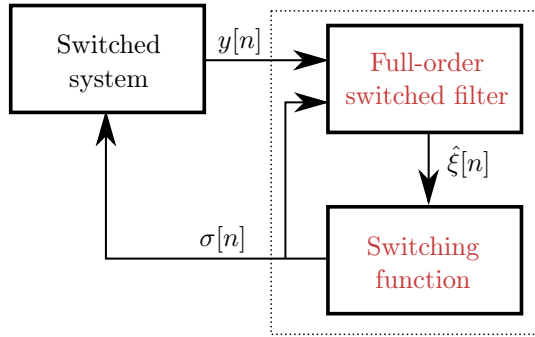


Figure 3.3: Block diagram showing the proposed output-dependent switching strategy.

The idea is to design the switching function $u(\hat{\xi})$ jointly with the filter matrices $(\hat{A}_i, \hat{B}_i, \hat{\ell}_i)$, $i \in \mathbb{K}$ to assure practical stability of the origin $\tilde{\xi} = 0$. This is done by optimizing an objective function related to the augmented set of attraction $\tilde{\mathcal{X}}$. To this end, we propose two objective functions:

- The first one is the volume minimization of the ellipsoidal set $\mathcal{X} \supset \tilde{\mathcal{X}}$, which is the projection of $\tilde{\mathcal{X}}$ on the subspace generated by the system state variable. The corresponding optimization problem is similar to the one presented in Theorem 3.1.
- The second objective function is based on the minimization of an upper bound for the Euclidean norm of the controlled output $\|z\|$ when the state variable is inside the set of attraction. In this case, the set of attraction becomes a ball in the vector space generated by the output $z[n]$.

Notice that, in our context, the role of the switched filter is restricted to provide information for the switching rule and, therefore, its steady state behavior is not of interest. For this reason, a measure of \mathcal{X} has to be defined depending only on the system state $\xi \in \mathbb{R}^{n_x}$. Moreover, to generalize the conditions in Theorem 3.1, the dependency of the switching function on ξ must be avoided, as this variable is no longer available. For this reason, consider the structured matrices

$$\tilde{Q}_i = \begin{bmatrix} Q & \bar{Q} \\ \bar{Q}' & \hat{Q}_i \end{bmatrix}, \quad \tilde{c}_i = \begin{bmatrix} c \\ \hat{c}_i \end{bmatrix}, \quad \tilde{\rho}_i = \rho_i \quad (3.50)$$

This structure is important to make the switching rule dependent only on the measured output through the filter state variable $\hat{\xi}$. Indeed, the evaluation of (3.10) for the augmented system with such structures provides

$$\begin{aligned} u(\tilde{\xi}) &= \arg \min_{i \in \mathbb{K}} -\tilde{\xi}' \tilde{Q}_i \tilde{\xi} + 2\tilde{c}_i' \tilde{\xi} + \tilde{\rho}_i \\ &= \arg \min_{i \in \mathbb{K}} -\hat{\xi}' \hat{Q}_i \hat{\xi} + 2\hat{c}_i' \hat{\xi} + \rho_i = u(\hat{\xi}) \end{aligned} \quad (3.51)$$

which is true since terms multiplying the system state are index independent.

Although the filter is essential for the switching function implementation, the optimization of the set of attraction must be focused only on the subspace generated by the system state variable $\xi \in \mathbb{R}^{n_x}$. Seeking to present a set of attraction independent of $\hat{\xi}$, let us define the degenerate ellipsoid

$$\tilde{\mathcal{X}} = \{\tilde{\xi} \in \mathbb{R}^{2n_x} : (\tilde{\xi} - \tilde{\mu})' \tilde{W} (\tilde{\xi} - \tilde{\mu}) \leq 1\} \quad (3.52)$$

with structured matrices

$$\tilde{W} = \begin{bmatrix} W & 0 \\ 0 & 0 \end{bmatrix}, \quad \tilde{\mu} = \begin{bmatrix} \mu \\ 0 \end{bmatrix} \quad (3.53)$$

where $W > 0$. The ellipsoid \mathcal{X} given by

$$\mathcal{X} = \{\xi \in \mathbb{R}^{n_x} : (\xi - \mu)' W (\xi - \mu) \leq 1\} \quad (3.54)$$

can be interpreted as the projection of a general ellipsoid $\tilde{\mathcal{X}}$ on the subspace generated by $\xi \in \mathbb{R}^{n_x}$ (see Appendix Section C, for more discussions).

The next theorem presents the control design condition of an output-dependent switching function, assuring practical stability through the volume minimization of the set of attraction given by (3.54).

Theorem 3.4. Consider the system (3.2) with $w[n] = 0, \forall n \in \mathbb{N}$ and let the equilibrium point $x_e \in X_e$ be given with its associated vector $\lambda \in \Lambda$. If there exist symmetric matrices Z, Q, \hat{Q}_i, Y, W , matrices J, L_i, M_i , vectors v_i, c, \hat{c}_i, h, g , and scalars ρ_i , solution to the convex optimization problem

$$\inf_{Z, Q, \hat{Q}_i, Y, W, J, L_i, M_i, v_i, c, \hat{c}_i, h, g, \rho_i} -\ln(\det(W)) \quad \text{s.t.} \quad (3.55)$$

$$\begin{bmatrix} Z - Q - J - J' - \hat{Q}_i & \bullet & \bullet & \bullet & \bullet \\ Z - Q - J & Y - Q & \bullet & \bullet & \bullet \\ c' + \hat{c}'_i + h'(I - A_i) & c' + h'(I - A_i) & \rho_i - 2\ell'_i h & \bullet & \bullet \\ ZA_i & ZA_i & Z\ell_i & Z & \bullet \\ YA_i + L_i C_i + M_i & YA_i + L_i C_i & Y\ell_i + \nu_i & Z & Y \end{bmatrix} > 0 \quad (3.56)$$

for all $i \in \mathbb{K}$ and

$$\begin{bmatrix} Q + J + J' + \hat{Q}_\lambda & \bullet & \bullet & \bullet \\ Q + J & Q & \bullet & \bullet \\ -c' - \hat{c}'_\lambda & -c' & 1 - \rho_\lambda & \bullet \\ W & W & g & W \end{bmatrix} > 0 \quad (3.57)$$

then the output-dependent switching function (3.51) and the switched filter (3.47) given by matrices

$$\hat{A}_i = (Z - Y)^{-1}M_i, \quad \hat{B}_i = (Z - Y)^{-1}L_i, \quad \hat{\ell}_i = (Z - Y)^{-1}\nu_i \quad (3.58)$$

assure that $\xi = 0$ is a globally practically stable equilibrium point and

$$\mathcal{X}_* = \{\xi \in \mathbb{R}^{n_x} : (\xi - \mu)'W(\xi - \mu) < 1\} \quad (3.59)$$

with $\mu = -W^{-1}g$, is an ellipsoidal set of attraction with minimum volume.

Proof: The proof consists in demonstrating that the LMIs (3.56) and (3.57) assure the validity of (3.8) and (3.9), respectively, whenever the augmented matrices (3.49) and the structured ones (3.50) and (3.53) are taken into account. Firstly, let us define the matrices

$$\tilde{P} = \begin{bmatrix} Y & V \\ V' & \hat{Y} \end{bmatrix}, \quad \tilde{S} = \tilde{P}^{-1} = \begin{bmatrix} X & U \\ U' & \hat{X} \end{bmatrix}, \quad \tilde{h} = \begin{bmatrix} h \\ 0 \end{bmatrix}, \quad \tilde{\Gamma} = \begin{bmatrix} X & I \\ U' & 0 \end{bmatrix} \quad (3.60)$$

The particular choice of \tilde{h} is important to guarantee that $\tilde{\rho}_\lambda > 0$ and, consequently, $0 \in \mathcal{X}_s$, as done in the proof of Theorem 3.1. Indeed, from (3.8) evaluated for the presented augmented matrices, we have that $\tilde{\rho}_i > 2\tilde{\ell}'_i \tilde{h} = 2\ell'_i h$ and, as $x_e \in X_e$ implies that $\ell_\lambda = 0$, we can conclude that $\tilde{\rho}_\lambda > 0$. Notice that inequality (3.8) multiplied to the left by $\text{diag}(\tilde{\Gamma}', I, \tilde{\Gamma}')$ and to the right by its transpose, yields

$$\begin{bmatrix} \tilde{\Gamma}' \tilde{P} \tilde{\Gamma} - \tilde{\Gamma}' \tilde{Q}_i \tilde{\Gamma} & \bullet & \bullet \\ \tilde{c}'_i \tilde{\Gamma} + \tilde{h}'(I - \tilde{A}_i) \tilde{\Gamma} & \tilde{\rho}_i - \tilde{\ell}'_i \tilde{h} - \tilde{h}' \tilde{\ell}_i & \bullet \\ \tilde{\Gamma}' \tilde{P} \tilde{A}_i \tilde{\Gamma} & \tilde{\Gamma}' \tilde{P} \tilde{\ell}_i & \tilde{\Gamma}' \tilde{P} \tilde{\Gamma} \end{bmatrix} > 0, \quad i \in \mathbb{K} \quad (3.61)$$

whereas inequality (3.9), multiplied to the left by $\text{diag}(\tilde{\Gamma}', I, I)$ and to the right by its transpose, produces

$$\begin{bmatrix} \tilde{\Gamma}'\tilde{Q}_\lambda\tilde{\Gamma} & \bullet & \bullet \\ -\tilde{c}'_\lambda\tilde{\Gamma} & 1 - \tilde{\rho}_\lambda & \bullet \\ \tilde{W}\tilde{\Gamma} & -\tilde{W}\tilde{\mu} & \tilde{W} \end{bmatrix} \geq 0 \quad (3.62)$$

From the fact that $\tilde{P}\tilde{S} = I$, we obtain the identities

$$\begin{aligned} YX + VU' &= I, & YU + V\hat{X} &= 0 \\ V'X + \hat{Y}U' &= 0, & V'U + \hat{Y}\hat{X} &= I \end{aligned} \quad (3.63)$$

which allows us to calculate

$$\tilde{\Gamma}'\tilde{P}\tilde{\Gamma} = \begin{bmatrix} X & \bullet \\ I & Y \end{bmatrix}, \quad \tilde{\Gamma}'\tilde{P}\tilde{A}_i\tilde{\Gamma} = \begin{bmatrix} A_iX & A_i \\ \Phi_i & YA_i + V\hat{B}_iC_i \end{bmatrix}, \quad \tilde{\Gamma}'\tilde{P}\tilde{\ell}_i = \begin{bmatrix} \ell_i \\ Y\ell_i + V\hat{\ell}_i \end{bmatrix}, \quad \tilde{W}\tilde{\Gamma} = \begin{bmatrix} WX & W \\ 0 & 0 \end{bmatrix} \quad (3.64)$$

$$\Gamma'\tilde{A}'_i\tilde{h} = \begin{bmatrix} XA'_ih \\ A'_ih \end{bmatrix}, \quad \tilde{\Gamma}'\tilde{Q}_i\tilde{\Gamma} = \begin{bmatrix} \Psi_i & \bullet \\ QX + \bar{Q}U' & Q \end{bmatrix}, \quad \tilde{\Gamma}'\tilde{h} = \begin{bmatrix} Xh \\ h \end{bmatrix}, \quad \tilde{\Gamma}'\tilde{c}_i = \begin{bmatrix} Xc + U\hat{c}_i \\ c \end{bmatrix} \quad (3.65)$$

with $\Phi_i = YA_iX + V\hat{B}_iC_iX + V\hat{A}_iU'$ and $\Psi_i = XQX + X\bar{Q}U' + U\bar{Q}'X + U\hat{Q}_iU'$. Replacing these identities in (3.61) and (3.62) and multiplying both sides of the first one by $\text{diag}(Z, I, I, Z, I)$ and the second one by $\text{diag}(Z, I, I, I, I)$, with $Z = X^{-1}$, we obtain

$$\begin{bmatrix} Z - Z\Psi_iZ & \bullet & \bullet & \bullet & \bullet \\ Z - Q - \bar{Q}U'Z & Y - Q & \bullet & \bullet & \bullet \\ \Pi_i & c' + h'(I - A_i) & \rho_i - 2\ell'_ih & \bullet & \bullet \\ ZA_i & ZA_i & Z\ell_i & Z & \bullet \\ \Phi_iZ & YA_i + V\hat{B}_iC_i & Y\ell_i + V\hat{\ell}_i & Z & Y \end{bmatrix} > 0 \quad (3.66)$$

$$\begin{bmatrix} Z\Psi_\lambda Z & \bullet & \bullet & \bullet \\ Q + \bar{Q}U'Z & Q & \bullet & \bullet \\ -c' - \tilde{c}'_\lambda U'Z & -c' & 1 - \tilde{\rho}_\lambda & \bullet \\ W & W & -W\mu & W \end{bmatrix} \geq 0 \quad (3.67)$$

with $\Pi_i = c' + \hat{c}'_iU'Z + h'(I - A_i)$, respectively. By replacing the variables $R_i = ZU\hat{Q}_iU'Z$, $J = \bar{Q}U'Z$, $M_i = V\hat{A}_iU'Z$, $L_i = V\hat{B}_i$, $\nu_i = V\hat{\ell}_i$, $d'_i = \hat{c}'_iU'Z$, notice that both (3.66) and (3.67) become linear matrix inequalities and independent of U and V . This shows that, without loss of generality, one of these matrix variables can be chosen arbitrarily such that $\det(V) \neq 0$ or $\det(U) \neq 0$, while the other has to be determined from the identity $YX + VU' = I$, which is one of the conditions that assures $\tilde{P}\tilde{S} = I$. Therefore, choosing matrix $U = X$ we have $V = Z - Y$, which provides the filter matrices (3.58). Moreover, inequalities (3.66) and (3.67) become (3.56) and (3.57), which assure the validity of (3.8) and (3.9) applied to the augmented system (3.48) and considering the structured matrices (3.50), (3.53) and (3.60). It is worth remembering that the structure of (3.50) is essential to make the switching rule dependent only on the filter state variable as demonstrated in (3.51). Finally, notice that $\tilde{\xi} = \tilde{\xi}_c \in \mathcal{X}$ and $\tilde{\xi} = 0 \in \mathcal{X}$ by the same arguments drawn in the state feedback case.

The proof is concluded. \square

We have just generalized Theorem 3.1 to cope with dynamic output feedback control design and the associated optimization problem is still a convex one. An important remark about this result is that LMIs (3.56) and (3.57) do not bound Y from above, a fact that may cause badly scaled filter matrices when the optimization problem is solved. Indeed, (3.57) does not depend on Y . To show that Y can be taken arbitrarily large in (3.56) as a feasible solution (whenever one exists), switch its second and fourth lines and columns and then, its second and third lines and columns to obtain the equivalent inequality

$$\begin{bmatrix} Z - Q - J - J' - \hat{Q}_i & \bullet & \bullet & \bullet & \bullet \\ c' + \hat{c}'_i + h'(I - A_i) & \rho_i - 2\ell'_i h & \bullet & \bullet & \bullet \\ ZA_i & Z\ell_i & Z & \bullet & \bullet \\ Z - Q - J & c + (I - A'_i)h & A'_i Z & Y - Q & \bullet \\ YA_i + L_i C_i + M_i & Y\ell_i + \nu_i & Z & YA_i + L_i C_i & Y \end{bmatrix} > 0 \quad (3.68)$$

Adopting new variables $\mathcal{Y}_i = YA_i + L_i C_i + M_i$ and $\mathcal{N}_i = Y\ell_i + \nu_i$, let us apply the Schur Complement Lemma with respect to the matrix block starting from (1, 1) to (3, 3), which results in two equivalent conditions

$$\mathcal{W}_i = \begin{bmatrix} Z - Q - J - J' - \hat{Q}_i & \bullet & \bullet \\ c' + \hat{c}'_i + h'(I - A_i) & \rho_i - 2\ell'_i h & \bullet \\ ZA_i & Z\ell_i & Z \end{bmatrix} > 0 \quad (3.69)$$

$$\begin{bmatrix} Y - Q & \bullet \\ YA_i + L_i C_i & Y \end{bmatrix} - \mathcal{U}_i \mathcal{W}_i^{-1} \mathcal{U}'_i > 0 \quad (3.70)$$

for all $i \in \mathbb{K}$, where

$$\mathcal{U}_i = \begin{bmatrix} Z - Q - J & c + (I - A'_i)h & A'_i Z \\ \mathcal{Y}_i & \mathcal{N}_i & Z \end{bmatrix} \quad (3.71)$$

Notice that Y and L_i are not present in (3.69) and can be taken arbitrarily large in (3.70) without restricting the feasibility domain regarding the remaining variables. As a consequence, replacing (Y, L_i) by $(\alpha Y, \alpha L_i)$ with $\alpha \rightarrow \infty$, we have from (3.58) written in terms of \mathcal{Y}_i and \mathcal{N}_i that

$$\hat{A}_i = A_i + Y^{-1}L_i C_i, \quad \hat{B}_i = -Y^{-1}L_i, \quad \hat{\ell}_i = \ell_i \quad (3.72)$$

which shows that the proposed filter also admits an observer form. Moreover, from (3.70) we have that

$$\begin{bmatrix} Y - Q & \bullet \\ YA_i + L_i C_i & Y \end{bmatrix} > 0 \quad (3.73)$$

and, therefore, (3.56) becomes equivalent to $\mathcal{W}_i > 0$ together with $(A_i - \hat{B}_i C_i)'Y(A_i - \hat{B}_i C_i) - Y < -Q < 0$, where this last constraint holds whenever pairs (A_i, C_i) are **quadratically detectable**, that is, there exist gains \hat{B}_i , $i \in \mathbb{K}$, such that the closed-loop matrices $A_i - \hat{B}_i C_i$, $i \in \mathbb{K}$, share a common quadratic Lyapunov function. With this in mind, the following theorem is of great importance to show that any set of attraction \mathcal{X} obtained

from the state-dependent switching function of Theorem 3.1 is also a set of attraction for the output-dependent switching strategy of Theorem 3.4.

Theorem 3.5. *For the discrete-time switched affine system (3.2) with $w[n] = 0$, $\forall n \in \mathbb{N}$, consider P^*, h^*, W^*, g^* , Q_i^*, c_i^*, ρ_i^* , $\forall i \in \mathbb{K}$ forming the optimal solution to Theorem 3.1 and assuring the existence of a minimal ellipsoidal set of attraction \mathcal{X} and the corresponding state-dependent switching function. The design conditions (3.56) and (3.57) for the output-dependent switching function in Theorem 3.4 hold for the same set of attraction \mathcal{X} if and only if matrix pairs (A_i, C_i) , $i \in \mathbb{K}$ are quadratically detectable.*

Proof: Assuming that (3.56) and (3.57) hold for the set of attraction \mathcal{X} defined by W^* and h^* , the necessity comes straightly from the fact that (3.56) implies (3.70), which implies quadratic detectability of the pairs (A_i, C_i) , $\forall i \in \mathbb{K}$.

The proof of the sufficiency consists in demonstrating that whenever (3.8) and (3.9) are verified for an arbitrary pair g^*, W^* , there exist matrices satisfying (3.56) and (3.57) for the same g^*, W^* . Let us firstly show that (3.56) holds under the assumptions made in the theorem statement. As discussed previously, notice that this LMI is equivalent to (3.69)-(3.70), which can be verified using the Schur Complement Lemma. Taking an arbitrary $\epsilon > 0$ and choosing $Z = P^*$, $h = h^*$, $Q = W^* + \epsilon I$, $J = -\epsilon I$, $\hat{Q}_i = Q_i^* - W^* + \epsilon I$, $c = -g^*$, $\hat{c}_i = g^* + c_i^*$ and $\rho_i = \rho_i^*$ we have that (3.69) becomes (3.8). Moreover, given the quadratic detectability of (A_i, C_i) , $i \in \mathbb{K}$, inequality (3.70) is always satisfied by taking Y and \hat{B}_i , $i \in \mathbb{K}$ that fulfill

$$(A_i - \hat{B}_i C_i)' Y (A_i - \hat{B}_i C_i) - Y < 0, \quad i \in \mathbb{K} \quad (3.74)$$

Now, to show that (3.57) is also true, let us multiply it to the left by Θ and to the right by Θ' with

$$\Theta = \begin{bmatrix} I & 0 & 0 & 0 \\ 0 & 0 & I & 0 \\ 0 & 0 & 0 & I \\ 0 & I & 0 & -I \end{bmatrix} \quad (3.75)$$

and replace the chosen variables together with $W = W^*$ and $g = g^*$, yielding

$$\begin{bmatrix} Q_\lambda^* & \bullet & \bullet & \bullet \\ -c_\lambda^{*\prime} & 1 - \rho_\lambda^* & \bullet & \bullet \\ W^* & g^* & W^* & \bullet \\ 0 & 0 & 0 & \epsilon I \end{bmatrix} > 0 \quad (3.76)$$

This is straightforwardly verified to be true from (3.9). The proof is concluded. \square

This result is important since it demonstrates how the design of the switching function and the full-order switched filter can be decoupled and the same optimal ellipsoidal set of attraction given by a state-dependent switching function (from Theorem 3.1) can be assured. It is somewhat surprising that the volume of the minimal ellipsoidal set of attraction for an output-dependent switching function does not depend on matrices C_i , $i \in \mathbb{K}$. Actually, if the system is practically stabilizable under state-dependent feedback, the only requirement for practical stability in the output-dependent case is the quadratic detectability of pairs (A_i, C_i) . Hence, for C_i

fulfilling this constraint, filter matrices can be readily computed from (3.72) with Y and L_i satisfying the LMI (3.73) and the output-dependent switching function is given by the same matrices as the state-dependent one, which is assured from the particular choice for $(\hat{Q}_i, \hat{c}_i, \rho_i)$, made in proof of Theorem 3.5.

Finally, notice that if the designer wants to solve the more general optimization problem in Theorem 3.4, numerical instability may be encountered given that Y is unbounded. To overcome this issue, we propose a two-step design:

1. Calculate optimal matrices W and g defining the minimum volume ellipsoidal set of attraction \mathcal{X} from the convex optimization problem (3.7), which regards the state-feedback case.
2. Obtain the remaining matrices from one of following convex or quasi-convex optimization problems:
 - Well scaled matrices can be obtained by employing

$$\inf_{Z, Q, \hat{Q}_i, Y, J, L_i, M_i, \nu_i, c, \hat{c}_i, h, \rho_i} \text{tr}(2Y - Z) \quad \text{s.t. (3.56)-(3.57)} \quad (3.77)$$

which is equivalent to minimize $\text{tr}(\tilde{P})$. This can be readily demonstrated from identities (3.63) along with the discussion in the proof of Theorem 3.4.

- Better transient responses can be found from

$$\inf_{Z, Q, \hat{Q}_i, Y, J, L_i, M_i, \nu_i, c, \hat{c}_i, h, \rho_i} \text{tr}(Z) \quad \text{s.t. (3.56)-(3.57)} \quad (3.78)$$

but matrices \hat{Q}_i , $i \in \mathbb{K}$, may be badly scaled. For this case, it has been empirically noticed that adopting new matrices $\hat{G}_i = \hat{Q}_i - Q$ provides a well-scaled equivalent switching function

$$\sigma[n] = u(\hat{\xi}[n]) = \arg \min_{i \in \mathbb{K}} -\hat{\xi}[n]' \hat{G}_i \hat{\xi}[n] + 2\hat{c}'_i \hat{\xi}[n] + \rho_i \quad (3.79)$$

- Similarly to what was done in Egidio et al. (2017), a minimum decay-rate guarantee $\beta = \sqrt{1 - \alpha}$ can be optimized. This is done by solving the generalized eigenvalue problem (see Boyd et al. (1994))

$$\inf_{Z, Q, \hat{Q}_i, Y, J, L_i, M_i, \nu_i, c, \hat{c}_i, h, \rho_i, \alpha} \alpha \quad \text{s.t. (3.57), } \alpha \leq 1 \text{ and} \quad (3.80)$$

$$\begin{bmatrix} \alpha Z - Q - J - J' - \hat{Q}_i & \bullet & \bullet & \bullet & \bullet \\ \alpha Z - Q - J & \alpha Y - Q & \bullet & \bullet & \bullet \\ c' + \hat{c}'_i + h'(I - A_i) & c' + h'(I - A_i) & \rho_i - 2\ell'_i h & \bullet & \bullet \\ ZA_i & ZA_i & Z\ell_i & Z & \bullet \\ YA_i + L_i C_i + M_i & YA_i + L_i C_i & Y\ell_i + \nu_i & Z & Y \end{bmatrix} > 0 \quad (3.81)$$

Three secondary optimization functions were presented which allows obtaining possibly different switching functions and filters for the same minimal ellipsoidal set of attraction \mathcal{X} . Further theoretical discussions about this topic are left for future works, as well as the adoption of other objective functions. The following example will illustrate these last aspects.

Example 3.3. Let us adopt the same discrete-time switched affine system given in Example 3.1 but now the state is not fully available to be measured. We have only access to the second state variable, which can be used as an input for the full-order switched filter (3.47), responsible to dynamically provide the switching function (3.51) with its state $\hat{\xi}$. The considered output matrices are $C_i = [0 \ 1]$, $\forall i \in \mathbb{K}$ and the desired equilibrium point is still the origin. To assure its global practical stability, the optimization problem given in Theorem 3.4 was solved providing matrices

$$W = \begin{bmatrix} 1.8397 & -0.2486 \\ -0.2486 & 1.8290 \end{bmatrix}, \quad g = 0, \quad (3.82)$$

which define the ellipsoidal set of attraction \mathcal{X} as in (3.59) with area 1.7826. Not surprisingly, this is the same (for the given precision) as the one obtained in the state-feedback case (see Example 3.1). With these matrices given, we could recalculate the remaining optimization variables by the optimization problem (3.77), yielding better-conditioned matrices

$$\hat{A}_1 = \begin{bmatrix} -0.1 & -0.008 \\ 0.4 & 0.032 \end{bmatrix}, \quad \hat{A}_2 = \begin{bmatrix} -0.9 & -0.072 \\ 0.6 & 0.048 \end{bmatrix} \quad (3.83)$$

$$\hat{A}_3 = \begin{bmatrix} 0.3 & 0.024 \\ 1 & 0.08 \end{bmatrix}, \quad \hat{A}_4 = \begin{bmatrix} -0.5 & -0.04 \\ 0.8 & 0.064 \end{bmatrix} \quad (3.84)$$

$$\hat{B}_1 = \begin{bmatrix} 0.8080 \\ -0.8320 \end{bmatrix}, \quad \hat{B}_2 = \begin{bmatrix} 0.8719 \\ 0.4520 \end{bmatrix}, \quad \hat{B}_3 = \begin{bmatrix} 0.4760 \\ 0.6201 \end{bmatrix}, \quad \hat{B}_4 = \begin{bmatrix} 1.0400 \\ 0.2361 \end{bmatrix} \quad (3.85)$$

$$\hat{\ell}_1 = \begin{bmatrix} -0.1 \\ 0 \end{bmatrix}, \quad \hat{\ell}_2 = \begin{bmatrix} 0.2 \\ 0.1 \end{bmatrix}, \quad \hat{\ell}_3 = \begin{bmatrix} 0 \\ -0.1 \end{bmatrix}, \quad \hat{\ell}_4 = \begin{bmatrix} -0.1 \\ 0 \end{bmatrix} \quad (3.86)$$

$$\hat{Q}_1 = \begin{bmatrix} 45.2317 & 15.1743 \\ 15.1743 & -31.3030 \end{bmatrix}, \quad \hat{c}_1 = \begin{bmatrix} 4.7455 \\ 10.5641 \end{bmatrix}, \quad \rho_1 = 2.1527 \quad (3.87)$$

$$\hat{Q}_2 = \begin{bmatrix} -18.1916 & 17.5550 \\ 17.5550 & 5.8980 \end{bmatrix}, \quad \hat{c}_2 = \begin{bmatrix} 0.3083 \\ 9.6440 \end{bmatrix}, \quad \rho_2 = -3.2522 \quad (3.88)$$

$$\hat{Q}_3 = \begin{bmatrix} 5.5572 & -44.9537 \\ -44.9537 & 15.1842 \end{bmatrix}, \quad \hat{c}_3 = \begin{bmatrix} -11.3510 \\ -3.2814 \end{bmatrix}, \quad \rho_3 = 2.9469 \quad (3.89)$$

$$\hat{Q}_4 = \begin{bmatrix} 1.9951 & 13.5361 \\ 13.5361 & -8.2319 \end{bmatrix}, \quad \hat{c}_4 = \begin{bmatrix} 5.6075 \\ -4.7086 \end{bmatrix}, \quad \rho_4 = 2.1527 \quad (3.90)$$

The correspondent filter and switching function assure global practical stability of the origin $x = 0$ and the existence of an ellipsoidal set of attraction \mathcal{X} . State and filter trajectories evolving from $x_0 = [0 \ 5]'$ $\hat{\xi}_0 = 0$ are depicted in Figure 3.4 and the resultant switching sequence, in Figure 3.5. As can be observed, this switched affine system, composed of four unstable subsystems, was also practically stabilized under the output-dependent switching strategy just presented.

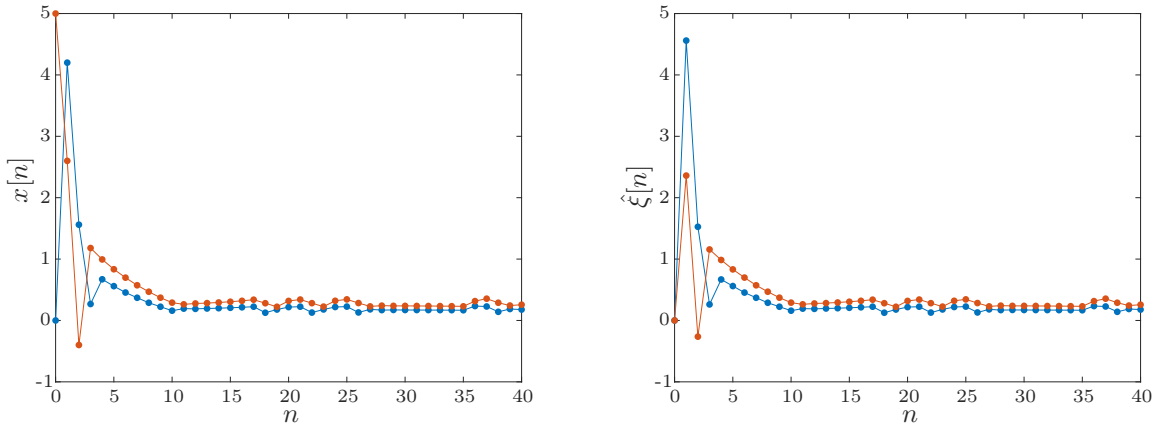


Figure 3.4: System and filter state over time under the output-dependent switching rule.

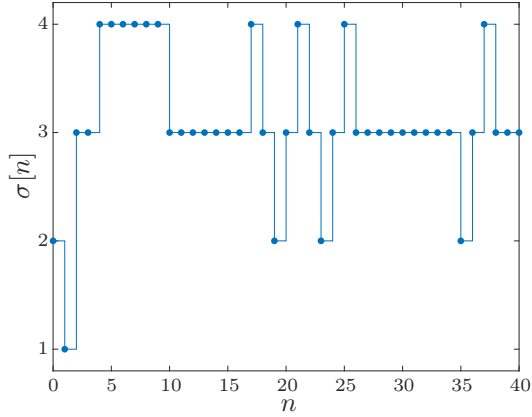


Figure 3.5: Switching signal generated by the output-dependent switching rule.

The second objective function, mentioned at the beginning of this subsection, can be now presented. Compared to the volume minimization, this approach may be very useful in practical applications when the designer is interested in the behavior of a specific controlled output instead of the full state variable $\xi \in \mathbb{R}^{n_x}$. Next corollary introduces the associated convex optimization problem.

Corollary 3.1. Consider the system (3.2) with $w[n], \forall n \in \mathbb{N}$ and let the equilibrium point $x_e \in X_e$ be given with its associated $\lambda \in \Lambda$. If there exist symmetric matrices Z, Q, \hat{Q}_i, Y , matrices J, L_i, M_i , vectors ν_i, c, \hat{c}_i, h , and scalars ρ_i, γ solution to the problem

$$\sup_{Z, Q, \hat{Q}_i, Y, J, L_i, M_i, \nu_i, c, \hat{c}_i, h, \rho_i, \gamma} \gamma \quad \text{s.t. (3.56) and} \quad (3.91)$$

$$\begin{bmatrix} Q + J + J' + \hat{Q}_\lambda - \gamma E'E & \bullet & \bullet \\ Q + J - \gamma E'E & Q - \gamma E'E & \bullet \\ -c' - \hat{c}'_\lambda & -c' & 1 - \rho_\lambda \end{bmatrix} > 0 \quad (3.92)$$

then the output-dependent switching function (3.51) and the filter (3.47) given by matrices (3.58) assure that the

origin is a globally practically stable equilibrium point and that the ball

$$\mathcal{B}_* = \{z \in \mathbb{R}^{n_z} : z' z \leq \gamma^{-1}\} \quad (3.93)$$

is a set of attraction.

Proof: The proof is analogous to the one of Theorem 3.4 and consists in showing that (3.92) is equivalent to (3.57) with $W = \gamma E'E$ and $g = 0$. This can be verified by applying the Schur Complement Lemma to (3.57) with respect to the last row and column. The set of attraction \mathcal{X} becomes thus

$$\{\xi \in \mathbb{R}^{n_x} : \xi' E'E\xi \leq \gamma^{-1}\} \quad (3.94)$$

which is equivalent to (3.93). \square

In certain practical applications this solution can be of greater interest than the volume minimization provided by (3.7), mainly when the idea is to assure a good steady state performance of a specific controlled output. In other words, this design procedure assures that,

$$z[n]' z[n] > \gamma^{-1} \implies \Delta v(\xi[n]) < 0 \quad (3.95)$$

Notice that the rank deficiency of $E'E$ might be a concern related to the boundedness of the set of attraction. Although the ball \mathcal{B}_* may be degenerate in the state-space, the existence of the bounded set of attraction \mathcal{X}_s , as given in (3.15), in its interior is always guaranteed by the strict inequality given in (3.92). Additionally, the same issues previously discussed regarding how matrix Y can grow arbitrarily apply to this approach as well, and a second step design might also be necessary, adapting the problems given in (3.77), (3.78) and (3.80). The following example illustrates the results from Corollary 3.1.

Example 3.4. Let a rectangular differential-drive robot as illustrated in Figure 3.6 (see Siegwart et al. (2011) for more information) which must move in circles on the plane. The forces f_1 and f_2 at the first and second wheels, respectively, are executed by DC motors with neglectable inductance which can be controlled in a bang-bang manner. This means that electronic switches can be commanded by a microprocessor to power each of them with a battery or short circuit them, at each sampling instant.

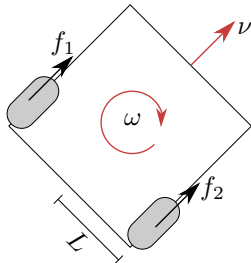


Figure 3.6: Differential-drive robot.

However, due to resource limitations, only one encoder is available and it was attached to the first wheel. This may also represent a fault context, where one of the encoders failed. The continuous-time dynamic

model for linear and rotational velocities $\nu(t)$ and $\omega(t)$ is given by

$$\begin{bmatrix} \dot{\nu}(t) \\ \dot{\omega}(t) \end{bmatrix} = \begin{bmatrix} -2k^2/(Rm) - c/m & 0 \\ 0 & -2L^2k^2/(RJ) - d/J \end{bmatrix} \begin{bmatrix} \nu(t) \\ \omega(t) \end{bmatrix} + \begin{bmatrix} k(u_{1\sigma(t)} + u_{2\sigma(t)})/(Rm) \\ kL(u_{1\sigma(t)} - u_{2\sigma(t)})/(RJ) \end{bmatrix} \quad (3.96)$$

where m is the robot mass, J is its moment of inertia, c and d are viscous friction coefficients, L represents half of its width, R is the armature resistance of the DC motor, k is its electric constant and u_{1i}, u_{2i} are applied voltages to the motor terminals, which depend on switching signal $\sigma(t)$ as shown in Table 3.1.

Table 3.1: Switching states and corresponding applied voltages for the differential-drive robot.

σ	$u_{1\sigma}$	$u_{2\sigma}$
1	0	0
2	0	V_{dc}
3	V_{dc}	0
4	V_{dc}	V_{dc}

The measured linear velocity of the first wheel can be written as

$$y(t) = [1 \quad L] \begin{bmatrix} \nu(t) \\ \omega(t) \end{bmatrix} \quad (3.97)$$

which allows us to define a continuous-time switched affine system. Consider a sampling period of $T = 0.01$ s and that the state of the switches is held constant between sampling instants, the step-invariant discretization procedure given in (2.77) can be applied to obtain an equivalent discrete-time switched affine system as (3.1). System data is given in Table 3.2.

Table 3.2: System parameters adopted for the differential-drive robot.

Quantity	Value	Unit
m	0.4	kg
L	0.2	m
J	$m(2L)^2/12$	kg.m ²
R	5	Ω
k	0.1	V.s/m
c	0.01	N.s/m
d	0.01	N.m.s/rad
V_{dc}	12	V

The desired circular trajectory is defined by $\nu_e = 4$ m/s and $\omega_e = 1$ rad/s which can be expressed as an equilibrium point $x_e = [\nu_e \omega_e]' \in X_e$ associated with $\lambda = [0.7721 \ 0.0054 \ 0.2171 \ 0.0054] \in \Lambda$. Solving the optimization problem of Corollary 3.1 with $E = \text{diag}(1, 6)$ we could obtain a set of attraction \mathcal{B}_* defined by $\gamma = 0.7301$. Taking this optimal solution and solving the problem (3.78) adapted for this case, we obtained the matrices

$$Y = \begin{bmatrix} 1.4649 & 0.0736 \\ 0.0736 & 1.4587 \end{bmatrix} \times 10^8, \quad Z = \begin{bmatrix} 1.0424 & -0.0000 \\ -0.0000 & 0.7024 \end{bmatrix} \times 10^3 \quad (3.98)$$

and the other matrix variables. By means of this solution, the switched full-order filter (3.47) and the

switching function (3.51) were implemented. A numerical simulation provided the state trajectories for the system and the filter depicted in Figure 3.7. Phase portraits for both filter and system state are given in Figure 3.8 along with its initial condition. In the system phase portrait, we highlighted the initial condition and the set of attraction \mathcal{B}_* defined in (3.93), while in the filter phase portrait, regions \mathcal{O}_i , $i \in \mathbb{K}$ for each subsystem were presented. The obtained switching sequence is also shown in Figure 3.9.

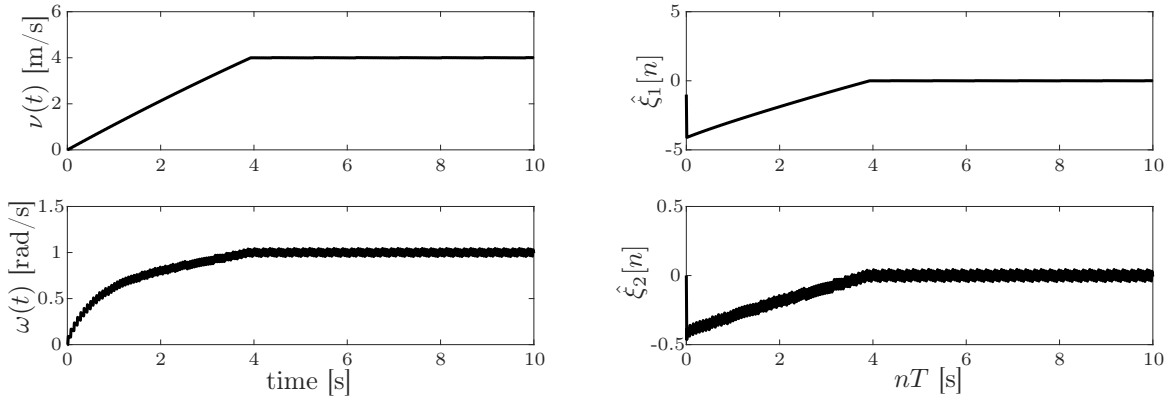


Figure 3.7: System and filter state over time.

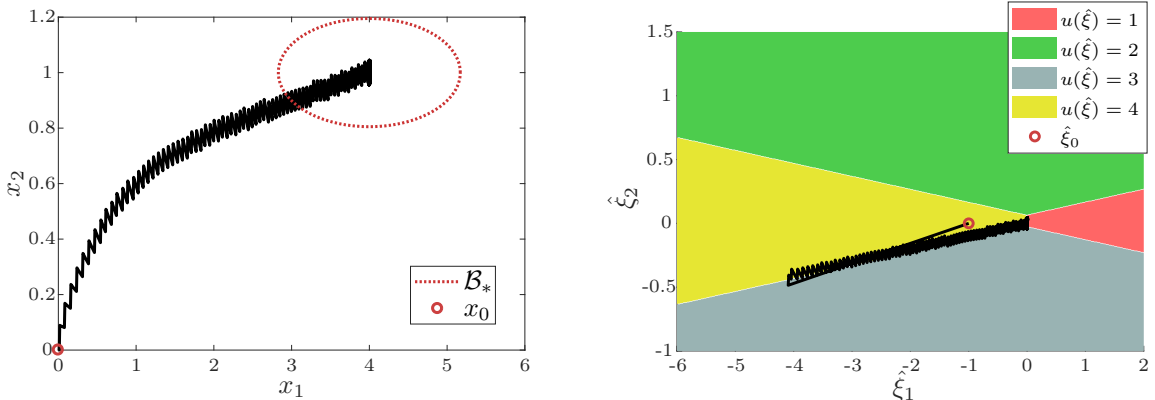


Figure 3.8: Phase portraits for both system and filter.

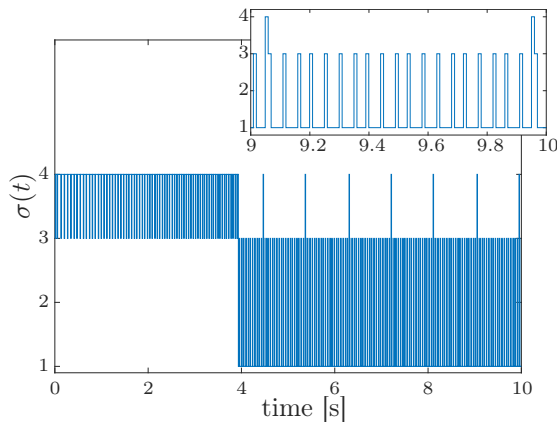


Figure 3.9: Obtained switching signal.

These examples demonstrated how limited information about the system state can be enough for our control methodology to assure global practical stability of a desired x_e . Indeed, the proposed full-order filter and switching function were successful in driving the robot by selecting properly when each motor should be powered, measuring the velocity of a single wheel.

Finally, some discussions regarding the invariance property are in order. Indeed, conditions in Theorem 3.2 are still valid for an augmented system to provide an augmented invariant set of attraction as a level set of the Lyapunov function. The following corollary relies on this fact to assure an invariant set of attraction independent of the filter variable.

Corollary 3.2. *For an optimal solution of Theorem 3.4, let the invariant set of attraction*

$$\tilde{\mathcal{V}} = \{\tilde{\xi} \in \mathbb{R}^{2n_x} : v(\tilde{\xi}) < r\} \quad (3.99)$$

be given by means of a matrix \tilde{P} , a vector h and a scalar $r > 0$, calculated through Theorem 3.2 with \tilde{W} , \tilde{P} and \tilde{h} provided in (3.53) and (3.60). There exists a time instant $n_0 \in \mathbb{N}$ such that for all $n \geq n_0$ the set

$$\mathcal{V} = \{\xi \in \mathbb{R}^{n_x} : (\xi - h)'(Y - V\hat{Y}^{-1}V')(\xi - h) < r\} \quad (3.100)$$

is an invariant set of attraction.

Proof: Consider the first instant n_0 such that $\tilde{\xi}[n_0] \in \tilde{\mathcal{V}}$. Due to Lemma C.1, the ellipsoid \mathcal{V} is the projection of $\tilde{\mathcal{V}}$ onto the subspace generated by the system state-space. For this reason, we can conclude that $\xi[n] \in \mathcal{V}$ for all $n \geq n_0$. \square

Obtaining an invariant set of attraction for all $n \in \mathbb{N}$ dependent only on the system state variable seems to be an intricate task, as the switching, critical for stability, is governed by the filter state. Notice that, as the invariant set of attraction $\tilde{\mathcal{V}}$ was not minimized, applying this corollary may lead to a set \mathcal{V} with large volume. For this reason, one may generalize Theorem 3.3 in a similar way to what was done to Theorem 3.1 to obtain conditions from Theorem 3.4, minimizing the projection set \mathcal{V} given in (3.100). However, I rather focus on minimizing the set of attraction \mathcal{X} exclusively, as it is clearly smaller than \mathcal{V} and sufficient to assure practical stability (see Lemma 3.2).

The next subsection presents novel practical stability conditions, based on a more elaborate Lyapunov function.

3.2.3 Min-type Lyapunov Functions

As the reader might have noticed so far, all stability conditions regarding discrete-time switched affine systems to date are based on quadratic Lyapunov functions. Let us now discuss how a special class of Lyapunov functions can be employed to reduce conservativeness and avoid some constraints. Firstly, notice that conditions in Deaecto and Egidio (2016), Deaecto and Geromel (2017) and Theorems 3.1 and 3.4 require that the desired equilibrium point x_e must belong to a specific set X_e (as defined in (3.5)) associated to a vector $\lambda \in \Lambda$ for which A_λ has to be a Schur stable matrix. Our goal is to obtain design conditions for a switching function assuring global practical stability of x_e without imposing that it belongs to X_e nor any other specific set. Additionally, the

existence of $\lambda \in \Lambda$ such that A_λ is Schur stable will no longer be required. This is done by employing a min-type Lyapunov function

$$v(\xi) = \min_{i \in \mathbb{K}} \xi' P_i \xi \quad (3.101)$$

and its associated switching function

$$\sigma[n] = u(\xi[n]) = \arg \min_{i \in \mathbb{K}} \xi[n]' P_i \xi[n] \quad (3.102)$$

which are common in the context of linear systems (see Section 2.4) but have never been adopted in the study of switched affine systems. Before presenting the results, let us recall an important family of matrices, which will be of great importance in our developments. The subclass of Metzler matrices for the discrete-time switched linear systems was previously defined as

$$\mathcal{M}_d = \left\{ \Pi = \{\pi_{ki}\} \in \mathbb{R}^{N \times N} : \sum_{k=1}^N \pi_{ki} = 1, \pi_{ki} \geq 0 \right\} \quad (2.114 \text{ r.})$$

and contains matrices with interesting properties. Due to the Gershgorin Circle Theorem, all eigenvalues of a matrix $\Pi \in \mathcal{M}_d$ are located in the complex plane inside circles centered at $\pi_{ii} \geq 0$ with radius $\sum_{k \in \mathbb{K} \setminus \{i\}} \pi_{ki} = 1 - \pi_{ii}$ and, therefore, all eigenvalues are inside the unit circle. Besides, since $e' \Pi = e'$ with $e' = [1 \ 1 \ \cdots \ 1]$, the Frobenius-Perron Theorem indicates that the eigenvalue of maximum modulus is equal to one (Perron-Frobenius eigenvalue) and the associated eigenvector is positive componentwise. Let us also recall the definition

$$P_{\pi i} = \sum_{k \in \mathbb{K}} \pi_{ki} P_k \quad (3.103)$$

which will be widely used afterward. The next theorem presents the conditions for which the switching function (3.102) is globally practically stabilizing.

Theorem 3.6. *Consider the system (3.1) and let $x_e \in \mathbb{R}^{n_x}$ be given. If there exist symmetric matrices W , P_i , a Metzler matrix $\Pi \in \mathcal{M}_d$, a vector g of compatible dimensions and positive scalars β_i , solution to the optimization problem*

$$\inf_{P_i, \Pi, W, h, \beta_i} -\ln(\det(W)) \quad \text{s.t.} \quad (3.104)$$

$$\begin{bmatrix} \beta_i P_i & \bullet & \bullet & \bullet \\ 0 & 1 & \bullet & \bullet \\ \beta_i P_{\pi i} A_i & \beta_i P_{\pi i} \ell_i & \beta_i P_{\pi i} & \bullet \\ W & g & 0 & W \end{bmatrix} > 0, \quad i \in \mathbb{K} \quad (3.105)$$

then the state-dependent switching function (3.102) assures that the set centered at $\mu = -W^{-1}g$ given by

$$\mathcal{E}_* = \{\xi \in \mathbb{R}^{n_x} : (\xi - \mu)' W (\xi - \mu) \leq 1\} \quad (3.106)$$

is an ellipsoidal set of attraction for the system.

Proof: Consider an arbitrary trajectory of the system (3.2) and that at an instant of time $n \in \mathbb{N}$ the switching rule is $\sigma[n] = u(\xi[n]) = i \in \mathbb{K}$. To ease the notation we drop the time dependency of the variables denoting

$\xi[n] = \xi$. The Lyapunov function (3.101) provides

$$\begin{aligned}\Delta v(\xi) &= \min_{\kappa \in \mathbb{K}} (A_i \xi + \ell_i)' P_\kappa (A_i \xi + \ell_i) - \xi' P_i \xi \\ &= \min_{\lambda \in \Lambda} (A_i \xi + \ell_i)' P_\lambda (A_i \xi + \ell_i) - \xi' P_i \xi \\ &\leq (A_i \xi + \ell_i)' P_{\pi i} (A_i \xi + \ell_i) - \xi' P_i \xi \\ &= \xi' (A_i' P_{\pi i} A_i - P_i) \xi + 2\xi' c_i + \rho_i\end{aligned}\quad (3.107)$$

where $c_i = A_i' P_{\pi i} \ell_i$ and $\rho_i = \ell_i' P_{\pi i} \ell_i$. Define the set \mathcal{X}_s as being $\mathcal{X}_s = \bigcup_{i \in \mathbb{K}} \mathcal{E}_i$ with

$$\mathcal{E}_i = \{\xi \in \mathbb{R}^{n_x} : (\xi - \mu_i)' Q_i (\xi - \mu_i) \leq c_i' Q_i^{-1} c_i + \rho_i\} \quad (3.108)$$

where $\mu_i = Q_i^{-1} c_i$ and $A_i' P_{\pi i} A_i - P_i = -Q_i$. Making $Q_i > 0$ and considering that the inequality (3.107) holds for every $u(\xi) = i \in \mathbb{K}$, we have the following properties: $0 \in \mathcal{X}_s$ and $\Delta v(\xi) < 0, \forall \xi \notin \mathcal{X}_s$. Notice that, \mathcal{X}_s is a nonconvex set of attraction whose volume is very hard to minimize or even compute. Then, let us find the smallest ellipsoid \mathcal{E} which contains \mathcal{X}_s in its interior. Indeed, from inequalities (3.105), eliminating the second and fourth rows and columns, it is simple to see that $Q_i = P_i - A_i' P_{\pi i} A_i > 0, \forall i \in \mathbb{K}$. Moreover, replacing $g = -W\mu$ in (3.105) and performing the Schur Complement with respect to the last two rows and columns we obtain

$$\begin{bmatrix} W & \bullet \\ -\mu' W & \mu' W \mu - 1 \end{bmatrix} < \beta_i \begin{bmatrix} Q_i & \bullet \\ -c_i' & -\rho_i \end{bmatrix}, \quad i \in \mathbb{K} \quad (3.109)$$

which multiplied to the right by $[\xi' \ 1]'$ and to the left by its transpose, assures by S-procedure (see Appendix Subsection A.4) that the ellipsoid \mathcal{E} in (3.106) contains the union of sets \mathcal{E}_i . The objective function is responsible for minimizing the volume of \mathcal{E} . The proof is concluded. \square

Concerning this last theorem, the first point to be highlighted is that the set of attraction of interest is actually

$$\mathcal{X} = \bigcup_{i \in \mathbb{K}} (\mathcal{E}_i \cap \mathcal{O}_i) \quad (3.110)$$

with the operating regions given as

$$\mathcal{O}_i = \bigcap_{j \in \mathbb{K} \setminus \{i\}} \{\xi \in \mathbb{R}^{n_x} : \xi' (P_i - P_j) \xi \leq 0\} \quad (3.111)$$

which is clearly smaller than the set \mathcal{X}_s considered in the proof of Theorem 3.6. Indeed, due to the switching rule $u(\xi) = i$, the set \mathcal{X} is determined taking into account that the ellipsoid \mathcal{E}_i is considered only within the region \mathcal{O}_i . Geometrically, \mathcal{X} represents the union of N ellipsoids, each of them intersected with $N - 1$ cones. A graphical representation of one possible set of attraction \mathcal{X} for $N = 2$ generated from Theorem 3.6 is depicted in Figure 3.10, along with ellipsoids $\mathcal{E}_1, \mathcal{E}_2$ and \mathcal{E}_* , switching surfaces \mathcal{C} and operating regions \mathcal{O}_1 and \mathcal{O}_2 , wherein the designed switching function chooses $u(\xi) = 1$ and $u(\xi) = 2$, respectively.

More accurate design conditions, which take into account the intersections of (3.110), could be obtained

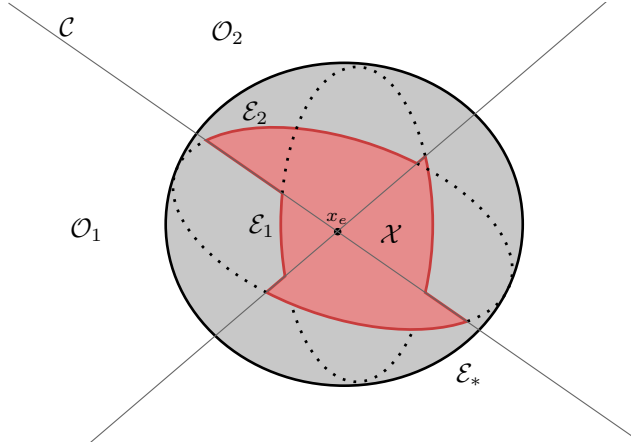


Figure 3.10: Graphical representation of a nonconvex set of attraction provided by Theorem 3.6.

whenever there exist scalars $\theta_{ij} > 0$ such that the inequalities

$$\begin{bmatrix} W & \bullet \\ -\mu'W & \mu'W\mu - 1 \end{bmatrix} < \beta_i \begin{bmatrix} Q_i + \sum_{j \in \mathbb{K} \setminus \{i\}} (\theta_{ij}/\beta_i)(P_i - P_j) & \bullet \\ -c'_i & -\rho_i \end{bmatrix}$$

replace (3.109) for all $i \in \mathbb{K}$. This implies the replacement of the first main diagonal block of (3.105) by $\beta_i P_i + \sum_{j \in \mathbb{K} \setminus \{i\}} \theta_{ij}(P_i - P_j)$. There is no doubt that the new conditions obtained after this replacement are extremely difficult to solve because they imply in searching for $N^2 - N$ new parameters besides the $N^2 - 1$ already existent in Theorem 3.6.

Notice that in this theorem the conditions form a nonconvex optimization problem due to the product of variables $\{\Pi, P_i, \beta_i\}$. A manner to solve (3.104) is by searching $N^2 - N$ elements of the Metzler matrix Π plus $N - 1$ positive scalars since, without loss of generality, we can assume that one of the N free scalars β_i is equal to one. This can be simply verified by replacing $P_i = S_i/\beta_1$ and defining $\psi_i = \beta_i/\beta_1$ in (3.105). With some abuse of notation, we represent $P_i \rightarrow S_i$ and $\beta_i \rightarrow \psi_i$ because this choice does not modify the result and the developments afterward. This confirms that we can fix $\beta_1 = 1$ in (3.105) and let the scalars $\beta_i > 0, \forall i \in \mathbb{K} \setminus \{1\}$.

To obtain more conservative, but simpler-to-solve conditions, where the only parameters to be searched are those of the Metzler matrix, we can consider $\beta_i = \beta > 0, \forall i \in \mathbb{K}$, as stated in the next corollary.

Corollary 3.3. *Theorem 3.6 remains valid whenever inequalities (3.105) are replaced by*

$$\begin{bmatrix} P_i & \bullet & \bullet & \bullet \\ 0 & 1 & \bullet & \bullet \\ P_{\pi i}A_i & P_{\pi i}\ell_i & P_{\pi i} & \bullet \\ W & g & 0 & W \end{bmatrix} > 0, \quad i \in \mathbb{K} \quad (3.112)$$

for all $P_i > 0$.

Proof: The proof comes from (3.105) by making $\beta_i = \beta > 0$ and redefining $P_i \rightarrow \beta P_i$. \square

About this result, some remarks are in order. Notice that, when compared to conditions of Theorem 3.6, the ones of this corollary are numerically more amenable and do not seem to be too restrictive as it will be

illustrated in Example 3.6. For a two subsystems case, the solution is obtained without difficulty by performing a bidimensional search and solving a set of LMIs. However, for a greater number of subsystems, we can adopt a more conservative but simpler-to-solve condition proposed in Geromel and Colaneri (2006b), derived from a Metzler matrix with equal elements in the main diagonal, which reduces the dimension of variables to be searched to one. Another point is that the condition for existence of a set of attraction proposed in Theorem 3.6 and Corollary 3.3 is

$$A_i' P_{\pi i} A_i - P_i < 0, \quad \forall i \in \mathbb{K} \quad (3.113)$$

and it contains the inequality

$$\sum_{i \in \mathbb{K}} \lambda_i A_i' S A_i - S < 0 \quad (3.114)$$

with $S > 0$ and $\lambda \in \Lambda$, as a particular case. At this point, recall that inequality (3.114) is the condition for the existence of a set of attraction in references Deaecto and Egidio (2016) and Deaecto and Geromel (2017), being the latter equivalent to Theorem 3.1 (see discussions after this theorem for further details). As it has been already mentioned, both references take into account a quadratic Lyapunov function (3.6), with $h = 0$ in Deaecto and Egidio (2016). Actually, conditions (3.113) and (3.114) are equivalent for the particular case where we restrict the Metzler matrices to those with equal columns $[\lambda \cdots \lambda] \in \mathcal{M}_d$, $\lambda \in \Lambda$, for which $P_{\pi i} = P_\lambda$. With this choice, inequality (3.113) multiplied by λ_i and summed up from $i = 1$ to N provides (3.114) for $S = P_\lambda$. Conversely, let us define $P_i = A_i' S A_i + \epsilon I > 0$ for all $i \in \mathbb{K}$ and $\epsilon > 0$. Hence, using (3.114) we have

$$\begin{aligned} P_\lambda - S &= \sum_{i \in \mathbb{K}} \lambda_i A_i' S A_i - S + \epsilon I \\ &\leq 0 \end{aligned} \quad (3.115)$$

for $\epsilon > 0$ sufficiently small. Thus, as a consequence

$$A_i' P_\lambda A_i - P_i \leq A_i' S A_i - P_i = -\epsilon I < 0 \quad (3.116)$$

which enables us to conclude that (3.113) with $P_{\pi i} = P_\lambda$ is satisfied. The first inequality comes from (3.115) and the second is obtained replacing $P_i = A_i' S A_i + \epsilon I$, see Fioravanti et al. (2013) for more details. The comparison of volumes with the cited references will be made numerically in Examples 3.6 and 3.7.

At this point, an interesting question that might emerge is why not apply a general min-type Lyapunov function with the structure $V(\xi) = \min_{i \in \mathbb{K}} (\xi - \xi_{ci})' P_i (\xi - \xi_{ci})$ where ξ_{ci} is determined adequately to minimize some upper bound of $\Delta V(\xi)$, as in Deaecto and Geromel (2017), or directly from the optimization procedure, as in Theorem 3.1. Unfortunately, the first option is not possible. Indeed, assuming that for an arbitrary instant of time $n \in \mathbb{N}$ the switching function is $\sigma[n] = u(\xi[n]) = i \in \mathbb{K}$, we have

$$\Delta V(\xi) \leq f_{ui}(\xi, \xi_{ci}) \quad (3.117)$$

where

$$f_{ui}(\xi, \xi_{ci}) = \begin{bmatrix} \xi \\ \xi_{ci} \end{bmatrix}' \mathcal{Q}_i \begin{bmatrix} \xi \\ \xi_{ci} \end{bmatrix} + 2\mathcal{C}_i' \begin{bmatrix} \xi \\ \xi_{ci} \end{bmatrix} + \rho_i \quad (3.118)$$

with $\rho_i = \ell'_i P_{\pi i} \ell_i$ and

$$\mathcal{Q}_i = \begin{bmatrix} -Q_i & \bullet \\ P_i - P_{\pi i} A_i & P_{\pi i} - P_i \end{bmatrix}, \quad \mathcal{C}'_i = \begin{bmatrix} A'_i P_{\pi i} \ell_i \\ -P_{\pi i} \ell_i \end{bmatrix}' \quad (3.119)$$

Notice that it is not possible to determine the upper bound

$$\Delta V(\xi) \leq \min_{\xi_{ci} \in \mathbb{R}^{n_x}} \max_{\xi \in \mathbb{R}^{n_x}} f_{ui}(\xi, \xi_{ci}) \quad (3.120)$$

because the function $f_{ui}(\xi, \xi_{ci})$ is concave with respect to ξ but it is not convex with respect to ξ_{ci} since

$$\begin{aligned} P_{\pi i} - P_i &= \sum_{j \in \mathbb{K} \setminus \{i\}} \pi_{ji} P_j - (1 - \pi_{ii}) P_i \\ &= \sum_{j \in \mathbb{K} \setminus \{i\}} \pi_{ji} (P_j - P_i) \end{aligned} \quad (3.121)$$

is a sign undefined matrix. Hence, the upper bound in (3.120) does not admit a saddle point. On the other hand, letting ξ_{ci} to be determined from the optimization procedure is a complex task, since the introduction of ξ_{ci} terms in inequalities (3.105) generate several bilinear terms and their linearization is left for future works.

The results presented so far regard the volume minimization of an ellipsoid as a manner of minimizing the volume of the set of attraction \mathcal{X} , but disregarding its invariance property. As previously discussed, nothing assures that the state trajectory ξ remains in its interior, once it is attained. This fact motivates the search for an associated invariant set of attraction

$$\mathcal{V} = \{\xi \in \mathbb{R}^{n_x} : v(\xi) < r_*\} \quad (3.122)$$

with $r_* > 0$ obtained from

$$r_* = \max_{\xi \in \mathcal{X}} v(\xi) = \inf_{r > 0} \{r : v(\xi) < r, \forall \xi \in \mathcal{X}\} \quad (3.123)$$

similarly to what was done in Theorem 3.2. The invariance property assures that whenever $\xi[n] \in \mathcal{V}$ then $\xi[n+1] \in \mathcal{V}$ as well. That is, once the state trajectory attains \mathcal{V} , its remaining part becomes confined to \mathcal{V} . The next theorem tackles this issue.

Theorem 3.7. Consider matrices P_i , $i \in \mathbb{K}$, and $\Pi \in \mathcal{M}_d$ that follow from the optimal solution to Theorem 3.6. The positive scalars r , β_i , $i \in \mathbb{K}$, and θ_{ij} , $i \neq j$, $(i, j) \in \mathbb{K} \times \mathbb{K}$, solution to the convex optimization problem

$$r_* = \inf_{r, \beta_i, \theta_{ij}} r \quad \text{s.t.} \quad (3.124)$$

$$\begin{bmatrix} \beta_i P_i + \sum_{j \in \mathbb{K} \setminus \{i\}} \theta_{ij} (P_i - P_j) & \bullet & \bullet & \bullet \\ 0 & r & \bullet & \bullet \\ \beta_i P_{\pi i} A_i & \beta_i P_{\pi i} \ell_i & \beta_i P_{\pi i} & \bullet \\ P_i & 0 & 0 & P_i \end{bmatrix} > 0 \quad (3.125)$$

for all $i \in \mathbb{K}$, assure that (3.122) is an invariant set of attraction.

Proof: Performing the Schur Complement with respect to the last two rows and columns of (3.125) and rearranging,

we obtain

$$\begin{bmatrix} P_i & \bullet \\ 0 & -r \end{bmatrix} < \beta_i \begin{bmatrix} Q_i + \sum_{j \in \mathbb{K} \setminus \{i\}} (\theta_{ij}/\beta_i)(P_i - P_j) & \bullet \\ -c'_i & -\rho_i \end{bmatrix} \quad (3.126)$$

for all $i \in \mathbb{K}$, which multiplied to the left by $[\xi' \ 1]$ and to the right by its transpose assures that $\mathcal{X} \subseteq \mathcal{V}$, with \mathcal{X} defined as in (3.110). As has already been discussed, the definition (3.110) allows us to take into account that each ellipsoid \mathcal{E}_i must be considered only in the operating region \mathcal{O}_i defined by the switching function $u(\xi) = i$. To prove the invariance property let us consider that for an arbitrary instant $n \in \mathbb{N}$ we have $\sigma[n] = i \in \mathbb{K}$ and that two important cases can occur:

1. If $\xi \in \mathcal{V}$ and $\xi \notin \mathcal{E}_i \cap \mathcal{O}_i$ then $\Delta v(\xi) < 0$ and ξ is converging to the origin. The same occurs if $\xi \notin \mathcal{V}$ because by consequence $\xi \notin \mathcal{E}_i \cap \mathcal{O}_i$ since $\mathcal{E}_i \cap \mathcal{O}_i \subseteq \mathcal{V}$.
2. If $\xi \in \mathcal{V}$ and $\xi \in \mathcal{E}_i \cap \mathcal{O}_i$, it follows from (3.107) that

$$\begin{aligned} v(A_i \xi + \ell_i) &< v(\xi) - (\xi' Q_i \xi - 2\xi' c_i - \rho_i) \\ &\leq \max_{\xi \in \mathcal{E}_i} \{\xi' P_i \xi - (\xi' Q_i \xi - 2\xi' c_i - \rho_i)\} \\ &= \max_{\xi \in \mathcal{E}_i} \{\xi' P_i \xi\} \\ &= r_i \end{aligned} \quad (3.127)$$

with some $r_i > 0$. The last two equalities have been obtained, performing similar steps to those in the proof of Theorem 3.3. In fact, taking into account that $P_i - Q_i = A'_i P_{\pi i} A_i > 0$, it is possible to use Lemma A.5 to obtain the first equality.

For all possible $i \in \mathbb{K}$ chosen by the switching function, a suitable upper bound for $v(A_\sigma \xi + \ell_\sigma)$ is $r = \max_{i \in \mathbb{K}} r_i$ which is obtained by solving problem (3.124). \square

Notice that the invariant set of attraction (3.122) is of min-type and, therefore, nonconvex. Alternatively, the region

$$\mathcal{V} = \bigcup_{i \in \mathbb{K}} \{\xi \in \mathbb{R}^{n_x} : \xi' P_i \xi \leq r\} \quad (3.128)$$

also represents this set.

The next academical examples illustrate the previous results. In particular, the first one is based on an affine system with two second order subsystems. It is presented a phase portrait containing the set of attraction and the associated invariant one as well as a possible state trajectory. The second one compares the present technique with the methodologies available in the literature in terms of volume minimization taking into account three different systems, two of them borrowed from the literature.

Example 3.5. Let us consider the discrete-time switched affine system (3.1) defined by matrices (3.30) for

all $i \in \mathbb{K}$, with $T = 0.5$ s obtained by the step-invariant discretization presented in (2.77) where

$$A_{c1} = \begin{bmatrix} -5.8 & -5.9 \\ -4.1 & -4.0 \end{bmatrix}, b_{c1} = \begin{bmatrix} 0 \\ -2 \end{bmatrix}, A_{c2} = \begin{bmatrix} 0.1 & -0.5 \\ -0.3 & -5.0 \end{bmatrix}, b_{c2} = \begin{bmatrix} -2 \\ 2 \end{bmatrix} \quad (3.129)$$

represent two unstable subsystems. Our goal is to stabilize this system around the origin $x_e = [0 \ 0]'$. Notice that this point does not belong to the set X_e normally adopted in the literature. The design of the switching function $\sigma[n] = u(x[n])$ follows from the solution of Corollary 3.3, performed by searching the elements (p, q) of the Metzler matrix

$$\Pi = \begin{bmatrix} p & 1-q \\ 1-p & q \end{bmatrix} \quad (3.130)$$

inside the box $[0, 1] \times [0, 1]$. The global optimal solution obtained for $(p_*, q_*) = (0, 0)$ has provided an ellipse \mathcal{E}_* with minimum area 19.54 and the matrices

$$P_1 = \begin{bmatrix} 0.3234 & 0.4329 \\ 0.4329 & 3.0385 \end{bmatrix}, \quad P_2 = \begin{bmatrix} 5.1154 & 4.5456 \\ 4.5456 & 4.5763 \end{bmatrix}$$

that are important to implement the stabilizing switching function $u(x[n])$. The associated set of attraction \mathcal{X} has presented an area of 6.29. Moreover, from Theorem 3.7 we have obtained the associated nonconvex invariant set \mathcal{V} with $r_* = 6.48$ and area of 28.23. These three sets together with the switching surface $\mathcal{C} = \{x \in \mathbb{R}^{n_x} : x' P_1 x = x' P_2 x\}$ are presented in Figure 3.11 as well as a trajectory $x[n]$ starting from $x_0 = [-10 \ 5]'$. Notice that the sequence $x[n]$ is attracted to the set \mathcal{X} but it can leave it at some instants. However, as expected, once the state $x[n]$ attains the invariant set, it remains confined to it. The time evolution of this trajectory and the corresponding switching sequence $\sigma[n]$ is shown in Figure 3.12, where it is clear that after the transient, the state remains near the desired equilibrium point.

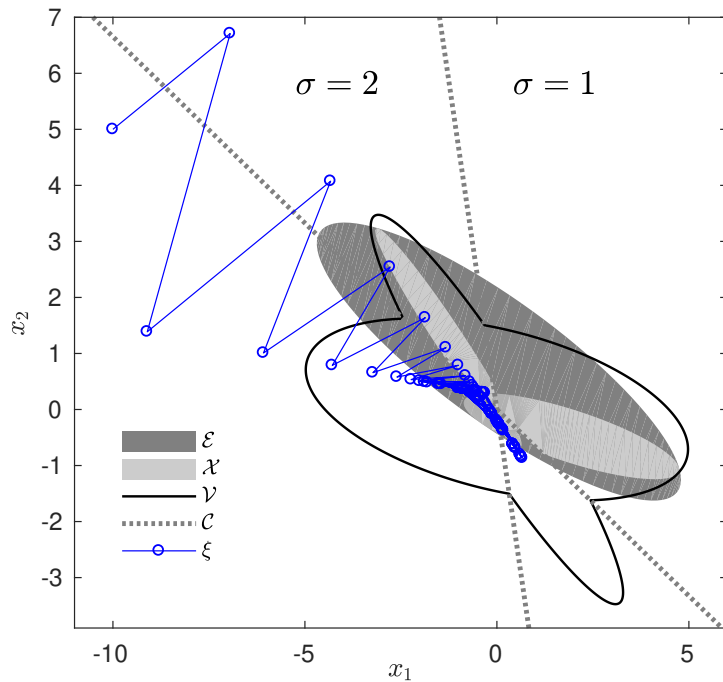


Figure 3.11: State trajectory ξ and sets of attraction assured from Corollary 3.3.

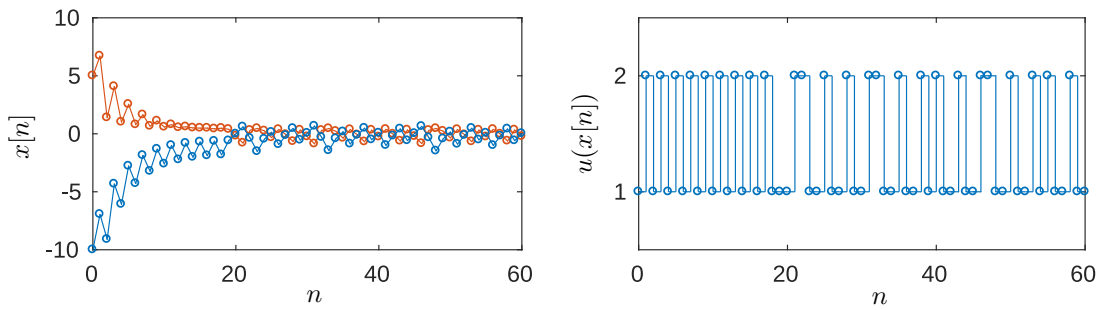


Figure 3.12: Time evolution of trajectories $\xi[n]$ and switching sequence $\sigma[n]$, obtained from Corollary 3.3.

Example 3.6. In order to compare the present methodology with those of Deaecto and Egidio (2016) and Theorem 3.1, in terms of volumes of the sets \mathcal{X} and \mathcal{V} , system data from Example 1 in Deaecto and Egidio (2016) and Example 1 in Deaecto and Geromel (2017) were borrowed and named \mathcal{D}_1 and \mathcal{D}_2 , respectively. We have adopted the same equilibrium point $x_e \in X_e$ of the respective references. A third system \mathcal{D}_3 was also compared, given by matrices A_i and b_i obtained from (3.30) with $T = 1$ s and

$$A_{c1} = \begin{bmatrix} -3 & -6 & 3 \\ 2 & 2 & -3 \\ 1.6 & 0 & -2 \end{bmatrix}, \quad b_{c1} = \begin{bmatrix} 0.5 \\ 0 \\ 0 \end{bmatrix}, \quad A_{c2} = \begin{bmatrix} 1 & 3 & 3 \\ -0.2 & -3 & -3 \\ 0 & 0 & -2 \end{bmatrix}, \quad b_{c2} = \begin{bmatrix} 0 \\ 0 \\ 0.5 \end{bmatrix} \quad (3.131)$$

together with the point $x_e = (I - A_\lambda)^{-1}b_\lambda = [0.0845 \ 0.0909 \ 0.0283]'$ for $\lambda = [0.56 \ 0.44]$.

Table 3.3 shows the volumes of the ellipsoid \mathcal{E}_* obtained by solving the conditions of Theorem 3.6, identified as T. 3.6, and Corollary 3.3, identified as C. 3.3, as well as the volumes of the set of attraction \mathcal{X} and the associated invariant set \mathcal{V} , obtained from Theorem 3.7. For sake of comparison, we have solved the conditions of Theorems 1 in Deaecto and Egidio (2016), identified as T. DE2016 and Theorem 3.1, as T. 3.1, to obtain the minimal ellipsoidal sets of attraction \mathcal{X} . The correspondent invariant set \mathcal{V} was obtained from Theorem 3.2.

Table 3.3: Volume comparison for several switching functions and system data.

	T. 3.6	C. 3.3	T. DE2016	T. 3.1
\mathcal{D}_1	\mathcal{E}_*	20.28	21.95	-
	\mathcal{X}	17.92	17.05	222.22
	\mathcal{V}	214.70	183.68	454.94
\mathcal{D}_2	\mathcal{E}_*	111.95	135.09	-
	\mathcal{X}	79.84	73.26	224.35
	\mathcal{V}	493.02	447.50	331.66
\mathcal{D}_3	\mathcal{E}_*	20.83	33.75	-
	\mathcal{X}	2.57	14.23	infeas.
	\mathcal{V}	162.58	225.70	infeas.

Notice that for the first system \mathcal{D}_1 , the volumes of \mathcal{X} and \mathcal{V} of T. 3.6 and C. 3.3 are always smaller than the ones of T. DE2016 and T. 3.1. The same is true for the volume of the auxiliary ellipsoid \mathcal{E}_* . This

conclusion can not be drawn for the system \mathcal{D}_2 , where the volumes of T. 3.1 are around 30% and 26% smaller than C. 3.3 with respect to \mathcal{X} and \mathcal{V} , respectively. This can happen since T. 3.1 is based on a quadratic but general Lyapunov function. However, the volumes in C. 3.3 are around 67% and 84% smaller than the sets \mathcal{X} and \mathcal{V} of T. DE2016 which adopts a simple quadratic Lyapunov function.

Although the volumes sometimes can be greater than those of T. 3.1, the conditions for the existence of a set of attraction in T. 3.6 and C. 3.3 are more general as previously proved. This fact was illustrated by system \mathcal{D}_3 in Table 3.3, which does not satisfy the condition (3.114), i.e., there is no $\lambda \in \Lambda$ such that A_λ is Schur stable. Therefore, T. DE2016 and T. 3.1 could not ensure its practical stability.

Another remark concerns the fact that, nevertheless Corollary 3.3 is derived as a particular case from Theorem 3.6, it presents smaller attraction set \mathcal{X} for both systems \mathcal{D}_1 and \mathcal{D}_2 . It may seem counterintuitive that a more general condition as T. 3.6 provided a greater volume. However, this phenomenon may occur since the minimized volume was that from ellipsoid \mathcal{E}_* and not that from set \mathcal{X} .

For system \mathcal{D}_3 the solution to Theorem 3.6 obtained for $(p_*, q_*) = (0, 0)$ in (3.130) has provided $(\beta_1, \beta_2) = (1, 0.1684)$ and matrices

$$P_1 = \begin{bmatrix} 1.5090 & 8.5303 & -2.8394 \\ 8.5303 & 64.0829 & -3.2703 \\ -2.8394 & -3.2703 & 66.2689 \end{bmatrix} \quad (3.132)$$

$$P_2 = \begin{bmatrix} 3.9551 & 5.3460 & -3.5290 \\ 5.3460 & 7.2309 & -4.7687 \\ -3.5290 & -4.7687 & 3.1548 \end{bmatrix} \times 10^3 \quad (3.133)$$

For this case, the invariant set \mathcal{V} , guaranteed by Theorem 3.7, is defined as the sublevel set $v(\xi) \leq r_* = 115.28$. For the system evolving from $\xi[0] = [20 \ -20 \ -20]'$, Figure 3.13 provides the time evolution of the Lyapunov function as well as the switching sequence $\sigma[n]$. Shown in Figure 3.14 is the invariant set \mathcal{V} and the state trajectories. This example illustrated the efficiency and the validity of the proposed theory.

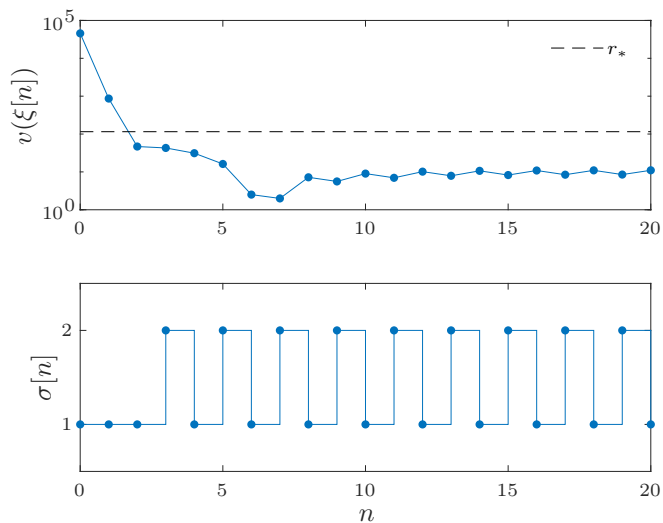


Figure 3.13: Lyapunov function trajectory and the upper bound r_* for the invariant set together with the switching function (3.102).

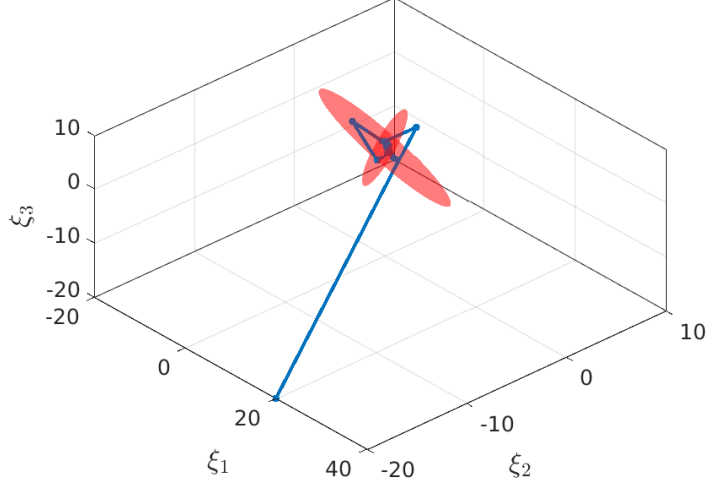


Figure 3.14: Phase portrait of a state trajectory converging to the invariant set of attraction \mathcal{V} , in red.

3.2.4 Sampled-data Application

In this subsection, some discussions on the application of the practical stability results on sampled-data control are given. As the reader could infer from some of the last examples, the stability conditions just presented are suitable to deal with continuous-time switched affine systems of the form

$$\dot{x}(t) = A_{\sigma(t)}x(t) + b_{\sigma(t)}, \quad x(0) = x_0 \quad (3.134)$$

under sampled-data switching control, where the switching signal is piecewise continuous

$$\sigma(t) = u(x(t_n)), \quad \forall t \in [t_n, t_{n+1}) \quad (3.135)$$

with $t_0 = 0$ and $t_{n+1} > t_n$ for all $n \in \mathbb{N}$ as it has been already defined in (2.139). For these cases, step-invariant or norm-equivalent discretizations might be used to generate a discrete-time switched affine system whose state trajectories $x[n]$ form exactly sequences $(x(t_n))_{n \in \mathbb{N}}$ with $t_n > 0$, $n \in \mathbb{N}$ being uniformly distributed sampling instants with $t_0 = 0$. Let us theoretically and numerically analyze the limit case where the sampling period $T = t_{n+1} - t_n \rightarrow 0$ to verify the behavior of the optimal solutions to Theorems 3.1 and 3.6. To this end, observe that the Taylor series expansion of the step-invariant discretization given in (2.77) for a continuous-time switched affine system defined by matrices (A_{ci}, b_{ci}) , $i \in \mathbb{K}$ is given as

$$A_i = I + TA_{ci} + O(T^2), \quad b_i = Tb_{ci} + O(T^2), \quad i \in \mathbb{K} \quad (3.136)$$

where $O(T^2)$ represents higher order terms on T . Whenever T is taken arbitrarily small, the approximation $A_i \approx I + TA_{ci}$, $b_i \approx Tb_{ci}$ is valid and consequently, the set of attainable equilibrium points of Theorem 3.1 becomes the one of Theorem 2.15, for the continuous-time case. This can be verified from the definition of X_e in (3.5) and of X_e^c in (2.125). Consequently $\ell_i \rightarrow T\ell_{ci}$ with $\ell_{ci} = A_{ci}x_e + b_{ci}$ and, therefore, $\ell_\lambda = \ell_{c\lambda} = 0$. Finally,

the switching function design conditions (3.8) and (3.9) are fulfilled for a singleton set of attraction $\mathcal{X}_* = \{0\}$ whenever there exists $S > 0$ such that $A'_\lambda S + SA_\lambda < 0$, which is the sufficient and necessary condition for feasibility of Theorem 2.15. Indeed, replacing the previously mentioned approximation in (3.8), after eliminating higher order terms, we have

$$T \begin{bmatrix} A'_{ci}P + PA_{ci} & \bullet \\ \ell'_{ci}P + h'A_{ci} & 2\ell'_{ci}h \end{bmatrix} < \begin{bmatrix} -Q_i & \bullet \\ c'_i & \rho_i \end{bmatrix} \quad (3.137)$$

Without loss of generality, choosing $h = 0$, $g = -W\mu = 0$, $-Q_i = T(A'_{ci}P + PA_{ci})$, $c_i = TP\ell_{ci}$ and $\rho_i = 1$ for all $i \in \mathbb{K}$ which clearly satisfy this inequality, condition (3.9) rewritten as

$$\begin{bmatrix} -Q_\lambda & \bullet \\ c_\lambda & \rho_\lambda - 1 \end{bmatrix} < - \begin{bmatrix} W & \bullet \\ -\mu'W & \mu'W\mu \end{bmatrix} \quad (3.138)$$

is turned to $T(A'_{c\lambda}P + PA_{c\lambda}) < -W$. Notice that choosing $P = T^{-1}S$ for some $S > 0$, the matrix $W > 0$ can be taken arbitrarily large whenever A_λ is a Hurwitz stable matrix, what makes $\mathcal{X}_* \rightarrow \{0\}$. Moreover, the switching function (3.10) becomes

$$\begin{aligned} u(\xi[n]) &= \arg \min_{i \in \mathbb{K}} -\xi[n]'Q_i\xi[n] + 2c'_i\xi[n] + \rho_i \\ &= \arg \min_{i \in \mathbb{K}} \xi[n]'S(A_{ci}\xi[n] + \ell_{ci}) \\ &= \arg \min_{i \in \mathbb{K}} \xi(t)'S(A_{ci}\xi(t) + \ell_{ci}) = u(\xi(t)) \end{aligned}$$

where the last equality takes into account that $u(\xi[n]) = u(\xi(t_n)) = u(\xi(t))$ whenever $T \rightarrow 0$, which is the same as the continuous-time one given in (2.130) considering only stability.

Regarding now stability conditions in Theorem 3.6, unfortunately, it is not possible to guarantee that \mathcal{X}_* turns into a singleton when $T \rightarrow 0$. This will be numerically illustrated in the sequel by means of an example. Additionally, it is important to remark that the continuous-time switching function cannot be written in the form of (3.102), from Theorem 3.6, due to the absence of a linear term inside the arg min expression. The next example compares both methodologies numerically.

Example 3.7. Consider the sampled-data switched affine system given as in (3.134) with matrices

$$A_{c1} = \begin{bmatrix} 0 & 1 \\ -1 & -3 \end{bmatrix}, A_{c2} = \begin{bmatrix} 0 & 1 \\ -5 & -3 \end{bmatrix}, A_{c3} = \begin{bmatrix} 0 & 1 \\ -3 & -1 \end{bmatrix}, b_{c1} = \begin{bmatrix} 1 \\ -4 \end{bmatrix}, b_{c2} = \begin{bmatrix} 1 \\ -1 \end{bmatrix}, b_{c3} = \begin{bmatrix} -2 \\ 3 \end{bmatrix} \quad (3.139)$$

where the goal is to stabilize the state $x(t)$ around the origin $x = 0$ by only commanding the switching signal. However, switching can only occur at sampling instants. In other words, the switching signal is constrained to be piecewise constant, as given in (2.139). Employing the step-invariant discretization (2.77), this system is exactly represented by a discrete-time switched affine system. For 20 evenly distributed values of sampling time $T \in [10^{-3}, 2]$ s, practical stability of the origin was verified via Theorem 3.1 and Corollary 3.3, adopting $\Pi = [\lambda \ \lambda \ \lambda]$ with $\lambda \in \Lambda$ associated with $0 \in X_e$. Along this grid, the existence of a globally practically stabilizing switching function was guaranteed for all T but $T = 2$ s (for which there is no $\lambda \in \Lambda$ such that $0 \in X_e$) and the area of the sets of attraction \mathcal{X} obtained from both methods are

presented in Figure 3.15. Observe that for $T = 10^{-3}$ s the area obtained from Theorem 3.1 (solid black line) tends to zero while the one of Corollary 3.3 (dashed red line) does not. However, for this example, smaller sets of attraction in terms of area are obtained from the corollary when larger values of T are adopted. This illustrates once more that none of the techniques overcome another in terms of volume minimization and that \mathcal{X} may not tend to a singleton when $T \rightarrow 0$ for Corollary 3.3 and the given Metzler matrix.

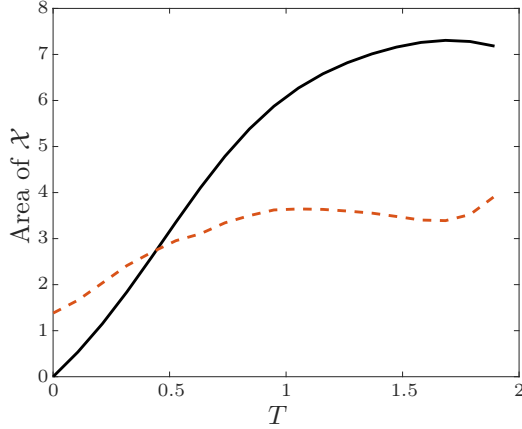


Figure 3.15: Area of the set of attraction \mathcal{X} calculated from Theorem 3.1 (solid black) and Corollary 3.3 (dashed red) for various sampling periods T .

A brief remark on this example is in order. The particular choice for the Metzler matrix is to certify that both conditions are equivalent in terms of the existence of \mathcal{X} . This is a consequence of equation (3.116) and following discussions.

This concludes our discussions about practical stability for switched affine systems. The next section presents the alternative approach previously discussed, which is based on limit cycles instead of sets of attraction.

3.3 Limit Cycle Stability

In the last section, state trajectories were guided to a sufficiently small set of attraction containing a desired point of interest. However, their behavior inside this set may not be predicted *a priori*. Indeed, in steady-state, nothing beyond bounds for the error can be derived. Consequently, neither \mathcal{H}_2 nor \mathcal{H}_∞ performance indexes can be studied, as they are defined only for asymptotically stable systems, see Section 2.4. To the best of my knowledge, there are only a few results available in the literature dealing with asymptotic stability of a limit cycle for switched affine systems, and none of them regards the discrete-time domain. Very recently, and only for the continuous-time domain, some references treated the asymptotic stabilization not to a single point but to a limit cycle as a manner of controlling the steady-state behavior, see Benmiloud et al. (2019) as an example of local stabilization and Patino et al. (2010), which is based on a predictive control approach. In the context of hybrid systems, global asymptotic stability of limit cycles was studied by Rubensson and Lennartson (2000), but this approach considers a given switching pattern and no design procedure is presented. Also, authors in Sferlazza et al. (2019) study the limit cycle generated by the trajectories of a DC-DC boost converter when the

dwell time constraints are imposed on the adopted hybrid control strategy.

A new design methodology for a min-type state-dependent switching function to assure global asymptotic stability of limit cycles will be addressed in this section. These results were accepted for publication in [Egidio et al. \(2020\)](#). Firstly, a set of possible limit cycles related to periodic switching sequences is determined, and a subset of candidates is chosen by the designer based on specific criteria related to the desired behavior of the trajectories in the steady state. Afterward, a min-type switching function is designed based on a time-varying convex Lyapunov function to assure global asymptotic stability of the chosen limit cycle, as well as \mathcal{H}_2 or \mathcal{H}_∞ guaranteed cost. In the context of switched affine systems, these indexes were only employed for the continuous-time case, see [Trofino et al. \(2012\)](#), [Deaecto and Santos \(2015\)](#) and [Deaecto \(2016\)](#) as instances. Finally, the adoption of time-varying Lyapunov functions also allows reducing the degree of conservativeness of the switching function design, as it will be later illustrated.

3.3.1 Problem Statement

Before beginning, let us recall system (3.1), repeated here for convenience

$$\begin{cases} x[n+1] = A_{\sigma[n]}x[n] + b_{\sigma[n]} + H_{\sigma[n]}w[n], & x[-1] = x_e[-1] \\ z[n] = E_{\sigma[n]}x[n] + G_{\sigma[n]}w[n] \end{cases} \quad (3.140)$$

but defined for all $n \in \mathbb{N}_-$ with $\mathbb{N}_- = \mathbb{N} \cup \{-1\}$. Consider that for $w[n] = 0, \forall n \in \mathbb{N}_-$ it admits a periodic solution $x_e[n]$ with period $\kappa \in \mathbb{N}_+$ chosen by the designer.

Let us now formally define the aforementioned **limit cycle** as a periodic sequence $\mathcal{X}_e(c)$, given as

$$\mathcal{X}_e(c) = \{x_e[k(n)] : x_e[n+1] = A_{c[k(n)]}x_e[n] + b_{c[k(n)]}, n \in \mathbb{N}_-\} \quad (3.141)$$

where $c = (c[0], \dots, c[\kappa - 1]) \in \mathbb{K}^\kappa$ is a sequence of indexes that defines the fundamental period, given by the finite sequence $(x_e[0], \dots, x_e[\kappa - 1])$. The function $k(n) = n \bmod \kappa$ will be extensively used from now on to indicate periodicity. Indeed, $x_e[n]$ is an equilibrium solution for the system (3.140) with $w[n] = 0$ and $\sigma[n] = c[k(n)]$, which satisfies

$$x_e[n+1] = A_{c[k(n)]}x_e[n] + b_{c[k(n)]} \quad (3.142)$$

The design of the limit cycle is connected to the choice of the sequence $c[n]$, which can be selected from a set \mathbb{K}^κ with N^κ possible ones. As will be discussed in the next subsection, this selection is made according to criteria related to the steady-state behavior of the trajectories.

Defining the auxiliary state variable $\xi[n] = x[n] - x_e[n]$, $x_e[n] \in \mathcal{X}_e^*$, we obtain from the original switched affine system (3.140) an equivalent time-varying system

$$\begin{cases} \xi[n+1] = A_{\sigma[n]}\xi[n] + \ell_{\sigma[n]}[n] + H_{\sigma[n]}w[n], & \xi[-1] = 0 \\ z_e[n] = E_{\sigma[n]}\xi[n] + G_{\sigma[n]}w[n] \end{cases} \quad (3.143)$$

For the sake of clarity, the initial time instant will be sometimes considered to be $n = -1$ and sometimes $n = 0$ and this will be made clear throughout this section. The time-varying vectors are given by $\ell_i[n] = A_i x_e[n] - x_e[n+1] + b_i$, $\forall i \in \mathbb{K}$, and the new performance output is $z_e[n] = z[n] - E_{\sigma[n]}x_e[n]$, $\forall n \in \mathbb{N}_-$. Notice

that, whenever the trajectories of (3.140) reach the limit cycle, i.e., $x[n] = x_e[n] \in \mathcal{X}_e^*$, we have $\xi[n] = 0$ and, therefore, the origin is an equilibrium point of the equivalent system (3.143). Hence, the following definition is welcome at this point.

Definition 3.3 (Globally asymptotically stable limit cycle). A limit cycle \mathcal{X}_e^* is a **globally asymptotically stable limit cycle** for the discrete-time switched affine system (3.140) if the origin of the equivalent time-varying system (3.143) is a globally asymptotically stable equilibrium point.

Our goal is to design a state-dependent switching function $u : \mathbb{R}^{n_x} \times \mathbb{N}_- \rightarrow \mathbb{K}$ to assure global asymptotic stability of the limit cycle \mathcal{X}_e^* . In other words, we want to design $\sigma[n] = u(x[n], n)$ to guarantee that the origin $\xi = 0$ of (3.143) be a globally asymptotically stable equilibrium point, assuring a suitable upper bound for the \mathcal{H}_2 and \mathcal{H}_∞ performance indexes, defined previously for (2.112), and redefined in this chapter for convenience as follows:

- **\mathcal{H}_2 performance index:** Considering that the system (3.143), defined for all $n \in \mathbb{N}_-$ with $\xi[-1] = 0$, is asymptotically stable, this index is given by

$$\mathcal{J}_2 = \sum_{r=1}^{n_w} \|z_{er}\|_2^2 + e_r' G'_{\sigma[-1]} G_{\sigma[-1]} e_r \quad (3.144)$$

where $z_{er}[n]$, is the controlled output corresponding to the impulsive inputs $w[n] = e_r \delta[n+1]$ with vector e_r , $r \in \{1, \dots, n_w\}$, forming the standard basis and $\delta[n]$ being the impulse function.

- **\mathcal{H}_∞ performance index:** Considering that the system (3.143), defined for $n \in \mathbb{N}$ with $\xi[0] = 0$, is asymptotically stable, this index is given by

$$\mathcal{J}_\infty = \sup_{w \in \mathcal{L}_2^d \setminus \{0\}} \frac{\|z_e\|_2^2}{\|w\|_2^2} \quad (3.145)$$

As has already been mentioned, these indexes equal the \mathcal{H}_2 or \mathcal{H}_∞ squared norm of the i -th subsystem translated to its equilibrium, whenever they exist and the switching rule is kept constant, that is, $\sigma[n] = i \in \mathbb{K}$, $\forall n \in \mathbb{N}_-$. Moreover, they require that the system be asymptotically stable and, therefore, cannot be evaluated by the methodologies available dealing with sets of attraction when only practical stability is assessed. This occurs because, under these methodologies, the \mathcal{L}_2^d -norm $\|z_e\|_2$ does not converge.

Our design conditions are based on the following convex time-varying Lyapunov function

$$v(\xi[n], n) = \xi[n]' P[k(n)] \xi[n] \quad (3.146)$$

with $P[n] > 0$, $n \in \{0, \dots, \kappa - 1\}$, to be determined. This function has been recently used in [Deaecto and Geromel \(2018\)](#) and [Daiha et al. \(2017\)](#) to study the stability of switched linear systems and, certainly, provides less conservative conditions than the time-invariant quadratic Lyapunov function, recurrent in the literature of switched affine systems.

3.3.2 Limit Cycle Generation

To avoid misinterpretations, let us firstly state that periodic switching functions will be employed strictly to generate candidate limit cycles. In the general case, the switching functions $\sigma[n] = u(\xi[n], n)$ that we seek to design do not generate periodic switching sequences since it is state-dependent. At this point some definitions, borrowed from [Deaecto and Geromel \(2018\)](#), are important. For a given positive $\kappa \in \mathbb{N}$ that defines the desired period of the limit cycle, let $\mathfrak{C}(\kappa) = \mathbb{K}^\kappa$ be the set obtained from the Cartesian product of \mathbb{K} by itself κ times. This set contains N^κ elements $c \in \mathfrak{C}(\kappa)$, which are finite sequences $c = (c[0], \dots, c[\kappa - 1])$.

Associated to each $c \in \mathfrak{C}(\kappa)$ there exists $\mathcal{X}_e(c)$, given in [\(3.141\)](#), of which first κ points $x_e[n], n \in \{0, \dots, \kappa - 1\}$, can be obtained from [\(3.142\)](#) with $x_e[0] = x_e[\kappa]$ as the solution of the linear equation

$$\tilde{A}(c)\tilde{x}_e = -\tilde{b}(c) \quad (3.147)$$

where $\tilde{x}_e = [x_e[0]' \ x_e[1]' \ \dots \ x_e[\kappa - 1]]'$, the matrix

$$\tilde{A}(c) = \begin{bmatrix} A_{c[0]} & -I & 0 & \cdots & 0 \\ 0 & A_{c[1]} & -I & \cdots & 0 \\ \vdots & \vdots & \vdots & \ddots & \vdots \\ -I & 0 & 0 & \cdots & A_{c[\kappa-1]} \end{bmatrix} \quad (3.148)$$

and $\tilde{b}(c) = [b'_{c[0]} \ b'_{c[1]} \ \dots \ b'_{c[\kappa-1]}]'$. Notice that the boundary condition $x_e[0] = x_e[\kappa]$ that naturally arises from the fact that $x_e[n] = x_e(k[n])$ has been taken into account in the last row of $\tilde{A}(c)$ and that due to [\(3.142\)](#) all the limit cycles satisfy the identity $\ell_{c[n]}[n] = 0$.

The N^κ different switching sequences $c \in \mathfrak{C}(\kappa)$ allow us to define the family of candidate limit cycles

$$\mathfrak{X} = \{\mathcal{X}_e(c) : c \in \mathfrak{C}(\kappa)\} \quad (3.149)$$

The search for a desired limit cycle $\mathcal{X}_e^* \in \mathfrak{X}$, defining properties of interest for the trajectories of [\(3.140\)](#) in the steady state, as ripple amplitude and oscillation frequency, can be constrained to a subset $\mathfrak{X}_s \subseteq \mathfrak{X}$, which is related to some criterion specified by the designer. Given a reference point x_* , a possible criterion is

$$\mathfrak{X}_s = \left\{ \mathcal{X}_e \in \mathfrak{X} : \frac{1}{\kappa} \sum_{n=0}^{\kappa-1} \|\Gamma(x_e[n] - x_*)\| < 1 \right\} \quad (3.150)$$

which contains candidate limit cycles with mean distance between $\Gamma x_e[n]$ and Γx_* over $n \in \{0, \dots, \kappa - 1\}$ smaller than 1. The matrix Γ provided by the designer is important when the interest is to optimize the steady-state behavior of only one or a combination of state components. Alternatively, when the goal is to bound the ripple amplitudes of the trajectories in the steady state, another possibility is to adopt the subset

$$\mathfrak{X}_s = \left\{ \mathcal{X}_e \in \mathfrak{X} : \max_{n \in \{0, \dots, \kappa - 1\}} \|\Gamma(x_e[n] - x_*)\|_\infty < 1 \right\} \quad (3.151)$$

with, as in the first case, Γ being a parameter provided by the designer. Notice that the criterion choice depends exclusively on the interest of the designer with respect to the steady-state behavior of the trajectories, which

can define different sets \mathfrak{X}_s . The subset of sequences c associated to $\mathcal{X}_e(c) \in \mathfrak{X}_s$ is defined as $\mathfrak{C}_s(\kappa) \subseteq \mathfrak{C}(\kappa)$. Sufficiently restricting the subset of candidates leads to a set $\mathfrak{C}_s(\kappa)$ with fewer elements, which will show to be an interesting aspect from a computational point of view. The next theorem relies upon the results of [Bittanti and Colaneri \(2009\)](#) to provide conditions that assure the existence of a globally asymptotically stable limit cycle $\mathcal{X}_e(c) \in \mathfrak{X}_s$ to be considered in the forthcoming developments.

Theorem 3.8. *Consider system (3.140) with $w[n] = 0$, $\forall n \in \mathbb{N}_-$, and let $\kappa \in \mathbb{N}_+$ and $c \in \mathfrak{C}_s(\kappa)$ be given. The limit cycle $\mathcal{X}_e(c) \in \mathfrak{X}_s$ under the periodic switching sequence $\sigma[n] = c[k(n)]$ is globally asymptotically stable if and only if there exist positive definite matrices $P[n] > 0$, $n \in \{0, \dots, \kappa - 1\}$, satisfying the linear matrix inequalities*

$$A'_{c[n]} P[n+1] A_{c[n]} - P[n] < 0 \quad (3.152)$$

for all $n \in \{0, \dots, \kappa - 1\}$, with the boundary condition $P[\kappa] = P[0]$.

Proof: Consider system (3.140) with $w[n] = 0$, $\forall n \in \mathbb{N}_-$, written alternatively as (3.143) and governed by the periodic switching sequence $\sigma[n] = c[k(n)] \in \mathfrak{C}_s(\kappa)$. Associated to this sequence, the limit cycle $\mathcal{X}_e(c) \in \mathfrak{X}_s$ defined in (3.141) assures that $\tilde{A}(c)\tilde{x}_e = -\tilde{b}(c)$ holds, which is equivalent to verify the identity

$$\ell_{c[n]}[n] = A_{c[n]}x_e[n] - x_e[n+1] + b_{c[n]} = 0 \quad (3.153)$$

for all $n \in \{0, \dots, \kappa - 1\}$ and $x_e[0] = x_e[\kappa]$. With the identity (3.153), the system becomes a periodic linear system $\xi[n+1] = A_{c[n]}\xi[n]$. Hence, due to Proposition 3.5 of [Bittanti and Colaneri \(2009\)](#), the condition (3.152) is necessary and sufficient for global asymptotic stability of the origin $\xi = 0$ regarding system (3.143), or equivalently, for the global asymptotic stability of the limit cycle $\mathcal{X}_e(c)$ concerning system (3.140). \square

As will be clear in the next subsection, for every limit cycle \mathcal{X}_e^* chosen inside \mathfrak{X}_s , that satisfies the conditions of Theorem 3.8, it is possible to determine state-dependent switching functions, which not only preserve global asymptotic stability of the limit cycle, but also optimize an upper bound for the previously defined \mathcal{H}_2 and \mathcal{H}_∞ performance indexes. Before proceeding, let us define the matrix function

$$\mathcal{L}_i[n] = \begin{bmatrix} A'_i P[n+1] A_i - P[n] & \bullet \\ \ell_i[n]' P[n+1] A_i & \ell_i[n]' P[n+1] \ell_i[n] \end{bmatrix} \quad (3.154)$$

since it will be useful afterward.

3.3.3 State and Time-dependent Switching

At this first moment, our goal is to determine a state-dependent switching function $\sigma[n] = u(x[n], n)$ that assures global asymptotic stability of the limit cycle $\mathcal{X}_e^* \in \mathfrak{X}_s$ chosen as the one that minimizes the upper bound for the square \mathcal{L}_2 -norm $\|z_e\|_2^2$. For this purpose, let us consider the simpler translated system

$$\begin{cases} \xi[n+1] = A_{\sigma[n]}\xi[n] + \ell_{\sigma[n]}[n], & \xi[0] = x[0] - x_e[0] \\ z_e[n] = E_{\sigma[n]}\xi[n] \end{cases} \quad (3.155)$$

with $x_e[n] \in \mathcal{X}_e^*$. The next theorem presents this result.

Theorem 3.9. Consider system (3.140) with $w[n] = 0$, $\forall n \in \mathbb{N}_-$, evolving from an arbitrary $x[0]$. Let the scalar $\kappa \in \mathbb{N}_+$ and the set of candidate limit cycles $\mathcal{X}_e(c) \in \mathfrak{X}_s$, $\forall c \in \mathfrak{C}_s(\kappa)$ be given. If there exist positive definite matrices $P[n] > 0$ satisfying the optimization problem

$$\min_{\mathcal{X}_e(c) \in \mathfrak{X}_s} \inf_{P[n]} (x[0] - x_e[0])' P[0] (x[0] - x_e[0]) \quad \text{s.t.} \quad (3.156)$$

$$A'_{c[n]} P[n+1] A_{c[n]} - P[n] + E'_{c[n]} E_{c[n]} < 0 \quad (3.157)$$

for all $n \in \{0, \dots, \kappa - 1\}$, $c \in \mathfrak{C}_s(\kappa)$ with the boundary condition $P[\kappa] = P[0]$, then the state-dependent switching function $\sigma[n] = u(\xi[n], n)$ with

$$u(\xi, n) = \arg \min_{i \in \mathbb{K}} \begin{bmatrix} \xi \\ 1 \end{bmatrix}' \mathcal{L}_i[k(n)] \begin{bmatrix} \xi \\ 1 \end{bmatrix} + \xi' E'_i E_i \xi \quad (3.158)$$

assures that the limit cycle $\mathcal{X}_e^* = \mathcal{X}_e(c)$, solution to (3.156), is globally asymptotically stable and that the following upper bound

$$\|z_e\|_2^2 < (x[0] - x_e[0])' P[0] (x[0] - x_e[0]) \quad (3.159)$$

is a guaranteed performance cost.

Proof: Notice that the system under consideration can be rewritten alternatively as (3.155) and adopt the switching function (3.158). For an arbitrary trajectory of (3.143) in the time interval $n \in \{0, \dots, \kappa - 1\}$, the Lyapunov function (3.146) provides

$$\begin{aligned} \Delta v(\xi, n) &= \begin{bmatrix} \xi \\ 1 \end{bmatrix}' \mathcal{L}_{\sigma[n]}[n] \begin{bmatrix} \xi \\ 1 \end{bmatrix} + \xi' E'_{\sigma[n]} E_{\sigma[n]} \xi - z'_e z_e \\ &= \min_{i \in \mathbb{K}} \begin{bmatrix} \xi \\ 1 \end{bmatrix}' \mathcal{L}_i[n] \begin{bmatrix} \xi \\ 1 \end{bmatrix} + \xi' E'_i E_i \xi - z'_e z_e \\ &\leq \begin{bmatrix} \xi \\ 1 \end{bmatrix}' \mathcal{L}_{c[n]}[n] \begin{bmatrix} \xi \\ 1 \end{bmatrix} + \xi' E'_{c[n]} E_{c[n]} \xi - z'_e z_e \\ &= \xi' (A'_{c[n]} P[n+1] A_{c[n]} - P[n] + E'_{c[n]} E_{c[n]}) \xi - z'_e z_e \\ &< -z'_e z_e \end{aligned} \quad (3.160)$$

where the second equality comes from the switching function (3.158), the first inequality is a consequence of the minimum operator and the third equality is due to the fact that the sequence $c \in \mathfrak{C}_s(\kappa)$, associated with the limit cycle $\mathcal{X}_e^* \in \mathfrak{X}_s$, assures that the identity (3.153) holds. Finally, the last inequality is verified by the validity of (3.157). From the periodic continuation $P[n] = P[k(n)]$ we have that $\Delta v(\xi, n) < -z'_e z_e < 0$ for all $n \in \mathbb{N}$ and, therefore, the equilibrium point $\xi = 0$ is globally asymptotically stable. Consequently, the same occurs for the limit cycle \mathcal{X}_e^* , regarding the original system. Moreover, summing both sides of (3.160) from $n = 0$ up to infinity, we obtain a telescoping series which assures

$$\sum_{n=0}^{\infty} \Delta v(\xi[n], n) = -v(\xi[0], 0) < - \sum_{n=0}^{\infty} \|z_e\|^2 \quad (3.161)$$

verifying (3.159) and concluding the proof. \square

About this result, some remarks are in order. This theorem presents conditions for the design of the mentioned state-dependent switching function. Notice that, for the particular case where $\sigma[n] = c[k(n)]$, it is simple to show that $\|z_e\|_2^2 = (x[0] - x_e[0])'P[0](x[0] - x_e[0])$ where $P[0] > 0$ is the solution of $A_{c[n]}'P[n+1]A_{c[n]} - P[n] + E_{c[n]}'E_{c[n]} = 0$ for all $n \in \{0, \dots, \kappa-1\}$ and $P[\kappa] = P[0]$. This indicates that the state-dependent switching function (3.158) provides an actual cost which is better than, or at least equal to, the one provided by a periodic switching function.

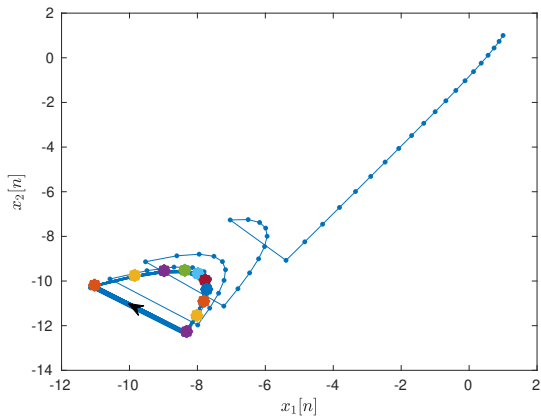
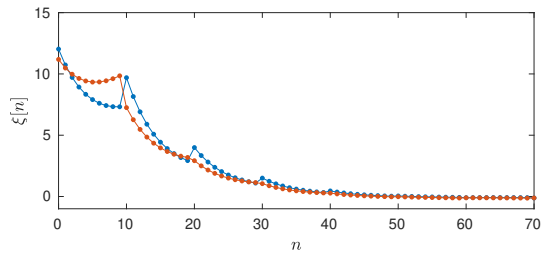
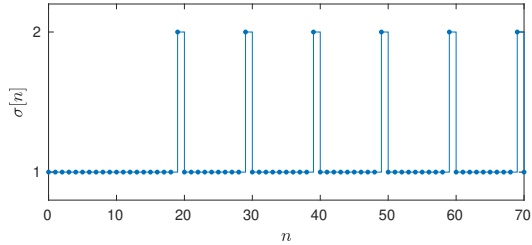
To the best of my knowledge, this is the first result dealing with global asymptotic stability of a desired limit cycle for discrete-time switched affine systems. Even for the continuous-time domain there are only few results in the literature, for instance, the recent reference Benmiloud et al. (2019) that deals with local asymptotic stability using a systematic methodology based on a Poincaré map approach. Differently, the conditions proposed in Theorem 3.9 are expressed by means of LMIs being, therefore, simple-to-solve by readily available algorithms. Compared to the conditions for practical stability, the inequalities (3.157) are less conservative than the methods based on a simple time-invariant quadratic Lyapunov function, as those in Theorems 3.1 and 3.3, and are not comparable to the Lyapunov-Metzler conditions, given in Theorem 3.6, as discussed in Daiha et al. (2017). The following example, borrowed from Egídio et al. (2020), illustrates this result.

Example 3.8. Consider the switched affine system (3.140) with $w[n] = 0$ and composed of two unstable subsystems defined by (3.30) with $T = 0.1$ s and

$$A_{c1} = \begin{bmatrix} -4 & 3 \\ -3 & 2.5 \end{bmatrix}, \quad b_{c1} = \begin{bmatrix} 0 \\ -2 \end{bmatrix}, \quad E_1 = I$$

$$A_{c2} = \begin{bmatrix} 4 & -1 \\ 1 & -2 \end{bmatrix}, \quad b_{c2} = \begin{bmatrix} 0 \\ 8 \end{bmatrix}, \quad E_2 = I$$

The goal is to control the first state component toward an average value near -9 in the steady state. To this end, for $\kappa = 10$, a set of candidate limit cycles was defined as in (3.150) with $x_* = [-9 \ ?]'$, where the symbol “?” indicates a value without importance, $\Gamma = [1 \ 0]$, which produced an $\mathfrak{X}_s \subset \mathfrak{X}$ with 10 candidate limit cycles whose average value of the first state component is inside the interval $(-10, -8)$. Solving the optimization problem of Theorem 3.9, matrices $P[n]$ and the optimal limit cycle \mathcal{X}_e^* , correspondent to the optimal sequence $c = (1, 1, 1, 1, 1, 1, 1, 1, 1, 2) \in \mathfrak{C}_s(\kappa)$ have been found, allowing the implementation of the switching function (3.158). The limit cycle \mathcal{X}_e^* is presented in the Figure 3.16 along with a trajectory $x[n]$ starting from $x[0] = [1 \ 1]'$, where the arrow represents the direction of the state trajectories on \mathcal{X}_e^* . Figure 3.17 and Figure 3.18 show, respectively, the state trajectories $\xi[n]$ and the switching signal $\sigma[n]$ over time instants n . Notice that the trajectories $x[n]$ converged to the chosen limit cycle while, as expected, $\xi[n]$ tended to zero. By numerical simulation, we have calculated $\|z\|_2^2 = 2417.53$ which respects its upper bound 3945.57, defined in (3.159). This puts in evidence the efficiency of the proposed switching strategy.

Figure 3.16: State trajectory $x[n]$ and limit cycle \mathcal{X}_e^* Figure 3.17: Time evolution of the auxiliary state $\xi[n]$.Figure 3.18: Obtained switching signal $\sigma[n]$.

An interesting remark about this result is that a better performance can be obtained by a suitable choice of κ , allowing performance optimization in the steady and transient states. Fortunately, $\kappa \in \mathbb{N}_+$ does not need to be large to achieve an adequate guaranteed cost. Actually, as it has been discussed in [Deaecto and Geromel \(2018\)](#), whenever $\hat{\kappa} = \eta\kappa$, for some $\eta \in \mathbb{N}_+$, it is possible to assure that the costs are non increasing as η increases since $\mathfrak{C}_s(\eta\kappa)$ contains all the periodic sequences $\mathfrak{C}_s(\kappa)$ as a particular case. However, nothing can be concluded about the costs for the case when $\hat{\kappa} > \kappa$ but $\hat{\kappa} \neq \eta\kappa$ for all $\eta \in \mathbb{N}$ such that $\eta \geq 2$. The next subsections generalize Theorem 3.8 to deal with \mathcal{H}_2 and \mathcal{H}_∞ control design.

3.3.4 \mathcal{H}_2 Performance

Consider the switched affine system (3.140) with an initial condition $x[-1] = x_e[-1]$ and an external input of impulsive type $w[n] = e_r \delta[n+1]$, where $e_r, r \in \{0, \dots, n_w\}$, are vectors forming the standard basis. This system can be equivalently rewritten as (3.155) but evolving from initial condition $\xi[0] = \ell_{\sigma[-1]}[-1] + H_{\sigma[-1]}e_r$. The next corollary presents an upper bound for the \mathcal{H}_2 performance index defined in (3.144).

Corollary 3.4. *Consider system (3.140) evolving from $x[-1] = x_e[-1]$ with $w[n] = e_r \delta[n+1]$. Let the scalar $\kappa \in \mathbb{N}_+$, the set of candidate limit cycles $\mathcal{X}_e(c) \in \mathfrak{X}_s$, $\forall c \in \mathfrak{C}_s(\kappa)$, and $\sigma[-1] = m$ be given. If there exist positive definite matrices $P[n] > 0$ satisfying the optimization problem*

$$\min_{\mathcal{X}_e(c) \in \mathfrak{X}_s} \inf_{P[n]} \text{tr}\left((L_m + H_m)' P[0] (L_m + H_m) + G_m' G_m\right) \quad (3.162)$$

where $L_m = [\ell_m[-1] \ \dots \ \ell_m[-1]] \in \mathbb{R}^{n_x \times n_w}$ and $\ell_m[-1] = A_m x_e[-1] - x_e[0] + b_m$, subject to the linear matrix inequalities (3.157), for all $n \in \{0, \dots, \kappa - 1\}$, $c \in \mathfrak{C}_s(\kappa)$ with the boundary condition $P[\kappa] = P[0]$, then the state-dependent switching function $\sigma[n] = u(\xi[n], n)$ with (3.158) assures that the limit cycle $\mathcal{X}_e^* = \mathcal{X}_e(c)$, solution to (3.162), is globally asymptotically stable and the upper bound

$$\mathcal{J}_2 < \text{tr}\left((L_m + H_m)' P[0] (L_m + H_m) + G_m' G_m\right) = \bar{\mathcal{J}}_2 \quad (3.163)$$

is an \mathcal{H}_2 guaranteed cost of performance.

Proof: From Theorem 3.9, asymptotic stability is assured by the switching function (3.158) and the inequality $\|z_e\|_2^2 < \xi[0]' P[0] \xi[0]$ with $\xi[0] = x[0] - x_e[0]$ holds. Hence, from (3.144), we have

$$\begin{aligned} \mathcal{J}_2 &= \sum_{r=1}^{n_w} \|z_{er}\|_2^2 + e_r' G_m' G_m e_r \\ &< \sum_{r=1}^{n_w} \xi[0]' P[0] \xi[0] + e_r' G_m' G_m e_r \\ &= \text{tr}\left((L_m + H_m)' P[0] (L_m + H_m) + G_m' G_m\right) \end{aligned} \quad (3.164)$$

where the inequality comes from the guaranteed cost of Theorem 3.9 and the last equality is obtained from $\xi[0] = (L_m + H_m)e_r$. The proof is concluded. \square

Notice that, for a given set of candidate limit cycles \mathfrak{X}_s associated to $c \in \mathfrak{C}_s(\kappa) \subseteq \mathfrak{C}(\kappa)$, the optimization problem (3.162) in Corollary 3.4 represents the solution of a certain number of convex subproblems that does not exceed N^κ , the number of elements of $\mathfrak{C}(\kappa)$. Making the optimization with respect to $c \in \mathfrak{C}_s(\kappa)$, we obtain the optimal limit cycle $\mathcal{X}_e^* \in \mathfrak{X}_s$, which minimizes the \mathcal{H}_2 guaranteed cost. Moreover, it is not difficult to conclude from its proof that for a periodic switching function the guaranteed and actual costs coincide, as already discussed just after Theorem 3.9. The following example illustrates these points.

Example 3.9. Consider a discrete-time switched affine system (3.140) with $N = 2$ subsystems defined by

the matrices

$$A_1 = \begin{bmatrix} 0.8 & 0 \\ -1 & -1.6 \end{bmatrix}, \quad A_2 = \begin{bmatrix} 1.2 & -0.5 \\ -0.2 & -0.1 \end{bmatrix}, \quad b_1 = \begin{bmatrix} 0.2 \\ 1.2 \end{bmatrix}, \quad b_2 = \begin{bmatrix} 0.2 \\ 0.1 \end{bmatrix} \quad (3.165)$$

$H_1 = H_2 = [-4 \ 2]', E_1 = E_2 = I$ and $G_1 = G_2 = 0$, defining two unstable subsystems which present no stable convex combination between them, i.e., there is no $\lambda \in \Lambda$ such that A_λ is Schur stable. The goal is to globally asymptotically stabilize the state trajectories to some limit cycle as close as possible to $x_* = [1.5 \ 0]'$, in terms of its mean value. Moreover, the switching function design must minimize an upper bound for the \mathcal{H}_2 performance index (3.145). To do so, for several values of $\kappa \in \{2, \dots, 10\}$ we built sets of candidate limit cycles \mathfrak{X}_s as in (3.150) with $\Gamma = (2/3)I$. Afterward, the candidate associated with the least upper bound $\bar{\mathcal{J}}_2$, given in (3.163), was selected by solving the optimization problem presented in Corollary 3.4 and the actual \mathcal{J}_2 performance index was obtained by means of numerical simulation. The obtained results are given in Table 3.4.

Table 3.4: Number of candidate limit cycles, upper bound $\bar{\mathcal{J}}_2$ and actual cost \mathcal{J}_2 for several κ .

κ	2	3	4	5	6	7	8	9	10
$ \mathfrak{X}_s $	3	4	7	6	24	22	47	76	108
$\bar{\mathcal{J}}_2$	infeas.	109.3246	infeas.	infeas.	109.3246	75.1449	235.2343	84.3215	92.9873
\mathcal{J}_2	infeas.	73.2469	infeas.	infeas.	73.2469	61.6781	119.4387	79.9657	62.4098

Considering values of κ for which feasible solutions were encountered, the actual costs \mathcal{J}_2 obtained from the switching function $\sigma[n] = u(\xi[n], n)$ were always smaller than their upper bounds $\bar{\mathcal{J}}_2$ assured by Corollary 3.4. Hence, we can conclude that the proposed state-dependent switching function is very efficient and a better option when compared to the periodic one.

Regarding this last example, a short remark is in order. For $\kappa = 10$, note that the full set of limit cycles \mathfrak{X} presents $N^\kappa = 1024$ elements. However, the adequate restriction of candidates provided by equation (3.150) reduced the number of convex optimization problems to be solved to 108. This shows that even though an exponential growth of complexity is expected with respect to κ , the designer can tune this constraint to avoid a large number of candidates and, consequently, convex optimization problems to solve.

3.3.5 \mathcal{H}_∞ Performance

Turning our attention to the \mathcal{H}_∞ control design, let us consider again system (3.143) but defined for $n \in \mathbb{N}$, with external input $w \in \mathcal{L}_2^d$ and $\xi[0] = 0$. Defining $\Xi_i[n] = H'_i P[n+1] H_i + G'_i G_i - \rho I$, the matrix

$$\mathcal{R}_i[n] = \begin{bmatrix} A'_i P[n+1] H_i + E'_i G_i \\ \ell_i[n]' P[n+1] H_i \end{bmatrix} \Xi_i[n+1]^{-1} \begin{bmatrix} A'_i P[n+1] H_i + E'_i G_i \\ \ell_i[n]' P[n+1] H_i \end{bmatrix}' \quad (3.166)$$

will be very useful to obtain the conditions for the \mathcal{H}_∞ control design as it will be clear in the next corollary.

Corollary 3.5. Consider system (3.140) defined for $n \in \mathbb{N}$ with $w \in \mathcal{L}_2^d$, evolving from $x[0] = x_e[0]$. Let the scalar $\kappa \in \mathbb{N}_+$ and the set of candidate limit cycles $\mathcal{X}_e(c) \in \mathfrak{X}_s$, $\forall c \in \mathfrak{C}_s(\kappa)$ be given. If there exist matrices $P[n] > 0$, a scalar $\rho > 0$, solution to the optimization problem

$$\min_{\mathcal{X}_e(c) \in \mathfrak{X}_s} \inf_{P[n], \rho} \rho \quad \text{s.t.} \quad (3.167)$$

$$\begin{bmatrix} P[n] & \bullet & \bullet & \bullet \\ 0 & \rho I & \bullet & \bullet \\ P[n+1]A_{c[n]} & P[n+1]H_{c[n]} & P[n+1] & \bullet \\ E_{c[n]} & G_{c[n]} & 0 & I \end{bmatrix} > 0 \quad (3.168)$$

$$H'_i P[n+1] H_i + G'_i G_i - \rho I < 0, \quad i \in \mathbb{K} \quad (3.169)$$

for all $n \in \{0, \dots, \kappa-1\}$, $c \in \mathfrak{C}_s(\kappa)$ with $P[\kappa] = P[0]$, then the switching function $\sigma[n] = u(\xi[n], n)$ with

$$u(\xi, n) = \arg \min_{i \in \mathbb{K}} \begin{bmatrix} \xi \\ 1 \end{bmatrix}' (\mathcal{L}_i[k(n)] - \mathcal{R}_i[k(n)]) \begin{bmatrix} \xi \\ 1 \end{bmatrix} + \xi' E'_i E_i \xi \quad (3.170)$$

assures that the limit cycle $\mathcal{X}_e^* = \mathcal{X}_e(c)$, solution to (3.167), is globally asymptotically stable and verifies the inequality $\mathcal{J}_\infty < \rho$.

Proof: Consider system (3.140) written alternatively as (3.143) with $\xi[0] = 0$, denote $\xi[n] = \xi$, $\sigma[n] = \sigma$ and $w[n] = w$, and define

$$\mathcal{F}_i[n] = \begin{bmatrix} A'_i P[n+1] A_i - P[n] + E'_i E_i & \bullet & \bullet \\ \ell_i[n]' P[n+1] A_i & \ell_i[n]' P[n+1] \ell_i[n] & \bullet \\ H'_i P[n+1] A_i + G'_i E_i & H'_i P[n+1] \ell_i[n] & \Xi_i[n] \end{bmatrix}$$

as well as the augmented variable $\tilde{\xi} = [\xi' \ 1 \ w']'$. Adopting the Lyapunov function (3.146), within the time interval $n \in \{0, \dots, \kappa-1\}$ we have the following developments

$$\begin{aligned} \Delta v(\xi, n) &= \tilde{\xi}' \mathcal{F}_\sigma[n] \tilde{\xi} - z'_e z_e + \rho w' w \\ &\leq \min_{i \in \mathbb{K}} \begin{bmatrix} \xi \\ 1 \end{bmatrix}' (\mathcal{L}_i[n] - \mathcal{R}_i[n]) \begin{bmatrix} \xi \\ 1 \end{bmatrix} + \xi' Q_i \xi - z'_e z_e + \rho w' w \\ &\leq \begin{bmatrix} \xi \\ 1 \end{bmatrix}' (\mathcal{L}_{c[n]}[n] - \mathcal{R}_{c[n]}[n]) \begin{bmatrix} \xi \\ 1 \end{bmatrix} + \xi' Q_{c[n]} \xi - z'_e z_e + \rho w' w \\ &= \xi' (A'_{c[n]} P[n+1] A_{c[n]} - P[n] + Q_{c[n]} - \mathcal{T}_{c[n]}[n] \Xi_{c[n]}[n]^{-1} \mathcal{T}_{c[n]}[n]') \xi - z'_e z_e + \rho w' w \\ &< -z'_e z_e + \rho w' w \end{aligned} \quad (3.171)$$

with $\mathcal{T}_i[n] = A'_i P[n+1] H_i + E'_i G_i$ and $Q_i = E'_i E_i$. The first inequality comes from the fact that function $h_i(\xi, w) = \tilde{\xi}' \mathcal{F}_i[n] \tilde{\xi}$ is concave with respect to w for all $i \in \mathbb{K}$ due to (3.169). Hence, it is possible to determine $\sup_{w \in \mathcal{L}_2^d} h_\sigma(\xi, w)$ which occurs for

$$w^* = -\Xi_\sigma[n]^{-1} (\mathcal{T}'_\sigma[n] \xi + H'_\sigma P[n+1] \ell_\sigma[n]) \quad (3.172)$$

This value, together with the switching function provided in (3.170), results in the expression of the right-hand side of the first inequality. The second inequality is a consequence of the minimum operator, the second equality is due to $\ell_{c[n]}[n] = 0$, since the sequence $c \in \mathfrak{C}_s(\kappa)$ is associated with the limit cycle $\mathcal{X}_e(c) \in \mathfrak{X}_s$. Finally, the last inequality comes from the validity of (3.168). The periodic continuation $P[n] = P[k(n)]$ assures that

$\Delta v(\xi, n) < -z'_e z_e + \rho w' w$ for all $n \in \mathbb{N}$. Summing both sides of this inequality from $n = 0$ up to infinity, and recalling that $v(\xi[0], 0) = 0$ since $\xi[0] = 0$ and $\lim_{n \rightarrow \infty} v(\xi[n], n) = 0$ as a consequence of the asymptotic stability of the origin $\xi = 0$, we obtain

$$\|z_e\|_2^2 - \rho \|w\|_2^2 < 0 \quad (3.173)$$

which assures the validity of the \mathcal{H}_∞ guaranteed cost, concluding thus the proof. \square

This corollary generalizes results from Theorem 3.9 to deal with \mathcal{H}_∞ performance optimization during the switching function design. An interesting remark at this point is that, considering one of the criteria (3.150) or (3.151), whenever \mathfrak{X}_s is non-empty it has at least κ candidate limit cycles, which are shifted versions of each other. In fact, as an example, the sequences $c \in \{(1, 2, 2, 1), (2, 2, 1, 1), (2, 1, 1, 2), (1, 1, 2, 2)\}$ provide the same limit cycle but with different initial points $x_e[0]$. Therefore, if one of them is inside $\mathfrak{C}_s(\kappa)$ the others are as well. Whenever this scenario takes place in the \mathcal{H}_2 control design, the optimization with respect to $\mathcal{X}_e(c) \in \mathfrak{X}_s$ consists in determining the best initial value $x_e[0]$ such that the guaranteed cost is minimized. On the other hand, the \mathcal{H}_∞ design procedure produces the same optimal upper bound ρ for all the shifted versions since the optimization problem (3.167) in Corollary 3.5 is independent of $x_e[0]$.

The next subsection presents examples illustrating both \mathcal{H}_2 and \mathcal{H}_∞ control design in a power electronics application.

3.3.6 Application for DC-DC Conversion

This application example was borrowed from the recent reference Benmiloud et al. (2019), which also treats the asymptotic stability of a limit cycle, but in the continuous-time domain and guaranteeing only local stability. It considers a multicellular DC-DC converter feeding an inductive load as depicted in Figure 3.19, which is composed of a series association of elementary commutation cells, each one consisting of a pair of complementary switches (i.e., when s_1 is open s_4 is closed). The system parameters are $V_{dc} = 60$ V, $C_1 = C_2 = 40 \mu\text{F}$, $L = 5 \text{ mH}$, and $R = 20 \Omega$. This topology presents $N = 8$ operation modes (or subsystems) from which a switching signal $\sigma(t)$ selects one of them as active at each instant of time. This system can be modeled as the continuous-time switched affine system

$$\begin{cases} \dot{x}(t) &= A_{c\sigma(t)}x(t) + b_{c\sigma(t)} + H_{c\sigma(t)}w(t) \\ z_c(t) &= E_{c\sigma(t)}x(t) + G_{c\sigma(t)}w(t) \end{cases} \quad (3.174)$$

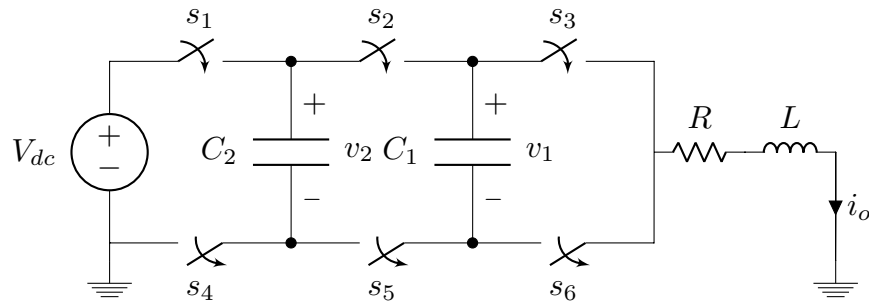


Figure 3.19: Schematic of a three-cell converter.

Table 3.5: Values u_1 , u_2 , and u_3 for each operation mode i

i	1	2	3	4	5	6	7	8
u_1	0	1	0	1	0	1	0	1
u_2	0	0	1	1	0	0	1	1
u_3	0	0	0	0	1	1	1	1

where the state is defined as $x(t) = [v_1(t) \ v_2(t) \ i_o(t)]'$, the exogenous input $w(t)$ represents a disturbance and $\sigma(t)$ must be governed by a switching function to be designed. The system matrices are

$$A_{ci} = \begin{bmatrix} 0 & 0 & \frac{u_2 - u_1}{C_1} \\ 0 & 0 & \frac{u_3 - u_2}{C_2} \\ \frac{u_1 - u_2}{L} & \frac{u_2 - u_3}{L} & \frac{-R}{L} \end{bmatrix}, \quad b_{ci} = \begin{bmatrix} 0 \\ 0 \\ \frac{V_{dc}u_3}{L} \end{bmatrix}, \quad (3.175)$$

$E_{ci} = \text{diag}([1 \ 1 \ 1])$ and $G_{ci} = [0 \ 0 \ 0]'$, $i \in \mathbb{K}$. The matrices $H_{ci} \in \mathbb{R}^3$, $\forall i \in \mathbb{K}$, will be defined afterward, for each control design case. The values for u_1 , u_2 , and u_3 are given in Table 3.5 as a function of the current value of the switching signal $\sigma(t) = i$. In order to treat this problem in the discrete-time domain, assuring an upper bound for the switching frequency, a sampling period $T = 0.1$ ms is taken into account, such that the switching signal must respect $\sigma(t) = \sigma(t_n)$ for all $t \in [t_n, t_{n+1})$ where $t_n = nT$ is the n -th sampling instant. Denoting $x(t_n) = x[n]$, $\forall n \in \mathbb{N}$, let us consider the norm-equivalent discretization procedure, presented in Subsection 2.2.3 which provides a controlled output $z[n]$ that satisfies

$$\|z\|_2^2 = \|z_c\|_2^2 = \int_0^\infty z_c(t)' z_c(t) dt \quad (3.176)$$

indicating that \mathcal{L}_2^d -norms of the controlled outputs $z_c(t)$ and $z[n]$ are identical. With this procedure, we can obtain the discrete-time switched affine system (3.140) with matrices

$$\begin{bmatrix} A_i & [b_i \ H_i] \\ 0 & I \end{bmatrix} = e^{\mathcal{A}_i T}, \quad \begin{bmatrix} E'_i \\ G'_i \end{bmatrix}' = \int_0^T e^{\mathcal{A}'_i t} \mathcal{E}'_i \mathcal{E}_i e^{\mathcal{A}_i t} dt \quad (3.177)$$

and

$$\mathcal{A}_i = \begin{bmatrix} A_{ci} & [b_{ci} \ H_{ci}] \\ 0 & 0 \end{bmatrix}, \quad \mathcal{E}_i = [E_{ci} \ G_{ci}]$$

for all $i \in \mathbb{K}$, where it is assumed that the external input $w(t) = w(t_n)$, $\forall t \in [t_n, t_{n+1})$, is piecewise constant, which can be a good approximation for a low-frequency disturbance $w(t)$.

Hence, concerning the discretized system, our goal is to design a limit cycle \mathcal{X}_e^* and a switching function $\sigma[n] = u(\xi[n], n)$ able to govern the state trajectories $x[n]$ from any initial condition towards \mathcal{X}_e^* , assuring \mathcal{H}_2 or \mathcal{H}_∞ performance indexes. In contrast with the local stability results of Benmiloud et al. (2019), the proposed methodology assures global asymptotic stability of \mathcal{X}_e^* .

Before proceeding to the control design, the set of candidate limit cycles has to be determined. The limit cycle \mathcal{X}_e^* must be chosen to keep a suitable maximum distance to the reference point $x_* = [V_{dc}/3 \ 2V_{dc}/3 \ I_{ref}]$, with a free $I_{ref} \in [0, I_{max}]$, where $I_{max} = V_{dc}/R$ is the maximum possible current at the output of the converter.

Notice that x_* is not an equilibrium point of any subsystem and its asymptotic stability is impossible in the discrete-time domain. Our goal is accomplished by taking $\kappa = 6$ and adopting (3.151) with $\Gamma = \text{diag}\{0.5, 0.5, 0\}$ in order to construct the set of candidate limit cycles \mathcal{X}_s . Using these parameters, we have obtained 30 candidates from which the one providing the best transient response is chosen. The given Γ imposes that the voltages v_1 and v_2 must not deviate more than 2 V from the references specified in x_* during the steady state. For organization purposes, the \mathcal{H}_2 and \mathcal{H}_∞ control design are presented separately in the following examples.

Example 3.10. (\mathcal{H}_2 case) Our interest is to design a switching function $\sigma[n] = u(\xi[n], n)$ to optimize the transient response of the discretized system, starting from a null initial condition $x[0] = 0$, which represents the system start-up. Considering that in the \mathcal{H}_2 case, the external input is not piecewise constant, but of impulsive type, matrices H_i , $\forall i \in \mathbb{K}$, are determined differently from those provided in the norm-equivalent discretization procedure. Indeed, for $w[n] = \delta[n+1]$, $x[-1] = x_e[-1]$ and choosing $\sigma[-1] = c[\kappa - 1] = m$, the discrete-time matrices are given by $H_i = -x_e[0]$, $\forall i \in \mathbb{K}$, which lead to $x[0] = 0$. Under these conditions, solving the optimization problem of Corollary 3.4 we have obtained an \mathcal{H}_2 guaranteed cost of $\bar{\mathcal{J}}_2 = 37.7903$ associated to the sequence $c = (5, 1, 3, 1, 2, 1)$ and the limit cycle \mathcal{X}_e^* defined by the fundamental period

$$(x_e[0], \dots, x_e[5]) = \left(\begin{bmatrix} 19.5989 \\ 39.4582 \\ 0.4031 \end{bmatrix}, \begin{bmatrix} 19.5989 \\ 40.7315 \\ 0.5983 \end{bmatrix}, \begin{bmatrix} 19.5989 \\ 40.7315 \\ 0.4011 \end{bmatrix}, \begin{bmatrix} 20.8722 \\ 39.4582 \\ 0.5961 \end{bmatrix}, \begin{bmatrix} 20.8722 \\ 39.4582 \\ 0.3996 \end{bmatrix}, \begin{bmatrix} 19.5989 \\ 39.4582 \\ 0.6014 \end{bmatrix} \right) \quad (3.178)$$

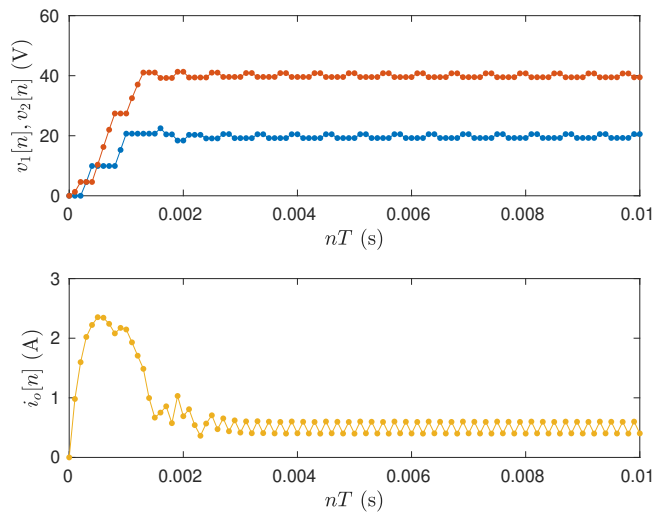


Figure 3.20: State trajectories for \mathcal{H}_2 control design.

Implementing the switching function $\sigma[n] = u(\xi[n], n)$, given in (3.158), Figure 3.20 presents the state trajectories and Figure 3.21 shows the corresponding switching signal obtained by the discrete-time simulation. A phase portrait of the system trajectories toward the limit cycle is given in Figure 3.22 and a zoom on the limit cycle under the steady-state operation is presented in Figure 3.23, where the arrow represents the direction of the state trajectory. Evaluating numerically the \mathcal{H}_2 performance index (3.144) we have obtained $\mathcal{J}_2 = 1.7632$, which shows the efficiency of the designed switching function, since by

adopting the periodic switching function $\sigma[n] = c[k(n)]$ the value $\mathcal{J}_2 = 37.7903$ is obtained.

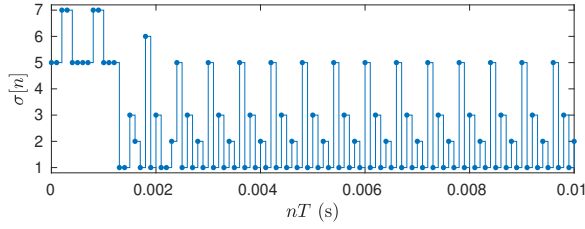


Figure 3.21: Obtained switching signal for \mathcal{H}_2 control design.

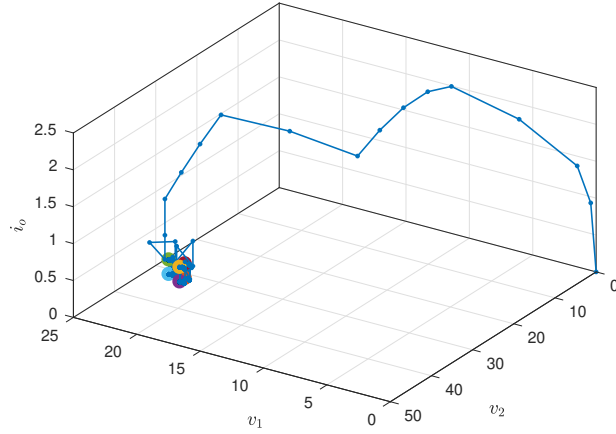


Figure 3.22: State trajectories converging to the limit cycle \mathcal{X}_e^* .

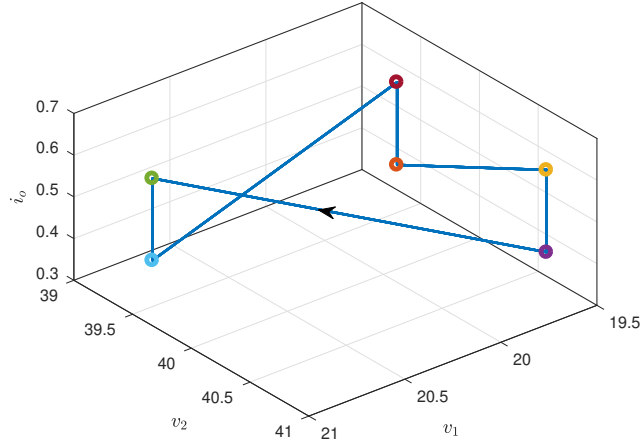


Figure 3.23: Zoom showing the limit cycle \mathcal{X}_e^* in steady-state.

Example 3.11. (\mathcal{H}_∞ case) Now our goal is to design a switching function $\sigma[n] = u(\xi[n], n)$ but to attenuate the influence of an exogenous input representing a voltage oscillation and a voltage dip of the input source

V_{dc} . Voltage dips (or voltage sags) are recurrent events that depreciate power quality and may generate failures in sensitive loads such as medical equipment, factory automations, among others, see Dargahi et al. (2012). Considering now the continuous-time matrices $H_{ci} = [0 \ 0 \ u_3/L]'$, $\forall i \in \mathbb{K}$, which model $w(t)$ as a deviation of the input voltage around the considered V_{dc} . Taking into account the discretized system, a limit cycle $\mathcal{X}_e^* \in \mathfrak{X}_s$ must now be chosen to minimize ρ . Solving the optimization problem of Corollary 3.5, we have assured an \mathcal{H}_∞ guaranteed cost of $\rho = 0.3633 \times 10^{-3}$ associated to the sequence $c = (3, 1, 2, 1, 5, 1)$ and the correspondent optimal limit cycle \mathcal{X}_e^* , which is the same of the \mathcal{H}_2 case but shifted by 2.

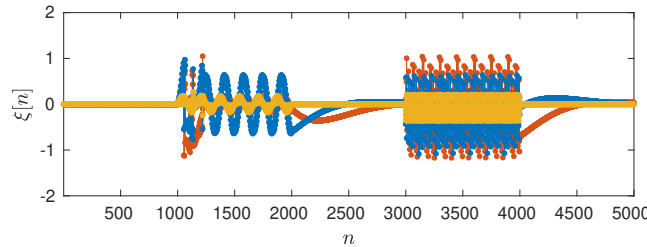


Figure 3.24: Discrete-time state $\xi[n]$ for \mathcal{H}_∞ control design.

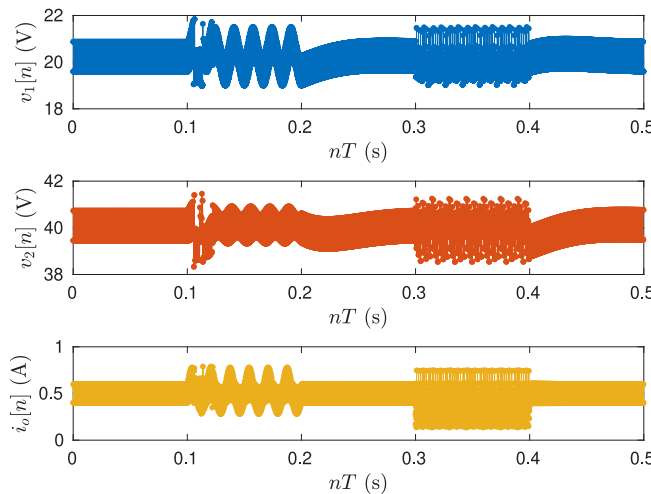


Figure 3.25: State trajectories for \mathcal{H}_∞ control design.

Implementing the switching function $\sigma[n] = u(\xi[n], n)$ with $u(\xi[n], n)$ given in (3.170), starting the system from $x[0] = [19.5989 \ 40.7315 \ 0.4011]'$ and considering the following exogenous input

$$w[n] = \begin{cases} 10 \sin(120\pi Tn), & n \in [0.1/T, 0.2/T] \\ -20, & n \in [0.3/T, 0.4/T] \\ 0, & \text{otherwise} \end{cases} \quad (3.179)$$

we have obtained a discrete-time state trajectories $\xi[n]$ and $x[n]$ depicted in Figures 3.24 and 3.25, respectively. Moreover, the RMS value of the output current $i_o[n]$ has been calculated over three different intervals, namely voltage oscillation $n \in [0.1/T, 0.2/T]$, voltage dip $n \in [0.3/T, 0.4/T]$ and regular operation $n \in [0, 0.1/T]$ providing 0.5161 A, 0.4231 A and 0.5096 A, respectively. This demonstrates that the designed switching function was successful in reducing the influence of the disturbance $w[n]$ on the system behavior,

guaranteeing an RMS deviation of approximately 17% during a voltage dip of 33%, compared to the regular operation.

3.4 Concluding Remarks

The results in this chapter treat the control of discrete-time switched affine systems where state and output-dependent switching functions are designed to govern system trajectories toward a desired reference. Two globally stabilizing approaches are presented, being the first one based on practical stability and the second one, on asymptotic stability of a desired limit cycle. More precisely, we have presented studies on the existence of a set of attraction \mathcal{X} containing the desired point x_e and whose volume is minimized in the design step. At the first moment, LMI conditions based on a general quadratic Lyapunov function (3.6) are presented and ellipsoidal sets of attraction are considered. These conditions are generalized to cope with output-dependent switching, where a full-order switched filter is proposed to orchestrate the switching function. This generalization is shown to be capable of equally assure the existence of any set of attraction \mathcal{X} obtained for the state feedback case, whenever matrix pairs (A_i, C_i) , $i \in \mathbb{K}$ are quadratically detectable. Later, departing from a min-type Lyapunov function, novel practical stability conditions are presented based on the Lyapunov-Metzler inequalities and guaranteeing the existence of a nonconvex set of attraction \mathcal{X} . This is the first time that these inequalities are used in the context of switched affine systems and are less restrictive in terms of assuring the existence of \mathcal{X} .

Another approach, based on asymptotic stability of limit cycles, is introduced afterward. In this case, performance optimization in the steady and transient states could be considered. More specifically, we have developed the design procedure of switching functions for this class of systems in two sequential steps. First, we have obtained a set of candidate limit cycles $\mathcal{X}_e(c) \in \mathfrak{X}_s$ based on some criteria specified by the designer, which involve aspects such as their periods, oscillation amplitudes and mean values. As a second step, we have determined a state and time-dependent switching function in order to assure global asymptotic stability of the “best” limit cycle $\mathcal{X}_e^* \in \mathfrak{X}_s$, that is, the one correspondent to the least \mathcal{H}_2 or \mathcal{H}_∞ guaranteed cost, provided in Corollary 3.4 or 3.5, respectively.

“Você me pergunta aonde que eu quero chegar / Se há tantos caminhos na vida e pouca esperança no ar.”

— RAUL SEIXAS, CAMINHOS (1975)

STUDIES regarding switched systems presenting some particular nonlinearities within their subsystem models are discussed in this chapter. The motivation is twofold, relying on applications to switching power electronic circuits and theoretical challenges of dealing with such nonlinear systems without using averaged models.

Practical interest follows from the fact that switched control strategies for alternating current (AC) systems seem to have received less investigation from the scientific community when compared to direct current (DC) power systems. Indeed, the time-varying nature of AC currents requires a class of parameter-dependent switched systems to precisely model these devices and allow switched control theory to be employed. As instances of currently existing research works in switched control of DC-AC conversion, state-dependent switching rules to command the switches of a three-phase inverter feeding a squirrel-cage induction motor in Scharlau et al. (2013) and a PMSM in Delpoux et al. (2014) are proposed to regulate the shaft rotational velocity using approaches based on auxiliary reference frames. Dealing with DC-AC power converter, reference Sanchez et al. (2019b) has proposed a switched control law based on the hybrid dynamic system theory, where the main goal is to track a sinusoidal reference trajectory assuring a minimum dwell time and guaranteeing practical stability. For AC-DC power converters there are only few results using techniques based on the switched control theory. See for instance the recent reference Hadjeras et al. (2019), where a hybrid control law is proposed for a three-level Neutral Point Clamped (NPC) converter, working as a rectifier to regulate the output DC voltage.

The common nonlinear phenomenon studied throughout this chapter is a periodic dependency on an angular parameter $\theta(t)$ whose variation rate, which can be regarded as an angular velocity, can be arbitrary or given as some function of the state variable. This is certainly a hindrance to employing results presented in the last chapters for designing switching functions. For this reason, specific Lyapunov functions will be employed, allowing an efficient stability analysis with a suitable system response and based on less conservative stability conditions. The problem of trajectory tracking will naturally arise and will be adequately explored.

First, a motivational case is presented where some properties of a parameter-dependent Lyapunov function are discussed. Afterward, two application cases will be studied and appropriate tools to assess the asymptotic stability of both cases will be developed. Namely, these cases consist of controlling the switches in three-phase converters to, firstly, control the velocity of a permanent magnet synchronous machine and, subsequently, achieve AC-DC conversion under unitary power factor operation.

4.1 Parameter-dependent Lyapunov Function

A **parameter-dependent Lyapunov function** can be regarded as a special class of time-varying ones given, for example, as

$$v(x(t), \theta(t)) = x(t)' P(\theta(t)) x(t) \quad (4.1)$$

where $x : \mathbb{R}_{0+} \rightarrow \mathbb{R}^{n_x}$ is the state variable, $\theta : \mathbb{R}_{0+} \rightarrow \mathbb{R}$ is a **time-varying angular parameter** and $P : \mathbb{R} \rightarrow \mathbb{R}^{n_x \times n_x}$ is a parameter-dependent positive definite matrix which is periodic with respect to $\theta(t)$, that is, we have $P(\theta + 2\pi k) = P(\theta)$ for all $\theta \in \mathbb{R}$ and $k \in \mathbb{Z}$. Notice that $v(\cdot)$ is convex and radially unbounded with respect to the state x and might be non-convex with respect to θ . Moreover, from Lemma A.1, it clearly admits parameter independent lower and upper bounds $v_{lb}(x) = \min_{\theta,i} \gamma_i(P(\theta)) \|x\|^2$ and $v_{ub}(x) = \max_{\theta,i} \gamma_i(P(\theta)) \|x\|^2$, respectively.

A Lyapunov function candidate given as (4.1) can be used, for example, to study the stability of the origin for a dynamic system given as

$$\dot{x}(t) = A(\theta(t))x(t), \quad x(0) = x_0 \quad (4.2)$$

where $\theta(t)$ and the matrix function $A : \mathbb{R} \rightarrow \mathbb{R}^{n_x \times n_x}$ are well defined. A periodic behavior is also considered for $A(\theta(t))$ with the same period 2π , making the Lyapunov function (4.1) well adapted to this system. Indeed, evaluating its time-derivative along arbitrary trajectories $x(t)$ and $\theta(t)$, yields

$$\dot{v}(x(t), \theta(t)) = x(t)' \left(A(\theta(t))' P(\theta(t)) + P(\theta(t))A(\theta(t)) + \dot{P}(\theta(t)) \right) x(t) \quad (4.3)$$

Notice the presence of the time derivative of $P(\theta)$ in the Lyapunov function derivative. A particular case that will serve as motivation for the following sections is presented in the next example.

Example 4.1. Consider a continuous-time system of the form (4.2) defined by a matrix

$$A(\theta(t)) = R(\theta(t))' \left(FR(\theta(t)) - \dot{R}(\theta(t)) \right) \quad (4.4)$$

with $\dot{\theta}(t) = \omega = 5$ rad/s, $\theta(0) = 0$ and

$$F = \begin{bmatrix} 0 & 1 \\ -10 & -7 \end{bmatrix}, \quad R(\theta) = \begin{bmatrix} \cos(\theta) & -\sin(\theta) \\ \sin(\theta) & \cos(\theta) \end{bmatrix}, \quad \dot{R}(\theta) = \omega \begin{bmatrix} -\sin(\theta) & -\cos(\theta) \\ \cos(\theta) & -\sin(\theta) \end{bmatrix} \quad (4.5)$$

Notice that F is a Hurwitz stable matrix and that $R(\theta)R(\theta)' = I$. Adopt the Lyapunov function (4.1) with $P(\theta) = R(\theta)'WR(\theta)$ and $W > 0$ satisfying $F'W + WF < 0$. Evaluating (4.3), yields

$$\begin{aligned} \dot{v}(x, \theta) &= x' \left(A(\theta)' P(\theta) + P(\theta)A(\theta) + \dot{P}(\theta) \right) x \\ &= x' \left(\text{He} \left((R(\theta)' F' - \dot{R}(\theta)') R(\theta) R(\theta)' W R(\theta) + \dot{R}(\theta)' W R(\theta) \right) \right) x \\ &= x' (R(\theta)' (F'W + WF) R(\theta)) x \\ &< 0 \end{aligned} \quad (4.6)$$

characterizing global asymptotic stability of the origin $x = 0$. Indeed, simulating the system state evolution departing from $x_0 = [0.6 \ - 0.6]'$, we obtain the phase portrait in Figure 4.1, where some level sets $\mathcal{V}_t = \{y \in \mathbb{R}^2 : v(y, \theta(t)) = x(t)'P(\theta(t))x(t)\}$ of the Lyapunov function are depicted for

$$W = \begin{bmatrix} 2.5643 & 0.0500 \\ 0.0500 & 0.2214 \end{bmatrix} \quad (4.7)$$

Figure 4.2 displays a three-dimensional representation of this phase portrait taking into account the time as one of the axis.

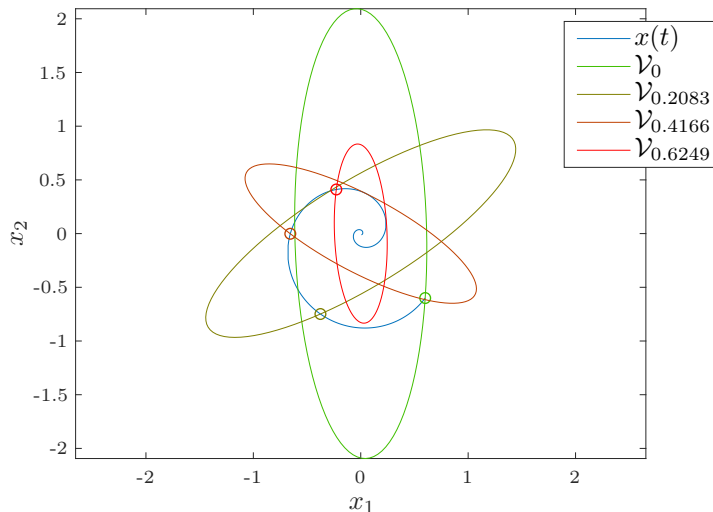


Figure 4.1: Phase portrait of a trajectory $x(t)$ along with some level sets \mathcal{V}_t .

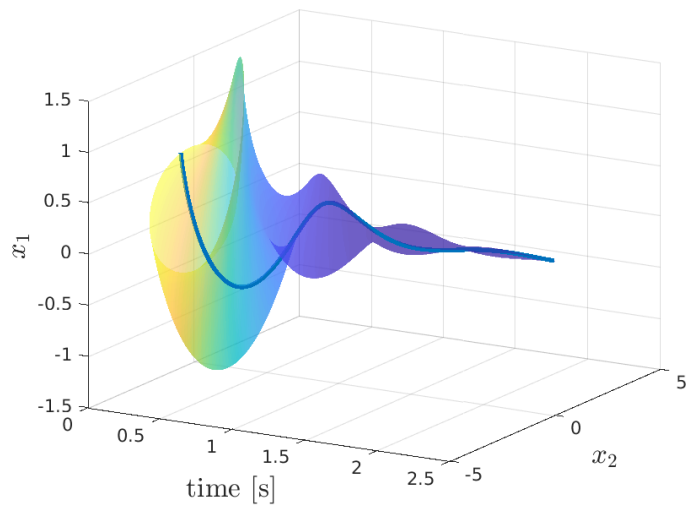


Figure 4.2: Level sets of the Lyapunov function evaluated along the trajectory $x(t)$ (in blue).

This example showed how a parameter-dependent Lyapunov function can capture key features of a dynamic system presenting dependency on the same parameter, easing its analysis and, as will be clear afterward,

control design. The Lyapunov function considered has a parameter-dependent matrix $P(\theta)$ whose eigenvalues do not depend on θ . This function possesses ellipsoid-shaped level sets that rotate with respect to θ and are periodic with period 2π . Even though a linear dependency with time was taken into account, notice that the reasoning within Example 4.1 can be employed to guarantee stability for an arbitrary trajectory $\theta(t)$.

As shown in Figure 4.1, the level set areas are decreasing over time but the system trajectory might leave the current level set in a subsequent instant of time, given the rotative nature of the system. The rotation causes non-convexity of $v(x, \theta)$ with respect to θ and, consequently, time. However, global asymptotic convergence is still assured because of the guaranteed contraction of the level sets \mathcal{V}_t , which was illustrated by means of Figure 4.2. In the next sections, two dynamical systems that model power electronic devices are presented and the adoption of parameter-dependent Lyapunov functions will be of main importance to obtain efficient methods for switching control design.

4.2 Permanent Magnet Synchronous Machines

A **permanent magnet synchronous machine** (PMSM) is an electrical drive characterized by the presence of permanent magnets in the rotor (not requiring magnetizing currents) and a set of windings in the stator. It presents a high torque density, low torque ripple, high efficiency and a wide range of velocities. These features make PMSMs desirable in several high-performance applications such as electrical and hybrid vehicles Yang et al. (2015), autonomous water-pumping stations Antonello et al. (2017), aerospace applications Kefalas and Kladas (2014), among others. References on modeling and classical control approaches for these machines are available in Krishnan (2009) and Krause et al. (2013).

Generally, PMSMs are fed by a **voltage source inverter** (VSI) whose switches are operated to command desired voltages to each machine terminal, as it is schematized in Figure 4.3. A standard approach to control these switches, known as field-oriented control (FOC), consists in modeling the machine in terms of an auxiliary rotating reference frame in which the currents are regulated by means of PID controllers together with feedback linearization techniques. Another recurrent approach in the literature is the direct-torque control (DTC) which, in general, controls the machine torque by adopting switching tables that depend on the estimated magnetic flux and torque signals. Nevertheless, both methods require reference frame transformations (e.g., Park and Clarke transformations) and a second slower feedback loop that provides the reference current or torque to the inner loop. This additional controller stabilizes the machine shaft velocity or its position to a desired reference. A detailed comparison of these schemes can be found in Casadei et al. (2002). To the best of my knowledge, the literature to date does not present results regarding the control of a PMSM in the framework of switched systems, where a switching function is designed to decide continuously the state (open or closed) of the VSI switches, without using auxiliary reference frames. This approach enables the control of the PMSM in a single loop, bringing the rotor velocity to a desired value in a simpler manner.

Consider the three-phase permanent magnet synchronous machine with one pair of poles fed by a three-phase inverter with switches $\{s_1, \dots, s_6\}$ and a DC source V_{dc} depicted in Figure 4.3. The dynamic model of

this assembly is described by the following coupled nonlinear differential equations

$$L \frac{di_a(t)}{dt} + Ri_a(t) = \nu_a(t) - \mu\omega(t)f_a(\theta(t)) \quad (4.8)$$

$$L \frac{di_b(t)}{dt} + Ri_b(t) = \nu_b(t) - \mu\omega(t)f_b(\theta(t)) \quad (4.9)$$

$$L \frac{di_c(t)}{dt} + Ri_c(t) = \nu_c(t) - \mu\omega(t)f_c(\theta(t)) \quad (4.10)$$

together with

$$J \frac{d\omega(t)}{dt} + c\omega(t) = \mu i_a(t)f_a(\theta(t)) + \mu i_b(t)f_b(\theta(t)) + \mu i_c(t)f_c(\theta(t)) - \tau \quad (4.11)$$

$$\frac{d\theta(t)}{dt} = \omega(t) \quad (4.12)$$

where $i_a(t)$, $i_b(t)$ and $i_c(t)$ are phase currents satisfying $i_a(t) + i_b(t) + i_c(t) = 0$ for all $t \in \mathbb{R}_{0+}$, $\nu_a(t)$, $\nu_b(t)$ and $\nu_c(t)$ are phase to neutral voltages, R and L are the resistance and the equivalent inductance per phase, respectively, J is the rotor moment of inertia, μ is the peak value of the mutual flux linkage, c is the viscous friction coefficient and τ is the external constant torque. The time-varying parameter $\theta(t)$ is the shaft angular displacement and $\omega(t)$ is its angular velocity. The auxiliary periodic functions $f_a(\theta)$, $f_b(\theta)$ and $f_c(\theta)$ are related to the shape of the back electromotive force (emf) and are defined as

$$f_a(\theta) = \sin(\theta) \quad (4.13)$$

$$f_b(\theta) = \sin(\theta - 2\pi/3) \quad (4.14)$$

$$f_c(\theta) = \sin(\theta - 4\pi/3) \quad (4.15)$$

An important remark is that the assumption of a single pole pair is done without loss of generality. For a machine with n_p pole pairs, a variable $\theta_e = n_p\theta$ can be defined to express the electrical angle on which $f(\cdot)$ should depend in equations (4.8)-(4.11), leading to similar developments. The voltages $\nu_a(t)$, $\nu_b(t)$ and $\nu_c(t)$ depend exclusively on the state (open or closed) assigned to the switches $\{s_1, \dots, s_6\}$, at each instant of time. More specifically, s_i is 1 when the switch is closed and 0 when it is open. The control of these switches is the only manner of actuating in the system to make the angular velocity $\omega(t)$ asymptotically convergent toward a pre-specified profile $\omega^*(t)$ chosen by the designer. Each pair of switches (s_1, s_4) , (s_2, s_5) , (s_3, s_6) is alternately commanded, for instance, s_1 is closed whenever s_4 is open, and *vice-versa*. Thus, there exist eight possible configurations for the switches, defining seven combinations for the triple $\nu_a(t)$, $\nu_b(t)$ and $\nu_c(t)$ that are represented by the

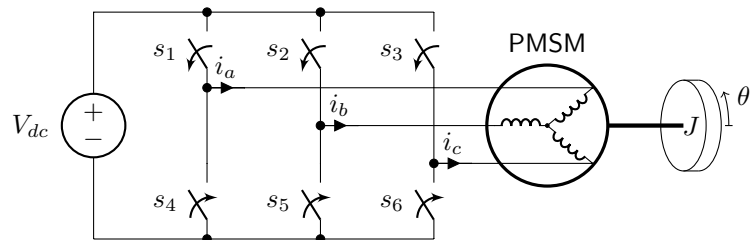


Figure 4.3: PMSM and inverter schematic.

σ	s_1	s_2	s_3	ν_a	ν_b	ν_c
1	0	0	1	$-V_{dc}/3$	$-V_{dc}/3$	$2V_{dc}/3$
2	0	1	0	$-V_{dc}/3$	$2V_{dc}/3$	$-V_{dc}/3$
3	0	1	1	$-2V_{dc}/3$	$V_{dc}/3$	$V_{dc}/3$
4	1	0	0	$2V_{dc}/3$	$-V_{dc}/3$	$-V_{dc}/3$
5	1	0	1	$V_{dc}/3$	$-2V_{dc}/3$	$V_{dc}/3$
6	1	1	0	$V_{dc}/3$	$V_{dc}/3$	$-2V_{dc}/3$
7	1	1	1	0	0	0
	0	0	0			

Table 4.1: Modes σ , switches state and phase voltages.

switching signal $\sigma : \mathbb{R}_{0+} \rightarrow \mathbb{K} = \{1, \dots, 7\}$, as detailed in Table 4.1. This allows us to describe (4.8)-(4.12) by the following state-space representation

$$\dot{x}(t) = A(\theta(t))x(t) + b_{\sigma(t)}, \quad x(0) = x_0 \quad (4.16)$$

$$\dot{\theta}(t) = \omega(t), \quad \theta(0) = \theta_0 \quad (4.17)$$

where $x(t) = [i_\phi(t)' \ \omega(t)]' : \mathbb{R}_{0+} \rightarrow \mathbb{R}^4$ is the state variable with $i_\phi(t) = [i_a(t) \ i_b(t) \ i_c(t)]'$ and the matrices $(A(\theta), b_\sigma)$ are given by

$$A(\theta) = \begin{bmatrix} -(R/L)I & -(\mu/L)f(\theta) \\ (\mu/J)f(\theta)' & -(c/J) \end{bmatrix}, \quad b_\sigma = \begin{bmatrix} (1/L)\nu_\sigma \\ -(\tau/J) \end{bmatrix} \quad (4.18)$$

where the vector valued function is $f(\theta) = [f_a(\theta) \ f_b(\theta) \ f_c(\theta)]' : \mathbb{R} \rightarrow \mathbb{R}^3$, and the voltage function $\nu_{\sigma(t)} = [\nu_a(t) \ \nu_b(t) \ \nu_c(t)]' : \mathbb{R}_{0+} \rightarrow \mathbb{R}^3$ takes the values shown in Table 4.1, for different modes $\sigma(t) \in \mathbb{K}$, $\forall t \in \mathbb{R}_{0+}$.

The main goal of this section is to design a state-dependent switching function $u : \mathbb{R}^4 \times \mathbb{R} \rightarrow \mathbb{K}$ such that the switching control $\sigma(t) = u(x(t), \theta(t))$ guarantees asymptotic tracking to a given rotational velocity profile $\omega^*(t)$, $\forall t \in \mathbb{R}_{0+}$, that is

$$\lim_{t \rightarrow \infty} \omega(t) = \omega^*(t) \quad (4.19)$$

Ideally, the switching function should be designed from the solution to the optimal control problem

$$\min_{\sigma} \int_0^{\infty} \left(\| (i_\phi(t) - i_\phi^*(t)) \|^2 + d(\omega(t) - \omega^*(t))^2 \right) dt \quad (4.20)$$

where $d \in \mathbb{R}_+$ is a parameter used by the designer to define an appropriate tradeoff between the two parts of the total cost and $i_\phi^*(t)$ is the phase current reference vector, to be determined as a function of $\omega^*(t)$. However, as it has been already discussed in the literature, see for instance Deaecto et al. (2010), this problem is extremely difficult to solve due to the nonlinear nature of the switching control and, therefore, a suboptimal solution is obtained by minimizing a suitable upper bound of (4.20). Actually, we are particularly interested in assuring the asymptotic convergence of the rotor velocity $\omega(t)$ to the desired profile expressed by $\omega^*(t)$ and, therefore, the correspondent phase current vector $i_\phi^*(t)$ is obtained accordingly from the knowledge of $\theta(t)$, $\omega^*(t)$ and $\dot{\omega}^*(t)$ as will be clear in the sequel.

4.2.1 Mathematical Properties of Function $f(\theta)$

The vector valued function $f : \mathbb{R} \rightarrow \mathbb{R}^3$ can be rewritten as $f(\theta) = Gh(\theta)$ with

$$G = \begin{bmatrix} 1 & 0 \\ -1/2 & -\sqrt{3}/2 \\ -1/2 & \sqrt{3}/2 \end{bmatrix}, \quad h(\theta) = \begin{bmatrix} \sin(\theta) \\ \cos(\theta) \end{bmatrix} \quad (4.21)$$

where the matrix $G \in \mathbb{R}^{3 \times 2}$ coincides with the inverse Clarke transformation, see Duesterhoeft et al. (1951). Using (4.21) and the fact that $G'G = (3/2)I$, simple algebraic manipulations show that for an arbitrary solution $\theta(t)$ and $\omega(t)$ satisfying (4.17) for all $t \in \mathbb{R}_{0+}$, the relations

$$f(\theta)'f(\theta) = \frac{3}{2}, \quad f(\theta, \omega)'f(\theta) = 0, \quad f(\theta, \omega)'f(\theta, \omega) = \frac{3}{2}\omega^2 \quad (4.22)$$

hold with $\dot{f}(\theta, \omega) = \omega(\partial f / \partial \theta)$. Finally, for the vector $e = [1 \ 1 \ 1]' \in \mathbb{R}^3$, along the same trajectories we also have $e'f(\theta) = 0$ and $e'\dot{f}(\theta, \omega) = 0$. This means that the images of functions $f(\theta)$ and $\dot{f}(\theta, \omega)$ are contained in a plane orthogonal to the vector $e \in \mathbb{R}^3$, formally defined as

$$\Upsilon = \{y \in \mathbb{R}^3 : y'e = 0\} \quad (4.23)$$

This plane is also known from the power electronics literature as the $\alpha\beta$ plane. Therefore, we can conclude that for every scalars $a_1, a_2 \in \mathbb{R}$, the linear combination of $f(\theta)$ and $\dot{f}(\theta, \omega)$ given by $m(\theta, \omega) = a_1f(\theta) + a_2\dot{f}(\theta, \omega)$ always belongs to the circumference

$$\mathbb{F}_\omega = \left\{ y \in \mathbb{R}^3 : e'y = 0, \|y\| = \sqrt{3(a_1^2 + a_2^2\omega^2)/2} \right\} \quad (4.24)$$

For a given $\kappa \in \mathbb{R}_+$, the set $\mathbb{F} = \bigcup_{|\omega| \leq \kappa} \mathbb{F}_\omega$ represents an annulus in the Υ plane with inner and outer radii defined by the boundary values of rotational velocity, whenever it varies in the interval $-\kappa \leq \omega \leq \kappa$. The maximal circumference with radius correspondent to $|\omega| = \kappa$ is denoted by \mathbb{F}_κ .

4.2.2 Switching Function Design

Within this section, we present the main results regarding the design of a state-dependent switching function capable of assuring asymptotic tracking and minimum guaranteed performance cost. More specifically, for a given $\kappa \in \mathbb{R}_+$, which defines the velocity domain of interest

$$\Omega_\kappa = \{\omega \in \mathbb{R} : |\omega| \leq \kappa\} \quad (4.25)$$

our main goal is to determine a set of attainable rotational velocity profiles $\omega^*(t) \in \Omega_*$, the associated harmonic currents $i_\phi^*(t)$ and a switching function $\sigma(t) = u(x(t), \theta(t))$ responsible to orchestrate the state trajectories asymptotically towards $x^*(t) = [i_\phi^*(t)' \ \omega^*(t)]'$, assuring a minimum upper bound for the optimal cost (4.20). Actually, given a set of initial conditions $(x_0, \theta_0) \in \mathbb{R}^4 \times \mathbb{R}$ and a pre-specified velocity profile $\omega^*(t) \in \Omega_*$, we need to assure that the rotational velocity $\omega(t)$ does not leave the region (4.25), i.e., $\omega(t) \in \Omega_\kappa$ for all $t \in \mathbb{R}_{0+}$ and attains the desired profile $\omega^*(t) \in \Omega_*$, asymptotically. Moreover, associated with each $\omega^*(t) \in \Omega_*$ we must

provide a current trajectory of the form $i_\phi^*(t) = i^*(t)f(\theta(t))$, where $i^* : \mathbb{R}_{0+} \rightarrow \mathbb{R}$ is a scalar valued function to be determined.

To accomplish this goal, consider the auxiliary state variable $\xi(t) = x(t) - x^*(t)$ and the following non-quadratic, radially unbounded (with respect to ξ), Lyapunov function candidate

$$v(\xi, \theta) = \xi' P(\theta) \xi \quad (4.26)$$

where the symmetric matrix valued function $P : \mathbb{R} \rightarrow \mathbb{R}^{4 \times 4}$ is of the form

$$P(\theta) = \begin{bmatrix} pI & \bullet \\ rf(\theta)' & q \end{bmatrix} > 0, \quad \forall \theta \in \mathbb{R} \quad (4.27)$$

The real scalars (p, q, r) are design variables whose determination is linked to the switching function design, as in the previous presented design methodologies. As will be clear in the sequel, this class of Lyapunov functions is comprehensive enough to accomplish our proposals and can provide less conservative results when compared to a quadratic one. We proceed by calculating its time derivative along an arbitrary solution $(x(t), \theta(t))$, $\forall t \in \mathbb{R}_{0+}$ of the system under consideration (4.16)-(4.17). After some algebraic manipulations we obtain

$$\dot{v}(\xi, \theta) = -\xi' W(\theta, \omega) \xi + 2\xi' P(\theta) h_\sigma(\theta, \omega) \quad (4.28)$$

which holds for all pairs $(\xi, \theta) \in \mathbb{R}^5$ and where the symmetric matrix valued function $W : \mathbb{R} \times \mathbb{R} \rightarrow \mathbb{R}^{4 \times 4}$ and the vector valued function $h_\sigma : \mathbb{R} \times \mathbb{R} \rightarrow \mathbb{R}^4$ are

$$W(\theta, \omega) = \begin{bmatrix} 2(Rp/L)I - 2(\mu r/J)f(\theta)f(\theta)' & \bullet \\ (Rr/L - \mu q/J + \mu p/L + rc/J)f(\theta)' - r\dot{f}(\theta, \omega)' & 3\mu r/L + 2cq/J \end{bmatrix} \quad (4.29)$$

$$h_\sigma(\theta, \omega) = \begin{bmatrix} \nu_\sigma/L - (Ri^* + \mu\omega^* + Ldi^*/dt)f(\theta)/L - i^*\dot{f}(\theta, \omega) \\ (3i^*\mu/2 - c\omega^* - \tau - J\dot{\omega}^*)/J \end{bmatrix} \quad (4.30)$$

Notice that, to impose the trajectory tracking condition, we need to determine a switching control $\sigma(t) = u(x(t), \theta(t))$ assuring that $\dot{v}(\xi, \theta) < 0$ for all $\xi \neq 0$, $\theta \in \mathbb{R}$ and $\omega(t) \in \Omega_\kappa$ for all $t \in \mathbb{R}_{0+}$. Although nontrivial, a solution to this task will be equivalently expressed as an optimization problem described in terms of LMIs and relying on key properties of the nonlinear function $f(\theta)$. The next theorem is of central importance as it provides sufficient conditions for the existence of the switching function $u(x, \theta)$, which is a solution to the previously stated control design problem.

Theorem 4.1. Consider the switched nonlinear system (4.16)-(4.17) with initial condition (x_0, θ_0) . Choose the diagonal matrix $Q = \text{diag}(I, d)$ and the scalar $\kappa \in \mathbb{R}_+$ that defines the stability domain of interest Ω_κ given in (4.25). Let the current trajectory $i_\phi^*(t)$ be defined with

$$i^*(t) = \left(\frac{2}{3\mu} \right) (c\omega^*(t) + J\dot{\omega}^*(t) + \tau) \quad (4.31)$$

where $\omega^*(t)$ is a desired rotational velocity profile such that $\omega^*(t) \in \Omega_*$ with

$$\Omega_* = \left\{ \omega(t) : \Delta(\omega(t))' (\psi\psi' + \kappa^2\varphi\varphi') \Delta(\omega(t)) \leq V_{dc}^2, |\omega(t)| \leq \kappa, \forall t \in \mathbb{R}_{0+} \right\} \quad (4.32)$$

whose indicated elements are

$$\psi = \left(\frac{2}{\sqrt{3}\mu} \right) \begin{bmatrix} Rc + 3\mu^2/2 & JR + Lc & JL & R \end{bmatrix}' \quad (4.33)$$

$$\varphi = \left(\frac{2}{\sqrt{3}\mu} \right) \begin{bmatrix} Lc & JL & 0 & L \end{bmatrix}' \quad (4.34)$$

$$\Delta(\omega(t)) = \begin{bmatrix} \omega(t) & \dot{\omega}(t) & \ddot{\omega}(t) & \tau \end{bmatrix}' \quad (4.35)$$

If there exist scalars (p, q, r) such that $P(\theta) > 0$ and $W(\theta, \omega) > Q$ for all $\theta \in \mathbb{R}$ and $\omega \in \Omega_\kappa$, then the state-dependent switching function $\sigma(t) = u(x(t), \theta(t))$ with

$$u(x, \theta) = \arg \min_{j \in \mathbb{K}} \left([pI \quad rf(\theta)](x - x^*) \right)' \nu_j \quad (4.36)$$

assures that $x(t) \rightarrow x^*(t)$ asymptotically. Moreover, the upper bound

$$\mathcal{J} = \int_0^\infty (x(t) - x^*(t))' Q (x(t) - x^*(t)) dt \leq \xi_0' P(\theta_0) \xi_0 = \bar{\mathcal{J}} \quad (4.37)$$

for the performance cost (4.20) holds with $\xi_0 = x(0) - x^*(0)$.

Proof: In order to prove asymptotic tracking towards $x^*(t)$, we need to show that for an arbitrary solution to (4.16)-(4.17) we have $\dot{v}(\xi, \theta) < 0$ for all $\xi \neq 0$, $\theta \in \mathbb{R}$ and $\omega \in \Omega_\kappa$. First of all, notice that the choice of the current $i^*(t)$ indicated in (4.31) makes null the last element of the vector (4.30). Now, from the first row of (4.30), let us define

$$m(\theta, \omega) = \left(Ri^* + \mu\omega^* + L \frac{di^*}{dt} \right) f(\theta) + Li^* \dot{f}(\theta, \omega) \quad (4.38)$$

which, as it has been earlier discussed, is a vector valued function that has the image set $\mathbb{F}_\omega \subset \Upsilon$ given by (4.24) with $a_1 = Ri^* + \mu\omega^* + Ldi^*/dt$ and $a_2 = Li^*$. On the other hand, from the values of the phase voltages provided in Table 4.1, it is a matter of immediate verification that $e'\nu_j = 0$ for all $j \in \mathbb{K}$ which means that all vectors ν_j , $j \in \mathbb{K}$, belong to the same Υ plane in \mathbb{R}^3 as $m(\theta, \omega)$ does. The consequence of this important fact that follows from the physical nature of the motor is that at each instant of time $t \in \mathbb{R}_{0+}$ the vector $m(\theta(t), \omega(t))$ can be alternatively written as a convex combination of the phase voltages ν_j , $j \in \mathbb{K}$ under certain conditions. Indeed, for each $\theta \in \mathbb{R}$ and $\omega \in \Omega_\kappa$, there exists a $\lambda^* \in \Lambda$ such that

$$\nu_{\lambda^*} = m(\theta, \omega) \quad (4.39)$$

if and only if

$$\mathbb{F}_\kappa \subseteq \mathbb{P} = \left\{ \nu \in \mathbb{R}^3 : \nu = \sum_{j \in \mathbb{K}} \lambda_j \nu_j, \lambda \in \Lambda \right\} \quad (4.40)$$

As illustrated in Figure 4.4, the circumference of radius $V_{dc}/\sqrt{2}$ is the one of maximum radius inscribed in the polytope \mathbb{P} . Thus, taking into account the definition of \mathbb{F}_κ just after (4.24), the inclusion (4.40) holds if and only if

$$\nu_{\lambda^*}' \nu_{\lambda^*} \leq 3(a_1^2 + a_2^2 \kappa^2)/2 \leq V_{dc}^2/2 \quad (4.41)$$

with a_1 and a_2 provided previously. Plugging the current i^* , given in (4.31), expressed as a function of $(\omega^*, \dot{\omega}^*)$

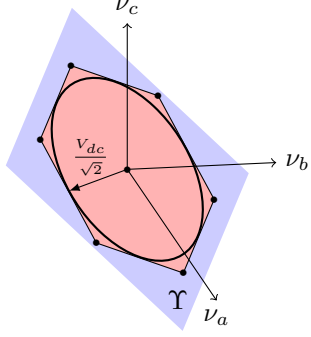


Figure 4.4: Graphical representation of polytope \mathbb{P} and inscribed circumference.

in a_1 and a_2 , a few algebraic manipulations lead to the fact that the second inequality in (4.41) holds whenever the desired rotational velocity profile $\omega^*(t)$ is chosen inside the set Ω_* defined in (4.32). Now taking into account the existence of $\lambda^* \in \Lambda$ satisfying (4.39), the equality (4.28) together with the switching rule (4.36) yield

$$\begin{aligned}
\dot{v}(\xi, \theta) &= -\xi' W(\theta, \omega)\xi + \min_{j \in \mathbb{K}} 2\xi' P(\theta)h_j(\theta, \omega) \\
&< -\xi' Q\xi + \min_{\lambda \in \Lambda} 2\xi' P(\theta)h_\lambda(\theta, \omega) \\
&\leq -\xi' Q\xi + 2\xi' P(\theta)h_{\lambda^*}(\theta, \omega) \\
&= -\xi' Q\xi \leq 0
\end{aligned} \tag{4.42}$$

where the first inequality comes from the fact that $W(\theta, \omega) > Q$ and the last equality holds from the fact that at each instant of time $t \in \mathbb{R}_{0+}$ we are able to find $\lambda^* \in \Lambda$ such that ν_{λ^*} satisfies (4.39), leading to $h_{\lambda^*} = 0$. Hence, $\dot{v}(\xi, \theta) < 0$ for all $\xi \neq 0$, $\theta \in \mathbb{R}$ and $\omega \in \Omega_\kappa$ implies that $\xi(t) \rightarrow 0$ asymptotically. Integrating both sides of (4.42) from $t = 0$ to $t \rightarrow \infty$ we obtain the upper bound (4.37). The proof is concluded. \square

This result provides a switching function that can be applied in the important context of trajectory tracking and a set of feasible trajectories has been identified. To this end a bounded rotational velocity profile with bounded first and second order time derivative must be provided. Moreover, an upper bound for the associated cost is determined and, as it will be seen next, it can be minimized by an adequate choice of the matrix function $P(\theta)$.

We turn our attention at this point to the determination of a set of initial conditions Ξ such that for a given rotational velocity profile $\omega^* \in \Omega_*$ any $(\xi_0, \theta_0) \in \Xi$ implies $\omega(t) \in \Omega_\kappa$ for all $t \in \mathbb{R}_{0+}$ and a given $\kappa \in \mathbb{R}_+$. The next theorem presents a key result that, together with the one of Theorem 4.1, assures the tracking property $\omega(t) \rightarrow \omega^*(t)$ and $\omega(t) \in \Omega_\kappa$ for any choice of the velocity profile such that $\omega^*(t) \in \Omega_*$ for all $t \in \mathbb{R}_{0+}$.

Theorem 4.2. *Let a rotational velocity profile $\omega^* \in \Omega_*$, a scalar $\kappa \in \mathbb{R}_+$ and a triple (p, q, r) satisfying the design conditions provided in Theorem 4.1 be given. Any solution for the system (4.16)-(4.17) evolving from $(\xi_0, \theta_0) \in \Xi$ with*

$$\Xi = \left\{ (\xi, \theta) \in \mathbb{R}^4 \times \mathbb{R} : v(\xi, \theta) \leq v_0 \right\} \tag{4.43}$$

$$v_0 = \left(q - \frac{3r^2}{2p} \right) \min_{\varsigma \in \mathbb{R}_+} (\kappa - |\omega^*(\varsigma)|)^2 \tag{4.44}$$

satisfies $\omega(t) \in \Omega_\kappa$ for all $t \in \mathbb{R}_{0+}$.

Proof: Before all, it is important to mention that from the application of the Schur Complement to (4.27) it is verified that $P(\theta) > 0$ for all $\theta \in \mathbb{R}$ if and only if $q > 3r^2/(2p) > 0$. First, considering $t \in \mathbb{R}_{0+}$ arbitrary and $(\xi(t), \theta(t)) \in \Xi$, we have

$$\begin{aligned} v_0 &\geq v(\xi(t), \theta(t)) \\ &\geq \min_{i_\phi(t) \in \mathbb{R}^3} v(\xi(t), \theta(t)) \\ &= \left(q - \frac{3r^2}{2p} \right) (\omega(t) - \omega^*(t))^2 \end{aligned} \quad (4.45)$$

which together with (4.44) yield

$$\begin{aligned} (\omega(t) - \omega^*(t))^2 &\leq \min_{\varsigma \in \mathbb{R}_+} (\kappa - |\omega^*(\varsigma)|)^2 \\ &\leq (\kappa - |\omega^*(t)|)^2 \end{aligned} \quad (4.46)$$

Taking into account that $\omega^* \in \Omega_*$ implies $|\omega^*(t)| \leq \kappa$, inequality (4.46) imposes $|\omega(t)| \leq \kappa$ as well, that is, $\omega(t) \in \Omega_\kappa$. From Theorem 4.1 it follows that $d\nu(\xi(t), \theta(t))/dt < 0$ whenever $\omega(t) \in \Omega_\kappa$ and we have shown that every $(\xi, \theta) \in \Xi$ is such that $\omega \in \Omega_\kappa$. Since Ξ is a level set of the Lyapunov function, putting all these properties together, we conclude that any trajectory starting in Ξ remains on this set for all $t \in \mathbb{R}_+$, concluding thus the proof. \square

It is important to provide an interpretation of the set Ξ , which is a level set of the Lyapunov function defined by v_0 . Using the fact that

$$\min_{i_\phi(\varsigma) \in \mathbb{R}^3, |\omega(\varsigma)| = \kappa} v(\xi(\varsigma), \theta(\varsigma)) = \left(q - \frac{3r^2}{2p} \right) (\kappa - |\omega^*(\varsigma)|)^2 \quad (4.47)$$

then it is readily verified that

$$\begin{aligned} v_0 &= \min_{\varsigma \in \mathbb{R}_+} \left(q - \frac{3r^2}{2p} \right) (\kappa - |\omega^*(\varsigma)|)^2 \\ &= \min_{\varsigma \in \mathbb{R}_+} \min_{i_\phi(\varsigma) \in \mathbb{R}^3, |\omega(\varsigma)| = \kappa} v(\xi(\varsigma), \theta(\varsigma)) \end{aligned} \quad (4.48)$$

which indicates that v_0 defines the largest level set of the Lyapunov function such that $|\omega(\varsigma)| = \kappa$ for all $\varsigma \in \mathbb{R}_{0+}$. Hence, the set of all initial conditions (ξ_0, θ_0) such that the resulting trajectory respects $\omega(t) \in \Omega_\kappa$ for all $t \geq 0$, fulfilling the assumption for Theorem 4.1, is composed by all pairs $(\xi_0, \theta_0) \in \Xi$.

The set Ω_* has an especial structure and for this reason it can be replaced by a simpler, although more conservative version

$$\Omega_c = \left\{ \omega(t) : \|\Delta(\omega(t))\|^2 \leq \frac{V_{dc}^2}{\|\psi\|^2 + \kappa^2 \|\varphi\|^2}, |\omega(t)| \leq \kappa, \forall t \in \mathbb{R}_{0+} \right\} \quad (4.49)$$

which imposes, as expected, a certain bound on the size of $\Delta(\omega(t))$ depending on the physical parameters of the motor and the design parameter $\kappa \in \mathbb{R}_+$. The application of this result in each case of interest requires some care as indicated in the sequel. Let us consider the following particular cases that are important in practice:

- **Case 1 :** Sufficiently realistic in some situations, when the viscous friction coefficient and the external torque can be neglected, that is, $(c, \tau) = (0, 0)$. This situation has been treated in Egidio et al. (2019), considering $\omega^*(t) = \omega^*$ a constant rotational velocity. It can be noticed that the conditions provided by Theorem 4.1 are considerably simplified, because $\Delta(\omega) = \omega$, $\psi = \sqrt{3}\mu$ and $\varphi = 0$ are scalars, yielding $\Omega_c \equiv \Omega_* \equiv \Omega_\kappa$ provided that

$$\kappa = V_{dc}/(\sqrt{3}\mu) \quad (4.50)$$

- **Case 2 :** Parameters $(c, |\tau|)$ are positive and $\omega^*(t) = \omega^*$ is a constant rotational velocity. The parameter τ represents the torque produced by Coulomb friction. The vector $\Delta(\omega(t)) = [\omega(t) \ \tau]'$ allows us to consider ψ and φ two vectors in \mathbb{R}^2 that follow from the elimination of the second and third elements of (4.33)-(4.34). Taking into account that matrix $\psi'\psi + \kappa^2\varphi\varphi' \geq 0$ and has only nonnegative elements, a necessary and sufficient condition for the convex set Ω_* be equal to Ω_κ follows by imposing that

$$\begin{bmatrix} \kappa \\ |\tau| \end{bmatrix}' (\psi\psi' + \kappa^2\varphi\varphi') \begin{bmatrix} \kappa \\ |\tau| \end{bmatrix} \leq V_{dc}^2 \quad (4.51)$$

holds for some design parameter $\kappa \in \mathbb{R}_+$. It must be chosen as small as possible in order to take into account the physical limitations on V_{dc} .

- **Case 3 :** This is the general case characterized by positive parameters $(c, |\tau|)$ but the goal now is to track a piecewise linear rotational velocity profile $\omega^*(t)$. This yields $\Delta(\omega(t)) = [\omega \ \dot{\omega}]'$ since $\ddot{\omega}^*(t) = 0$ almost everywhere. This is not an overwhelming restriction as, at nondifferentiable points of $\omega^*(t)$ this trajectory can be adequately smoothed. This situation is of great practical appeal as it can attenuate required phase currents in the transient state, reducing component wear. It will be illustrated by means of an experiment in the next chapter.

Now, an essential point about Theorem 4.1 is how to obtain the parameters (p, q, r) that satisfy the inequality $W(\theta, \omega) > Q > 0$ and $P(\theta) > 0$ for all $\theta \in \mathbb{R}$ and $\omega \in \Omega_\kappa$. A computationally intensive approach to this problem would be to exploit the periodicity of $f(\theta)$ by imposing these conditions on a sufficiently fine discrete grid on the box defined by the intervals $|\theta| \leq \pi$ and $|\omega| \leq \kappa$. However, a more efficient manner can be adopted by using the result presented in the next lemma that follows from the properties of functions $f(\theta)$ and $\dot{f}(\theta, \omega)$ previously stated.

Lemma 4.1. *Let the real parameters $(\alpha, \beta, \rho, \eta, \vartheta)$ with $\beta \in \mathbb{R}_{0+}$ and $\kappa \in \mathbb{R}_+$ be given. The symmetric matrix valued function $S : \mathbb{R} \times \mathbb{R} \rightarrow \mathbb{R}^{4 \times 4}$ defined by*

$$S(\theta, \omega) = \begin{bmatrix} \alpha I - \beta f(\theta)f(\theta)' & \bullet \\ \rho f(\theta)' - \eta \dot{f}(\theta, \omega)' & \vartheta \end{bmatrix} \quad (4.52)$$

is positive definite for all $\theta \in \mathbb{R}$ and $\omega \in \Omega_\kappa$ if and only if the following conditions

$$2\alpha/3 > \beta, \quad 2\vartheta/3 > \left(\frac{\eta^2}{\alpha}\right)\kappa^2 + \left(\frac{\rho^2}{\alpha - 3\beta/2}\right) \quad (4.53)$$

hold simultaneously.

Proof: Since by assumption $\beta \geq 0$ then the first diagonal block of $S(\theta, \omega)$ is positive definite if and only if

$$\begin{bmatrix} \alpha I & \bullet \\ \sqrt{\beta} f(\theta)' & 1 \end{bmatrix} > 0 \quad (4.54)$$

and the Schur Complement with respect to the first diagonal element indicates that (4.54) holds if and only if $\alpha > 0$ and $1 > (\beta/\alpha)f(\theta)'f(\theta) = 3\beta/(2\alpha), \forall \theta \in \mathbb{R}$, which is exactly the first condition in (4.53). Using this fact, the Schur Complement of (4.52) with respect to the first diagonal element indicates that $W(\theta, \omega) > 0$ if and only if

$$\vartheta > (\rho f(\theta) - \eta \dot{f}(\theta, \omega))' (\alpha I - \beta f(\theta)f(\theta)')^{-1} (\rho f(\theta) - \eta \dot{f}(\theta, \omega)) \quad (4.55)$$

Using Lemma A.2, it follows that

$$(\alpha I - \beta f(\theta)f(\theta)')^{-1} = (1/\alpha)I + (\beta/\alpha) \left(\frac{f(\theta)f(\theta)'}{\alpha - 3\beta/2} \right) \quad (4.56)$$

which, replaced into (4.55) and recalling the properties in (4.22), leads to

$$\begin{aligned} \vartheta &> 3\rho^2/(2\alpha) + 3\eta^2\omega^2/(2\alpha) + (\beta/\alpha) \left(\frac{(3/2)^2\rho^2}{\alpha - 3\beta/2} \right) \\ &= 3\eta^2\omega^2/(2\alpha) + \left(\frac{(3/2)\rho^2}{\alpha - 3\beta/2} \right) \end{aligned} \quad (4.57)$$

which must be verified for all $\omega \in \Omega_\kappa$. This provides the second inequality in (4.53) after multiplying both sides by the factor $2/3$, concluding the proof. \square

Since the vector valued function $f(\theta)$ is nonlinear, the result of Lemma 4.1 is somewhat surprising. Moreover, it is interesting to notice that the conditions (4.53) can be equivalently rewritten by means of a single LMI, making possible and simple the determination of the free parameters involved. Hence, this result can be adopted to express the conditions of Theorem 4.1 in terms of LMIs as it is stated in the next corollary.

Corollary 4.1. *Let the initial conditions (ξ_0, θ_0) , the matrix $Q > 0$, and $\kappa \in \mathbb{R}_+$ be given. The parameters (p, q, r) solution to the optimization problem*

$$\min_{(p,q,r) \in \mathbb{R}^3} \xi_0' P(\theta_0) \xi_0 \quad \text{s.t. } P(\theta) > 0, W(\theta, \omega) > Q \quad (4.58)$$

for all $(\theta, \omega) \in \mathbb{R} \times \Omega_\kappa$ are equivalently determined from the following convex optimization problem

$$\min_{(p,q,r) \in \mathbb{R}^3} \xi_0' P(\theta_0) \xi_0 \quad \text{s.t.} \quad (4.59)$$

$$\begin{bmatrix} (2/3)q & \bullet \\ r & p \end{bmatrix} > 0 \quad (4.60)$$

$$\begin{bmatrix} (2\mu/L)r + (4c/(3J))q - 2d/3 & \bullet & \bullet & \bullet \\ \kappa r & (2R/L)p - 1 & \bullet & \bullet \\ (R/L + c/J)r - (\mu/J)q + (\mu/L)p & 0 & (2R/L)p - (3\mu/J)r - 1 \end{bmatrix} > 0 \quad (4.61)$$

Proof: First, notice that the conditions (4.53) can be expressed in terms of a linear matrix inequality of the form

$$\begin{bmatrix} 2\vartheta/3 & \bullet & \bullet \\ \kappa\eta & \alpha & \bullet \\ \rho & 0 & \alpha - 3\beta/2 \end{bmatrix} > 0 \quad (4.62)$$

Now, making $S(\theta, \omega) = P(\theta)$, Lemma 4.1 assures that inequality (4.60) is equivalent to $P(\theta) > 0$ for all $\theta \in \mathbb{R}$. In the same manner, writing $S(\theta, \omega) = W(\theta, \omega) - Q$, Lemma 4.1 assures that inequality (4.61) is equivalent to $W(\theta, \omega) - Q > 0$ for all $\theta \in \mathbb{R}$ and $\omega \in \Omega_\kappa$. \square

An interesting remark at this point is the fact that problem (4.58) always admits a feasible solution (p, q, r) with $q = (J/L)p > 0$, r small enough and $p > 0$ large enough. This puts in evidence the fact that the present design conditions are always feasible and, consequently, valid. This result is very important in practical applications, mainly related to control of electrical drives, see Krishnan (2009), Pillay and Krishnan (1989), Matsui and Shigyo (1992), as some examples. A useful application, very common in control of electrical machines, is to adopt a velocity reference of ramp type in order to smooth the transient response by reducing current peaks. This aspect will be fully illustrated by the forthcoming experimental results. To conclude the theoretical discussion in this section, some remarks about the computational complexity of the proposed methodology are in order.

4.2.3 Computational Analysis

The proposed switching function (4.36) can be equivalently replaced by a more efficient one, in terms of required computational effort. In fact, from (4.36) we have

$$u(x, \theta) = \arg \min_{j \in \mathbb{K}} \left(pi_\phi + (r\omega - r\omega^* - pi^*)f(\theta) \right)' \nu_j \quad (4.63)$$

$$= \arg \min_{j \in \mathbb{K}} \left(pGG^\# i_\phi + (r\omega - r\omega^* - pi^*)Gh(\theta) \right)' \nu_j \quad (4.64)$$

$$= \arg \min_{j \in \mathbb{K}} \left(G^\# i_\phi + ((r/p)\omega - (r/p)\omega^* - i^*)h(\theta) \right)' G' \nu_j \quad (4.65)$$

where $G^\#$ is given by

$$G^\# = \frac{2}{3} \begin{bmatrix} 1 & -1/2 & -1/2 \\ 0 & -\sqrt{3}/2 & \sqrt{3}/2 \end{bmatrix} \quad (4.66)$$

and coincides with the Clarke transform, see Duesterhoeft et al. (1951). Despite the fact that $GG^\# = I - (1/3)ee'$ is not the identity matrix, we always have $GG^\# i_\phi = i_\phi$ whenever $i_a + i_b + i_c = 0$. This is a consequence of the fact that $GG^\#$ is symmetric and has one null eigenvalue associated to the vector $e = [1 \ 1 \ 1]'$ and two unitary eigenvalues associated to linearly independent eigenvectors that are orthogonal to e , namely ζ_1 and ζ_2 . Thus one can always rewrite i_ϕ as a linear combination of ζ_1 and ζ_2 which shows that $GG^\#$ is an identity operator for i_ϕ .

Notice that while (4.63) requires the evaluation of three sine functions and two dot products between vectors in \mathbb{R}^3 , expression (4.65) requires only one sine and one cosine (to evaluate $h(\theta)$) along with two dot products of vectors in \mathbb{R}^2 , given that $G' \nu_j$ can be calculated *a priori* for all $j \in \mathbb{K}$. Moreover, observing that the expression inside the min-operator is linear with respect to ν_j , it always returns 0 for $\nu_7 = 0$ and opposite

results for the pairs (ν_1, ν_6) , (ν_2, ν_5) and (ν_3, ν_4) , implying that this expression must be evaluated for only 3 instead of 7 subsystems. Finally, using the fact that $i_c = -i_a - i_b$ we can expand $G^\# i_\phi = [i_a \ (-\sqrt{3}/3)(i_a + 2i_b)]'$, simplifying this matrix product to one multiplication and two additions. The division (r/p) and possible scaling factors can also be computed offline.

The numerical validation of this approach will be tackled in the following subsection. Experimental results will be carried out in Chapter 5, where two experiments are presented.

4.2.4 Simulation Results

Some simulations with data borrowed from the literature were made and the results are gathered in this section. The next example illustrates the case where a constant output velocity must be reached.

Example 4.2. Let us consider a PMSM with system data presented in [Zhang et al. \(2013\)](#), given in our notation as in Table 4.2.

Table 4.2: System data employed

Parameter	Value	Unit
R	3.5	Ω
L	11.5	mH
μ	0.321	V.s/rad
c	10^{-5}	N.m.s/rad
τ	0	N.m
J	0.44	$\text{g} \cdot \text{m}^2$
V_{dc}	100	V
n_p	3	pole pairs

Adopting a $\kappa = 314.1593$ rad/s (or 3000 rpm), which defines the velocity domain of interest Ω_κ as in (4.25), and $d = 0.01$ that defines the quadratic cost \mathcal{J} in (4.37) with $Q = \text{diag}(I, d)$. Our goal is to bring the rotational velocity to a constant value of $\omega^* = 104.7197$ rad/s (or 1000 rpm). Considering null initial conditions, we solved the optimization problem in Corollary 4.1 obtaining a matrix $P(\theta)$ as given in (4.27) defined by the scalars $p = 0.0039$, $q = 1.7901 \times 10^{-4}$ and $r = 1.9446 \times 10^{-4}$. This solution defines an upper bound for the quadratic cost (4.37) given by $\bar{\mathcal{J}} = \xi'_0 P(\theta_0) \xi_0 = 1.9632$. Through a numerical simulation, we have obtained the system trajectories evolving from $x_0 = 0$, $\theta_0 = 0$ and governed by the switching function (4.36). These trajectories are shown in Figure 4.5 and 4.6 and the associated switching signal, in Figure 4.7. The corresponding quadratic cost obtained via numerical integration was $\mathcal{J} = 0.3704$, which respected its upper bound.

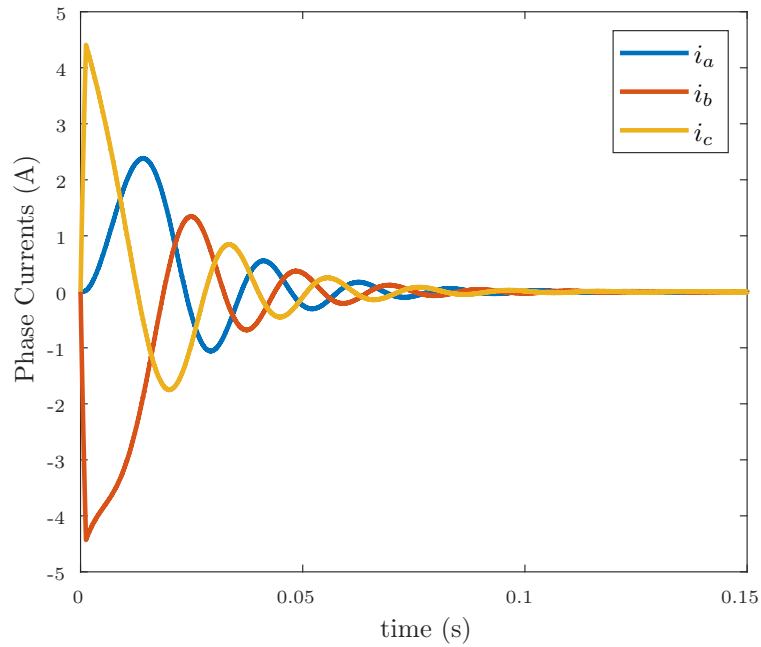


Figure 4.5: Phase currents of a PMSM controled by switching rule (4.36).

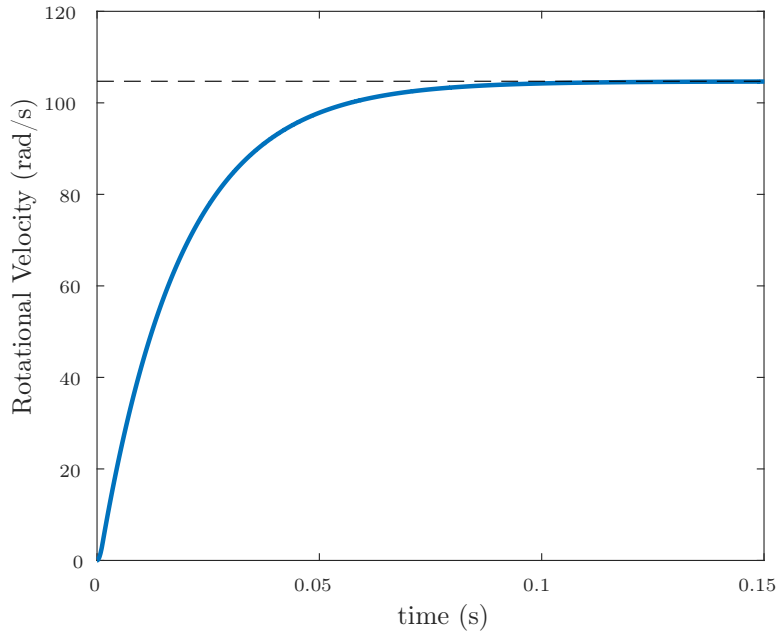


Figure 4.6: Rotational velocity of a PMSM controled by switching rule (4.36) and desired reference ω^* (dashed line).

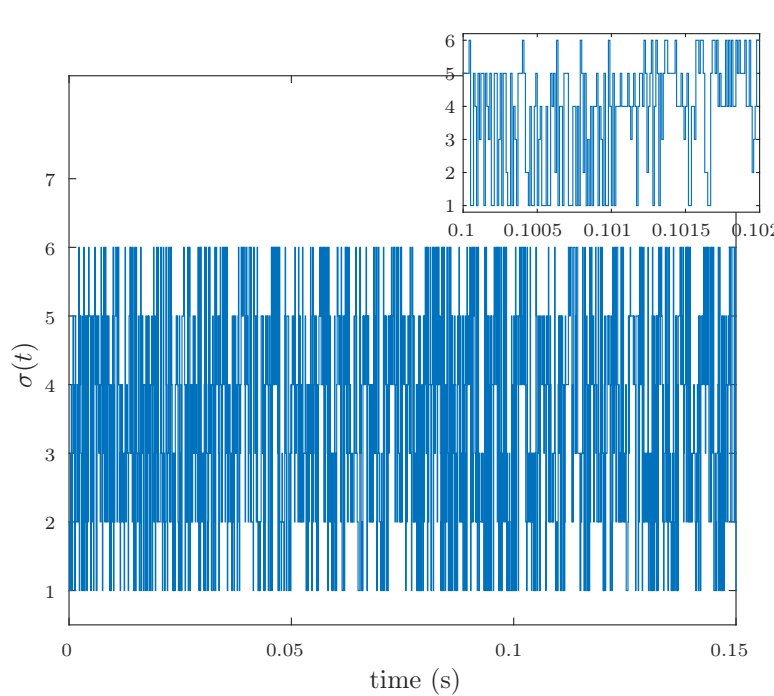


Figure 4.7: Corresponding switching signal associated to the switching rule (4.36).

This example illustrated the efficiency of the proposed methodology. An important question to be made in view of these results is whether a less conservative result could be found if a full constant matrix $P > 0$ were taken in the Lyapunov function (4.27). Certainly, contrasting these two scenarios might not lead to a fair comparison since different structures are being considered for the Lyapunov function but alternative stability conditions might be of interest, as a 4th order matrix P provides 10 optimization variables while the presented methodology only takes into account 3.

Adopting the simple quadratic Lyapunov function $\hat{v}(\xi) = \xi' P \xi$ with $P > 0$, asymptotic stability is assured by analogous developments to those of Theorem 4.1 when the inequality

$$A(\theta)'P + PA(\theta) < -Q \quad (4.67)$$

holds for all $\theta \in [0, 2\pi]$. The next example compares the guaranteed cost for this case with Theorem 4.1.

Example 4.3. To assure that inequality (4.67) holds for every $\theta \in [0, 2\pi]$ the optimization problem

$$\min_{P>0} \xi_0' P \xi_0 \quad \text{s.t.} \quad (4.68)$$

$$A(\theta_k)'P + PA(\theta_k) < -Q \quad (4.69)$$

with $\theta_k = 2\pi k/n$, for all $k \in \{0, \dots, M\}$ and $M = 100$ is proposed. This is a sufficiently fine discretization of the interval $[0, 2\pi]$ since greater values of M yielded the same results. Employing the same data from

Example 4.2, the solution obtained was a badly scaled matrix

$$P = \begin{bmatrix} 1.146 \times 10^{11} & 1.033 \times 10^6 & 1.033 \times 10^6 & 0 \\ 1.033 \times 10^6 & 2.924 \times 10^7 & 2.924 \times 10^7 & 0 \\ 1.033 \times 10^6 & 2.924 \times 10^7 & 2.924 \times 10^7 & 0 \\ 0 & 0 & 0 & 0.22 \end{bmatrix} \quad (4.70)$$

whose eigenvalues are $\{0.22, 5.75, 5.8485 \times 10^7, 1.1458 \times 10^{11}\}$, leading to an upper bound for the cost (4.37) given by $\xi_0' P \xi_0 = 2.4125 \times 10^3$, which is approximately 1228 times greater than the one guaranteed by Theorem 4.1 in Example 4.2.

This last example was important to show that the non-quadratic structure adopted for the Lyapunov function is capable of adequately capture the nonlinear parameter-dependency of the PMSM dynamic model. In fact, even with less decision variables, the minimum upper bound for the quadratic cost \mathcal{J} , defined in (4.37), was smaller when the Lyapunov function (4.26) had been employed, compared to a constant quadratic one.

Finally, effects of the choice of the cost weight $d \in \mathbb{R}_+$ must be discussed. Intuitively, larger values of d should provide faster convergence of $\omega(t)$ towards the desired reference. On the other hand, smaller d will reduce current peak values, which is generally a desired scenario to avoid equipment damage. The next example quantitatively illustrates this aspect.

Example 4.4. To explore the effects of different $d \in \mathbb{R}_+$ values in the definition of the weight matrix Q and the quadratic cost \mathcal{J} in (4.37), the optimization problem of Corollary 4.1 was solved for a set of different d values for the same data employed in Example 4.2. Via numerical simulation, different state trajectories were obtained for the same null initial conditions. In Table 4.3, two performance indexes for each trajectory are presented, namely, the absolute peak of the phase currents $i_p = \max_{t \geq 0} \|i_\phi(t)\|_\infty$ and the settling time $t_{2\%}$ at which the rotational velocity $\omega(t)$ attains an error less than 2% with respect to the reference ω^* .

Table 4.3: Absolute current peak and settling time for $\omega(t)$ obtained for several values of d .

d	0.001	0.0022	0.0046	0.01	0.0215	0.0464	0.1	0.2154	0.4642	1
i_p (A)	0.9494	1.7886	3.0263	4.4306	5.6087	6.3718	6.7894	7.0006	7.1037	7.1515
$t_{2\%}$ (s)	0.2592	0.1776	0.1060	0.0714	0.0554	0.0481	0.0447	0.0431	0.0424	0.0420

Indeed, the value d is an important parameter which has to be chosen adequately by the designer in order to state a trade-off between current intensity and settling time, as shown in the last example. Other situations will be studied from an experimental perspective in Chapter 5.

In the following section, another switched nonlinear system that arises in power electronics domain is discussed.

4.3 AC-DC Converter

The contributions presented in this section were submitted in Egidio et al. (nd) and consist in developing a framework to design a switching function, capable of deciding the state of switches in a three-phase bidirectional

AC-DC power converter, also known as a controlled rectifier. The project must assure global asymptotic stability of the state variable, composed of phase currents and output voltage, towards a desired reference trajectory in a single control loop and avoiding using auxiliary reference frames or modulation strategies.

More precisely, while the output voltage must be maintained constant at some desired value, the input currents have to track a sinusoidal reference to attain a unitary power factor operation, guaranteeing an efficient use of the three-phase source. A set of attainable references is presented, which is not more restrictive than the one for approaches based on averaged models. A parameter-dependent Lyapunov function was adopted, allowing us to obtain less conservative solutions when compared to a classical quadratic one, regarding the minimization of a performance index. Moreover, design conditions are written in terms of linear matrix inequalities making the design step easily implementable using off-the-shelf optimization tools.

Consider a topology for the three-phase AC-DC power converter given in Figure 4.8, which is based on a three-phase controlled rectifier with an inductive input filter and an output capacitor feeding a resistive load. By means of Kirchoff's voltage and current laws, the dynamic model of this system can be given by the switched nonlinear system

$$\dot{x}(t) = A_{\sigma(t)}x(t) + b(\theta(t)), \quad x(0) = x_0 \quad (4.71)$$

where $x(t) = [i_\phi(t)' \quad \nu_o(t)]' \in \mathbb{R}^4$ is the state vector, $i_\phi(t) = [i_a(t) \ i_b(t) \ i_c(t)]' \in \mathbb{R}^3$ are input phase currents and $\nu_o(t) \in \mathbb{R}$ is the output voltage. The switching signal $\sigma(t) \in \mathbb{K} = \{1, \dots, 7\}$ is responsible to select one of the seven possible subsystems at each instant of time. System matrices are given by

$$A_\sigma = \begin{bmatrix} -(R_L/L)I & -(1/L)S_\sigma \\ (1/C)S'_\sigma & -1/(R_oC) \end{bmatrix}, \quad b(\theta) = \begin{bmatrix} (\nu_m/L)f(\theta) \\ 0 \end{bmatrix} \quad (4.72)$$

where R_L and L are the resistance and inductance of each coupling inductor, C is the dc-link capacitance, ν_m is the peak phase-to-neutral voltage, R_o is the load resistance, the vector function $f(\theta) = [f_a(\theta) \ f_b(\theta) \ f_c(\theta)]' \in \mathbb{R}^3$ is defined from (4.13)-(4.15), as in the previous section. Vectors S_i , $i \in \mathbb{K}$ take values according to Table 4.4. A time-varying angular parameter $\theta(t)$ represents the instantaneous electrical angle and is assumed to respect $\theta(t) = \omega t + \theta_0$ with constant angular frequency ω . In our context, this parameter is considered to be measured by sensors or adequately estimated.

Our main goal is to design a state-dependent switching function capable of orchestrating the switching

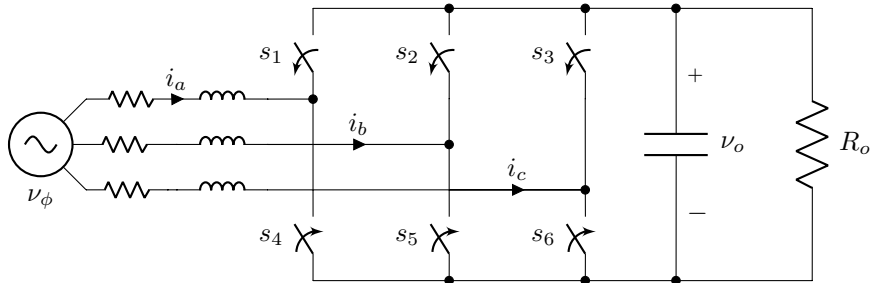


Figure 4.8: Three-phase AC-DC power converter.

Table 4.4: Modes σ , switch states and vector S_i

σ	s_1	s_2	s_3	S'_σ
1	0	0	1	$[-1/3 \ -1/3 \ 2/3]$
2	0	1	0	$[-1/3 \ 2/3 \ -1/3]$
3	0	1	1	$[-2/3 \ 1/3 \ 1/3]$
4	1	0	0	$[2/3 \ -1/3 \ -1/3]$
5	1	0	1	$[1/3 \ -2/3 \ 1/3]$
6	1	1	0	$[1/3 \ 1/3 \ -2/3]$
7	1 0	1 0	1 0	$[0 \ 0 \ 0]$

events of this system, bringing $\nu_o(t)$ to a constant reference value ν_o^* chosen by the designer. In order to operate in unitary power factor situation, phase currents $i_\phi(t)$ must track a sinusoidal reference $i_\phi^*(\theta(t)) = i^* f(\theta(t))$, synchronized with the source phase voltages. The control problem also allows for the minimization of an upper bound for the cost integral

$$\mathcal{J} = \int_0^\infty \left(d \|i_\phi(t) - i_\phi^*(t)\|^2 + (\nu_o(t) - \nu_o^*)^2 \right) dt \quad (4.73)$$

with the weight $d \in \mathbb{R}_{0+}$ chosen by the designer to state a trade-off between input current behavior in transient state and the output voltage settling time.

Adopting the auxiliary state variable $\xi(t) = x(t) - x^*(\theta(t))$ with the equilibrium trajectory $x^*(\theta(t)) = [i_\phi^*(\theta(t))' \ \nu_o^*]'$, we can write the equivalent switched nonlinear system

$$\dot{\xi}(t) = A_{\sigma(t)} \xi(t) + \ell_{\sigma(t)}(\theta(t)), \quad \xi(0) = \xi_0 \quad (4.74)$$

with $\ell_j(\theta) = A_j x^*(\theta) + b(\theta) - \dot{x}^*(\theta)$, $j \in \mathbb{K}$ and $\xi_0 = x_0 - x^*(\theta_0)$. This permits to tackle the trajectory tracking problem

$$\lim_{t \rightarrow \infty} x(t) = x^*(\theta(t)) \quad (4.75)$$

for the original system (4.71) by assuring global asymptotic stability of the origin $\xi = 0$ of system (4.74).

The set of equilibrium pairs (i^*, ν_o^*) defining the attainable trajectories $x^*(t)$ is given by

$$X^* = \mathcal{E} \cap \mathcal{H} \quad (4.76)$$

with the ellipse \mathcal{E} and the region \mathcal{H} given, respectively, by

$$\mathcal{E} = \{(i^*, \nu_o^*) \in \mathbb{R}^2 : R_L i^{*2} - \nu_m i^* + 2\nu_o^{*2}/(3R_o) = 0\} \quad (4.77)$$

$$\mathcal{H} = \{(i^*, \nu_o^*) \in \mathbb{R}^2 : (\nu_m - R_L i^*)^2 + (L\omega i^*)^2 \leq \nu_o^{*2}/3\} \quad (4.78)$$

An illustration of one possible set X^* is depicted in Figure 4.9. From the definition of \mathcal{E} it can be concluded that a necessary condition on ν_o^* for the existence of an i^* such that $(i^*, \nu_o^*) \in X^*$ is that $|\nu_o^*| \leq \nu_m \sqrt{(3R_o)/(8R_L)} = \bar{\nu}_o^*$. Hence, a pair $(i^*, \nu_o^*) \in X^*$ can be obtained by taking the desired ν_o^* to solve the second order equation in (4.77) for i^* , providing up to two candidate pairs (i^*, ν_o^*) each of which can be tested to $(i^*, \nu_o^*) \in \mathcal{H}$.

At this point some trigonometric properties must be presented and discussed. They encompass some of

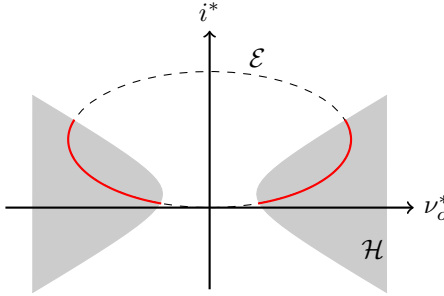


Figure 4.9: Representation of X^* (in red) as $\mathcal{E} \cap \mathcal{H}$.

the properties presented in Subsection 4.2.1.

4.3.1 Trigonometric Properties

Consider the vector function $f(\theta)$ defined by identities (4.13)-(4.15). As discussed previously, we have that $e' f(\theta) = 0$, $\forall \theta \in \mathbb{R}$ with $e = [1 \ 1 \ 1]'$, which let us shows that $f(\theta)$ belongs to the same Υ plane in \mathbb{R}^3 perpendicular to vector e , formally defined in (4.23).

Consequently, along a trajectory of $\theta(t)$, time derivative of $f(\theta)$ also belongs to the plane Υ and it is given by $\dot{f}(\theta) = \omega g(\theta)$ with $g(\theta) = [g_a(\theta) \ g_b(\theta) \ g_c(\theta)]'$ and

$$g_a(\theta) = \cos(\theta) \quad (4.79)$$

$$g_b(\theta) = \cos(\theta - 2\pi/3) \quad (4.80)$$

$$g_c(\theta) = \cos(\theta - 4\pi/3) \quad (4.81)$$

with $e' g(\theta) = 0$. Moreover, it also follows that

$$f(\theta)' f(\theta) = \frac{3}{2}, \quad f(\theta)' g(\theta) = 0, \quad g(\theta)' g(\theta) = \frac{3}{2} \quad (4.82)$$

The matrix

$$R(\theta) = \begin{bmatrix} f(\theta) & g(\theta) & 0 \\ 0 & 0 & \sqrt{3/2} \end{bmatrix} \quad (4.83)$$

will be extensively employed throughout this section and some of its properties have to be highlighted. Firstly, from (4.82), we have that

$$R(\theta)' R(\theta) = \frac{3}{2} I \quad (4.84)$$

Additionally, it is also true that $\dot{g}(\theta) = -\omega f(\theta)$ for any trajectory $\theta(t)$, allowing to demonstrate that

$$\dot{R}(\theta(t)) = R(\theta(t)) \Omega \quad (4.85)$$

with the skew-symmetric matrix

$$\Omega = \begin{bmatrix} 0 & -\omega & 0 \\ \omega & 0 & 0 \\ 0 & 0 & 0 \end{bmatrix} \quad (4.86)$$

Even though these properties resemble those from rotation matrices, notice that $R(\theta)$ is not square, so it may not be considered one. Finally, for an arbitrary diagonal matrix $D = \text{diag}(d_1 I, d_2)$ we also have that

$$DR(\theta) = R(\theta)V'DV \quad (4.87)$$

with the full rank matrix

$$V = \begin{bmatrix} 1 & 0 & 0 \\ 0 & 1 & 0 \\ 0 & 0 & 0 \\ 0 & 0 & 1 \end{bmatrix} \quad (4.88)$$

4.3.2 Switching Function Design

To present design conditions based on LMIs capable of guaranteeing global asymptotic stability of the origin $\xi = 0$ for system (4.74), the next lemma will be of main importance.

Lemma 4.2. *Let scalars $(\kappa, \eta, \alpha, \beta, \gamma, \mu, \vartheta, \rho)$ of the structured positive definite matrices*

$$T_I = \begin{bmatrix} \kappa I & 0 \\ 0 & \eta \end{bmatrix}, \quad T_R = \begin{bmatrix} \alpha & \beta & \mu \\ \beta & \gamma & \vartheta \\ \mu & \vartheta & \rho \end{bmatrix} \quad (4.89)$$

be given. The inequality

$$T_I - R(\theta)T_RR(\theta)' > 0 \quad (4.90)$$

holds for every $\theta \in \mathbb{R}$ if and only if

$$J'T_IJ - T_R > 0 \quad (4.91)$$

holds for $J = \sqrt{2/3}V$.

Proof: Firstly, notice that performing the Schur Complement Lemma in (4.90) with respect to T_R and multiplying both sides of the result by $\text{diag}(I, T_R)$, we obtain

$$\begin{bmatrix} \kappa I & \bullet & \bullet & \bullet & \bullet \\ 0 & \eta & \bullet & \bullet & \bullet \\ \alpha f(\theta)' + \beta g(\theta)' & \sqrt{3/2}\mu & \alpha & \bullet & \bullet \\ \beta f(\theta)' + \gamma g(\theta)' & \sqrt{3/2}\vartheta & \beta & \gamma & \bullet \\ \mu f(\theta)' + \vartheta g(\theta)' & \sqrt{3/2}\rho & \mu & \vartheta & \rho \end{bmatrix} > 0 \quad (4.92)$$

Now, multiplying the second row and column by $\sqrt{2/3}$ and applying once more the Schur Complement Lemma, but now with respect to κ , we obtain

$$\begin{bmatrix} 2\eta/3 & \bullet & \bullet & \bullet \\ \mu & \alpha & \bullet & \bullet \\ \vartheta & \beta & \gamma & \bullet \\ \rho & \mu & \vartheta & \rho \end{bmatrix} - \kappa^{-1} \begin{bmatrix} 0 & \alpha f(\theta)' + \beta g(\theta)' \\ \beta f(\theta)' + \gamma g(\theta)' & \mu f(\theta)' + \vartheta g(\theta)' \end{bmatrix} \begin{bmatrix} 0 & \alpha f(\theta)' + \beta g(\theta)' \\ \beta f(\theta)' + \gamma g(\theta)' & \mu f(\theta)' + \vartheta g(\theta)' \end{bmatrix}' =$$

$$= \begin{bmatrix} 2\eta/3 & \bullet & \bullet & \bullet \\ \mu & \alpha & \bullet & \bullet \\ \vartheta & \beta & \gamma & \bullet \\ \rho & \mu & \vartheta & \rho \end{bmatrix} - \frac{3}{2}\kappa^{-1} \begin{bmatrix} 0 & 0 \\ \alpha & \beta \\ \beta & \gamma \\ \mu & \vartheta \end{bmatrix} \begin{bmatrix} 0 & 0 \\ \alpha & \beta \\ \beta & \gamma \\ \mu & \vartheta \end{bmatrix}' > 0 \quad (4.93)$$

where the equality follows from the identities (4.82). Finally, performing the Schur Complement Lemma in (4.93) with respect to κ , rearranging rows and columns and applying once more the Schur Complement Lemma with respect to T_R we have (4.91), concluding the proof. \square

This last lemma provides a tool to efficiently verify that a matrix function as given in (4.90) is positive definite for all $\theta \in \mathbb{R}$ by evaluating the LMI in (4.91). Its importance will be clear in the proof of the next theorem.

To present globally asymptotically stabilizing design conditions, let us adopt a parameter-dependent Lyapunov function

$$v(\xi, \theta) = \xi' P(\theta) \xi \quad (4.94)$$

with the positive definite matrix

$$P(\theta) = P_I - R(\theta)P_RR(\theta)' \quad (4.95)$$

where

$$P_I = \begin{bmatrix} pI & 0 \\ 0 & q \end{bmatrix} > 0 \quad (4.96)$$

and $P_R > 0$ are to be determined.

Notice that the Lyapunov function (4.26) is a particular case of (4.94), with

$$P_R = \begin{bmatrix} 0 & 0 & -\sqrt{2/3}r \\ 0 & 0 & 0 \\ -\sqrt{2/3}r & 0 & 0 \end{bmatrix} \quad (4.97)$$

but this matrix is not positive definite as here imposed.

Evaluating the time derivative of $v(\xi, \theta)$ along trajectories $\xi(t)$ and $\theta(t)$, we obtain

$$\dot{v}(\xi, \theta) = \xi' W_\sigma(\theta) \xi + 2\xi' P(\theta) \ell_\sigma(\theta) \quad (4.98)$$

with

$$W_\sigma(\theta) = A'_\sigma P(\theta) + P(\theta)A_\sigma + \dot{P}(\theta) \quad (4.99)$$

The next theorem presents sufficient conditions for guaranteeing that $\dot{v}(\xi, \theta) < 0$ for all $\xi \neq 0$.

Theorem 4.3. Consider system (4.74) evolving from $\xi(0) = \xi_0$, a nonnegative scalar d composing $Q = \text{diag}(dI, 1)$ and a desired pair $(i^*, \nu_o^*) \in X^*$ be given. If there exist positive scalars p, q composing $P_I = \text{diag}(pI, q)$ and a positive definite matrix P_R satisfying the following LMIs

$$J' P_I J - P_R > 0 \quad (4.100)$$

$$J'(-Q - 2P_I A_I)J - \Psi > 0, \quad \Psi > 0 \quad (4.101)$$

with

$$\Psi = \text{He}\left(P_R((3/2)A_R - V'A_I V - \Omega') - V'P_I V A_R\right) \quad (4.102)$$

$$A_I = \begin{bmatrix} -(R_L/L)I & 0 \\ 0 & -1/(R_o C) \end{bmatrix} \quad (4.103)$$

$$A_R = \frac{\sqrt{6}}{3\nu_o^*} \begin{bmatrix} 0 & 0 & -\nu_d/L \\ 0 & 0 & -\omega i^* \\ \nu_d/C & L\omega i^*/C & 0 \end{bmatrix} \quad (4.104)$$

and $\nu_d = R_L i^* - \nu_m$, then the switching function $\sigma(t) = u(\xi(t), \theta(t))$ with

$$u(\xi, \theta) = \arg \min_{j \in \mathbb{K}} \xi'(W_j(\theta)\xi + 2P(\theta)\ell_j(\theta)) \quad (4.105)$$

assures that the origin of (4.74) is a globally asymptotically stable equilibrium point and that

$$\mathcal{J} \leq v(\xi_0, \theta_0) = \bar{\mathcal{J}} \quad (4.106)$$

for all $\xi_0 \in \mathbb{R}^{n_x}$.

Proof: The proof follows from (4.98), which evaluated along an arbitrary trajectory of system (4.74), under the switching function $\sigma(t) = u(\xi(t), \theta(t))$, yields

$$\begin{aligned} \dot{v}(\xi, \theta) &= \min_{j \in \mathbb{K}} \xi' W_j(\theta) \xi + 2\xi' P(\theta) \ell_j(\theta) \\ &= \min_{\lambda \in \Lambda} \xi' W_\lambda(\theta) \xi + 2\xi' P(\theta) \ell_\lambda(\theta) \\ &\leq \xi' W_{\lambda^*(\theta)}(\theta) \xi + 2\xi' P(\theta) \ell_{\lambda^*(\theta)}(\theta) \end{aligned} \quad (4.107)$$

where $\lambda^*(\theta)$ is an arbitrary vector inside Λ . If for each θ , there exists $\lambda^*(\theta) \in \Lambda$ such that the inequality $W_{\lambda^*(\theta)}(\theta) < -Q$ is satisfied and $\ell_{\lambda^*(\theta)}(\theta) = 0$, then we have $\dot{v}(\xi, \theta) < 0$ and the origin $\xi = 0$ is globally asymptotically stable. In order to verify that $\ell_{\lambda^*(\theta)}(\theta) = 0$, let us write

$$\ell_{\lambda^*(\theta)}(\theta) = \begin{bmatrix} L^{-1}((\nu_m - R_L i^*)f(\theta) - L\omega i^*g(\theta) - \nu_o^* S_{\lambda^*(\theta)}) \\ C^{-1}(i^* S'_{\lambda^*(\theta)} f(\theta) - \nu_o^*/R_o) \end{bmatrix} \quad (4.108)$$

Now, observe that the polytope \mathbb{P} formed by vertices (S_1, \dots, S_7) is a regular hexagon perpendicular to the vector $e = [1 \ 1 \ 1]'$, with an inscribed circumference of radius $1/\sqrt{2}$, as shown in Figure 4.10. Hence, $S_{\lambda^*(\theta)} \in \Upsilon$ can be chosen as any linear combination of $f(\theta)$ and $g(\theta)$ as long as its length does not exceed $1/\sqrt{2}$, given that both $f(\theta), g(\theta) \in \Upsilon$ for all $\theta \in \mathbb{R}$. Indeed, choosing

$$S_{\lambda^*(\theta)} = \frac{\nu_m - R_L i^*}{\nu_o^*} f(\theta) - \frac{L\omega i^*}{\nu_o^*} g(\theta) \quad (4.109)$$

that makes null the first term of (4.108), the constraint $S'_{\lambda^*(\theta)} S_{\lambda^*(\theta)} \leq 1/2$ yields the region \mathcal{H} , as defined in (4.78). Moreover, replacing $S_{\lambda^*(\theta)}$ in the second term of (4.108), it is simple to verify that this element becomes null whenever the pair (i^*, ν_o^*) is chosen as a point of the ellipse \mathcal{E} . Hence, choosing $(i^*, \nu_o^*) \in X^*$ assures that for each $\theta \in \mathbb{R}$ there exists $\lambda^*(\theta)$ such that $\ell_{\lambda^*(\theta)}(\theta) = 0$. For the same $\lambda^*(\theta)$, let us now show

that inequality $W_{\lambda^*(\theta)}(\theta) < -Q$ holds for all $\theta \in \mathbb{R}$ whenever inequalities in (4.101) are satisfied. Firstly, let us rewrite $A_{\lambda^*(\theta)} = A_I - R(\theta)A_R R(\theta)'$ and evaluate $W_{\lambda^*(\theta)}(\theta)$ as

$$W_{\lambda^*(\theta)}(\theta) = 2P_I A_I + R(\theta)\Psi R(\theta)' \quad (4.110)$$

with Ψ defined in (4.102) obtained after applying (4.84), (4.85) and (4.87) adequately. Now, by applying Lemma 4.2 in (4.101) for $T_I = -Q - 2P_I A_I$ and $T_R = \Psi$, and observing that $T_R > 0$, we have that

$$-Q - 2P_I A_I > R(\theta)\Psi R(\theta)' \quad (4.111)$$

showing that $W_{\lambda^*(\theta)}(\theta) < -Q$. The positive definiteness of $P(\theta)$ is guaranteed by (4.100) together with Lemma 4.2, but now with $T_I = P_I$ and $T_R = P_R$. Finally, from (4.107), we obtain $\dot{v}(\xi, \theta) < -\xi' Q \xi$ for all $\xi \neq 0$, assuring global asymptotic stability of the origin. At last, integrating this last inequality from $t = 0$ up to infinity allows us to determine the upper bound (4.106), concluding the proof. \square

The above theorem provides sufficient conditions for the design of a switching function able to assure global asymptotic tracking of $x^*(\theta(t))$, bringing the AC-DC converter to a steady output v_o^* and controlling input currents to assure unitary power factor operation. It is important to notice that the design conditions are given in terms of LMIs, being, therefore, easy-to-solve with readily available tools. Another remark is that the proposed switching function (4.105) can be interpreted as a selection of the subsystem $j \in \mathbb{K}$ such that the steepest possible descend direction for the Lyapunov function occurs.

A parameter-dependent Lyapunov function was employed and showed to be adapted to the system dependency on $\theta(t)$. Indeed, an alternative approach, based on a simple quadratic Lyapunov function $\hat{v}(\xi) = \xi' P \xi$ with a constant $P > 0$, could be considered. However, this requires to impose the condition

$$A'_{\lambda^*(\theta)} P + P A_{\lambda^*(\theta)} < -Q \quad (4.112)$$

for all $\theta \in [0, 2\pi]$ that can be done by assuring this inequality over a sufficiently fine grid of points. This alternative strategy is not only less efficient but also provided more conservative results in our tests, in spite of the fact that it takes into account more optimization variables. This will be illustrated in Section 4.3.5. Finally, notice that the stability conditions in this theorem require only that $A_{\lambda^*(\theta)}$ is Hurwitz stable, making no

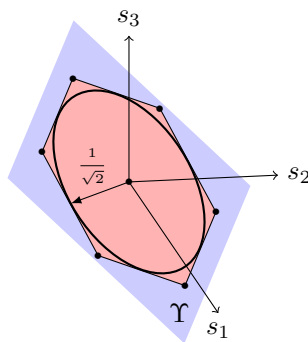


Figure 4.10: Graphical representation of polytope \mathbb{P} and inscribed circumference.

imposition regarding stability of matrices A_j , $j \in \mathbb{K}$, isolatedly considered, although all of them are also stable.

In the sequel, we present some theoretical comparisons with techniques based on an averaged system response and also discussions regarding computational issues.

4.3.3 Averaged Model Comparison

Averaged model techniques are extensively used in switched systems such as the proposed converter, for instance in Wu et al. (1990). Indeed, these techniques rely upon the fact that sufficiently fast switching between subsystems creates an averaged dynamics, which governs the state evolution. Surely, this takes into account Filippov solutions $\xi(t)$ for the error system (4.74) that must satisfy the differential inclusion

$$\dot{\xi}(t) \in \{A_\lambda \xi(t) + \ell_\lambda(\theta(t)) : \lambda \in \Lambda\} \quad (4.113)$$

Notice that the origin $\xi = 0$ of this system (4.74) is an equilibrium point if and only if there exist for each $\theta \in \mathbb{R}$ a $\lambda(\theta) \in \Lambda$ such that $\ell_{\lambda(\theta)}(\theta) = 0$, assuring $\dot{\xi}(t) = 0$. Given the discussions presented in the proof of Theorem 4.3, we can conclude that, for this particular system, this requirement is fulfilled if and only if $(i^*, \nu_o^*) \in X^*$, with X^* given in (4.76). Hence, we can conclude that the proposed set X^* contains all pairs (i^*, ν_o^*) defining a steady-state response $x^*(\theta(t))$ for (4.71) attainable by a averaged model strategy.

4.3.4 Computational Analysis

From a computational point of view, the evaluation of the proposed switching function (4.105) is of low complexity since it can be recast in a simpler equivalent form, that is given in this subsection. Indeed, we have that

$$\begin{aligned} h_j(\xi, \theta) &= \xi'(W_j(\theta)\xi + 2P(\theta)\ell_j(\theta)) \\ &= \xi'\left(2P(\theta)\left(A_j(\xi + x_e(\theta)) + b(\theta) - \dot{x}_e(\theta)\right) + \dot{P}(\theta)\xi\right) \end{aligned}$$

Note that the dependency on index $j \in \mathbb{K}$ is present only in term $2\xi'P(\theta)A_j(\xi + x^*(\theta))$, indicating that it is unnecessary to evaluate the remaining ones. Moreover, employing trigonometric identities, we can decompose

$$R(\theta) = G\bar{R}(\theta) \quad (4.114)$$

with

$$G = \frac{1}{2} \begin{bmatrix} 2 & 0 & 0 \\ -1 & -\sqrt{3} & 0 \\ -1 & \sqrt{3} & 0 \\ 0 & 0 & \sqrt{6} \end{bmatrix}, \quad \bar{R}(\theta) = \begin{bmatrix} \sin(\theta) & \cos(\theta) & 0 \\ \cos(\theta) & -\sin(\theta) & 0 \\ 0 & 0 & 1 \end{bmatrix} \quad (4.115)$$

Consider now the matrix $G^\# = (2/3)G'$. Notice that $GG^\# = I - (1/3)\tilde{e}\tilde{e}'$ with $\tilde{e} = [1 \ 1 \ 1 \ 0]'$ and that $\tilde{e}'\xi = \tilde{e}'x^*(\theta) = 0$, assuring the identities

$$GG^\#\xi = \xi, \quad GG^\#x^*(\theta) = x^*(\theta) \quad (4.116)$$

Defining $\bar{h}_j(\xi, \theta) = \xi' P(\theta) A_j (\xi + x_e(\theta))$, given the previous discussion we have that

$$\begin{aligned}\bar{h}_j(\xi, \theta) &= \xi' G^{\#'} G' (P_I A_j - R(\theta) P_R R(\theta)' A_j) G G^{\#} (\xi + x^*(\theta)) \\ &= \xi' G^{\#'} (\mathcal{P}_j - \mathcal{R}(\theta) \mathcal{A}_j) G^{\#} (\xi + x^*(\theta))\end{aligned}$$

with $\mathcal{P}_j = G' P_I A_j G$, $\mathcal{R}(\theta) = (3/2) \bar{R}(\theta) P_R \bar{R}(\theta)'$ and $\mathcal{A}_j = G' A_j G$. Observe that matrices \mathcal{P}_j and \mathcal{A}_j can be calculated *a priori*. Finally, taking into account that $i_c = -i_a - i_b$, the vectors $\bar{x} = G^{\#} x$ and $\bar{x}^*(\theta) = G^{\#} x^*(\theta)$ can be calculated as

$$\bar{x} = \begin{bmatrix} i_a \\ -(\sqrt{3}/3)(i_a + 2i_b) \\ (\sqrt{6}/3)\nu_o \end{bmatrix}, \quad \bar{x}^*(\theta) = \begin{bmatrix} i^* \sin(\theta) \\ i^* \cos(\theta) \\ (\sqrt{6}/3)\nu_o^* \end{bmatrix} \quad (4.117)$$

leading to an equivalent switching function

$$u(\bar{x}, \theta) = \arg \min_{j \in \mathbb{K}} (\bar{x} - \bar{x}^*(\theta))' (\mathcal{P}_j - \mathcal{R}(\theta) \mathcal{A}_j) \bar{x} \quad (4.118)$$

which is more adapted for implementation in microcontrollers. Indeed, at each control update the most demanding operations required are two trigonometric function evaluations (i.e. $\sin(\theta)$ and $\cos(\theta)$), two 3x3 matrix products for determining $\mathcal{R}(\theta)$ and then 7 evaluations of the expression in (4.118), which can be efficiently performed for each $j \in \mathbb{K}$. The next subsection presents simulation results of the presented approach.

4.3.5 Simulation Results

Some numerical results are discussed in this subsection. Firstly, let us demonstrate the efficiency of the proposed methodology by means of the following example, with data borrowed from the literature.

Example 4.5. The goal is to bring the output voltage of the AC-DC converter given in Figure 4.8 to a steady-state value of $\nu_o^* = 120$ V while operating in unitary power factor. The numerical data were borrowed from Bouafia et al. (2009) and are given in Table 4.5.

Table 4.5: System parameters adopted in simulations.

Quantity	Value	Unit
R_o	175	Ω
R_L	0.56	Ω
L	19.5	mH
ω	$2\pi \times 50$	rad/s
C	2.35	mF
ν_M	40.825	V

To this end we could verify that, for $i^* = 1.369$ A, the pair $(i^*, \nu_o^*) \in X^*$ defines a reachable steady state trajectory $x^*(\theta) = [i^* f(\theta)' \nu_o^*]'$. Adopting this equilibrium pair, we have solved the optimization problem

$$\min_{p, q, P_R} (x_0 - x^*(\theta_0))' P(\theta_0) (x_0 - x^*(\theta_0)) \quad (4.119)$$

subject to (4.100)-(4.102) considering $x_0 = 0$ and $\theta_0 = 0$. Moreover, to obtain a fast convergence of $\nu_o(t)$ toward ν_o^* , we chose $d = 0$. This objective function is responsible for minimizing the upper bound $\bar{\mathcal{J}}$ defined in (4.106). An optimal solution was obtained for $p = 6.2576 \times 10^4$, $q = 5.6854 \times 10^3$ and

$$P_R = \begin{bmatrix} 4.1718 \times 10^4 & -0.0082 & -0.0155 \\ -0.0082 & 4.1718 \times 10^4 & -0.0487 \\ -0.0155 & -0.0487 & 3.7902 \times 10^3 \end{bmatrix} \quad (4.120)$$

assuring an upper bound in (4.106) of $\bar{\mathcal{J}}_2 = 1975.32 > \mathcal{J}$. For sake of comparison, solving the analogous problem with the constraint (4.112), related to a quadratic Lyapunov function $\hat{v}(\xi) = \xi' P \xi$, yields an upper bound $\bar{\mathcal{J}} = 2965.81$, showing that the proposed Lyapunov function is better adapted to this system.

Simulating the system response from $x_0 = 0$, the state trajectories obtained and the correspondent switching signal are shown in Figure 4.11, 4.12 and 4.13. From these data we can conclude that the proposed switching function was successful in controlling the converter output voltage towards a constant value of 120 V, under unitary power factor operation.

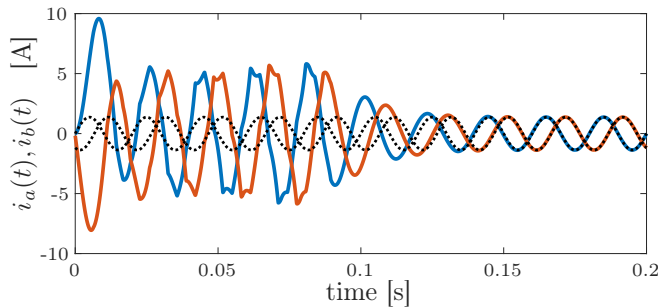


Figure 4.11: Phase currents $i_a(t)$ (blue) and $i_b(t)$ (red) and steady-state references (dashed lines).

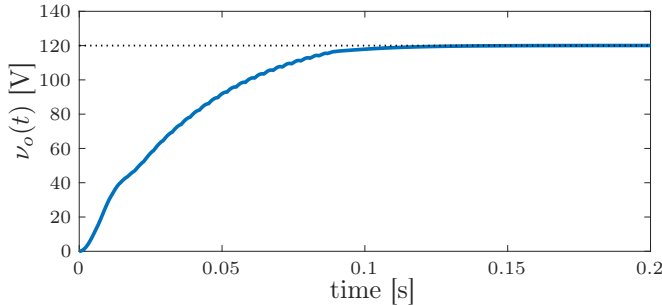


Figure 4.12: Output voltage $\nu_o(t)$ and correspondent steady-state reference (dashed line).

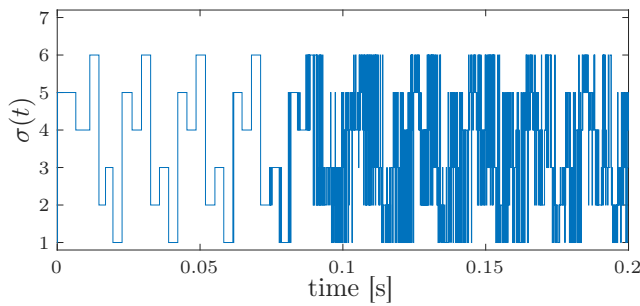


Figure 4.13: Switching signal $\sigma(t)$ generated by the proposed switching function.

As it can be noticed in Figure 4.13, the switching frequency during the transient response was relatively low, when compared to the steady-state. This implies that the present methodology may be of interest in contexts where reducing the number of switching events is desirable. However, notice that no bounds on the switching frequency were presented. This issue is still to be studied in this context of the parameter-dependent systems, presented in this chapter and the next example serves as a motivation for this topic.

Example 4.6. For the sake of curiosity, let us investigate the effects of employing a piecewise constant switching function as

$$\sigma(t) = u(\xi(t_n), \theta(t_n)), \quad \forall t \in [t_n, t_{n+1}) \quad (4.121)$$

where $t_n, n \in \mathbb{N}$ are switching instants respecting $t_0 = 0$ and the switching period $T = t_{n+1} - t_n$. For several values of T , the steady-state behavior of the phase current $i_a(t)$ and output voltage $v_o(t)$ are shown in Figure 4.14 along with the corresponding references (dotted lines).

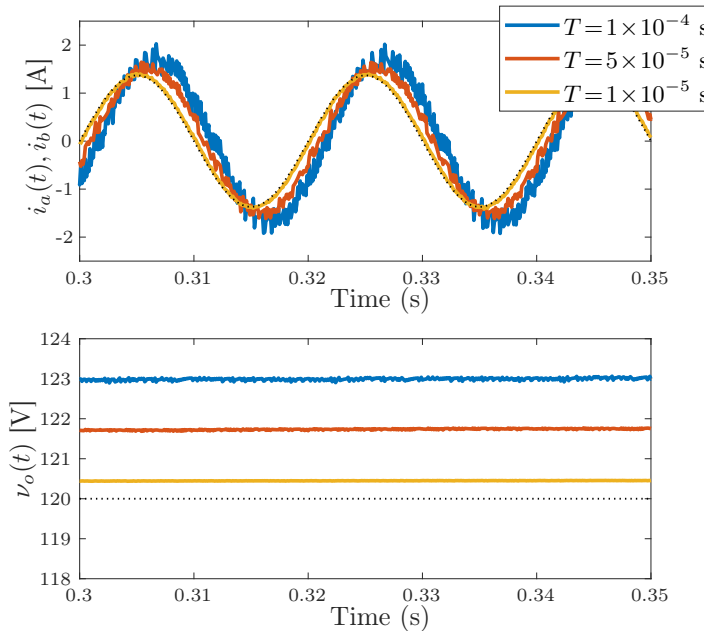


Figure 4.14: Steady-state response of current $i_a(t)$ (above) and voltage $v_o(t)$ (below) for several values of T .

Notice that the performance is impaired as larger values of switching period T are adopted. This demonstrates the importance of taking into account this aspect into the design step, motivating future works.

4.4 Concluding Remarks

This chapter presented design methodologies for switching functions capable of controlling the state variables of two switched nonlinear systems, assuring asymptotic stability of a desired trajectory. The first system, consists of a PMSM fed by a VSI, where the switches in the inverter are commanded to make the velocity $\omega(t)$ track a desired profile $\omega^*(t)$. The second system is a three-phase AC-DC rectifier, whose output voltage is kept constant while sinusoidal currents as drawn from each input phase, to preserve unitary power factor. Both methodologies have in common the adoption of parameter-dependent Lyapunov functions, which was shown to be more adapted

for these problems. Indeed, the time-varying parameter $\theta(t)$, regarded as the electrical angle of these AC systems, is took into account in the design step and in both switching functions. This particular choice of Lyapunov function provided efficient design methodologies, based on LMIs, assuring guaranteed quadratic costs and leading to less conservative results, when compared to a classical quadratic Lyapunov function, in our examples.

The proposed approaches dismiss the use of auxiliary reference frames or space-vector modulation and are of low computational complexity. Moreover, they seem to be adaptable to AC systems with higher numbers of phases or the control of synchronous and brushless DC machines, which are topics to be addressed in related future works.

"A minha alucinação é suportar o dia-a-dia / E meu delírio é a experiência com coisas reais."
— ANTONIO CARLOS BELCHIOR, ALUCINAÇÃO (1976)

Although this dissertation is mainly devoted to control theory studies, some experiments were carried out to validate theoretical results previously presented. The tests employed power electronic devices largely diffused in the industry. Our goal is to evaluate the performance of these devices, usually controlled by averaged model approaches, under the switched control strategies that were developed. Part of the results in this chapter are available in [Egidio et al. \(2017\)](#). Another reference containing experimental verification of techniques presented in this dissertation is [Garcia et al. \(2009\)](#), where switching functions designed by Theorem 2.15 are implemented to control a boost converter, in the continuous-time domain.

5.1 Buck-boost DC-DC Converter

A bidirectional buck-boost DC-DC converter is a versatile power switching converter topology, allowing to step-up or step-down the output voltage, only by varying the switching pattern. A simplified schematic of this circuit is shown in Figure 5.1. A DC source with voltage E and internal resistance R_s supplies the converter input. An inductor with inductance L , winding resistance R_L and a capacitor with capacitance C integrate the buck-boost circuit together with two switches sw_1 and sw_2 . These switches are commanded alternately and are responsible for the existence of two subsystems that are numbered 1, when sw_1 is closed, and 2, otherwise. Applying the Kirchhoff's circuit laws for each case, we obtain the following dynamic equations for this system.

$\sigma = 1$: sw_1 closed and sw_2 open:

$$L \frac{di_L(t)}{dt} = E - (R_s + R_L)i_L(t) \quad (5.1)$$

$$C \frac{d\nu_c(t)}{dt} = -\frac{\nu_c(t)}{R_o} \quad (5.2)$$

$\sigma = 2$: sw_2 closed and sw_1 open:

$$L \frac{di_L(t)}{dt} = -R_L i_L(t) - \nu_c(t) \quad (5.3)$$

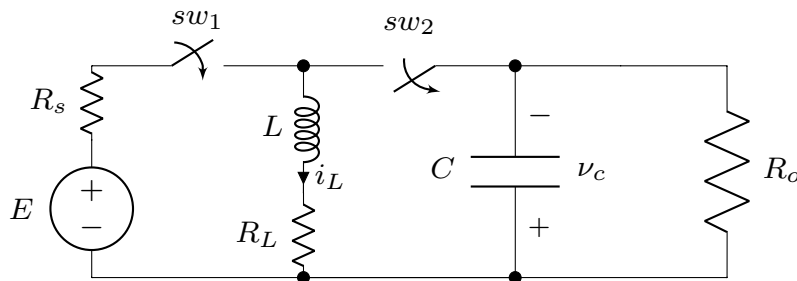


Figure 5.1: Buck-boost circuit schematic.

Table 5.1: Identified parameters for the built buck-boost converter.

Quantity	Value	Unit
E	10.75	V
C	2.2	mF
L	0.848	mH
R_L	1.129	Ω
R_o	68	Ω
R_s	0.45	Ω

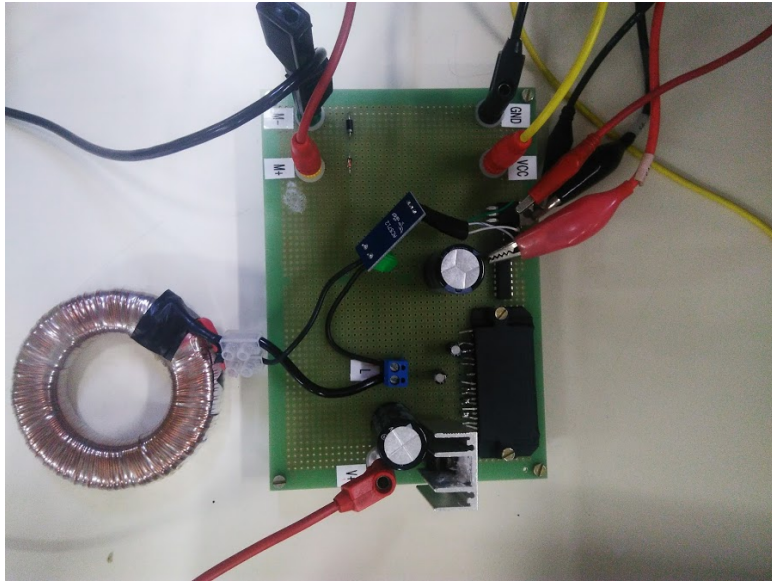


Figure 5.2: Photo of the developed buck-boost converter.

$$C \frac{d\nu_c(t)}{dt} = -\frac{\nu_c(t)}{R_o} + i_L(t) \quad (5.4)$$

Defining the system state vector as being $x(t) = [i_L(t) \ \nu_c(t)]'$, the converter can be represented by the continuous-time switched affine system with state-space realization

$$\frac{dx(t)}{dt} = F_\sigma x(t) + g_\sigma, \quad x(0) = x_0 \quad (5.5)$$

with matrices given by

$$F_1 = \begin{bmatrix} -(R_L + R_s)/L & 0 \\ 0 & -1/(R_o C) \end{bmatrix}, \quad g_1 = \begin{bmatrix} E/L \\ 0 \end{bmatrix}, \quad F_2 = \begin{bmatrix} -R_L/L & -1/L \\ 1/C & -1/(R_o C) \end{bmatrix}, \quad g_2 = \begin{bmatrix} 0 \\ 0 \end{bmatrix} \quad (5.6)$$

which defines $N = 2$ affine subsystems with $\sigma(t)$ being the switching function that selects one of them to be activated at each instant of time.

An experimental setup was designed to allow the validation of some of the proposed switching techniques. System parameters were measured and are available in Table 5.1. Additionally, a photo of the circuit is given in Figure 5.2. The switches sw_1 and sw_2 are a pair of built-in IGBTs from International Rectifier found inside the IRAMX20UP60A hybrid IC. This IC integrates the half-H bridge and the gate drivers as well as the appropriate protections. A Hall effect-based current sensor, namely the Allegro ACS712, allows the acquisition of i_L ,

appending an insignificant impedance to the circuit. The acquisition and control system were implemented in a dSPACE DS1104 controller board, which is capable of running the required real-time routine. An analog-to-digital converter acquires the current sensor output and the voltage ν_c .

The fixed sampling rate of $f_s = 1/T = 1$ kHz was chosen, at which the real-time program is responsible for acquiring the state variables and for digital conditioning. Whenever the updated state is available, the board microprocessor evaluates a proposed control law to decide whether the switches have to be closed or opened. At this instant of time, the controller board sends the suitable signal to the IC, directly to the input of sw_1 and passing through a NOT gate to sw_2 . The propagation delay of the NOT gate, the HD74LS04P, is negligible.

The goal is to design a suitable state-dependent switching function taking into account an upper bound for the switching frequency in order to avoid chattering occurrence and to make possible that some important aspects appearing in practical implementations be considered, as for instance, the response time of the converter switches. Hence, the idea is to impose a constraint on the switching rule that must remain constant during all $t \in [t_n, t_{n+1})$ with $t_{n+1} - t_n = T > 0$ where $T > 0$ is the defined sampling period. This constraint is introduced in equation (2.139) and allows to bound the switching frequency from above by the sampling frequency f_s . In this case, we can employ the step-invariant discretization procedure (2.77) for each subsystem, defining an equivalent discrete-time switched affine system with state-space realization given as (3.1), where $x[n] = x(t_n) = x(nT) \in \mathbb{R}^n$ for all $n \in \mathbb{N}$.

The following experiment demonstrates how a state-dependent switching function can be designed adopting the switching strategy proposed by Theorem 3.3 which, as has been discussed just after Theorem 3.1, is equivalent to Theorem 1 of Deaecto and Geromel (2017) adopted in Egidio et al. (2017) from where the experimental results of the next two experiments were borrowed.

Experiment 5.1. Consider the buck-boost converter circuit presented above. In order to control its output voltage around $\nu_c(t) = 4$ V, the optimization problem in Theorem 3.3, was solved for $\lambda = [0.5339 \ 0.4661]'$, which is associated to the equilibrium point $x_e = [i_{Le} \ \nu_{ce}]' = [0.3915 \ 4.0000]' \in X_e$, defined in (3.5). Details about the implementation of this solution are available in Appendix B. The solution found for $\beta = 6.06$ provided matrices

$$P = \begin{bmatrix} 0.0113 & 0.0486 \\ 0.0486 & 0.4150 \end{bmatrix} \quad (5.7)$$

Q_i , vectors h , c_i and scalars ρ_i for $i \in \{1, 2\}$ and allowed the implementation of the switching function (3.10), capable of assuring global practical stability of the desired x_e and the existence of an invariant set of attraction \mathcal{V} , as defined in (3.42). A comparison between the experimental and the simulated evolution of state variables from $x_0 = [0 \ 0]'$ is carried out in Figure 5.3. At the beginning, notice that the current in the real inductor increases in a smaller rate than in the simulation due to the DC supply slew rate. Nevertheless, this difference is only relevant during the beginning of the transient response.

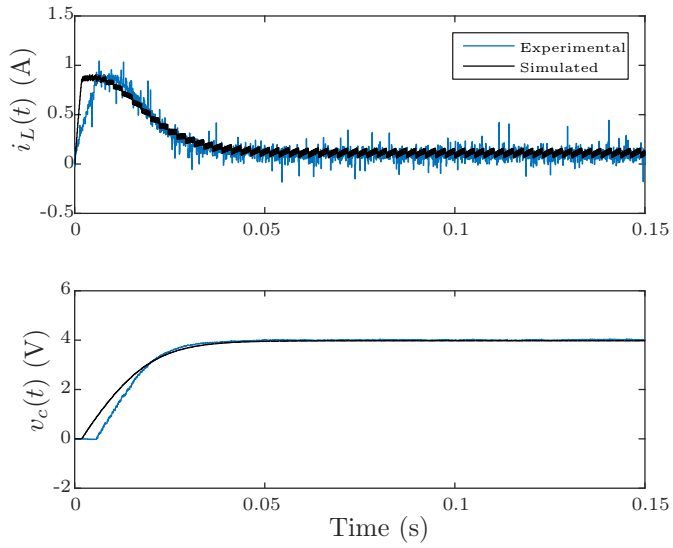


Figure 5.3: Experimental response of a buck-boost converter controled by the switching function (3.10).

This experiment showed how a buck-boost DC-DC converter can be controlled by the state-dependent switching function (3.10). Indeed, the proposed methodology was successful in achieving the desired output voltage. A more involving case is presented in the next section where the output load is replaced by a DC motor and a switching function will be designed to control its velocity and the electrical variables in a single control loop.

5.2 DC-DC Converter Feeding DC Motor

Let us now replace the resistor R_o by a DC motor, as depicted in Figure 5.4. The DC motor is considered to have a winding inductance L_m , winding resistance R_m , electrical and mechanical constants K_e and K_m . Moreover an inertia was attached to its shaft, and the total inertia is given by J . The mechanical modeling assumes the existence of a friction torque which depends on the rotational velocity and is composed of a combination of

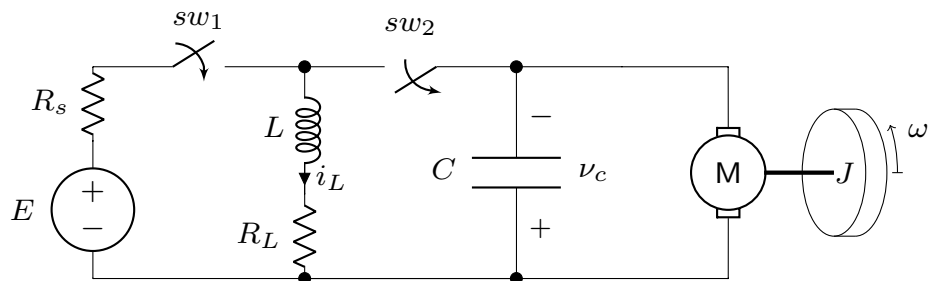


Figure 5.4: Buck-boost and DC-motor circuit schematic.

viscous and Coulomb frictions. This external torque is taken as

$$T_f(\omega) = T_v\omega + T_d \text{sign}(\omega) \quad (5.8)$$

This nonlinearity is illustrated in Figure 5.5. In the context of this experiment, the motor shaft only turns in one direction since the buck-boost converter output is always inverted with respect to the input supply. Hence, a simplification can be adopted concerning the sign function, leading to an affine dynamic model for the mechanical part, obtained through the Newton-Euler equations and given by

$$J \frac{d\omega(t)}{dt} + T_v\omega(t) + T_d = K_m i_m(t). \quad (5.9)$$

The updated electrical model is also defined for each subsystem as it follows.

$\sigma = 1$: sw_1 closed and sw_2 opened:

$$L \frac{di_L(t)}{dt} = E - (R_s + R_L)i_L(t) \quad (5.10)$$

$$L_m \frac{di_m(t)}{dt} = -R_m i_m(t) - K_e \omega(t) - \nu_c(t) \quad (5.11)$$

$$C \frac{d\nu_c(t)}{dt} = i_m(t) \quad (5.12)$$

$\sigma = 2$: sw_2 closed and sw_1 opened:

$$L \frac{di_L(t)}{dt} = -R_L i_L(t) - \nu_c(t) \quad (5.13)$$

$$L_m \frac{di_m(t)}{dt} = -R_m i_m(t) - K_e \omega(t) - \nu_c(t) \quad (5.14)$$

$$C \frac{d\nu_c(t)}{dt} = i_m(t) + i_L(t) \quad (5.15)$$

Let us consider L_m sufficiently small, such that the motor electrical dynamics can be neglected. However, for motors that this assumption is not consistent, L_m can be included in the affine model by simply adding a state variable i_m . Defining the system state vector as being $x = [i_L \ \nu_c \ \omega]'$, the combination DC motor/Buck-boost converter can be represented by the continuous-time switched affine system with state-space realization

$$\frac{dx(t)}{dt} = F_\sigma x(t) + g_\sigma, \quad x(0) = x_0 \quad (5.16)$$

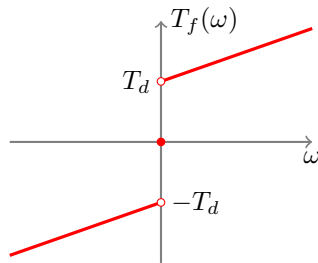


Figure 5.5: Friction torque in function of the rotational velocity.

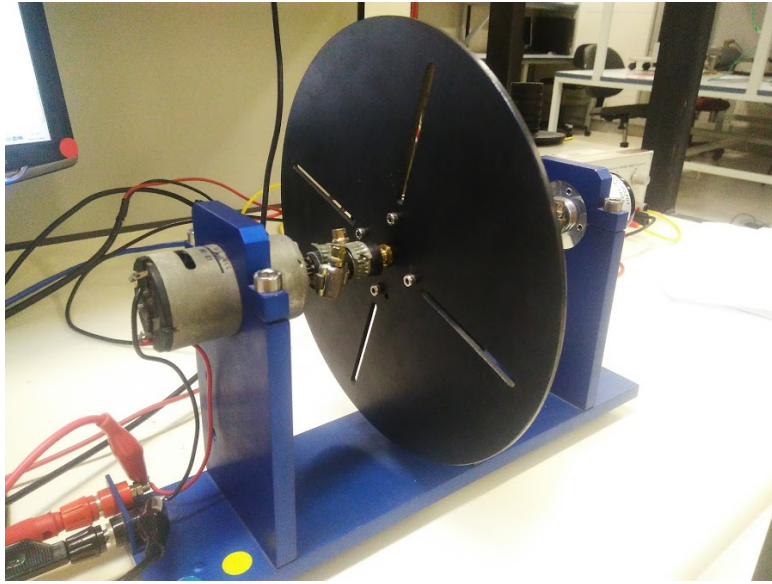


Figure 5.6: Photo of the considered DC motor.

Table 5.2: Identified parameters for the DC motor.

Quantity	Value	Unit
K_e	0.051	V.s/rad
K_m	0.051	N.m/A
R_m	10.207	Ω
J	3.792	$\text{g} \cdot \text{m}^2$
T_d	6.195	mN.m
T_v	76.220	$\mu\text{N} \cdot \text{m} \cdot \text{s}/\text{rad}$

with matrices given by

$$F_1 = \begin{bmatrix} \frac{-(R_L+R_s)}{L} & 0 & 0 \\ 0 & -1/(R_m C) & -K_e/(R_m C) \\ 0 & -K_m/(J R_m) & \frac{-T_v R_m - K_m K_e}{J R_m} \end{bmatrix}, \quad F_2 = \begin{bmatrix} -R_L/L & -1/L & 0 \\ 1/C & -1/(R_m C) & -K_e/(R_m C) \\ 0 & -K_m/(J R_m) & \frac{-T_v R_m - K_m K_e}{J R_m} \end{bmatrix} \quad (5.17)$$

$$g_1 = \begin{bmatrix} E/L \\ 0 \\ T_d/J \end{bmatrix}, \quad g_2 = \begin{bmatrix} 0 \\ 0 \\ T_d/J \end{bmatrix} \quad (5.18)$$

which defines $N = 2$ affine subsystems with $\sigma(t)$ being once more the switching signal that selects one of them to be activated at each instant of time.

The same setup presented in the last section was adopted. The considered DC motor is shown in Figure 5.6 and the identified parameters are given in Table 5.2. To acquire the rotational velocity $\omega(t)$, the motor shaft is coupled to an incremental encoder that produces a square wave of which time differences between rising edges are measured by a hardware interruption handler. The experimental validation of the switching function proposed in Theorem 3.3 was done in this system and is given in the following experiment.

Experiment 5.2. Firstly, let us investigate which are the rotational velocities ω_e that are attainable by the methodology proposed in Theorem 3.3. Naturally, let us turn our attention to the associated set of attainable equilibrium points X_e , which is defined in equation (3.5). By evaluating x_e for every $\lambda \in \Lambda$, the attainable set of steady state velocities is given in Figure 5.7 as a function of the first element of λ . For comparison, the same was done regarding the continuous-time case, whose set X_e^c is given in (2.125).

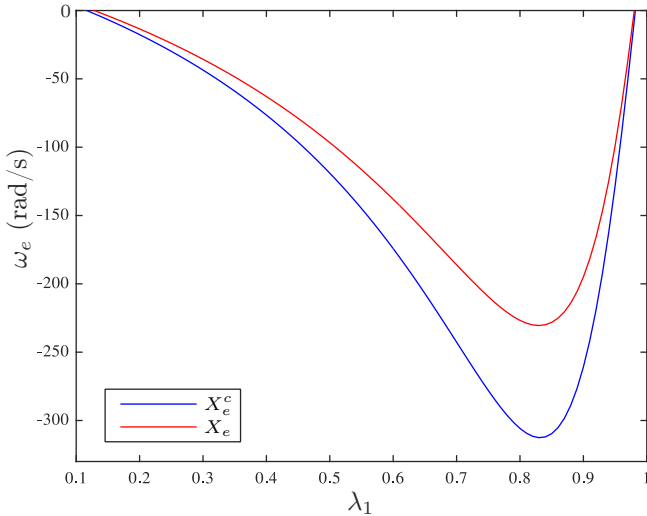


Figure 5.7: Attainable rotational velocities for continuous and discrete-time switched control techniques.

Notice that bounding the switching frequency, in the discrete-time case, has restricted the range of attainable velocities for this approach. However, as previously discussed in Subsection 3.2.4, adopting small enough sampling period makes X_e become closer to X_e^c .

For the sake of comparison, four switching functions were implemented to bring the motor rotational velocity to a steady value of $\omega_e = -40$ rad/s. To this end, we have chosen the vector $\lambda = [0.3171 \ 0.6829]'$ correspondent to $x_e = [0.5173 \ 3.8744 \ -39.9493]'$ $\in X_e$, allowing to write the equivalent discrete-time system (3.2) on the auxiliary state variable $\xi[n]$.

The first switching function, denoted by $u_a(t)$, is a periodic time-dependent signal known as PWM, previously presented in (2.88). The duty-cycle $\alpha = 0.30$ was chosen from the averaged model (see discussions following (2.88) for more details) in order to guarantee $\omega(t) \rightarrow \omega_e$. Its period $T_P = 2T$ assures a fair comparison with the state-dependent rule, i.e., the state-dependent switching functions will not switch more than the time-dependent function inside any interval of time. The second switching function, represented by $u_{\mathcal{V}}(\xi)$, is defined as (3.10) and was designed from the solution to the optimization problem of Theorem 3.3, which minimizes the invariant set of attraction given in (3.42). For more details regarding the optimization procedure, refer to Appendix B. A third switching function $u_{\mathcal{X}}(\xi)$ was designed solving the conditions of Theorem 3.1 that takes into account the volume minimization of the set of attraction \mathcal{X} , defined in (3.11). The last adopted switching function, denoted $u_d(\xi)$, was implemented considering the same conditions as in Deaecto and Geromel (2017) but bounding the volume of the set of attraction \mathcal{X} and optimizing the decay rate. Hence, we have solved the generalized eigenvalue minimization problem (see Boyd et al. (1994))

$$\min_{P > 0, \rho \in [0,1]} \rho \quad \text{s.t.} \tag{5.19}$$

$$\sum_{i \in \mathbb{K}} \lambda_i A'_i P A_i - \rho P < -\gamma I, \quad \sum_{i \in \mathbb{K}} \lambda_i \ell'_i P \ell_i < 1, \quad (5.20)$$

for $\gamma = 3 \times 10^{-6}$, which constrains the volume to obtain a suitable decay rate of $\sqrt{1-\rho} = 0.0121$. For the two last rules, the correspondent invariant set could be obtained by solving the conditions of Theorem 3.2.

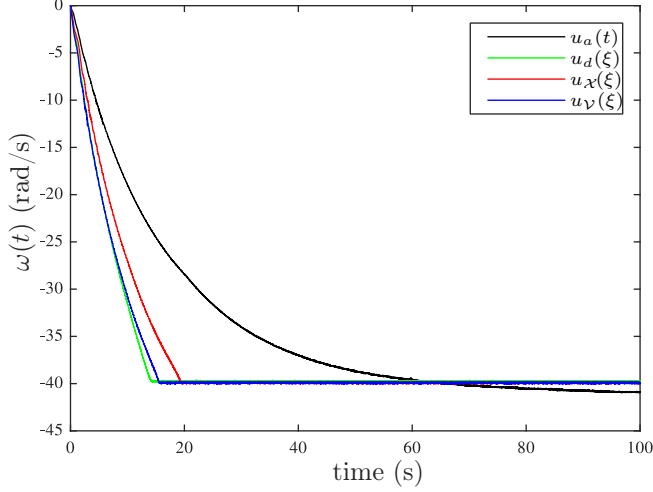


Figure 5.8: Experimental response of a DC motor fed by buck-boost converter under several switching functions.

Time evolution of $\omega(t)$, measured through the motor shaft encoder, is presented in Figure 5.8. Not surprisingly, it can be noticed that u_a with a settling time of $t_e = 53.93$ s presented the worst performance compared with the other three switching functions. This is natural since it is an open-loop technique whereas the others take into account the measurement of the discrete-time state $\xi[n]$. Notice that, for this function, the velocity in steady state was slightly different from the desired one since the model does not reflect a perfect behavior of the real system (for example, neglecting temperature transient, parasitic elements, etc.).

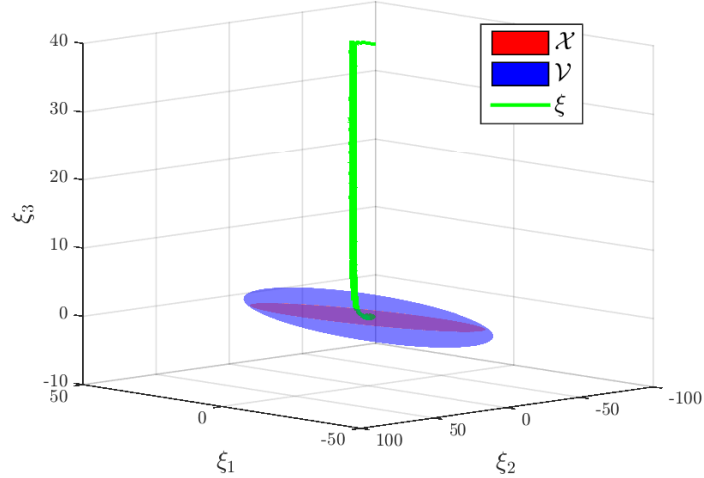


Figure 5.9: State trajectory ξ under u_V , obtained experimentally, and sets V and X .

Finally, Figure 5.9 presents the time evolution of the state trajectory ξ , obtained experimentally, and the sets of attraction \mathcal{V} and \mathcal{X} . Also as expected, the state ξ does not leave the invariant set \mathcal{V} once it is attained.

From the results presented in this experiment, we can conclude that the proposed state-dependent switching functions were able to successfully control the motor rotational velocity. As showed in Figure 5.8, the nonlinear behavior of the switching function is evident in all state-dependent rules. It is important to remark that as we adopt greater values of $T > 0$ the steady-state velocity may become different from ω_e also presenting an oscillatory behavior. However, the state vector ξ will always be inside the invariant set of attraction and the volume minimization procedure assures that ξ is as near as possible the desired equilibrium.

Let us now compare quantitatively the switching functions designed previously. Calculating the error

$$\bar{\epsilon} = \frac{\omega_e - \omega_\infty}{\omega_e} \quad (5.21)$$

where ω_∞ denotes the average steady-state rotational velocity, and the settling time t_e within 5% of the steady-state reference, these values for each experimentally obtained state trajectory are given in Table 5.3. These quantities lead to the conclusion that all switching functions presented a very small steady-state error and that σ_d , as expected, provided the fastest transient response.

	u_d	$u_{\mathcal{X}}$	$u_{\mathcal{V}}$
$vol(\mathcal{X})/vol(\mathcal{V}_*)$	2.25%	0.13%	3.09%
$vol(\mathcal{V})/vol(\mathcal{V}_*)$	2363.92%	133.66%	100%
$\bar{\epsilon}$	0.48%	0.05%	0.05%
t_e [s]	12.91	17.77	14.30

Table 5.3: Quantitative comparison of switching functions.

A comparison of the volumes, which were expressed relatively to the set of attraction \mathcal{V} of Theorem 3.3, is also shown in Table 5.3. As it can be verified, $u_{\mathcal{V}}$ guarantees the invariant set \mathcal{V} with the smallest volume while $u_{\mathcal{X}}$ has the smallest set \mathcal{X} among the switching functions implemented. This fact puts in evidence the effect of volume minimization in each design method.

The results presented in this section validated experimentally some methodologies for practical stability introduced in Chapter 3. Two experiments based on a classical buck-boost converter were provided and the performance of each case was evaluated.

5.3 PMSM and Voltage Source Inverter

Regarding the validation of the methodology for controlling a PMSM fed by a voltage source inverter presented in Section 4.2, it was experimentally implemented in a system whose parameters are given in Table 5.4. The following experimental results have been obtained embedding the proposed switching function in a Texas

Table 5.4: Identified system parameters.

Quantity	Value	Unit
R	2.19	Ω
L	8.1	mH
λ	6.0×10^{-2}	V.s/rad
c	3.1×10^{-4}	N.m.s/rad
J	3.0×10^{-4}	kg.m ²
V_{dc}	100	V
τ	8.7×10^{-3}	N.m

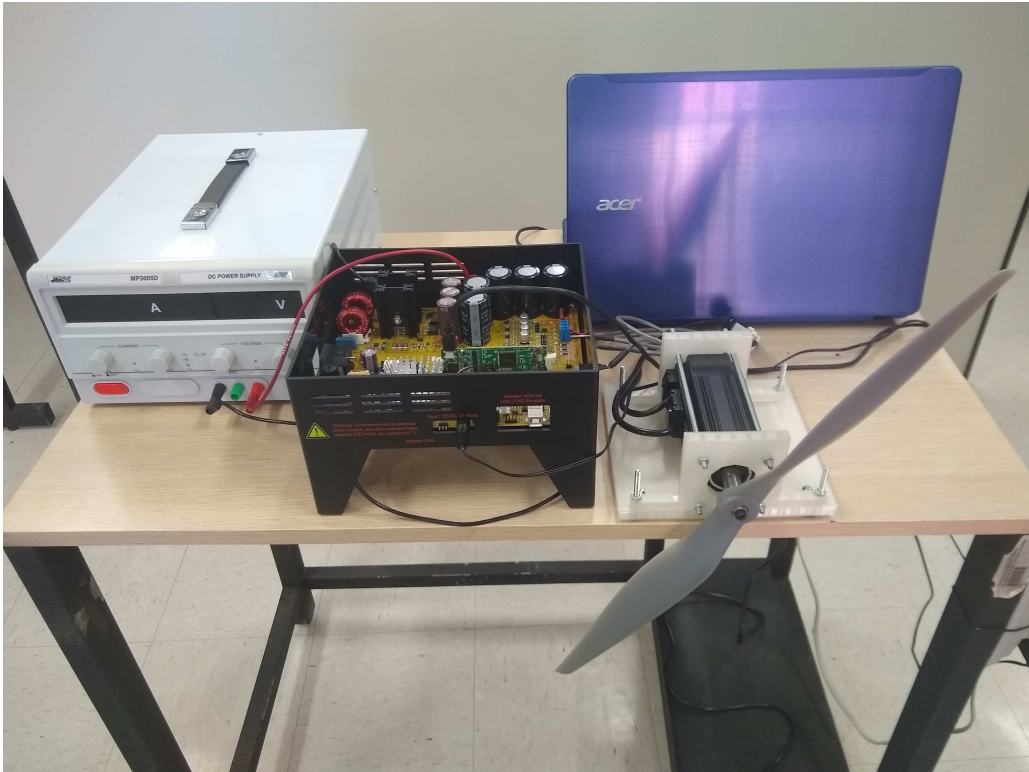


Figure 5.10: Photo of the experimental setup for controlling the PMSM.

Instruments TMS320F28069 microcontroller (MCU) under sampling frequency $f_s = 40$ kHz. Phase currents were measured through shunt resistors and data were acquired by means of built-in analog-to-digital converter and quadrature encoder pulse modules. The motor is the Estun EMJ-04APB24 and a propeller with a diameter of 50.8 cm was attached to its shaft, as shown in Fig. 5.10. An incremental encoder with 2,500 steps per rotation was used to measure both rotational velocity and displacement. The rotational velocity signal has been filtered by means of a first order Butterworth filter with cutoff frequency $\omega_c = 4,000$ rad/s, discretized through the bilinear transformation. This allows to calculate the rotational velocity within a suitable precision. The next experiment shows a comparison between experimental and simulated responses for this system controlled under the switching function proposed in Theorem 4.1.

Experiment 5.3. We have designed the switching function (4.36) to assure asymptotic convergence of $\omega(t)$ toward various velocity profiles. Particularly in this experiment, a constant $\omega^* = 100$ rad/s is adopted

as reference. To this end, we have considered $\kappa = 314.1593$ rad/s (or 3,000 rpm, the motor rated speed), which assures that the chosen $\omega^* \in \Omega_*$ is reachable. Solving the optimization problem (4.59) stated in Corollary 4.1 for $x(0) = 0$, $\theta(0) = 0$, $\omega^*(t) = 100$ rad/s and $Q = \text{diag}(I, 1)$, we have obtained the solution

$$p = 2.8790, r = 0.0672, q = 0.1111 \quad (5.22)$$

and the upper bound for (4.37) given by $\xi'_0 P(\theta_0) \xi_0 = 1120.23$. This solution allows the implementation of the switching function (4.36). Figures 5.11 and 5.12 show the experimentally obtained rotational velocity $\omega(t)$ and phase current $i_a(t)$, respectively, along with their simulated responses. The resulting switching signal is given in Figure 5.13. The simulated and experimental responses are very close and the angular velocity $\omega(t)$ has attained the desired ω^* as expected, thus validating the proposed control technique as well as the adopted experimental arrangement.

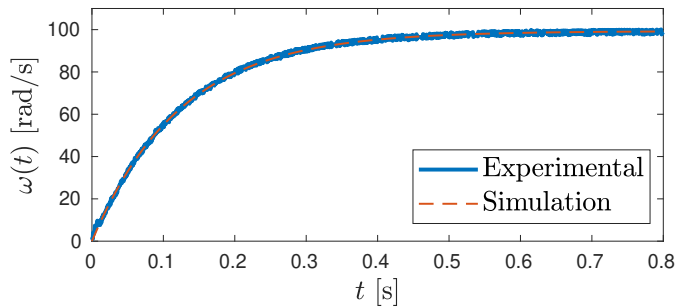


Figure 5.11: Experimental and simulated rotational velocities for $\omega^* = 100$ rad/s.

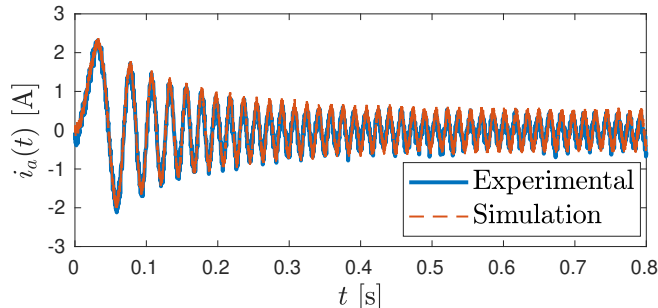


Figure 5.12: Experimental and simulated phase current $i_a(t)$ correspondent to $\omega^* = 100$ rad/s.

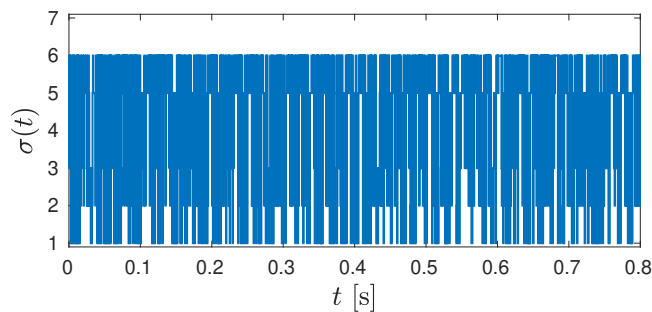


Figure 5.13: Switching signal for a constant $\omega^* = 100$ rad/s.

This experiment showed how the proposed model precisely captured the dynamics of the PMSM fed by the voltage source inverter and that the methodology provided by Theorem 4.1 successfully controlled the rotational velocity toward the desired reference. Now, our goal is to investigate the effects of the adoption of a time-varying reference $\omega^*(t) \in \Omega_*$. Notice that the switching function designed in Example 5.3 is robust with respect to the reference trajectory being capable of assuring asymptotic stability of any $\omega^*(t) \in \Omega_*$. This situation is explored in the following experiment.

Experiment 5.4. To avoid the current overshoot present in Figure 5.12 during the motor start-up, a piecewise linear reference $\omega^*(t)$ was adopted to bring gradually the rotational velocity to 50 rad/s, 100 rad/s and then to a complete stop. This will be done by limiting the angular acceleration $|\dot{\omega}(t)| < 50$ rad/s², in order to avoid high peak currents. For the given κ , we have verified that even though discontinuities are present in the time-derivative of the desired velocity profile, $\omega^*(t)$ does belong to the set of attainable ones Ω_* for almost every $t \in \mathbb{R}_{0+}$. Indeed, all the piecewise linear parts of $\omega^*(t)$ belong to Ω_* and, therefore, asymptotic stability is assured along them. In this sense, the discontinuities can be interpreted as new initial conditions for the remaining state trajectory. The transient response for the rotational velocity $\omega(t)$ along with the desired $\omega^*(t)$ is given in Figure 5.14. The obtained current trajectory for the phase current $i_a(t)$ is shown in Figure 5.15 keeping the same vertical scale as Figure 5.12.

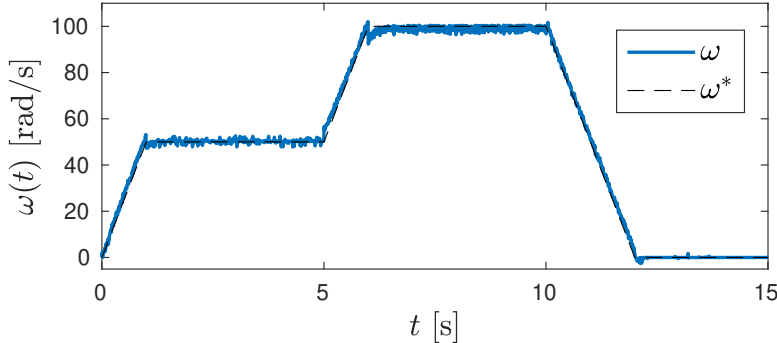


Figure 5.14: Experimental rotational velocity $\omega(t)$ and corresponding reference $\omega^*(t)$.

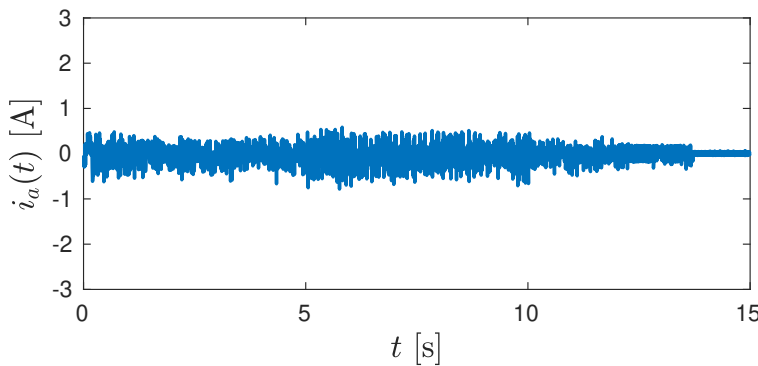


Figure 5.15: Experimental phase currents $i_a(t)$ obtained considering the reference $\omega^*(t)$.

This allows us to verify that the current peak was drastically reduced. This point is of great practical interest as high peak currents may cause premature failure and equipment wear.

Some comments are in order regarding the computational complexity of the proposed approach. We were able to perform the calculation of (4.65) and (4.31) within 477 clock cycles, using floating-point arithmetic. For the sake of comparison, the field-oriented control approach provided by Texas Instruments ControlSuite must compute a Clarke and a Park Transform, three discrete-time PI controller updates, an inverse Park Transform and a Space-Vector generation of PWM signals, which is done within 535 clock cycles also using floating-point arithmetic in the same microprocessor. Further investigations and other accelerations should be applied, but this preliminary comparison shows that our approach is implementable and may prosper in terms of demanding lower computational effort.

5.4 Concluding Remarks

Three experiments were presented in this chapter. The first two were based on a buck-boost DC-DC converter feeding, respectively, a resistive load and a DC motor. These setups, modeled as switched affine systems, allowed to validate the design methodology presented in Section 3.2, regarding practical stability. In this case, bounding the switching frequency accordingly, the state trajectories were globally guided to an invariant set of attraction containing the desired reference point x_e . Different switching functions were compared experimentally and theoretically.

The third experiment adopted a permanent magnet synchronous machine fed by a voltage source inverter. The methodology present in Section 4.2 was considered and the rotational velocity of the PMSM was controlled, first toward a constant reference and, subsequently, toward a piecewise linear trajectory. This last approach showed to be efficient in reducing current peaks, avoiding premature system damage.

Although not extensively, the experiments presented in this chapter close the exposition of results obtained throughout my Ph.D. and motivate the applicability of some developed techniques. Indeed, further tests and other experimental setups must be employed to investigate undisclosed aspects of these methodologies. This will certainly put in evidence practical issues that make arise new control problems and, consequently, let us search for their solutions.

“Corra não pare, não pense demais / Repare essas velas no cais / Que a vida é cigana”

— ALÇEU VALENÇA & GERALDO AZEVEDO, CARAVANA (1985)

6.1 Conclusions

This conclusion is devoted to highlight the main contributions presented in this Ph.D dissertation. Firstly, fundamental results gathered from the literature composed Chapter 2, which was the basis for the subsequent chapters.

In Chapter 3, three novel methodologies for designing globally stabilizing switching functions for discrete-time switched affine systems were provided. The first one is inspired in practical stability studies, where the existence of a set of attraction, to where the system trajectories are globally attracted, is assured. An approach inspired by existing results was given in Theorem 3.1 and then generalized to cope with the output feedback problem in Theorem 3.4. This generalization took into account a full-order switched affine filter and it was shown that any set of attraction assured by the state feedback case can also be assured under output-dependent switching. Less conservative conditions with respect to practical stability guarantees were provided in Theorem 3.6, pioneering the adoption of Lyapunov-Metzler inequalities and min-type Lyapunov functions in the context of switched affine systems. Finally, instead of assuring stability towards a set of attraction containing the desired equilibrium, an approach to design a suitable limit cycle taking into account the desired steady-state behavior of the system trajectories and to guarantee its global asymptotic stability was given in Theorem 3.9. This approach allowed to adopt \mathcal{H}_2 and \mathcal{H}_∞ performance index for the first time in the context of discrete-time switched affine systems, being possible to optimize the transient response of this class of systems.

Studies regarding the control of particular switched nonlinear systems, which are harmonically dependent on a time-varying parameter, were performed throughout Chapter 4. The main interest behind these classes arises from AC power systems where an angular parameter called the electrical angle governs the oscillatory behavior in the system dynamics. Namely, the considered systems were the a permanent magnet synchronous machine fed by a voltage source inverter and an AC-DC power converter based on a controlled rectifier. The approaches in this chapter took into account the original reference frame, introducing a new fashion of controlling these type of systems. To obtain design conditions written in terms of LMIs, a new class of parameter-dependent Lyapunov functions was introduced, which also allowed to reduce the conservativeness compared to when a simple quadratic one is adopted.

Finally, some experiments were presented in Chapter 5, validating theoretical results developed in the previous chapters and motivating the practical interest on these methodologies. In the next section, topics related to this dissertation that require further investigation in future works, are discussed.

6.2 Future Works

Regarding discrete-time switched affine systems, discussed in Chapter 3, open problems are the design of switching functions under uncertainties, such as of polytopic type. Moreover, generalizing those methodologies to stabilizing system whose subsystems present integrator dynamics could allow these approaches to be employed in some robotics contexts, for instance controlling the linear velocity and orientation of the robot in Example 3.4, while regulating its rotational velocity to zero. Unfortunately, this cannot be done in that example using methodologies derived from Theorem 3.1 because there is no $\lambda \in \Lambda$ such that A_λ is Schur when the integrator is included and, as discussed in Subsection 3.2.4, Theorem 3.6 might not produce results well adapted for sampled-data control.

With respect to results in Chapter 4, lots of studies are still to be done. Indeed, a more general framework must be developed to cope with systems presenting the exposed parameter dependency. Additionally, more nonlinear phenomena may arise when considering induction motors instead of PMSM or more complex AC-DC conversion typologies and active power filters. Discrete-time domain approaches should also be investigated but no state transition matrices were found so far for these classes of systems. Other methodologies to bound the switching frequency should also be considered, as for example, taking into account dwell-time within the switching function design step. Finally, coping with model uncertainties is a topic of great interest in these cases as, generally, loads might be unknown and system parameters are subject to temperature transients.

REFERENCES

- Albea, C., Garcia, G., and Zaccarian, L. (2015). Hybrid dynamic modeling and control of switched affine systems: application to DC-DC converters. In *IEEE Conference on Decision and Control (CDC)*, pages 2264–2269.
- 2 citations in pages 18 and 52.
- Angeli, D. and Kountouriotis, P. (2011). A stochastic approach to “dynamic-demand” refrigerator control. *IEEE Transactions on Control Systems Technology*, 20(3):581–592.
- One citation in page 42.
- Antonello, R., Carraro, M., Costabeber, A., Tinazzi, F., and Zigliotto, M. (2017). Energy-efficient autonomous solar water-pumping system for permanent-magnet synchronous motors. *IEEE Transactions on Industrial Electronics*, 64(1):43–51.
- One citation in page 114.
- Apkarian, P. and Tuan, H. D. (2000). Robust control via concave minimization local and global algorithms. *IEEE Transactions on Automatic Control*, 45(2):299–305.
- One citation in page 174.
- Bellman, R. E. (1961). *Adaptive control processes: a guided tour*. Princeton University Press.
- One citation in page 52.
- Beneux, G., Riedinger, P., Daafouz, J., and Grimaud, L. (2019). Adaptive stabilization of switched affine systems with unknown equilibrium points: Application to power converters. *Automatica*, 99:82–91.
- 2 citations in pages 51 and 52.
- Benmiloud, M., Benalia, A., Djemai, M., and Defoort, M. (2019). On the local stabilization of hybrid limit cycles in switched affine systems. *IEEE Transactions on Automatic Control*, 64:841–846.
- 4 citations in pages 94, 100, 105, and 106.
- Bittanti, S. and Colaneri, P. (2009). *Periodic systems: filtering and control*. Springer Science & Business Media.
- 2 citations in pages 45 and 98.
- Blanchini, F. and Miani, S. (2008). *Set-theoretic methods in control*. Springer.
- One citation in page 177.
- Blondel, V. and Tsitsiklis, J. N. (1997). NP-hardness of some linear control design problems. *SIAM Journal on Control and Optimization*, 35(6):2118–2127.
- 2 citations in pages 46 and 53.
- Bolzern, P. and Spinelli, W. (2004). Quadratic stabilization of a switched affine system about a nonequilibrium point. In *IEEE American Control Conference (ACC)*, volume 5, pages 3890–3895.
- 4 citations in pages 18, 51, 52, and 58.

Bose, B. K. (2010). Global warming: Energy, environmental pollution, and the impact of power electronics. *IEEE Industrial Electronics Magazine*, 4(1):6–17.

One citation in page 20.

Bouafia, A., Krim, F., and Gaubert, J. (2009). Fuzzy-logic-based switching state selection for direct power control of three-phase PWM rectifier. *IEEE Transactions on Industrial Electronics*, 56(6):1984–1992.

One citation in page 137.

Boyd, S., Ghaoui, L., Feron, E., and Balakrishnan, V. (1994). *Linear Matrix Inequalities in System and Control Theory*. Studies in Applied Mathematics. SIAM.

10 citations in pages 19, 23, 35, 63, 76, 147, 169, 170, 173, and 175.

Boyd, S. and Vandenberghe, L. (2004). *Convex optimization*. Cambridge University Press.

One citation in page 173.

Branicky, M. S. (1998). Multiple Lyapunov functions and other analysis tools for switched and hybrid systems. *IEEE Transactions on Automatic Control*, 43(4):475–482.

2 citations in pages 41 and 46.

Buisson, J., Richard, P., and Cormerais, H. (2005). On the stabilisation of switching electrical power converters. In *International Workshop on Hybrid Systems: Computation and Control*, pages 184–197.

One citation in page 52.

Casadei, D., Profumo, F., Serra, G., and Tani, A. (2002). FOC and DTC: two viable schemes for induction motors torque control. *IEEE Transactions on Power Electronics*, 17(5):779–787.

One citation in page 114.

Chan, C. C. (2007). The state of the art of electric, hybrid, and fuel cell vehicles. *Proceedings of the IEEE*, 95(4):704–718.

One citation in page 20.

Chen, C. (1995). *Linear System Theory and Design*. Oxford University Press, 2nd edition.

One citation in page 28.

Chen, T. and Francis, B. A. (2012). *Optimal sampled-data control systems*. Springer Science & Business Media.

4 citations in pages 19, 39, 40, and 58.

Chow, T. P. and Guo, Z. (2019). GaN smart power devices and integrated circuits. In *Wide Bandgap Semiconductor Power Devices*, pages 151–208.

3 citations in pages 8, 17, and 18.

Colaneri, P., Geromel, J. C., and Locatelli, A. (1997). *Control Theory and Design: An RH₂ and RH_∞ Viewpoint*. Elsevier Science.

One citation in page 176.

- Corona, D., Buisson, J., De Schutter, B., and Giua, A. (2007). Stabilization of switched affine systems: An application to the buck-boost converter. In *IEEE American Control Conference (ACC)*, pages 6037–6042.
2 citations in pages 18 and 52.
- Cuk, S. and Middlebrook, R. D. (1977). A general unified approach to modelling switching DC-to-DC converters in discontinuous conduction mode. In *IEEE Power Electronics Specialists Conference*, pages 36–57.
One citation in page 44.
- Daiha, H. R., Egidio, L. N., Deaecto, G. S., and Geromel, J. C. (2017). \mathcal{H}_∞ state feedback control design of discrete-time switched linear systems. In *IEEE Conference on Decision and Control (CDC)*, pages 5882–5887.
3 citations in pages 51, 96, and 100.
- Dargahi, V., Sadigh, A. K., Pahlavani, M. R. A., and Shoulaie, A. (2012). DC (direct current) voltage source reduction in stacked multicell converter based energy systems. *Energy*, 46:649–663.
One citation in page 109.
- Dayawansa, W. P. and Martin, C. F. (1999). A converse Lyapunov theorem for a class of dynamical systems which undergo switching. *IEEE Transactions on Automatic Control*, 44(4):751–760.
One citation in page 45.
- Deaecto, G. S. (2016). Dynamic output feedback \mathcal{H}_2 control of continuous-time switched affine systems. *Automatica*, 71:44–49.
3 citations in pages 18, 70, and 95.
- Deaecto, G. S., Daafouz, J., and Geromel, J. C. (2012). \mathcal{H}_2 and \mathcal{H}_∞ performance optimization of singularly perturbed switched systems. *SIAM Journal on Control and Optimization*, 50(3):1597–1615.
One citation in page 47.
- Deaecto, G. S. and Egidio, L. N. (2016). Practical stability of discrete-time switched affine systems. In *IEEE European Control Conference (ECC)*, pages 2048–2053.
4 citations in pages 62, 82, 86, and 90.
- Deaecto, G. S. and Geromel, J. C. (2010). \mathcal{H}_∞ control for continuous-time switched linear systems. *Journal of Dynamic Systems, Measurement, and Control*, 132(4):041013.
One citation in page 48.
- Deaecto, G. S. and Geromel, J. C. (2017). Stability analysis and control design of discrete-time switched affine systems. *IEEE Transactions on Automatic Control*, 62(8):4058–4065.
14 citations in pages 60, 61, 62, 64, 65, 68, 70, 82, 86, 90, 143, 147, 171, and 173.
- Deaecto, G. S. and Geromel, J. C. (2018). Stability and performance of discrete-time switched linear systems. *Systems & Control Letters*, 118:1–7.
5 citations in pages 18, 51, 96, 97, and 101.

Deaecto, G. S., Geromel, J. C., and Daafouz, J. (2011a). Dynamic output feedback \mathcal{H}_∞ control of switched linear systems. *Automatica*, 47(8):1713–1720.

3 citations in pages 18, 50, and 70.

Deaecto, G. S., Geromel, J. C., and Daafouz, J. (2011b). Switched state-feedback control for continuous time-varying polytopic systems. *International Journal of Control*, 84(9):1500–1508.

One citation in page 17.

Deaecto, G. S., Geromel, J. C., Garcia, F., and Pomilio, J. (2010). Switched affine systems control design with application to DC–DC converters. *IET Control Theory & Applications*, 4(7):1201–1210.

6 citations in pages 18, 51, 52, 53, 62, and 116.

Deaecto, G. S. and Santos, G. C. (2015). State feedback \mathcal{H}_∞ control design of continuous-time switched affine systems. *IET Control Theory & Applications*, 9(10):1511–1516.

3 citations in pages 18, 52, and 95.

Deaecto, G. S., Souza, M., and Geromel, J. C. (2014). Chattering free control of continuous-time switched linear systems. *IET Control Theory & Applications*, 8(5):348–354.

4 citations in pages 18, 19, 56, and 65.

DeCarlo, R. A., Branicky, M. S., Pettersson, S., and Lennartson, B. (2000). Perspectives and results on the stability and stabilizability of hybrid systems. *Proceedings of the IEEE*, 88(7):1069–1082.

One citation in page 17.

Delpoux, R., Hetel, L., and Kruszewski, A. (2014). Parameter-dependent relay control: Application to PMSM. *IEEE Transactions on Control Systems Technology*, 23(4):1628–1637.

One citation in page 111.

Dinh, Q. T., Gumussoy, S., Michalek, W., and Diehl, M. (2011). Combining convex–concave decompositions and linearization approaches for solving BMIs, with application to static output feedback. *IEEE Transactions on Automatic Control*, 57(6):1377–1390.

One citation in page 174.

Doyle, J. C., Glover, K., Khargonekar, P. P., and Francis, B. A. (1989). State-space solutions to standard \mathcal{H}_2 \mathcal{H}_∞ control problems. *IEEE Transactions on Automatic Control*, 34(8):831–847.

One citation in page 34.

Duesterhoeft, W. C., Schulz, M. W., and Clarke, E. (1951). Determination of instantaneous currents and voltages by means of alpha, beta, and zero components. *Transactions of the American Institute of Electrical Engineers*, 70(2):1248–1255.

2 citations in pages 117 and 124.

Egidio, L. N. (2016). Controle via realimentação de estado de sistemas afins com comutação a tempo discreto. Master's thesis (in portuguese), FEM - Universidade Estadual de Campinas.

2 citations in pages 53 and 62.

Egidio, L. N., Daiha, H. R., and Deaecto, G. S. (2020). Limit cycle global asymptotic stability and $\mathcal{H}_2/\mathcal{H}_\infty$ performance of discrete-time switched affine systems. *Automatica*. Accepted.

3 citations in pages 19, 95, and 100.

Egidio, L. N., Daiha, H. R., Deaecto, G. S., and Geromel, J. C. (2017). DC motor speed control via buck-boost converter through a state dependent limited frequency switching rule. In *IEEE Conference on Decision and Control (CDC)*, pages 2072–2077.

5 citations in pages 60, 76, 141, 143, and 173.

Egidio, L. N. and Deaecto, G. S. (2019). Novel practical stability conditions for discrete-time switched affine systems. *IEEE Transactions on Automatic Control*, 64(11):4705–4710.

One citation in page 19.

Egidio, L. N. and Deaecto, G. S. (n.d.). Dynamic output feedback control of discrete-time switched affine systems. Submitted.

3 citations in pages 19, 62, and 70.

Egidio, L. N., Deaecto, G. S., and Barros, T. A. S. (n.d.). Switched control of three-phase ac-dc power converter. Submitted.

3 citations in pages 20, 51, and 128.

Egidio, L. N., Deaecto, G. S., Hespanha, J. P., and Geromel, J. C. (2019). A nonlinear switched control strategy for permanent magnet synchronous machines. In *IEEE Conference on Decision and Control (CDC)*, pages 3411–3416.

3 citations in pages 20, 51, and 122.

Farey, J. (1827). *A Treatise on the Steam Engine: Historical, Practical, and Descriptive*. Longman, Rees, Orme, Brown, and Green.

One citation in page 17.

Fiacchini, M. and Jungers, M. (2014). Necessary and sufficient condition for stabilizability of discrete-time linear switched systems: A set-theory approach. *Automatica*, 50(1):75–83.

2 citations in pages 18 and 50.

Filippov, A. (1967). Classical solutions of differential equations with multi-valued right-hand side. *SIAM Journal on Control*, 5(4):609–621.

One citation in page 44.

Fioravanti, A. R., Gonçalves, A. P. C., Deaecto, G. S., and Geromel, J. C. (2013). Obtaining alternative LMI constraints with applications to discrete-time MJLS and switched systems. *Journal of the Franklin Institute*,

350(8):2212 – 2228.

One citation in page 86.

Frank, M. and Wolfe, P. (1956). An algorithm for quadratic programming. *Naval research logistics quarterly*, 3(1-2):95–110.

One citation in page 173.

Garcia, F. S., Pomilio, J. A., Deaecto, G. S., and Geromel, J. C. (2009). Analysis and control of DC-DC converters based on Lyapunov stability theory. In *IEEE Energy Conversion Congress and Exposition*, pages 2920–2927.

One citation in page 141.

Geromel, J. C. and Colaneri, P. (2006a). Stability and stabilization of continuous-time switched linear systems. *SIAM Journal on Control and Optimization*, 45(5):1915–1930.

3 citations in pages 18, 46, and 47.

Geromel, J. C. and Colaneri, P. (2006b). Stability and stabilization of discrete time switched systems. *International Journal of Control*, 79(7):719–728.

4 citations in pages 18, 46, 49, and 86.

Geromel, J. C., Colaneri, P., and Bolzern, P. (2008). Dynamic output feedback control of switched linear systems. *IEEE Transactions on Automatic Control*, 53(3):720–733.

2 citations in pages 48 and 50.

Geromel, J. C., Deaecto, G. S., and Daafouz, J. (2013). Suboptimal switching control consistency analysis for switched linear systems. *IEEE Transactions on Automatic Control*, 58(7):1857–1861.

One citation in page 48.

Geromel, J. C. and Korogui, R. H. (2011). *Controle Linear de Sistemas Dinâmicos : Teoria, Ensaios Práticos e Exercícios*. Edgard Blucher. (in portuguese).

One citation in page 29.

Gilpin, M. E. (1973). Do hares eat lynx? *The American Naturalist*, 107(957):727–730.

One citation in page 24.

Goebel, R. and Sanfelice, R. (2012). *Hybrid Dynamical Systems: Modeling, Stability, and Robustness*. Princeton University Press.

One citation in page 43.

Goudarzian, A. and Khosravi, A. (2019). Application of DC/DC Cuk converter as a soft starter for battery chargers based on double-loop control strategy. *International Journal of Circuit Theory and Applications*, 47(5):753–781.

One citation in page 51.

- Hadjeras, S., Sanchez, C. A., Gomez-Estern Aguilar, F., Gordillo, F., and Garcia, G. (2019). Hybrid control law for a three-level npc rectifier. In *IEEE European Control Conference (ECC)*, pages 281–286.
- 3 citations in pages 19, 51, and 111.
- Hale, J. (1969). *Ordinary Differential Equations*. Wiley.
- One citation in page 24.
- Hassibi, A., How, J., and Boyd, S. (1999). A path-following method for solving BMI problems in control. In *IEEE American Control Conference (ACC)*, volume 2, pages 1385–1389.
- One citation in page 174.
- Hauroigne, P., Riedinger, P., and Iung, C. (2011). Switched affine systems using sampled-data controllers: Robust and guaranteed stabilization. *IEEE Transactions on Automatic Control*, 56:2929–2935.
- One citation in page 57.
- Henrion, D., Arzelier, D., Peaucelle, D., and Šebek, M. (2001). An LMI condition for robust stability of polynomial matrix polytopes. *Automatica*, 37(3):461–468.
- One citation in page 53.
- Hespanha, J. P. (2004). Uniform stability of switched linear systems: Extensions of LaSalle’s invariance principle. *IEEE Transactions on Automatic Control*, 49(4):470–482.
- 2 citations in pages 18 and 40.
- Hespanha, J. P. (2018). *Linear Systems Theory*. Princeton Press, Princeton, New Jersey.
- One citation in page 29.
- Hespanha, J. P., Liberzon, D., and Morse, A. S. (2003). Hysteresis-based switching algorithms for supervisory control of uncertain systems. *Automatica*, 39(2):263–272.
- 2 citations in pages 17 and 56.
- Hespanha, J. P., Naghshtabrizi, P., and Xu, Y. (2007). A survey of recent results in networked control systems. *Proceedings of the IEEE*, 95(1):138–162.
- 2 citations in pages 17 and 39.
- Hetel, L. and Bernauau, E. (2014). Local stabilization of switched affine systems. *IEEE Transactions on Automatic Control*, 60(4):1158–1163.
- One citation in page 52.
- Hetel, L. and Fridman, E. (2013). Robust sampled-data control of switched affine systems. *IEEE Transactions on Automatic Control*, 58(11):2922–2928.
- 3 citations in pages 18, 58, and 62.
- Horn, R. A. and Johnson, C. R. (1990). *Matrix Analysis*. Cambridge university press.
- One citation in page 169.

Karmarkar, N. (1984). A new polynomial-time algorithm for linear programming. In *ACM Symposium on Theory of Computing*, pages 302–311.

One citation in page 173.

Kefalas, T. D. and Kladas, A. G. (2014). Thermal investigation of permanent-magnet synchronous motor for aerospace applications. *IEEE Transactions on Industrial Electronics*, 61(8):4404–4411.

One citation in page 114.

Khalil, H. K. (2002). *Nonlinear systems*. Prentice Hall.

6 citations in pages 23, 24, 27, 29, 56, and 58.

Kolotelo, G. K., Egidio, L. N., and Deaecto, G. S. (2018). \mathcal{H}_2 and \mathcal{H}_∞ filtering for continuous-time switched affine systems. In *IFAC Symposium on Robust Control Design (ROCOND)*, pages 184–189.

2 citations in pages 51 and 70.

Krause, P., Wasynczuk, O., Sudhoff, S., and Pekarek, S. (2013). *Analysis of Electric Machinery and Drive Systems*. John Wiley & Sons.

One citation in page 114.

Krishnan, R. (2009). *Permanent Magnet Synchronous and Brushless DC Motor Drives*. CRC press.

2 citations in pages 114 and 124.

Lee, H. and Utkin, V. I. (2007). Chattering suppression methods in sliding mode control systems. *Annual reviews in control*, 31(2):179–188.

One citation in page 56.

Lee, Y. I. and Kouvaritakis, B. (2009). Receding horizon control of switching systems. *Automatica*, 45(10):2307–2311.

One citation in page 57.

Liberzon, D. (2003). *Switching in systems and control*. Birkhäuser Boston.

6 citations in pages 17, 40, 41, 43, 44, and 58.

Lin, H. and Antsaklis, P. J. (2009). Stability and stabilizability of switched linear systems: a survey of recent results. *IEEE Transactions on Automatic Control*, 54(2):308–322.

3 citations in pages 17, 18, and 45.

Luenberger, D. (1979). *Introduction to Dynamic Systems: Theory, Models, and Applications*. Wiley.

3 citations in pages 24, 27, and 58.

Matsui, N. and Shigyo, M. (1992). Brushless DC motor control without position and speed sensors. *IEEE Transactions on Industry Applications*, 28(1):120–127.

One citation in page 124.

- Milnor, J. (1985). On the concept of attractor. In *The theory of chaotic attractors*, pages 243–264. Springer.
- 2 citations in pages 60 and 61.
- Mohan, N., Undeland, T. M., and Robbins, W. P. (2003). *Power electronics: Converters, Applications, and Design*. John Wiley & Sons.
- 2 citations in pages 17 and 51.
- Nemirovskii, A. (1993). Several NP-hard problems arising in robust stability analysis. *Mathematics of Control, Signals and Systems*, 6(2):99–105.
- One citation in page 53.
- Nesterov, Y. and Nemirovskii, A. (1994). *Interior-point polynomial algorithms in convex programming*, volume 13. SIAM.
- 2 citations in pages 35 and 173.
- Oppenheim, A. and Schafer, R. W. (2014). *Discrete-Time Signal Processing*. Pearson Education.
- 2 citations in pages 37 and 58.
- Oppenheim, A., Willsky, A., and Nawab, S. (1997). *Signals and Systems*. Prentice Hall.
- 3 citations in pages 33, 35, and 58.
- Patino, D., Riedinger, P., and Iung, C. (2009). Practical optimal state feedback control law for continuous-time switched affine systems with cyclic steady state. *International Journal of Control*, 82(7):1357–1376.
- 3 citations in pages 18, 51, and 52.
- Patino, D., Riedinger, P., and Ruiz, F. (2010). A predictive control approach for DC–DC power converters and cyclic switched systems. In *IEEE International Conference on Industrial Technology*, pages 1259–1264.
- One citation in page 94.
- Philippe, M., Athanasopoulos, N., Angeli, D., and Jungers, R. M. (2018). On path-complete Lyapunov functions: geometry and comparison. *IEEE Transactions on Automatic Control*, 64(5):1947–1957.
- One citation in page 46.
- Pillay, P. and Krishnan, R. (1989). Modeling, simulation, and analysis of permanent-magnet motor drives. I. The permanent-magnet synchronous motor drive. *IEEE Transactions on Industry Applications*, 25(2):265–273.
- One citation in page 124.
- Pinto, L. P. G. and Trofino, A. (2014). State and parameter estimation based on switched observers-an LMI approach. In *IEEE American Control Conference (ACC)*, pages 3249–3254.
- One citation in page 70.
- Qin, J. and Saeedifard, M. (2013). Reduced switching-frequency voltage-balancing strategies for modular multilevel HVDC converters. *IEEE Transactions on Power Delivery*, 28(4):2403–2410.
- One citation in page 17.

Rashid, M. (2014). *Power Electronics: Devices, Circuits, and Applications, International Edition*. Pearson Education Limited.

One citation in page 51.

Rockafellar, R. T. (1970). *Convex analysis*. Princeton University Press.

2 citations in pages 64 and 171.

Rubensson, M. and Lennartson, B. (2000). Stability of limit cycles in hybrid systems using discrete-time Lyapunov techniques. In *IEEE Conference on Decision and Control (CDC)*, volume 2, pages 1397–1402.

2 citations in pages 57 and 94.

Sanchez, C. A., Garcia, G., Sabrina, H., Heemels, W., and Zaccarian, L. (2019a). Practical stabilisation of switched affine systems with dwell-time guarantees. *IEEE Transactions on Automatic Control*.

4 citations in pages 18, 41, 52, and 62.

Sanchez, C. A., Santos, O. L., Prada, D. A. Z., Gordillo, F., and Garcia, G. (2019b). On the practical stability of hybrid control algorithm with minimum dwell time for a DC-AC converter. *IEEE Transactions on Control Systems Technology*, 27(6):2581–2588.

4 citations in pages 19, 51, 58, and 111.

Scharlau, C. C., de Oliveira, M. C., Trofino, A., and Dezuo, T. J. (2014). Switching rule design for affine switched systems using a max-type composition rule. *Systems & Control Letters*, 68:1–8.

2 citations in pages 18 and 52.

Scharlau, C. C., Dezuo, T. J. M., Trofino, A., and Reginatto, R. (2013). Switching rule design for inverter-fed induction motors. In *IEEE Conference on Decision and Control (CDC)*, pages 4662–4667.

One citation in page 111.

Seron, M. M., Zhuo, X. W., De Doná, J. A., and Martínez, J. J. (2008). Multisensor switching control strategy with fault tolerance guarantees. *Automatica*, 44(1):88–97.

One citation in page 17.

Sferlazza, A., Martínez-Salamero, L., Sanchez, C. A., Garcia, G., and Alonso, C. (2019). Min-type control strategy of a DC-DC synchronous boost converter. *IEEE Transactions on Industrial Electronics*.

One citation in page 94.

Shakhatreh, H., Sawalmeh, A. H., Al-Fuqaha, A., Dou, Z., Almaita, E., Khalil, I., Othman, N. S., Khreishah, A., and Guizani, M. (2019). Unmanned aerial vehicles (UAVs): A survey on civil applications and key research challenges. *IEEE Access*, 7:48572–48634.

One citation in page 20.

Shorten, R., Wirth, F., Mason, O., Wulff, K., and King, C. (2007). Stability criteria for switched and hybrid systems. *SIAM review*, 49(4):545–592.

2 citations in pages 17 and 46.

Siegwart, R., Nourbakhsh, I., and Scaramuzza, D. (2011). *Introduction to Autonomous Mobile Robots*. Intelligent Robotics and Autonomous Agents series. MIT Press.

One citation in page 79.

Slotine, J.-J. E., Li, W., et al. (1991). *Applied nonlinear control*. Prentice-Hall.

3 citations in pages 24, 29, and 58.

Souza, M., Deaecto, G. S., Geromel, J. C., and Daafouz, J. (2014). Self-triggered linear quadratic networked control. *Optimal Control Applications and Methods*, 35:524–538.

One citation in page 19.

Sun, Z. and Ge, S. S. (2011). *Stability theory of switched dynamical systems*. Springer Science & Business Media.

3 citations in pages 17, 18, and 58.

Trofino, A., Assmann, D., Scharlau, C. C., and Coutinho, D. F. (2009). Switching rule design for switched dynamic systems with affine vector fields. *IEEE Transactions on Automatic Control*, 54(9):2215–2222.

One citation in page 18.

Trofino, A., Scharlau, C. C., Dezuo, T. J., and de Oliveira, M. C. (2012). Switching rule design for affine switched systems with \mathcal{H}_∞ performance. In *IEEE Conference on Decision and Control*, pages 1923–1928.

3 citations in pages 18, 52, and 95.

Tuy, H. (1998). *Convex analysis and global optimization*. Springer.

One citation in page 171.

Utkin, V. and Lee, H. (2006). Chattering problem in sliding mode control systems. In *International Workshop on Variable Structure Systems*,, pages 346–350.

One citation in page 56.

Vangipuram, L. et al. (1990). *Practical stability of nonlinear systems*. World Scientific.

One citation in page 26.

Wu, R., Dewan, S. B., and Slemon, G. R. (1990). A PWM AC-to-DC converter with fixed switching frequency. *IEEE Transactions on Industry Applications*, 26(5):880–885.

One citation in page 136.

Xiao, F. and Wang, L. (2008). Asynchronous consensus in continuous-time multi-agent systems with switching topology and time-varying delays. *IEEE Transactions on Automatic Control*, 53(8):1804–1816.

One citation in page 17.

Xu, X., Zhai, G., and He, S. (2008). On practical asymptotic stabilizability of switched affine systems. *Nonlinear Analysis: Hybrid Systems*, 2(1):196–208.

One citation in page 58.

Xu, X., Zhai, G., and He, S. (2010). Some results on practical stabilizability of discrete-time switched affine systems. *Nonlinear Analysis: Hybrid Systems*, 4(1):113–121.

2 citations in pages 57 and 67.

Yakubovich, V. (1992). Nonconvex optimization problem: The infinite-horizon linear-quadratic control problem with quadratic constraints. *Systems & Control Letters*, 19(1):13–22.

One citation in page 171.

Yang, Z., Shang, F., Brown, I. P., and Krishnamurthy, M. (2015). Comparative study of interior permanent magnet, induction, and switched reluctance motor drives for ev and hev applications. *IEEE Transactions on Transportation Electrification*, 1(3):245–254.

One citation in page 114.

Zhang, X., Sun, L., Zhao, K., and Sun, L. (2013). Nonlinear speed control for PMSM system using sliding-mode control and disturbance compensation techniques. *IEEE Transactions on Power Electronics*, 28(3):1358–1365.

One citation in page 125.

Zhao, X., Shi, P., Yin, Y., and Nguang, S. K. (2016). New results on stability of slowly switched systems: A multiple discontinuous Lyapunov function approach. *IEEE Transactions on Automatic Control*, 62(7):3502–3509.

One citation in page 46.

Some results from the literature given in terms of lemmas are gathered together in this appendix. They were cited in this dissertation but, for sake of organization, their presentations are done here.

A.1 Rayleigh quotient

The **Rayleigh quotient** is a scalar ratio defined for an arbitrary symmetric matrix $Q \in \mathbb{R}^{n_x \times n_x}$ as

$$R(x) = \frac{x'Qx}{x'x} \quad (\text{A.1})$$

This quotient appears in several control problems and it allows determining suitable upper and lower bounds for quadratic forms, as the next lemma presents

Lemma A.1. *For any symmetric matrix $Q \in \mathbb{R}^{n_x \times n_x}$ the Rayleigh quotient is bounded for all $x \in \mathbb{R}^{n_x}$ as*

$$\min_{i \in \{1, \dots, n_x\}} \gamma_i(Q) \leq R(x) \leq \max_{i \in \{1, \dots, n_x\}} \gamma_i(Q) \quad (\text{A.2})$$

The proof is left as an exercise and, then, omitted.

A.2 Matrix Inversion Lemma

An important result for calculating an inverse matrix follows from the Sherman-Morrison-Woodbury formula, see [Horn and Johnson \(1990\)](#). Under certain conditions, this formula presents an alternative manner to evaluate the inverse of a matrix expression, which might be useful for obtaining equivalent expressions. The next lemma presents this result.

Lemma A.2 (Matrix Inversion Lemma). *Consider a matrix written as $A + XCY$ with $C \in \mathbb{R}^{m \times m}$, $X \in \mathbb{R}^{n \times m}$ and $Y \in \mathbb{R}^{m \times n}$. If A , C and $C^{-1} + YA^{-1}X$ are regular matrices, then*

$$(A + XCY)^{-1} = A^{-1} - A^{-1}X(C^{-1} + YA^{-1}X)^{-1}YA^{-1} \quad (\text{A.3})$$

This proof is also omitted.

A.3 Schur Complement Lemma

The Schur Complement Lemma, widely disseminated in mathematical literature, is a powerful tool in semi-definite programming context. This lemma is stated below as it follows in [Boyd et al. \(1994\)](#).

Lemma A.3 (Schur Complement Lemma). Consider an arbitrary symmetric matrix $S \in \mathbb{R}^{(n_x+n_y) \times (n_x+n_y)}$, which can be split in blocks as

$$S = \begin{bmatrix} U & V \\ V' & X \end{bmatrix} \quad (\text{A.4})$$

being $U \in \mathbb{R}^{n_x \times n_x}$, $V \in \mathbb{R}^{n_x \times n_y}$ and $X \in \mathbb{R}^{n_y \times n_y}$. We have that $S > 0$ if and only if

$$U > 0 \text{ and } X - V'U^{-1}V > 0 \quad (\text{A.5})$$

or

$$X > 0 \text{ and } U - VX^{-1}V' > 0 \quad (\text{A.6})$$

Proof: Consider the regular matrix

$$T = \begin{bmatrix} I & U^{-1}V \\ 0 & I \end{bmatrix} \quad (\text{A.7})$$

that can be used to factorize $S = T'KT$ with

$$K = \begin{bmatrix} U & 0 \\ 0 & X - V'U^{-1}V \end{bmatrix}$$

This shows that $S > 0$ if and only if $K > 0$, which is true whenever (A.5) hold. For (A.6) the proof is done analogously. \square

Throughout this dissertation, the just presented lemma is employed extensively as it allows stating equivalence between matrix inequalities. Whenever we want to replace (A.4) by (A.5) or vice-versa, we say that we will apply the Schur Complement Lemma with respect to U . The same holds for (A.6), when we say that the Schur Complement Lemma is applied with respect to X .

A.4 S-procedure

Another relevant result in our context is the S-procedure, which is also extracted from Boyd et al. (1994). In our context, it takes into account quadratic functions on a vector variable $x \in \mathbb{R}^n$ given as $F(x) = x'Qx + 2c'x + \rho$ with a symmetric matrix Q , a vector c and a scalar ρ arbitrarily given. The S-procedure statement is presented in the following lemma.

Lemma A.4 (S-Procedure Lemma). Consider quadratic functions $F_i: \mathbb{R}^n \rightarrow \mathbb{R}$, $i \in \{0, \dots, p\}$ with $p \in \mathbb{N}$. The inequality

$$F_0(x) > 0 \quad (\text{A.8})$$

holds $\forall x \neq 0: F_i(x) \geq 0, \forall i \in \{1, \dots, p\}$ if there exist $\tau_i \in \mathbb{R}_{0+}$, $i \in \{1, \dots, p\}$ such that for all $x \in \mathbb{R}^n$ we have that

$$F_0(x) - \sum_{i=1}^p \tau_i F_i(x) > 0 \quad (\text{A.9})$$

Proof: Consider that (A.9) holds for given τ_i , $i \in \{1, \dots, p\}$. Hence, for all x such that $F_i(x) \geq 0$, $\forall i \in \{1, \dots, p\}$ we have

$$\begin{aligned} F_0(x) &> \sum_{i=1}^p \tau_i F_i(x) \\ &\geq 0 \end{aligned} \tag{A.10}$$

showing that $F_0(x) \geq 0$ holds as well. \square

An interesting fact about the S-procedure is that, for the special case where $p = 1$, this lemma becomes lossless. In other words, the existence of $\tau_1 \geq 0$ such that $F_0(x) > \tau_1 F_1(x)$ is necessary and sufficient for having $F_0(x) > 0$ for all $x \neq 0$ such that $F_1(x) \geq 0$. More discussions regarding this lemma can be found in Yakubovich (1992).

A.5 Convex maximization

Maximizing convex functions (or minimizing concave ones) is generally a non-convex optimization problem that can have none, one or various local maxima. This fact makes these problems more intricate from a computational viewpoint, as efficient algorithms to enumerate and compare the local maxima (if any) are still lacking in the optimization literature. However, a clue on how to find these local maxima is that their occurrences happen at extreme points of the feasible domain, see Rockafellar (1970); Tuy (1998) for further discussions. In this context, the next lemma, borrowed from Deaecto and Geromel (2017), plays a key role in some developments within this dissertation.

Lemma A.5. *Consider the solution*

$$r_* = \sup_{z \in \mathbb{R}^n} q_1(z) \quad \text{s.t. } q_2(z) < 0 \tag{A.11}$$

being $q_1(z)$ and $q_2(z)$ quadratic convex functions on $z \in \mathbb{R}^n$ and an $\alpha \in \mathbb{R}$ such that

$$Q_1 - \alpha Q_2 > 0 \tag{A.12}$$

where Q_1 and Q_2 are Hessian matrices of $q_1(z)$ and $q_2(z)$, respectively. The global optimal solution to

$$\bar{r}_* = \sup_{z \in \mathbb{R}^n} q_1(z) - \alpha q_2(z) \quad \text{s.t. } q_2(z) < 0 \tag{A.13}$$

is $\bar{r}_* = r_*$.

Proof: If (A.12) hold for some $\alpha \in \mathbb{R}$ then $p(z) = q_1(z) - \alpha q_2(z)$ is a convex quadratic function. Being z_* the optimal solution of (A.11) and \bar{z}_* the one of (A.13), we can conclude that

$$\lim_{z \rightarrow z_*} q_2(z) = \lim_{z \rightarrow \bar{z}_*} q_2(z) = 0 \tag{A.14}$$

since $q_2(z) < 0$ defines a convex feasible set and will be an active constraint in both cases. From (A.11) and (A.13), we have

$$r_* = q_1(z_*) \geq q_1(\bar{z}_*) = \bar{r}_* + \alpha q_2(\bar{z}_*),$$

$$\bar{r}_* = p(\bar{z}_*) \geq p(z_*) = r_* - \alpha q_2(z_*).$$

Taking into account that $q_2(z_*) = q_2(\bar{z}_*) = 0$, obtained from (A.14), we can show that $\bar{r}_* = r_*$, concluding the demonstration. \square

The analysis and design conditions presented in this dissertation are written in terms of matrix inequalities, which comprises matrices whose terms are variables to be determined by an optimization procedure. The most desired scenario is when these inequalities are given by affine functions on these decisions variables. In these cases, we have one **linear matrix inequality (LMI)** or more, which define convex cones as feasible sets, called spectrahedra. Formally, an LMI can be written in a general form as

$$\mathcal{W}(x) = \mathcal{W}_0 + \sum_{i=1}^n x_i \mathcal{W}_i > 0, \quad (\text{B.1})$$

where $\mathcal{W}_i \in \mathbb{R}^{m \times m}$, $i \in \{0, \dots, n\}$, are symmetric matrices and $x \in \mathbb{R}^n$ is the vector of decision variables. Deciding whether there exist x that satisfies an LMI is a tractable problem and can be efficiently done in polynomial-time complexity, see [Boyd et al. \(1994\)](#) and [Boyd and Vandenberghe \(2004\)](#). Moreover, for a convex function $f : \mathbb{R}^n \rightarrow \mathbb{R}$, computing a feasible x for which $f(x)$ exceeds the global minimum of

$$\min_{x \in \mathbb{R}^n} f(x) \quad \text{s.t. } \mathcal{W}(x) > 0 \quad (\text{B.2})$$

by less than a given ϵ is still a task that can be accomplished in polynomial-time complexity. Indeed, the interest in linear matrix inequalities has grown over the last decades as many contributions from the literature, for instance [Karmarkar \(1984\)](#); [Nesterov and Nemirovskii \(1994\)](#); [Boyd and Vandenberghe \(2004\)](#), provided interior-point and first-order methods (among others) to globally solve optimization problems subject to LMIs with great reliability, allowing the development of semidefinite programming (SDP).

All the optimization problems in this dissertation were solved using the standard LMI framework, available in [Matlab Robust Control Toolbox](#) between 2017 and 2019 versions. The computer used in the numerical examples had Ubuntu as operating system between 16 and 18 versions. Many other (SDP) solvers are available for free such as [cvx](#) and [SeDuMi](#) and may provide slightly different numerical results.

Along this dissertation the determinant minimization problem

$$\min_{R > 0} -\ln(\det(R)) \quad (\text{B.3})$$

arises in Theorems [3.1](#), [3.3](#), [3.4](#) and [3.6](#), among others. This objective function is nonlinear but convex, as it is demonstrated in Appendix [C.1](#), and can be used to minimize the n -volume of ellipsoids. A specific subroutine was implemented based on the Frank-Wolfe algorithm (see [Frank and Wolfe \(1956\)](#)), in a more general fashion than it was provided in [Deaecto and Geromel \(2017\)](#) and [Egidio et al. \(2017\)](#). This algorithm is available in the public repository

<https://github.com/lucasegidio1/frankwolfe>

and requires the [Matlab Robust Control Toolbox](#).

B.1 BMIs

In some optimization problems in this dissertation, such as those from Theorems 3.3 and 3.6, constraints containing scalar and matrix variables multiplying each other are present, characterizing a **bilinear matrix inequality** (BMI). Luckily, fixing the scalar variables, the constraints become linear and, thus, convex. The adopted methodology to deal with these cases in this dissertation is to search for these scalars inside a discrete grid of values, solving a finite set of convex optimization problems. However, some strategies to locally solve optimization problems subject to BMIs are given in Hassibi et al. (1999); Apkarian and Tuan (2000); Dinh et al. (2011), for instance.

A generalized n -dimensional ellipsoid \mathcal{E} is given as a set of points $x \in \mathbb{R}^n$ defined as

$$\mathcal{E} = \{x \in \mathbb{R}^n : x'Qx + 2c'x + \rho \leq 0\} \quad (\text{C.1})$$

with a symmetric positive definite $Q \in \mathbb{R}^{n \times n}$, a vector $c \in \mathbb{R}^n$ and a scalar $\rho \in \mathbb{R}$ satisfying $\rho < c'Q^{-1}c$. An alternative representation can be given as

$$\mathcal{E} = \{x \in \mathbb{R}^n : (x - x_c)'Q(x - x_c) \leq r\} \quad (\text{C.2})$$

with $r = c'Q^{-1}c - \rho$ and center $x_c = -Q^{-1}c$. This ellipsoid has n orthogonal semi-axis whose lengths are given as $\|s_i\| = (\gamma_i(Q)/r)^{-1/2}$, $i \in \{1, \dots, n\}$.

Notice that, since the ellipsoid can be defined by a quadratic form (C.1), the S-procedure, introduced in Lemma A.4 is well adapted to determine whether an ellipsoid contains unions or intersections of other ellipsoids. Indeed, this aspect was explored by Theorem 3.6. More discussions about employing the S-procedure to this end are available in Boyd et al. (1994).

C.1 Volume

The generalized volume of an ellipsoid \mathcal{E} is given by

$$vol(\mathcal{E}) = \frac{\pi^{\frac{n}{2}}}{\Gamma(n/2 + 1)} \det\left(\frac{Q}{r}\right)^{-1/2} \quad (\text{C.3})$$

where $\Gamma(\cdot)$ is the Gamma function. This equation can be obtained from the n -volume of a unit ball after applying the endomorphism $(Q/r)^{1/2}$ over its space.

Taking $r = 1$, without loss of generality, the volume of \mathcal{E} is proportional to $g(Q) = \det(Q^{-1/2})$. This expression is non-convex in the elements of Q , since the determinant is defined from products between them. Nevertheless, the minimum of $g(Q)$ coincides with the one of

$$f(Q) = 2 \ln(g(Q)) = -\ln(\det(Q))$$

because the logarithm function is injective and increasing. Moreover, we can show that $f(Q)$ is a convex function

on Q , see Colaneri et al. (1997). For an arbitrary symmetric $Q_0 \in \mathbb{R}^{n \times n}$ we have

$$\begin{aligned} f(Q) - f(Q_0) &= -\ln(\det(Q_0^{-1}Q)) \\ &= -\sum_{i \in \mathbb{N}_n} \ln(\gamma_i(Q_0^{-1}Q)) \\ &\geq -\sum_{i \in \mathbb{N}_n} \{\gamma_i(Q_0^{-1}Q) - 1\} \\ &= -\text{Tr}(Q_0^{-1}Q - I) \end{aligned} \quad (\text{C.4})$$

where the first inequality follows from the fact that $\ln(\cdot)$ is a concave function, hence, $\ln(z) \leq z - 1$. Hence,

$$\begin{aligned} f(Q) &\geq f(Q_0) - \text{Tr}(Q_0^{-1}Q) + \text{Tr}(Q_0^{-1}Q_0) \\ &= f(Q_0) + \text{Tr}(-Q_0^{-1}(Q - Q_0)) \end{aligned} \quad (\text{C.5})$$

showing the convexity of $f(Q)$, according to Colaneri et al. (1997). Therefore, we can conclude that minimizing $f(Q)$ implies in minimizing the volume of the associated ellipsoid.

Moreover, making Q arbitrarily close to Q_0 , we have

$$f(Q) \approx f(Q_0) + \text{Tr}(-Q_0^{-1}(Q - Q_0)) \quad (\text{C.6})$$

allowing to conclude that the gradient of $f(Q)$ is

$$\nabla_Q f(Q) = -Q^{-1} \quad (\text{C.7})$$

This expression is the key for implementing the Frank-Wolfe algorithm employed to minimize $f(Q)$ along this dissertation, as discussed in Appendix B. Information about the gradient $\nabla_Q f(Q)$ is used by this algorithm at each iteration to minimize the linear approximation given in (C.6).

C.2 Projection

The next lemma provides an instrumental result about the projection of an ellipsoid onto a lower-dimensional space.

Lemma C.1. *Consider a generic ellipsoid*

$$\tilde{\mathcal{E}} = \{\tilde{x} \in \mathbb{R}^{2n} : p(\tilde{x}) \leq 0\} \quad (\text{C.8})$$

with $\tilde{x} = [x' \ \hat{x}']'$ and

$$p(\tilde{x}) = \begin{bmatrix} x \\ \hat{x} \\ 1 \end{bmatrix}' \begin{bmatrix} \Sigma & \Xi' & 0 \\ \Xi & \Upsilon & 0 \\ 0 & 0 & -1 \end{bmatrix} \begin{bmatrix} x \\ \hat{x} \\ 1 \end{bmatrix} \quad (\text{C.9})$$

where $\Upsilon > 0$ and $\Sigma - \Xi'\Upsilon^{-1}\Xi > 0$. The projection of $\tilde{\mathcal{E}}$ onto the subspace generated by $x \in \mathbb{R}^n$ is the ellipsoid

$$\mathcal{E} = \{x \in \mathbb{R}^n : x'(\Sigma - \Xi'\Upsilon^{-1}\Xi)x \leq 1\} \quad (\text{C.10})$$

Proof: The projection of $\tilde{\mathcal{E}}$ onto the subspace generated by x is also an ellipsoid (see [Blanchini and Miani \(2008\)](#)) defined in a general form $\mathcal{E} = \{x \in \mathbb{R}^n : x'\Omega x \leq 1\}$ such that $x \in \mathcal{E} \forall \tilde{x} : \tilde{x} \in \tilde{\mathcal{E}}$. From the S-procedure (see Appendix [A.4](#)), a necessary and sufficient condition for that is the existence of a scalar $\tau \in \mathbb{R}_{0+}$ such that

$$x'\Omega x - 1 < \tau p(\tilde{x}) \quad (\text{C.11})$$

As $p(\tilde{x})$ is a convex function in \hat{x} , this last inequality holds for every \hat{x} if and only if

$$x'\Omega x - 1 \leq \inf_{\hat{x} \in \mathbb{R}^n} \tau p(\tilde{x}) \quad (\text{C.12})$$

Evaluating the minimum of $p(\tilde{x})$ with respect to \hat{x} by making $\partial p(\tilde{x})/\partial \hat{x} = 0$ we have that it occurs for $\hat{x}_* = -\Upsilon^{-1}\Xi x$. Replacing \hat{x}_* into [\(C.12\)](#), we obtain

$$\begin{bmatrix} x \\ 1 \end{bmatrix} \begin{bmatrix} \Omega & 0 \\ 0 & -1 \end{bmatrix} \begin{bmatrix} x \\ 1 \end{bmatrix} \leq \tau \begin{bmatrix} x \\ 1 \end{bmatrix}' \begin{bmatrix} \Sigma - \Xi'\Upsilon^{-1}\Xi & 0 \\ 0 & -1 \end{bmatrix} \begin{bmatrix} x \\ 1 \end{bmatrix} \quad (\text{C.13})$$

The minimum ellipsoid $\tilde{\mathcal{E}}$ must satisfies this constraint at the equality, which is evident to occur for $\tau = 1$ and $\Omega = \Sigma - \Xi'\Upsilon^{-1}\Xi > 0$, providing the ellipsoid [\(C.10\)](#). \square

A useful remark is that although the generic ellipsoid defined in this lemma presents its center at the origin it is still general since x can define any translated vector.

INDEX

- \mathcal{H}_2 norm
 - continuous-time, 33
 - discrete-time, 37
- \mathcal{H}_2 performance index
 - continuous-time, 47
 - discrete-time, 50
- \mathcal{H}_∞ norm
 - continuous-time, 35
 - discrete-time, 38
- \mathcal{H}_∞ performance index
 - continuous-time, 48
 - discrete-time, 50
- \mathcal{L}_2^c space, 33
- \mathcal{L}_2^c -norm, 33
- \mathcal{L}_2^d space, 33
- \mathcal{L}_2^d -norm, 33
- autonomous switching law, 41
- averaged system, 44
- bilinear matrix inequality, 174
- chattering phenomenon, 56
- circularity of $\text{tr}(\cdot)$, 34
- common Lyapunov function, 46
- controllability gramian
 - continuous-time, 34
- controlled switching law, 41
- differential inclusion, 44
- discretized system, 39
- duty cycle, 44
- dwell-time, 41
- equilibrium point, 24
 - stable, 24
- asymptotically stable, 25
- globally asymptotically stable, 25
- globally practically stable, 26
- practically stable, 26
- unstable, 24
- Euclidean norm, 23
- full-order switched affine filter, 70
- guaranteed cost, 48
- Hare-Lynx System, 24
- Hurwitz stable matrix, 29
- impulse response
 - continuous-time, 33
 - discrete-time, 37
- limit cycle, 95
 - globally asymptotically stable, 96
- linear matrix inequality (LMI), 23, 35, 173
- Linear Time-Invariant System (LTI), 28
- LTI \mathcal{H}_2 performance
 - continuous-time, 34
 - discrete-time, 37
- LTI \mathcal{H}_∞ performance
 - continuous-time, 36
 - discrete-time, 38
- Lyapunov equation
 - continuous-time, 30
 - discrete-time, 31
- Lyapunov function, 27
 - min-type, 47
 - parameter-dependent, 112
 - quadratic, continuous-time, 30
 - quadratic, discrete-time, 32

- Lyapunov Stability Theorem, 26
 continuous-time, 27
 discrete-time, 27
- Lyapunov-Metzler inequalities
 continuous-time, 47
 discrete-time, 49
- Matrix Inversion Lemma, 169
- nonlinear system, 23
- norm-equivalent discretization, 40
- observability gramian
 continuous-time, 34
 discrete-time, 37
- operating region, 41
- permanent magnet synchronous machine, 114
- poles, 29
- pulse-width modulated (PWM), 44
- quadratically detectable, 74
- Rayleigh quotient, 169
- reset map, 41
- S-Procedure Lemma, 170
- sampled-data LTI systems, 39
- Schur Complement Lemma, 170
- Schur stable matrix, 31
- set of attraction, 60
 invariant, 60
- singleton set, 41
- sliding mode, 43
 sliding surface, 43
 stabilizable, 45
 stable LTI system, 29
 state vector, 23
 state-dependent switching law, 41
 state-space, 23
 step-invariant discretization, 39
 subsystems, 40
- switched affine system
 continuous-time, 51
 discrete-time, 59
- switched linear system
 continuous-time, 46
 discrete-time, 49
- switched system, 40
- switching function, 43
 switching sequence, 40
 switching signal, 40
 switching surfaces, 41
- system trajectory, 24
- time-dependent switching law, 41
 time-varying angular parameter, 112
 transfer function, 29
- voltage source inverter, 114
- Zeno Behavior, 43
 zeros, 29